MONOGRAPHS ON STATISTICS AND APPLIED PROBABILITY

General Editors

D.R. Cox, V. Isham, N. Keiding, T. Louis, N. Reid, R. Tibshirani, and H. Tong

1 Stochastic Population Models in Ecology and Epidemiology *M.S. Barlett* (1960)
2 Queues *D.R. Cox and W.L. Smith* (1961)
3 Monte Carlo Methods *J.M. Hammersley and D.C. Handscomb* (1964)
4 The Statistical Analysis of Series of Events *D.R. Cox and P.A.W. Lewis* (1966)
5 Population Genetics *W.J. Ewens* (1969)
6 Probability, Statistics and Time *M.S. Barlett* (1975)
7 Statistical Inference *S.D. Silvey* (1975)
8 The Analysis of Contingency Tables *B.S. Everitt* (1977)
9 Multivariate Analysis in Behavioural Research *A.E. Maxwell* (1977)
10 Stochastic Abundance Models *S. Engen* (1978)
11 Some Basic Theory for Statistical Inference *E.J.G. Pitman* (1979)
12 Point Processes *D.R. Cox and V. Isham* (1980)
13 Identification of Outliers *D.M. Hawkins* (1980)
14 Optimal Design *S.D. Silvey* (1980)
15 Finite Mixture Distributions *B.S. Everitt and D.J. Hand* (1981)
16 Classification *A.D. Gordon* (1981)
17 Distribution-Free Statistical Methods, 2nd edition *J.S. Maritz* (1995)
18 Residuals and Influence in Regression *R.D. Cook and S. Weisberg* (1982)
19 Applications of Queueing Theory, 2nd edition *G.F. Newell* (1982)
20 Risk Theory, 3rd edition *R.E. Beard, T. Pentikäinen and E. Pesonen* (1984)
21 Analysis of Survival Data *D.R. Cox and D. Oakes* (1984)
22 An Introduction to Latent Variable Models *B.S. Everitt* (1984)
23 Bandit Problems *D.A. Berry and B. Fristedt* (1985)
24 Stochastic Modelling and Control *M.H.A. Davis and R. Vinter* (1985)
25 The Statistical Analysis of Composition Data *J. Aitchison* (1986)
26 Density Estimation for Statistics and Data Analysis *B.W. Silverman* (1986)
27 Regression Analysis with Applications *G.B. Wetherill* (1986)
28 Sequential Methods in Statistics, 3rd edition
G.B. Wetherill and K.D. Glazebrook (1986)
29 Tensor Methods in Statistics *P. McCullagh* (1987)
30 Transformation and Weighting in Regression
R.J. Carroll and D. Ruppert (1988)
31 Asymptotic Techniques for Use in Statistics
O.E. Bandorff-Nielsen and D.R. Cox (1989)
32 Analysis of Binary Data, 2nd edition *D.R. Cox and E.J. Snell* (1989)

33 Analysis of Infectious Disease Data *N.G. Becker* (1989)

34 Design and Analysis of Cross-Over Trials *B. Jones and M.G. Kenward* (1989)

35 Empirical Bayes Methods, 2nd edition *J.S. Maritz and T. Lwin* (1989)

36 Symmetric Multivariate and Related Distributions
K.T. Fang, S. Kotz and K.W. Ng (1990)

37 Generalized Linear Models, 2nd edition *P. McCullagh and J.A. Nelder* (1989)

38 Cyclic and Computer Generated Designs, 2nd edition
J.A. John and E.R. Williams (1995)

39 Analog Estimation Methods in Econometrics *C.F. Manski* (1988)

40 Subset Selection in Regression *A.J. Miller* (1990)

41 Analysis of Repeated Measures *M.J. Crowder and D.J. Hand* (1990)

42 Statistical Reasoning with Imprecise Probabilities *P. Walley* (1991)

43 Generalized Additive Models *T.J. Hastie and R.J. Tibshirani* (1990)

44 Inspection Errors for Attributes in Quality Control
N.L. Johnson, S. Kotz and X, Wu (1991)

45 The Analysis of Contingency Tables, 2nd edition *B.S. Everitt* (1992)

46 The Analysis of Quantal Response Data *B.J.T. Morgan* (1992)

47 Longitudinal Data with Serial Correlation—A state-space approach
R.H. Jones (1993)

48 Differential Geometry and Statistics *M.K. Murray and J.W. Rice* (1993)

49 Markov Models and Optimization *M.H.A. Davis* (1993)

50 Networks and Chaos—Statistical and probabilistic aspects
O.E. Barndorff-Nielsen, J.L. Jensen and W.S. Kendall (1993)

51 Number-Theoretic Methods in Statistics *K.-T. Fang and Y. Wang* (1994)

52 Inference and Asymptotics *O.E. Barndorff-Nielsen and D.R. Cox* (1994)

53 Practical Risk Theory for Actuaries
C.D. Daykin, T. Pentikäinen and M. Pesonen (1994)

54 Biplots *J.C. Gower and D.J. Hand* (1996)

55 Predictive Inference—An introduction *S. Geisser* (1993)

56 Model-Free Curve Estimation *M.E. Tarter and M.D. Lock* (1993)

57 An Introduction to the Bootstrap *B. Efron and R.J. Tibshirani* (1993)

58 Nonparametric Regression and Generalized Linear Models
P.J. Green and B.W. Silverman (1994)

59 Multidimensional Scaling *T.F. Cox and M.A.A. Cox* (1994)

60 Kernel Smoothing *M.P. Wand and M.C. Jones* (1995)

61 Statistics for Long Memory Processes *J. Beran* (1995)

62 Nonlinear Models for Repeated Measurement Data
M. Davidian and D.M. Giltinan (1995)

63 Measurement Error in Nonlinear Models
R.J. Carroll, D. Rupert and L.A. Stefanski (1995)

64 Analyzing and Modeling Rank Data *J.J. Marden* (1995)

65 Time Series Models—In econometrics, finance and other fields
D.R. Cox, D.V. Hinkley and O.E. Barndorff-Nielsen (1996)

66 Local Polynomial Modeling and its Applications *J. Fan and I. Gijbels* (1996)

67 Multivariate Dependencies—Models, analysis and interpretation
D.R. Cox and N. Wermuth (1996)

68 Statistical Inference—Based on the likelihood *A. Azzalini* (1996)

69 Bayes and Empirical Bayes Methods for Data Analysis
B.P. Carlin and T.A Louis (1996)

70 Hidden Markov and Other Models for Discrete-Valued Time Series
I.L. Macdonald and W. Zucchini (1997)

71 Statistical Evidence—A likelihood paradigm *R. Royall* (1997)

72 Analysis of Incomplete Multivariate Data *J.L. Schafer* (1997)

73 Multivariate Models and Dependence Concepts *H. Joe* (1997)

74 Theory of Sample Surveys *M.E. Thompson* (1997)

75 Retrial Queues *G. Falin and J.G.C. Templeton* (1997)

76 Theory of Dispersion Models *B. Jørgensen* (1997)

77 Mixed Poisson Processes *J. Grandell* (1997)

78 Variance Components Estimation—Mixed models, methodologies and applications
P.S.R.S. Rao (1997)

79 Bayesian Methods for Finite Population Sampling
G. Meeden and M. Ghosh (1997)

80 Stochastic Geometry—Likelihood and computation
O.E. Barndorff-Nielsen, W.S. Kendall and M.N.M. van Lieshout (1998)

81 Computer-Assisted Analysis of Mixtures and Applications—
Meta-analysis, disease mapping and others *D. Böhning* (1999)

82 Classification, 2nd edition *A.D. Gordon* (1999)

83 Semimartingales and their Statistical Inference *B.L.S. Prakasa Rao* (1999)

84 Statistical Aspects of BSE and vCJD—Models for Epidemics
C.A. Donnelly and N.M. Ferguson (1999)

85 Set-Indexed Martingales *G. Ivanoff and E. Merzbach* (2000)

86 The Theory of the Design of Experiments *D.R. Cox and N. Reid* (2000)

87 Complex Stochastic Systems
O.E. Barndorff-Nielsen, D.R. Cox and C. Klüppelberg (2001)

88 Multidimensional Scaling, 2nd edition *T.F. Cox and M.A.A. Cox* (2001)

Multidimensional Scaling

SECOND EDITION

TREVOR F. COX
Senior Lecturer in Statistics
University of Newcastle Upon Tyne, UK

AND

MICHAEL A. A. COX
Lecturer in Business Management
University of Newcastle Upon Tyne, UK

CHAPMAN & HALL/CRC

Boca Raton London New York Washington, D.C.

Library of Congress Cataloging-in-Publication Data

Cox, Trevor F.
Multidimensional scaling / Trevor F. Cox, Michael A.A. Cox.--2nd ed.
p. cm. -- (Monographs on statistics and applied probability ; 88)
Includes bibliographical references and indexes.
ISBN 1-58488-094-5 (alk. paper)
1. Multivariate analysis. 2. Multideminsional scaling. I. Cox, Michael A.A. II. Title.
III. Series.

QA278 .C7 2000
519.5′35--dc21 00-060180
CIP

International Standard Book Number 1-58488-094-5
Library of Congress Card Number 00-060180
Printed in the United States of America 2 3 4 5 6 7 8 9 0
Printed on acid-free paper

Contents

Preface

It has been a pleasure for us to write the second edition of this book on multidimensional scaling. The second edition extends the first with recent references, a new chapter on biplots, a section on the Gifi system of nonlinear multivariate analysis and an extended version of the suite of computer programs.

Multidimensional scaling covers a variety of techniques, with its main development having rested in the hands of mathematical psychologists and the journal *Psychometrika* having championed the publication of articles in the subject. Multidimensional scaling has now become popular and has extended into areas other than its traditional place in the behavioural sciences. Many statistical computer packages now include multidimensional scaling.

The book has a review style to it which has been necessitated in attempting to cover several areas, but wanting to keep the size of the book of manageable proportions. The techniques covered have been applied to interesting data sets, hopefully giving insight into the data and the application of the theories. We hope readers will try out some of the techniques themselves, using the suite of computer programs provided. These run under DOS or Windows; a full Windows version will be available by the end of 2000.

Again, in this edition, we thank the many authors who have contributed to the theory of multidimensional scaling - not just the giants of the subject, Arabie, Benzécri, Carroll, Coombs, de Leeuw, Gower, Greenacre, Groenen, Guttman, Harshman, Heiser, Hubert, Kiers, Kroonenberg, Kruskal, Meulman, Ramsay, Schönemann, Shepard, Sibson, Takane, ten Berge, Torgerson, van der Heijden and Young, but every one of them. For without them, this book would not exist. Also, we would like to thank those who pointed out errors in the first edition, especially Jos ten Berge.

Newcastle upon Tyne
June 2000

Trevor F. Cox
Michael A. A. Cox

CHAPTER 1

Introduction

1.1 Introduction

Suppose a set of n objects is under consideration and between each pair of objects (r, s) there is a measurement δ_{rs} of the "dissimilarity" between the two objects. For example the set of objects might be ten bottles of whisky, each one from a different distillery. The dissimilarity δ_{rs} might be an integer score between zero and ten given to the comparison of the rth and sth whiskies by an expert judge of malt whisky. The judge would be given a tot from the rth bottle and one from the sth and then score the comparison: 0–the whiskies are so alike she cannot tell the difference, to 10–the whiskies are totally different. The judge is presented with all forty-five possible pairs of whiskies, and after a pleasant day's work, provides the data analyst with a total set of dissimilarities $\{\delta_{rs}\}$. Indeed Lapointe and Legendre (1994) understand the importance of a proper statistical comparison of whiskies, using data from a connoisseur's guide to malt whiskies written by Jackson (1989). In the same spirit, two much smaller analyses of whiskies are given in Chapters 6 and 9.

A narrow definition of multidimensional scaling (often abbreviated to MDS) is the search for a low dimensional space, usually Euclidean, in which points in the space represent the objects (whiskies), one point representing one object, and such that the distances between the points in the space, $\{d_{rs}\}$, match, as well as possible, the original dissimilarities $\{\delta_{rs}\}$. The techniques used for the search for the space and the associated configuration of points form metric and nonmetric multidimensional scaling.

An example

A classic way to illustrate multidimensional scaling is to use journey times between a set of cities in order to reconstruct a map of the cities. Greenacre and Underhill (1982) use flying times between

Southern African airports, Mardia *et al.* (1979) use road distances between some British cities.

For illustration here, the journey times by road between twelve British cities were subjected to multidimensional scaling, using classical scaling, which is described fully in Chapter 2. Figure 1.1 shows the configuration of points produced by the technique. There is a striking similarity between the positions of the points representing the cities and the positions of the same cities seen in a geographical map of Great Britain, except of course the cities in Figure 1.1 appear to be reflected about a line and rotated from the geographical map usually presented in an atlas.

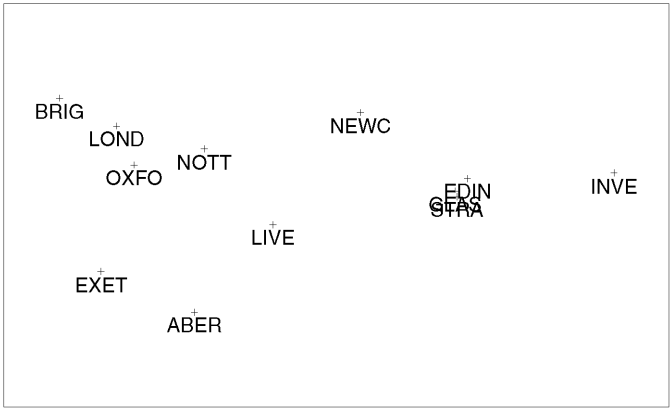

Figure 1.1 *A map of British cities reconstituted from journey time by road. ABER - Aberystwyth, BRIG - Brighton, EDIN - Edinburgh, EXET - Exeter, GLAS - Glasgow, INVE - Inverness, LIVE - Liverpool, LOND - London, NEWC - Newcastle, NOTT - Nottingham, OXFO - Oxford, STRA - Strathclyde.*

Multidimensional scaling is not only about reconstructing maps, but can be used on a wide range of dissimilarities arising from various situations, as for example, the whisky tasting experiment or other situations as described later in the chapter.

A wider definition of multidimensional scaling can subsume several techniques of multivariate data analysis. At the extreme, it

covers any technique which produces a graphical representation of objects from multivariate data. For example the dissimilarities obtained from the whisky comparisons could be used in a cluster analysis to find groups of similar whiskies. This text does not attempt to cover all these possibilities, as there are many books covering multivariate data analysis in general, for example Mardia *et al.* (1979), Chatfield and Collins (1980), Krzanowski (1988)and Krzanowski and Marriott (1994, 1995). The aim here is to give an account of the main topics that could be said to constitute the theory of multidimensional scaling.

Much of the theory of multidimensional scaling was developed in the behavioural sciences, with *Psychometrika* publishing many papers on the subject. It is a tribute to the journal that multidimensional scaling techniques are becoming a popular method of data analysis, with major statistical software packages now incorporating them into their repertoire.

1.2 A look at data and models

Several types of data lend themselves to analysis by multidimensional scaling. Behavioural scientists have adopted several terms relating to data which often are not familiar to others.

1.2.1 Types of data

Variables can be classified according to their "measurement scale". The four scales are the nominal scale, the ordinal scale, the interval scale and the ratio scale.

Nominal scale
Data measured on the nominal scale are classificatory, and only different classes are distinguishable, for example, hair colour, eye colour.

Ordinal scale
Data on the ordinal scale can be ordered, but are not quantitative data. For instance, whisky from bottle number 3 might be judged to be of better quality than that from bottle number 7.

Interval scale
Quantitative data where the difference between two values is meaningful are measured on the interval scale. For example, temperature in degrees Celsius, the difference in pulse rate before and after exercise.

Ratio scale
Data measured on the ratio scale are similar to those on the interval scale, except that the scale has a meaningful zero point, for example, weight, height, temperature recorded in degrees Kelvin.

Multidimensional scaling is carried out on data relating objects, individuals, subjects or stimuli to one another. These four terms will often be used interchangeably, although objects usually refers to inanimate things, such as bottles of whisky, individuals and subjects refering to people or animals, while stimuli usually refers to non-tangible entities, such as the taste of a tot of whisky.

The most common measure of the relationship of one object (stimulus, etc.) to another is a proximity measure. This measures the "closeness" of one object to another, and can either be a "similarity" measure where the similarity of one object to another, s_{rs}, is measured, or a "dissimilarity" measure where the dissimilarity, δ_{rs}, between the two objects is measured.

Suppose for the whisky tasting exercise, several more judges are brought in and each one of them compares all the pairs of whiskies. Then the available data are $\delta_{rs,i}$ where r, s refer to the bottles of whisky, and i refers to the ith judge. The situation now comprises a set of whiskies (stimuli) and a set of judges (subjects).

Number of modes
Each set of objects that underlie the data for multidimensional scaling is called a mode. Thus the dissimilarities $\delta_{rs,i}$ from the whisky tasting above are two-mode data, one-mode being the whiskies and the other the judges.

Number of ways
Each index in the measurement between objects etc. is called a way. So the $\delta_{rs,i}$ above are three-way data.

Thus data for multidimensional scaling are described by their number of modes and number of ways. With only one whisky judge, the data are one-mode, two-way, which is the commonest form.

The entries in a two-way contingency table form two-mode, two-way data. An appropriate method of analysis is correspondence analysis described in Chapter 9. Another form of two-mode, two-way data is where n judges each rank m stimuli. These data can be subjected to unfolding analysis described in Chapter 8. The two-mode, three-way data obtained from the judges of whisky can be analysed by individual differences models of Chapter 10. Three-mode, three-way, or even higher-mode and -way data can be analysed by using some of the methods described in Chapter 12. Data with large number of ways and modes are not very common in practice.

Coombs (1964) gives a classification of types of data. This was updated by Carroll and Arabie (1980) who classify data and also classify types of multidimensional scaling analyses. In so doing, they have constructed a useful review of the area. Other useful reviews have been given by Greenacre and Underhill (1982), de Leeuw and Heiser (1982), Wish and Carroll (1982), Gower (1984) and Mead (1992). An introductory book on multidimensional scaling is Kruskal and Wish (1978). Fuller accounts of the subject are given by Schiffman *et al.* (1981), Davidson (1983), Young (1987) and Borg and Groenen (1997) among others.

This book attempts to cover the main constituents of multidimensional scaling, giving much, but not all, of the mathematical theory. Also included in the book is a CD-ROM enabling the reader to try out some of the techniques. Instructions for loading the CD-ROM and running the programs are given in the appendix.

1.2.2 Multidimensional scaling models

Some models used for multidimensional scaling are outlined before fuller definition and development in later chapters. The starting point is one-mode, two-way proximity data, and in particular, dissimilarity measurements.

Suppose a set of n objects have dissimilarities $\{\delta_{rs}\}$ measured between all pairs of objects. A configuration of n points representing the objects is sought in a p dimensional space. Each point represents one object, with the rth point representing object r. Let the distances, not necessarily Euclidean, between pairs of points be $\{d_{rs}\}$. Then as stated before, the aim of multidimensional scaling is to find a configuration such that the distances $\{d_{rs}\}$ "match",

as well as possible, the dissimilarities $\{\delta_{rs}\}$. It is the different notions of "matching" that give rise to the different techniques of multidimensional scaling.

Classical scaling
If the distances in the configuration space are to be Euclidean and

$$d_{rs} = \delta_{rs} \qquad r, s = 1, \ldots, n \tag{1.1}$$

so that the dissimilarities are precisely Euclidean distances, then it is possible to find a configuration of points ensuring the equality in (1.1). Classical scaling treats dissimilarities $\{\delta_{rs}\}$ directly as Euclidean distances and then makes use of the spectral decomposition of a doubly centred matrix of dissimilarities. The technique is discussed fully in Chapter 2.

Metric least squares scaling
Least squares scaling matches distances $\{d_{rs}\}$ to transformed dissimilarities $\{f(\delta_{rs})\}$, where f is a continuous monotonic function. The function f attempts to transform the dissimilarities into distances whereupon a configuration is found by fitting its associated distances by least squares to $\{f(\delta_{rs})\}$. For example, a configuration may be sought such that the loss function

$$\frac{\sum_r \sum_s (d_{rs} - (\alpha + \beta\delta_{rs}))^2}{\sum_r \sum_s d_{rs}^2}$$

is minimized where α and β are positive constants which are to be found.

Classical scaling and least squares scaling are examples of "metric scaling", where metric refers to the type of transformation of the dissimilarities and not the space in which a configuration of points is sought. Critchley's intermediate method (Critchley, 1978) is another example of metric scaling and is also described in the second chapter.

Unidimensional scaling
A special case of multidimensional scaling occurs when the configuration of points representing the objects is sought in only one dimension. This is unidimensional scaling. The single dimension produces an ordering of the objects which can be useful in an analysis. An example of this is given in Chapter 2 where the technique

is used on classic data relating to the works of Plato. Unidimensional scaling can be plagued with a plethora of local minima when attempting to minimise the loss function.

Nonmetric scaling
If the metric nature of the transformation of the dissimilarities is abandoned, nonmetric multidimensional scaling is arrived at. The transformation f can now be arbitrary, but must obey the monotonicity constraint

$$\delta_{rs} < \delta_{r's'} \Rightarrow f(\delta_{rs}) \leq f(\delta_{r's'}) \qquad \text{for all } 1 \leq r, s, r', s' \leq n.$$

Thus only the rank order of the dissimilarities has to be preserved by the transformation and hence the term nonmetric. Nonmetric multidimensional scaling is discussed in Chapter 3.

Procrustes analysis
Suppose multidimensional scaling has been carried out on some dissimilarity data using two different methods giving rise to two configurations of points representing the same set of objects. A Procrustes analysis dilates, translates, reflects and rotates one of the configurations of points to match, as well as possible, the other, enabling a comparison of the two configurations to be made. Procrustes analysis is covered in Chapter 5.

Biplots
Biplots attempt to plot not only a configuration of points representing objects, but also axes within the plots that represent the variables upon which the dissimilarities were calculated. In the simplest case, the axes are linear, but with generalization the axes can be curvilinear. Chapter 7 explains the theory.

Unfolding
Suppose n judges of m types of whisky each rank the whiskies in order of their personal preference. Unfolding attempts to produce a configuration of points in a space with each point representing one of the judges, together with another configuration of points in the same space, these points representing the whiskies. The configurations are sought so that the rank order of the distances from the ith "judge" point to the "whisky" points, matches, as well as possible, the original whisky rankings of the ith judge. This is to

be the case for all of the judges. Unfolding analysis is the subject of Chapter 8.

Correspondence analysis
Data in the form of a two-way contingency table can be analysed by correspondence analysis. A space is found in which row profiles can be represented by points, and similarly, another space is also found for representing the column profiles. Distances in these spaces reproduce chi-square distances between row/column profiles. Full discussion is given in Chapter 9.

Indvidual differences
Again, if m judges each compare all pairs of whiskies, then either m separate multidimensional scaling analyses can be carried out or an attempt can be made at a combined approach. Individual differences models produce an overall configuration of points representing the whiskies in what is called the group stimulus space, together with a configuration of points representing the judges in a different space called the subject space. The position of a particular judge in the subject space depends on the weights needed on the axes of the stimulus space to transform the configuration of points in the group stimulus space into the configuration that would have been peculiar to that judge. Individual differences models are the subject of Chapter 10.

Gifi
The Gifi system of nonlinear multivariate analysis extends various techniques, such as principal components analysis. It has links to multidimensional scaling which are explored in Chapter 11. Multidimensional scaling based on alternating least squares scaling (ALSCAL) and by "majorization a complicated function" (SMACOF) are also discussed in Chapter 11.

Chapter 12 gives a brief summary of further multidimensional scaling models that involve data of more than 2 ways and 1 mode.

1.3 Proximities

Proximity literally means nearness in space, time or in some other way. The "nearness" of objects, individuals, stimuli needs definition and measurement prior to statistical analysis. In some situations, this is straightforward, but in others, difficult and controversial.

Measures of proximity are of two types: similarity and dissimilarity with the obvious interpretation of measuring how similar or dissimilar objects are to each other.

Let the objects under consideration comprise a set O. The similarity/dissimilarity measure between two objects is then a real function defined on $O \times O$, giving rise to similarity s_{rs}, or dissimilarity δ_{rs} between the rth and sth objects. Usually $\delta_{rs} \geq 0$, $s_{rs} \geq 0$, and the dissimilarity of an object with itself is taken to be zero, i.e. $\delta_{rr} = 0$. Similarities are usually scaled so that the maximum similarity is unity, with $s_{rr} = 1$.

Hartigan (1967) gives twelve possible proximity structures, S, that might need to be considered before a particular proximity measure is chosen. These are listed in Cormack (1971) and also below.

S1 S defined on $O \times O$ is Euclidean distance,
S2 S defined on $O \times O$ is a metric,
S3 S defined on $O \times O$ is symmetric real-valued,
S4 S defined on $O \times O$ is real-valued,
S5 S is a complete ordering $\preceq$ on $O \times O$,
S6 S is a partial ordering $\preceq$ on $O \times O$,
S7 S is a tree τ on O (a partial similarity order $(r, s) \preceq (r', s')$ whenever $\sup_\tau(r, s) \geq \sup_\tau(r', s')$, see Hartigan or Cormack for further details),
S8 S is a complete relative similarity ordering $\preceq_r$ on O; for each r in O, $s \preceq_r t$ means s is no more similar to r than t is,
S9 S is a partial relative similarity order $\preceq_r$ on O,
S10 S is a similarity dichotomy on $O \times O$ in which $O \times O$ is divided into a set of similar pairs and a set of dissimilar pairs,
S11 S is a similarity trichotomy on $O \times O$ consisting of similar pairs, dissimilar pairs, and the remaining pairs,
S12 S is a partition of O into sets of similar objects.

Structure S1 is a very strict structure with dissimilarity defined as Euclidean distance. Relaxing this to the requirement of a metric gives S2, where it is recalled that δ_{rs} is a metric if

$$\begin{aligned}
&\delta_{rs} = 0 \qquad \text{if and only if } r = s,\\
&\delta_{rs} = \delta_{sr} \qquad \text{for all } 1 \leq r, s \leq n,\\
&\delta_{rs} \leq \delta_{rt} + \delta_{ts} \qquad \text{for all } 1 \leq r, s, t \leq n.
\end{aligned}$$

Relaxing the metric requirement to δ_{rs} being symmetric real-valued or real-valued gives structures S3 and S4. Losing ratio/interval scales of measurement of δ_{rs} leads to the nonmetric structures S5 to S12. Of these the highest structure, S5, has a complete ordering of the $\{\delta_{rs}\}$. The lowest structure, S12, simply partitions O into sets of similar objects.

Choice of proximity measure depends upon the problem at hand, and is often not an easy task. Sometimes similarity between two objects is not based on any underlying data recorded on the objects. For example, in the whisky tasting exercise, the judge simply uses taste and smell sensations to produce a score between zero and ten. The similarity/dissimilarity measurement is totally subjective. It is extremely unlikely that the dissimilarities arrived at by the judge would obey proximity structure S1, since they are all integer-valued. The only possibility would be if the whiskies could be represented by integer points on a one dimensional Euclidean space and differences between points generated all forty-five dissimilarities correctly. It is even unlikely that S2 would be satisfied. The most likely structure is S3, or possibly S5 if actual scores were ignored and only the rank order of the dissimilarities taken into account.

In other situations, similarities (dissimilarities) are constructed from a data matrix for the objects. These are then called similarity (dissimilarity) coefficients. Several authors, for example Cormack (1971), Jardine and Sibson (1971), Anderberg (1973), Sneath and Sokal (1973), Diday and Simon (1976), Mardia *et al.* (1979), Gordon (1999), Hubálek (1982), Gower (1985b), Gower and Legendre (1986), Digby and Kempton (1987), Jackson *et al.* (1989), Baulieu (1989), Snijders *et al.* (1990) discuss various similarity and dissimilarity measures together with their associated problems. The following synthesis of the work of these authors attempts to outline the main ideas behind forming dissimilarities from a data matrix.

Table 1.1 *Dissimilarity measures for quantitative data*

Euclidean distance	$\delta_{rs} = \left\{ \sum_i (x_{ri} - x_{si})^2 \right\}^{\frac{1}{2}}$
Weighted Euclidean	$\delta_{rs} = \left\{ \sum_i w_i (x_{ri} - x_{si})^2 \right\}^{\frac{1}{2}}$
Mahalanobis distance	$\delta_{rs} = \{(\mathbf{x}_r - \mathbf{x}_s)^T \boldsymbol{\Sigma}^{-1} (\mathbf{x}_r - \mathbf{x}_s)\}^{\frac{1}{2}}$
City block metric	$\delta_{rs} = \sum_i \lvert x_{ri} - x_{si} \rvert$
Minkowski metric	$\delta_{rs} = \left\{ \sum_i w_i \lvert x_{ri} - x_{si} \rvert^{\lambda} \right\}^{\frac{1}{\lambda}} \quad \lambda \geq 1$
Canberra metric	$\delta_{rs} = \sum_i \lvert x_{ri} - x_{si} \rvert / (x_{ri} + x_{si})$
Divergence	$\delta_{rs} = \frac{1}{p} \sum_i (x_{ri} - x_{si})^2 / (x_{ri} + x_{si})^2$
Bray-Curtis	$\delta_{rs} = \frac{1}{p} \frac{\sum_i \lvert x_{ri} - x_{si} \rvert}{\sum_i (x_{ri} + x_{si})}$
Soergel	$\delta_{rs} = \frac{\sum_i \lvert x_{ri} - x_{si} \rvert}{\sum_i \max(x_{ri}, x_{si})}$
Bhattacharyya distance	$\delta_{rs} = \left\{ \sum_i (x_{ri}^{\frac{1}{2}} - x_{si}^{\frac{1}{2}})^2 \right\}^{\frac{1}{2}}$
Wave-Hedges	$\delta_{rs} = \frac{1}{p} \sum_i \left(1 - \frac{\min(x_{ri}, x_{si})}{\max(x_{ri}, x_{si})} \right)$
Angular separation	$\delta_{rs} = 1 - \frac{\sum_i x_{ri} x_{si}}{[\sum_i x_{ri}^2 \sum_i x_{si}^2]^{\frac{1}{2}}}$
Correlation	$\delta_{rs} = 1 - \frac{\sum_i (x_{ri} - \bar{x}_r)(x_{si} - \bar{x}_s)}{\left\{ \sum_i (x_{ri} - \bar{x}_r)^2 \sum_i (x_{si} - \bar{x}_s)^2 \right\}^{\frac{1}{2}}}$

Let $\mathbf{X} = [x_{ri}]$ denote the data matrix obtained for n objects on p variables. The vector of observations for the rth object is denoted by $\mathbf{x}_r$, and so $\mathbf{X} = [\mathbf{x}_r^T]$.

Quantitative data

Table 1.1 gives a list of possible dissimilarity measures for quantitative data that are in particular, continuous, possibly discrete, but not binary.

Binary data

		Object s		
		1	0	
Object r	1	a	b	$a+b$
	0	c	d	$c+d$
		$a+c$	$b+d$	$p=a+b+c+d$

When all the variables are binary, it is usual to construct a similarity coefficient and then to transform this into a dissimilarity coefficient. The measure of similarity between objects r and s is based on the above table. The table shows the number of variables, a, out of the total p variables where both objects score "1", the number of variables, b, where r scores "1" and s scores "0", etc. Table 1.2 gives a list of similarity coefficients based on the four counts a, b, c, d. Various situations call for particular choices of coefficients. In practice, more than one can be tried hoping for some robustness against choice. Hubálek (1982) gives the most comprehensive list of similarity coefficients for binary data and groups them into five clusters based on an empirical evaluation using data on the occurrence of fungal species of the genus *Chaetomium*.

Nominal and ordinal data

If, for the ith nominal variable, objects r and s share the same categorization, let $s_{rsi} = 1$, and 0 otherwise. A similarity measure is then $p^{-1}\sum_i s_{rsi}$. Of course, if other information is available regarding the relationship of various categories for the variables, then s_{rsi} can be given an appropriate value. For example, if the variable "bottle shape" has categories: standard (st); short cylindrical

Table 1.2 *Similarity coefficients for binary data*

Braun, Blanque	$s_{rs} = \dfrac{a}{\max\{(a+b),(a+c)\}}$
Czekanowski, Sørensen, Dice	$s_{rs} = \dfrac{2a}{2a+b+c}$
Hamman	$s_{rs} = \dfrac{a-(b+c)+d}{a+b+c+d}$
Jaccard coefficient	$s_{rs} = \dfrac{a}{a+b+c}$
Kulczynski	$s_{rs} = \dfrac{a}{b+c}$
Kulczynski	$s_{rs} = \dfrac{1}{2}\left(\dfrac{a}{a+b} + \dfrac{a}{a+c}\right)$
Michael	$s_{rs} = \dfrac{4(ad-bc)}{\{(a+d)^2+(b+c)^2\}}$
Mountford	$s_{rs} = \dfrac{2a}{a(b+c)+2bc}$
Mozley, Margalef	$s_{rs} = \dfrac{a(a+b+c+d)}{(a+b)(a+c)}$
Ochiai	$s_{rs} = \dfrac{a}{[(a+b)(a+c)]^{\frac{1}{2}}}$
Phi	$s_{rs} = \dfrac{ad-bc}{[(a+b)(a+c)(b+d)(c+d)]^{\frac{1}{2}}}$
Rogers, Tanimoto	$s_{rs} = \dfrac{a+d}{a+2b+2c+d}$
Russell, Rao	$s_{rs} = \dfrac{a}{a+b+c+d}$
Simple matching coefficient	$s_{rs} = \dfrac{a+d}{a+b+c+d}$
Simpson	$s_{rs} = \dfrac{a}{\min\{(a+b),(a+c)\}}$
Sokal, Sneath, Anderberg	$s_{rs} = \dfrac{a}{a+2(b+c)}$
Yule	$s_{rs} = \dfrac{ad-bc}{ad+bc}$

(sh); tall cylindrical (ta); and square section (sq), the following "agreement scores" may be appropriate for bottles r and s.

		bottle r			
		st	sh	ta	sq
bottle s	st	1.0	0.5	0.5	0.0
	sh	0.5	1.0	0.3	0.0
	ta	0.5	0.3	1.0	0.0
	sq	0.0	0.0	0.0	1.0

So if bottle r is "tall cylindrical" and bottle s "standard" then $s_{rsi} = 0.5$, for example.

If a variable is ordinal with k categories, then $k - 1$ indicator variables can be used to represent these categories. The indicator variables can then be subjected to similarity coefficients in order to give a value to s_{rsi}. For instance, if a bottle variable is "height of the bottle" with categories: small; standard; tall; long and thin, then the variable might be categorized as follows.

	Indicator variable		
category	I_1	I_2	I_3
small	0	0	0
standard	1	0	0
tall	1	1	0
long and thin	1	1	1

If bottle r is "standard" and bottle s is "long and thin", then using the simple matching coefficient to measure similarity for this variable, s_{rsi}=0.33. For further details see Sneath and Sokal (1973) or Gordon (1999).

1.3.1 Similarity/dissimilarity coefficients for mixed data

When data are of mixed type where binary, categorical, ordinal and quantitative variables might be measured, the similarity and

dissimilarity measures in Table 1.1 and 1.2 cannot sensibly be applied directly. To overcome this, Gower (1971) introduced a general similarity coefficient, s_{rs} defined as follows

$$s_{rs} = \frac{\sum_{i=1}^{p} \omega_{rsi} s_{rsi}}{\sum_i \omega_{rsi}},$$

where s_{rsi} is the similarity between the rth and sth objects based on the ith variable alone, and ω_{rsi} is unity if the rth and sth objects can be compared on the ith variable and zero if they cannot. Thus s_{rsi} is an average over all possible similarities s_{rsi} for the rth and sth objects. So for example, if some data are missing the overall coefficient is comprised of just those observations which are present for both the rth and sth objects.

Gower suggests the following values for s_{rsi} and ω_{rsi} for binary variables measuring presence/absence.

object r	object s	s_{rsi}	ω_{rsi}
+	+	1	1
+	-	0	1
-	+	0	1
-	-	0	0

For nominal variables, Gower suggests $s_{rsi} = 1$ if objects r and s share the same categorization for variable i, $s_{rsi} = 0$ otherwise. Of course other measures such as those described in the previous section can be used.

For quantitative variables,

$$s_{rsi} = 1 - |x_{ri} - x_{si}|/R_i,$$

where R_i is the range of the observations for variable i.

Gower's coefficient can be generalized using weights $\{w_i\}$ for the variables to

$$s_{rsi} = \frac{\sum_i s_{rsi} \omega_{rsi} w_i}{\sum_i \omega_{rsi} w_i}.$$

Further discussion, see for example Gordon (1990, 1999), can be found on missing values, incompatibility of units of measurement, conditionally present variables and the weighting of variables. Cox and Cox (2000) extend Gower's general dissimilarity coefficient producing a flexible method for producing two sets of dissimilarities simultaneously, one for the objects and one for the variables.

The method uses the idea of reciprocal averaging, a technique discussed in Chapter 9, and so further discussion is left until then.

Ichino and Yaguchi (1994) introduce a generalized Minkowski dissimilarity in the context of pattern recognition, where "features" are measured as opposed to random variables. The following summarises their measure. Firstly, the usual range of type of variables (features) measured is increased to include random intervals, and tree structures. Figure 1.2 shows a tree structure based on the body. Measurements are made as values at its terminal nodes, e.g. *(fracture, deafness)* in Figure 1.2.

The *Cartesian join*, $\oplus$, is defined as follows:

If the variable X_i is quantitative, ordinal, or a random interval, then

$$x_{ri} \oplus x_{si} = [\min(x_{ri}, x_{si}), \max(x_{ri}, x_{si})].$$

If X_i is categorical and where more than one category may be recorded for each object

$$x_{ri} \oplus x_{si} = x_{ri} \cup x_{si}.$$

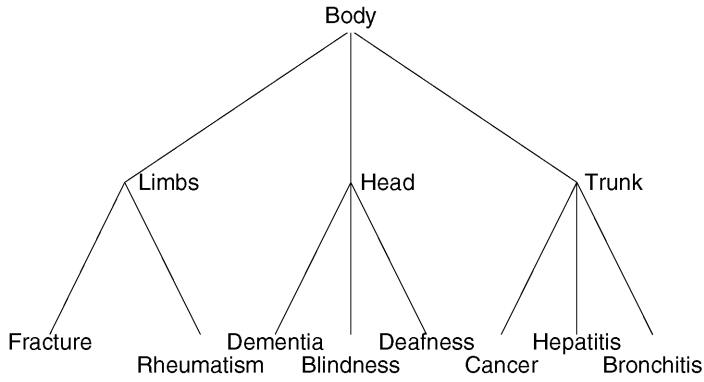

Figure 1.2 *A tree based on the body*

For a tree structure, let $n(x_{ri})$ be the nearest parent node for x_{ri} (e.g. the node "body" is the parent of *(fracture, deafness)*. If $n(x_{ri}) = n(x_{si})$ then

$$x_{ri} \oplus x_{si} = x_{ri} \cup x_{si},$$

but if $n(x_{ri}) \neq n(x_{si})$ then

$$x_{ri} \oplus x_{si} = (all\ terminal\ values\ branching\ from\ the\ node\ n(x_{ri} \cup x_{si})).$$

Also, if $x_{ri} = x_{si}$ then define

$$x_{ri} \oplus x_{si} = x_{ri}.$$

For example for the tree in Figure 1.2,

$$(fracture, blindness) \oplus (fracture, blindness) = (fracture, blindness)$$

$$(cancer, hepatitis) \oplus (bronchitis) = (cancer, hepatitis\ bronchitis)$$

$$(dementia, blindness) \oplus (cancer) = (fracture, rheumatism, dementia, blindness, deafness, cancer, hepatitis, bronchitis).$$

The *Cartesian meet*, $\otimes$, is defined as

$$x_{ri} \otimes x_{si} = x_{ri} \cap x_{si}.$$

Now define $\phi(x_{ri}, x_{si})$ as

$$\phi(x_{ri}, x_{si}) = |x_{ri} \oplus x_{si}| - |x_{ri} \otimes x_{si}| + \alpha(2|x_{ri} \otimes x_{si}| - |x_{ri}| - |x_{si}|),$$

where $|x_{ri}|$ denotes the length of the interval x_{ri} and $0 \leq \alpha \leq 0.5$ is a parameter that adjusts the measure when x_{ri} and x_{si} are intervals.

Now ϕ is normalized by defining

$$\psi(x_{ri}, x_{si}) = \phi(x_{ri}, x_{si})/|R_i|,$$

where $|R_i|$ is the range of X_i if X_i is quantitative and is the number of categories or terminal nodes if X_i is categorical or a tree structure.

The generalized Minkowski measure is then defined as

$$\delta_{rs} = \left\{ \sum_i w_i \psi^{\lambda}(x_{ri}, x_{si}) \right\}^{1/\lambda},$$

where w_i is a weight for the ith variable. Ichino and Yaguchi (1994) show that δ_{rs} is a metric.

1.3.2 *Distribution of proximity coefficients*

In calculating the similarity between a pair of objects, it might be of interest to establish whether the value obtained is significantly different from that expected for two arbitrary objects. This is usually not an easy task since the underlying distribution of the data vector needs to be known. If multivariate normality can be assumed, then some progress is possible with the dissimilarity measures in Table 1.1. For example for the Mahalanobis distance, $\delta_{rs} \sim 2\chi^2_p$.

For similarities based on binary variables, Goodall (1967) found the mean and variance for the simple matching coefficient, assuming independence of the variables. For the simple matching coefficient

$$s_{rs} = p^{-1}(a+d) = p^{-1}(I_1 + I_2 + \ldots + I_p),$$

where $I_i = 1$ if objects r and s agree (i.e. are both 0 or 1) on the ith variable. Let $Pr\{X_{ri} = 1\} = p_i$. Then

$$\mathrm{E}(s_{rs}) = p^{-1} \sum_{i=1}^{p} (p_i^2 + (1-p_i)^2) = \mu,$$

and after some algebra

$$\mathrm{Var}(s_{rs}) = p^{-1}\left\{\mu(1-\mu) - p^{-1} \sum_{i=1}^{p} \left(p_i^2 + (1-p_i)^2 - \mu^2\right)^2\right\}.$$

These results can be generalized to the case where the objects can come from different groups which have differing p_i's.

Moments for other coefficients which do not have a constant denominator are much more difficult to obtain. Snijders *et al.* (1990) give a brief review of the derivation of the moments for the Jaccard coefficient and the Dice coefficient. They also extend the results to the case where the binary variables are dependent. Approximate distributions can be found using these moments and hence the significance of an observed value of the similarity coefficient can be assessed.

1.3.3 *Similarity of species populations*

There is a large interest in measures of diversity within populations and similarity between populations with many papers in the

ecological literature, see for instance Rao (1982) and Jackson *et al.* (1989). Various authors have investigated the distribution of some of these similarity coefficients. Following Heltshe (1988) consider two sites A and B, where the presence/absence of various species is recorded. Let $a =$ the number of species found at both sites, $b =$ the number of species found at site B but not at site A, $c =$ the number of species found at site A but not at site B and $d =$ the number of species absent from both sites. The similarity between the two sites can be measured by one of the similarity coefficients of Table 1.2, the notation just described fitting with that for the 2×2 table formed for calculating these similarity coefficients.

Sampling of the sites is by use of quadrats which are areas of fixed size and shape, usually circular or rectangular, placed within the sampling frame sometimes at random and sometimes systematically. Measurements are then made within the quadrats, for example, counts of individuals for each species, or in this case, the recording of presence/absence for each species. Let there be n_1 quadrats used in site A and n_2 in site B. Several authors have used the jackknife estimator for measuring diversity and similarity between the sites (populations), see for example Farewell (1978), Smith *et al.* (1979), Heltshe and Forrester (1983) and Heltshe (1988).

Firstly, the similarity, s, between sites is calculated using the Jaccard coefficient say, and using the amalgamated presence/absence data from all the $n_1 + n_2$ quadrats. Thus $s = a/(a + b + c)$. Then the ith quadrat is removed from site A and s is recalculated with the reduced data. Let the value of this similarity be $s_{1(i)}$. This procedure is carried out for all n_1 quadrats for site A, and then for all n_2 quadrats of site B giving $s_{2(i)}$. If a removed quadrat from site A does not contain a species unique to that quadrat compared to all the other quadrats for site A, then $s_{1(i)} = s$. On the other hand, if the removed quadrat has $\alpha + \beta$ species unique to that quadrat for site A, but with α of these species also present at the other site B, and β species absent from B. Then $s_{1(i)} = (a - \alpha)/(a + b + c - \beta)$. Let $f_{1\alpha\beta}$ be the frequency of quadrats for site A in this situation, and similarly, for $s_{2(i)}$ and $f_{2\alpha\beta}$ when quadrats are removed from site B.

In general, the jackknife estimate of similarity is

$$\tilde{s} = (n_1 + n_2 - 1)s - (n_1 - 1)\bar{s}_1 - (n_2 - 1)\bar{s}_2,$$

where $\bar{s}_j = n_j^{-1} \sum_i s_{j(i)}$ $(j = 1, 2)$. The estimated variance of $\tilde{s}$ is

$$n_1^{-1}(n_1 - 1)^2 \hat{\sigma}_1^2 + n_2^{-1}(n_2 - 1)^2 \hat{\sigma}_2^2,$$

with

$$\hat{\sigma}_j^2 = (n_j - 1)^{-1} \left[\sum_{i=1}^{n_j} s_{j(i)}^2 - n_j^{-1} \left(\sum_{i=1}^{n_j} s_{j(i)} \right)^2 \right].$$

Heltshe (1988) shows that for the Jaccard coefficient

$$\bar{s}_{j(i)} = n_j^{-1} \sum_{\alpha=0}^{a+b+c} \sum_{\beta=0}^{a+b+c} \left(\frac{a - \alpha}{a + b + c - \beta} \right) f_{j\alpha\beta},$$

and

$$\hat{\sigma}_j^2 = (n_j - 1)^{-1} \left[\sum_{\alpha=0}^{a+b+c} \sum_{\beta=0}^{a+b+c} \left(\frac{a - \alpha}{a + b + c - \beta} \right) f_{j\alpha\beta} - n_j \bar{s}_j^2 \right].$$

Heltshe also gives the equivalent expressions for the simple matching coefficient.

Lim and Khoo (1985) considered sampling properties of Gower's general similarity coefficient for artificial communities. These communities were simulated in a rectangular region and random species abundance data generated. The proportion of individuals simulated that belong to species i was $\theta(1 - \theta)^{i-1}/(1 - \theta)^N$ $(i = 1, \ldots N)$, where $0 < \theta < 1$. So the first species is the most abundant, followed by the second, the third, etc., with N species in total. Let x_{ri} be the abundance of species i in the rth simulated community. Then the similarity between the rth and sth communities is measured by

$$s_{rs} = N^{-1} \sum_{i=1}^{N} (1 - |x_{ri} - x_{si}|/R_i),$$

where R_i is the range of the abundance data for the ith species.

Lim and Khoo study bias and variability of s_{rs} in this ecological setting. They show that s_{rs} has smallest bias when the true value of s_{rs} is close to 0.5 with bias increasing as the true value of s_{rs} approaches zero or unity. As expected, bias reduces as the sample size increases. The standard error of s_{rs} is largest when the true value of s_{rs} is close to 0.6.

1.3.4 Transforming from similarities to dissimilarities

Often similarity coefficients have to be transformed into dissimilarity coefficients. Possible transformations are

$$\delta_{rs} = 1 - s_{rs}$$
$$\delta_{rs} = c - s_{rs} \text{ for some constant } c$$
$$\delta_{rs} = \{2(1 - s_{rs})\}^{\frac{1}{2}}.$$

Choice will depend on the problem at hand.

1.3.5 The metric nature of dissimilarities

Gower and Legendre (1986) discuss in detail metric and Euclidean properties of many dissimilarity coefficients. A summary is given of some of the important results they establish or report on.

Let the dissimilarities $\{\delta_{rs}\}$ be placed in a matrix $\mathbf{D}$, the dissimilarity matrix. Similarly, let similarities $\{s_{rs}\}$ be placed in a similarity matrix $\mathbf{S}$. Then $\mathbf{D}$ is called metric if δ_{rs} is a metric. Matrix $\mathbf{D}$ is also Euclidean if n points can be embedded in a Euclidean space such that the Euclidean distance between the rth and sth points is δ_{rs}, for all $1 \leq r, s \leq n$.

If $\mathbf{D}$ is nonmetric then the matrix with elements $\delta_{rs} + c$ $(r \neq s)$ is metric where $c \geq \max_{i,j,k} |\delta_{ij} + \delta_{ik} - \delta_{jk}|$.

If $\mathbf{D}$ is metric then so are matrices with elements (i) $\delta_{rs} + c^2$ (ii) $\delta_{rs}^{1/\lambda}$ $(\lambda \geq 1)$ (iii) $\delta_{rs}/(\delta_{rs} + c^2)$ for any real constant c, and $r \neq s$.

Let matrix $\boldsymbol{\Lambda} = [-\frac{1}{2} d_{rs}^2]$.

Then $\mathbf{D}$ is Euclidean if and only if the matrix $(\mathbf{I} - \mathbf{1}\mathbf{s}^T)\boldsymbol{\Lambda}(\mathbf{I} - \mathbf{s}\mathbf{1}^T)$ is positive semi-definite, where $\mathbf{I}$ is the identity matrix, $\mathbf{1}$ is a vector of ones, and $\mathbf{s}$ is a vector such that $\mathbf{s}^T\mathbf{1} = 1$.

If $\mathbf{S}$ is a positive semi-definite similarity matrix with elements $0 \leq s_{rs} \leq 1$ and $s_{rr} = 1$, then the dissimilarity matrix with elements $d_{rs} = (1 - s_{rs})^{\frac{1}{2}}$ is Euclidean.

If $\mathbf{D}$ is a dissimilarity matrix, then there exists a constant h such that the matrix with elements $(\delta_{rs}^2 + h)^{\frac{1}{2}}$ is Euclidean, where $h \geq -\lambda_n$, the smallest eigenvalue of $\boldsymbol{\Lambda}_1 = \mathbf{H}\boldsymbol{\Lambda}\mathbf{H}$, $\mathbf{H}$ being the centring matrix $(\mathbf{I} - \mathbf{1}\mathbf{1}^T/n)$.

If $\mathbf{D}$ is a dissimilarity matrix, then there exists a constant k such that the matrix with elements $(\delta_{rs}+k)$ is Euclidean, where $k \geq \mu_n$, the largest eigenvalue of

$$\begin{bmatrix} \mathbf{0} & 2\boldsymbol{\Lambda}_1 \\ -\mathbf{I} & -4\boldsymbol{\Lambda}_2 \end{bmatrix}$$

where $\boldsymbol{\Lambda}_2 = [-\frac{1}{2}d_{rs}]$.

These last two theorems give solutions to the additive constant problem which is discussed further in Chapter 2.

For binary variables, Gower and Legendre define

$$S_\theta = \frac{a+d}{a+d+\theta(b+c)} \qquad T_\theta = \frac{a}{a+\theta(b+c)}.$$

Then for the appropriate choice of θ similarity coefficients in Table 1.2 can be obtained. Gower and Legendre show:

For $\theta \geq 1$, $1-S_\theta$ is metric; $\sqrt{1-S_\theta}$ is metric for $\theta \geq \frac{1}{3}$; if $\theta < 1$ then $1-S_\theta$ may be nonmetric; if $\theta < \frac{1}{3}$ then $\sqrt{1-S_\theta}$ may be nonmetric. There are similar results when S_θ is replaced by T_θ.

If $\sqrt{1-S_\theta}$ is Euclidean then so is $\sqrt{1-S_\phi}$ for $\phi \geq \theta$, with a similar result for T_θ.

For $\theta \geq 1$, $\sqrt{1-S_\theta}$ is Euclidean; for $\theta \geq \frac{1}{2}$, $\sqrt{1-T_\theta}$ is Euclidean. However $1-S_\theta$ and $1-T_\theta$ may be non-Euclidean.

Gower and Legendre give a table of various similarity/dissimilarity coefficients and use these results to establish which coefficients are metrics and which are also Euclidean. Further results can also be found in Fichet (1983), Gower (1985) and Caillez and Kuntz (1996)

1.3.6 Dissimilarity of variables

Sometimes it is not the objects that are to be subjected to multidimensional scaling, but the variables. One possibility for defining dissimilarities for variables is simply to reverse the roles of objects and variables and to proceed regardless, using one of the dissimilarity measures. Another possibility is to choose a dissimilarity more appropriate to variables than objects.

The sample correlation coefficient r_{ij} is often used as the basis for dissimilarity among variables. For instance $\delta_{ij} = 1 - r_{ij}$ could

be used. This measure has its critics. A similar dissimilarity can be based on the angular separation of the vectors of observations associated with the ith and jth variables,

$$\delta_{ij} = 1 - \frac{\sum_r x_{ri}x_{rj}}{(\sum_r x_{ri}^2 \sum_r x_{rj}^2)^{\frac{1}{2}}}.$$

Zegers and ten Berge (1985), Zegers (1986) and Fagot and Mazo (1989) consider general similarity coefficients for variables measured on different metric scales. The argument is that the similarity coefficient has to be invariant under admissible transformations of the variables. The scales considered are: the absolute scale where only the identity transformation is possible; the difference scale which is only invariant under additive transformations; the ratio scale which is only invariant under positive multiplicative transformations; and the interval scale which is invariant up to positive linear transformations. The variables are transformed to "uniformity" according to type:

$$u_{ri} = x_{ri} \quad \text{for the absolute scale}$$

$$u_{ri} = x_{ri} - \bar{x}_i \quad \text{for the difference scale}$$

$$u_{ri} = \left(\frac{1}{n}\sum_s x_{si}^2\right)^{-\frac{1}{2}} x_{ri} \quad \text{for the ratio scale}$$

$$u_{ri} = \left(\frac{1}{n-1}\sum_s (x_{si} - \bar{x}_i)^2\right)^{-\frac{1}{2}} (x_{ri} - \bar{x}_i) \quad \text{for the interval scale.}$$

Consider a general similarity coefficient, s_{ij}, based on the mean squared difference,

$$s_{ij} = 1 - cn^{-1}\sum_r (u_{ri} - u_{rj})^2,$$

where c is a constant. This is to have maximum value unity when $u_{ri} = u_{rj}$ $(1 \leq r \leq n)$. Hence c can be determined from the requirement that $s_{ij} = s_{ji}$, and then after some algebra

$$s_{ij} = \frac{2\sum_r u_{ri}u_{rj}}{(\sum_r u_{ri}^2 + \sum_r u_{rj}^2)}.$$

This can be a considered alternative to the haphazard use of the sample correlation coefficient.

1.3.7 Similarity measures on fuzzy sets

Fuzzy set theory has found several application areas. Klir and Folger (1988) describe its uses in such areas as meteorology, traffic control, aircraft control, medicine, management, expert systems and pattern recognition. Manton *et al.* (1994) discuss statistical theory and applications of fuzzy sets.

Without delving too deeply into fuzzy set theory, consider a universal set X. Let A be a subset of X, and suppose its membership is absolutely determined. To each element $x \in X$ assign the value 1 if $x \in A$ and the value 0 if $x \notin A$. The set A is known as a crisp set. Suppose it is not now certain as to whether x belongs to A or not. Then the 0/1 valued membership function for the crisp set can be replaced by a membership function μ_A, usually with range $[0, 1]$, that gives the "degree of membership" of x to A. The set A then becomes a fuzzy set.

Example
Let $X = R$, and $\mu_A(x) = \exp(-100x^2)$. Then A is a fuzzy set of numbers close to zero. The number zero has membership value unity. The number 0.1 has membership value 0.368.

For the purposes here, the universal set will be a set of objects O. Let O consist of n objects, $o_1, \ldots, o_n$, and let there be g sets (groups) $G_1, \ldots, G_g$. It is not known which objects belong to which groups, but suppose for each group there is a membership function $\mu_{G_i}(.)$. So $\mu_{G_i}(o_r)$ is the value of the membership for object o_r to be in group G_i. There have been various similarity measures proposed to measure the similarity between these fuzzy sets and also between the objects. Wang (1997) discusses some of these and suggests two of his own. Other references are Chen (1997), Fan and Xie (1999). The following are some of the similarity measures denoted by $s(G_i, G_j)$ where the notation μ_{G_i} is shortened to μ_i.

$$s(G_i, G_j) = \max_{o \in O} \min(\mu_i, \mu_j)$$

$$s(G_i, G_j) = \frac{C(G_i, G_j)}{\sqrt{T(G_i)T(G_j)}},$$

where

$$C(G_i, G_j) = \sum_{k=1}^{n} [\mu_i(o_k)\mu_j(o_k) + (1 - \mu_i(o_k))(1 - \mu_j(o_k))],$$

and

$$T(G_i) = \sum_{k=1}^{n} [\mu_i^2(o_k) + (1 - \mu_i(o_k))^2]$$

$$s(G_i, G_j) = \sum_{k=1}^{n} \min(\mu_i(o_k), \mu_j(o_k)) / \sum_{k=1}^{n} \max(\mu_i(o_k), \mu_j(o_k))$$

$$s(G_i, G_j) = 1 - \max_i(|\mu_i(o_k) - \mu_j(o_k)|)$$

$$s(G_i, G_j) = 1 - \sum_{k=1}^{n} |\mu_i(o_k) - \mu_j(o_k)| / \sum_{k=1}^{n} (\mu_i(o_k) + \mu_j(o_k))$$

$$s(G_i, G_j) = n^{-1} \sum_{k=1}^{n} \left[\frac{\min(\mu_i(o_k), \mu_j(o_k))}{\max(\mu_i(o_k), \mu_j(o_k))} \right]$$

$$s(G_i, G_j) = n^{-1} \sum_{k=1}^{n} [1 - |\mu_i(o_k) - \mu_j(o_k)|]$$

These last two measures were proposed by Wang (1997). He also proposed the following similarity measures between elements.

$$s(o_r, o_s) = g^{-1} \sum_{i=1}^{g} \left[\frac{\min(\mu_i(o_r), \mu_i(o_s))}{\max(\mu_i(o_r), \mu_i(o_s))} \right]$$

$$s(o_r, o_s) = g^{-1} \sum_{i=1}^{g} [1 - |\mu_i(o_r) - \mu_j(o_s)|]$$

1.4 Matrix results

A review of matrix algebra is not given here, as it is assumed that the reader is familiar with such. However, a brief reminder is given of the spectral decomposition of a symmetric matrix, the singular value decomposition of a rectangular matrix, and the Moore-Penrose inverse of a matrix. For outlines of matrix algebra relevant to statistics, see Mardia *et al.* (1979), Healy (1986) for example.

1.4.1 The spectral decomposition

Let $\mathbf{A}$ be an $n \times n$ symmetric matrix, with eigenvalues $\{\lambda_i\}$ and associated eigenvectors $\{\mathbf{v}_i\}$, such that $\mathbf{v}_i^T\mathbf{v}_i = 1 \quad (i = 1, \ldots, n)$. Then $\mathbf{A}$ can be written

$$\mathbf{A} = \mathbf{V}\boldsymbol{\Lambda}\mathbf{V}^T = \sum_{i=1}^{n} \lambda_i \mathbf{v}_i \mathbf{v}_i^T,$$

where

$$\boldsymbol{\Lambda} = \text{diag}(\lambda_1, \ldots, \lambda_n), \quad \mathbf{V} = [\mathbf{v}_1, \ldots, \mathbf{v}_n].$$

Matrix $\mathbf{V}$ is orthonormal, so that $\mathbf{V}\mathbf{V}^T = \mathbf{V}^T\mathbf{V} = \mathbf{I}$. Also if $\mathbf{A}$ is nonsingular

$$\mathbf{A}^m = \mathbf{V}\boldsymbol{\Lambda}^m\mathbf{V}^T$$

with $\boldsymbol{\Lambda}^m = \text{diag}(\lambda_1^m, \ldots, \lambda_n^m)$ for any integer m. If the eigenvalues $\{\lambda_i\}$ are all positive then rational powers of $\mathbf{A}$ can be defined in a similar way and in particular for powers $\frac{1}{2}$ and $-\frac{1}{2}$.

1.4.2 The singular value decomposition

If $\mathbf{A}$ is an $n \times p$ matrix of rank r, then $\mathbf{A}$ can be written as

$$\mathbf{A} = \mathbf{U}\boldsymbol{\Lambda}\mathbf{V}^T,$$

where $\boldsymbol{\Lambda} = \text{diag}(\lambda_1, \lambda_2, \ldots, \lambda_r)$, with $\lambda_1 \geq \lambda_2 \geq \ldots \geq \lambda_r \geq 0$, $\mathbf{U}$ is an orthonormal matrix of order $n \times r$, and $\mathbf{V}$ an orthonormal matrix of order $r \times r$, i.e. $\mathbf{U}^T\mathbf{U} = \mathbf{V}^T\mathbf{V} = \mathbf{I}$. The set of values $\{\lambda_i\}$ are called the singular values of $\mathbf{A}$. If $\mathbf{U}$ and $\mathbf{V}$ are written in terms of their column vectors, $\mathbf{U} = [\mathbf{u}_1, \ldots, \mathbf{u}_r]$, $\mathbf{V} = [\mathbf{v}_1, \ldots, \mathbf{v}_r]$, then $\{\mathbf{u}_i\}$ are the left singular vectors of $\mathbf{A}$ and $\{\mathbf{v}_i\}$ are the right singular vectors. The matrix $\mathbf{A}$ can then be written as

$$\mathbf{A} = \sum_{i=1}^{r} \lambda_i \mathbf{u}_i \mathbf{v}_i^T.$$

It can be shown that $\{\lambda_i^2\}$ are the nonzero eigenvalues of the symmetric matrix $\mathbf{A}\mathbf{A}^T$ and also of the matrix $\mathbf{A}^T\mathbf{A}$. The vectors $\{\mathbf{u}_i\}$ are the corresponding normalized eigenvectors of $\mathbf{A}\mathbf{A}^T$, and the vectors $\{\mathbf{v}_i\}$ are the corresponding normalized eigenvectors of $\mathbf{A}^T\mathbf{A}$.

An example
As an example let

$$\mathbf{A} = \begin{bmatrix} 5 & 2 & 9 \\ 0 & 1 & 2 \\ 2 & 1 & 4 \\ -4 & 3 & 2 \end{bmatrix}.$$

Then the SVD $\mathbf{A}$ is

$$\mathbf{A} = \begin{bmatrix} 0.901 & 0.098 \\ 0.169 & -0.195 \\ 0.394 & 0.000 \\ 0.056 & -0.980 \end{bmatrix} \begin{bmatrix} 11.619 & 0 \\ 0 & 5.477 \end{bmatrix} \times \begin{bmatrix} 0.436 & 0.218 & 0.873 \\ 0.802 & -0.535 & -0.267 \end{bmatrix}$$

or equivalently

$$\mathbf{A} = 11.619 \begin{bmatrix} 0.393 & 0.196 & 0.787 \\ 0.074 & 0.037 & 0.148 \\ 0.172 & 0.086 & 0.344 \\ 0.024 & 0.012 & 0.049 \end{bmatrix} + 5.477 \begin{bmatrix} 0.079 & -0.052 & -0.026 \\ -0.156 & 0.104 & 0.052 \\ 0.000 & 0.000 & 0.000 \\ -0.786 & 0.524 & 0.262 \end{bmatrix}$$

If there are no multiplicities within the singular values then the SVD is unique. If k of the singular values are equal, then the SVD is unique only up to arbitrary rotations in the subspaces spanned by the corresponding left and right singular vectors. Greenacre (1984) gives a good review of the SVD of a matrix and its use in statistical applications.

The usefulness of the SVD of a matrix is that it can be used to approximate matrix $\mathbf{A}$ of rank r by matrix

$$\tilde{\mathbf{A}}_{r^\star} = \sum_{i=1}^{r^\star} \lambda_i \mathbf{u}_i \mathbf{v}_i^T$$

which is of rank $r^\star < r$. The approximation is, in fact, the least squares approximation of $\mathbf{A}$ found by minimising

$$\sum_i \sum_j (a_{ij} - x_{ij})^2 = \mathrm{tr}\{(\mathbf{A} - \mathbf{X})(\mathbf{A} - \mathbf{X}^T)\},$$

for all matrices $\mathbf{X}$ of rank $r^\star$ or less. This is a classical result originating from Eckart and Young (1936).

For example, with $r^\star = 1$, $\mathbf{A}$ above is approximated by

$$\tilde{\mathbf{A}}_1 = \begin{bmatrix} 4.56 & 2.28 & 9.14 \\ 0.86 & 0.42 & 1.71 \\ 2.00 & 1.00 & 4.00 \\ 0.28 & 0.14 & 0.57 \end{bmatrix}$$

and noting that the second and third columns of $\tilde{\mathbf{A}}_1$ are simply multiples of the first column. This is, of course, expected since $\tilde{\mathbf{A}}_1$ is of rank one. If $\mathbf{A}$ is viewed as a matrix representing four points in a three dimensional space, it is noted that only two dimensions are in fact needed to represent the points since $\mathbf{A}$ has rank 2. A one dimensional space approximating to the original configuration is given by $\tilde{\mathbf{A}}_1$ giving an ordering of the points as 4,2,3,1.

Note that the singular value decomposition can be defined so that $\mathbf{U}$ is an $n \times n$ matrix, $\boldsymbol{\Lambda}$ is an $n \times p$ matrix and $\mathbf{V}$ is a $p \times p$ matrix. These matrices are the same as those just defined but contain extra rows/columns of zeros.

Generalized SVD

Suppose now weighted Euclidean distances are used in the spaces spanning the columns and rows of $\mathbf{A}$. Then the generalized SVD of matrix $\mathbf{A}$ is given by

$$\mathbf{A} = \mathbf{U}\boldsymbol{\Lambda}\mathbf{V}^T,$$

where $\boldsymbol{\Lambda} = \text{diag}(\lambda_1, \lambda_2, \ldots, \lambda_r)$, with $\lambda_1 \geq \lambda_2 \geq \ldots \geq \lambda_r \geq 0$, are the generalized singular values of $\mathbf{A}$, $\mathbf{U}$ is an $n \times r$ matrix, orthonormal with respect to $\boldsymbol{\Omega}$,and $\mathbf{V}$ is a $p \times r$ matrix orthonormal with respect to $\boldsymbol{\Phi}$, i.e. $\mathbf{U}^T\boldsymbol{\Omega}\mathbf{U} = \mathbf{V}^T\boldsymbol{\Phi}\mathbf{V} = \mathbf{I}$.

Let $\mathbf{U} = [\mathbf{r}_1, \ldots, \mathbf{r}_n]$ and $\mathbf{V} = [\mathbf{c}_1, \ldots, \mathbf{c}_p]$. The approximation of $\mathbf{A}$ by a lower rank matrix $\tilde{\mathbf{A}}_{r^\star}$ is given by

$$\tilde{\mathbf{A}}_{r^\star} = \sum_{i=1}^{r^\star} \lambda_i \mathbf{u}_i \mathbf{v}_i^T$$

where $\tilde{\mathbf{A}}_{r^\star}$ is the matrix that minimises

$$\text{tr}\{\boldsymbol{\Omega}(\mathbf{A} - \mathbf{X})\boldsymbol{\Phi}(\mathbf{A} - \mathbf{X})^T\}$$

over all matrices $\mathbf{X}$ of rank $r^\star$ or less.

1.4.3 The Moore-Penrose inverse

Consider the matrix equation

$$\mathbf{AX} = \mathbf{B}$$

where $\mathbf{A}$ is an $n \times p$ matrix, $\mathbf{X}$ is a $p \times n$ matrix and $\mathbf{B}$ is an $n \times n$ matrix. The matrix $\mathbf{x}$ which minimises the sum of squares $\mathrm{tr}(\mathbf{AX} - \mathbf{B})^T(\mathbf{AX} - \mathbf{B})$ and itself has the smallest value of $\mathrm{tr}\mathbf{X}^T\mathbf{X}$ among all least squares solutions is given by

$$\mathbf{X} = \mathbf{A}^+\mathbf{B},$$

where $\mathbf{A}^+$ is the unique $p \times n$ Moore-Penrose generalized inverse of $\mathbf{A}$, defined by the equations

$$\begin{aligned}
\mathbf{AA}^+\mathbf{A} &= \mathbf{A} \\
\mathbf{A}^+\mathbf{AA}^+ &= \mathbf{A}^+ \\
(\mathbf{AA}^+)^\star &= \mathbf{AA}^+ \\
(\mathbf{A}^+\mathbf{A})^\star &= \mathbf{A}^+\mathbf{A},
\end{aligned}$$

$\mathbf{A}^\star$ being the conjugate transpose of $\mathbf{A}$. As only real matrices are used in this book "$\star$" can be replaced by "T" the usual matrix transpose. For further details see Barnett (1990) for example.

CHAPTER 2

Metric multidimensional scaling

2.1 Introduction

Suppose there are n objects with dissimilarities $\{\delta_{rs}\}$. Metric MDS attempts to find a set of points in a œspace where each point represents one of the objects and the distances between points $\{d_{rs}\}$ are such that

$$d_{rs} \approx f(\delta_{rs}),$$

where f is a continuous parametric monotonic function. The function f can either be the identity function or a function that attempts to transform the dissimilarities to a distance-like form.

Mathematically, let the objects comprise a set O. Let the dissimilarity, defined on $\mathrm{O} \times \mathrm{O}$, between objects r and s be δ_{rs} $(r, s \in \mathrm{O})$. Let ϕ be an arbitrary mapping from O to E, where E is usually a Euclidean space, but not necessarily so, in which a set of points are to represent the objects. Thus let $\phi(r) = x_r \quad (r \in \mathrm{O},\ x_r \in \mathrm{E})$, and let $\mathrm{X} = \{x_r : r \in \mathrm{O}\}$, the image set. Let the distance between the points x_r, x_s in X be given by d_{rs}. The aim is to find a mapping ϕ, for which d_{rs} is approximately equal to $f(\delta_{rs})$ for all $r, s \in \mathrm{O}$.

The two main metric MDS methods, classical scaling and least squares scaling, will be considered in this chapter, with most emphasis placed on the former.

2.2 Classical scaling

Classical scaling originated in the 1930s when Young and Householder (1938) showed how starting with a matrix of distances between points in a Euclidean space, coordinates for the points can be found such that distances are preserved. Torgerson (1952) brought the subject to popularity using the technique for scaling.

2.2.1 Recovery of coordinates

Chapter 1 saw an application of classical scaling where a map of British cities was constructed from journey times by road between the cities. Suppose the starting point for the procedure had been the actual Euclidean distances between the various cities (making the assumption that Great Britain is a two dimensional Euclidean plane). Can the original positions of the cities be found? They can, but only relative to each other since any solution can be translated, rotated and reflected, giving rise to another equally valid solution. The method for finding the original Euclidean coordinates from the derived Euclidean distances was first given by Schoenberg (1935) and Young and Householder (1938). It is as follows.

Let the coordinates of n points in a p dimensional Euclidean space be given by $\mathbf{x}_r$ $(r = 1, \ \ldots \ , n)$, where $\mathbf{x}_r = (x_{r1}, \ldots, x_{rp})^T$. Then the Euclidean distance between the rth and sth points is given by

$$d_{rs}^2 = (\mathbf{x}_r - \mathbf{x}_s)^T(\mathbf{x}_r - \mathbf{x}_s). \tag{2.1}$$

Let the inner product matrix be $\mathbf{B}$, where

$$[\mathbf{B}]_{rs} = b_{rs} = \mathbf{x}_r^T\mathbf{x}_s.$$

From the known squared distances $\{d_{rs}\}$, this inner product matrix $\mathbf{B}$ is found, and then from $\mathbf{B}$ the unknown coordinates.

To find $\mathbf{B}$

Firstly, to overcome the indeterminancy of the solution due to arbitrary translation, the centroid of the configuration of points is placed at the origin. Hence

$$\sum_{r=1}^{n} x_{ri} = 0 \qquad (i = 1, \ldots, p).$$

To find $\mathbf{B}$, from (2.1)

$$d_{rs}^2 = \mathbf{x}_r^T\mathbf{x}_r + \mathbf{x}_s^T\mathbf{x}_s - 2\mathbf{x}_r^T\mathbf{x}_s, \tag{2.2}$$

and hence

$$\frac{1}{n}\sum_{r=1}^{n} d_{rs}^2 = \frac{1}{n}\sum_{r=1}^{n} \mathbf{x}_r^T\mathbf{x}_r + \mathbf{x}_s^T\mathbf{x}_s,$$

$$\frac{1}{n}\sum_{s=1}^{n} d_{rs}^2 = \mathbf{x}_r^T\mathbf{x}_r + \frac{1}{n}\sum_{s=1}^{n} \mathbf{x}_s^T\mathbf{x}_s,$$

$$\frac{1}{n^2}\sum_{r=1}^{n}\sum_{s=1}^{n} d_{rs}^2 = \frac{2}{n}\sum_{r=1}^{n} \mathbf{x}_r^T\mathbf{x}_r. \tag{2.3}$$

Substituting into (2.2) gives

$$\begin{aligned} b_{rs} &= \mathbf{x}_r^T\mathbf{x}_s, \\ &= -\frac{1}{2}\left(d_{rs}^2 - \frac{1}{n}\sum_{r=1}^{n} d_{rs}^2 - \frac{1}{n}\sum_{s=1}^{n} d_{rs}^2 + \frac{1}{n^2}\sum_{r=1}^{n}\sum_{s=1}^{n} d_{rs}^2\right), \\ &= a_{rs} - a_{r.} - a_{.s} + a_{..}, \end{aligned} \tag{2.4}$$

where $a_{rs} = -\frac{1}{2}d_{rs}^2$, and

$$a_{r.} = n^{-1}\sum_{s} a_{rs}, \quad a_{.s} = n^{-1}\sum_{r} a_{rs}, \quad a_{..} = n^{-2}\sum_{r}\sum_{s} a_{rs}.$$

Define matrix $\mathbf{A}$ as $[\mathbf{A}]_{rs} = a_{rs}$, and hence the inner product matrix $\mathbf{B}$ is

$$\mathbf{B} = \mathbf{HAH} \tag{2.5}$$

where $\mathbf{H}$ is the centring matrix,

$$\mathbf{H} = \mathbf{I} - n^{-1}\mathbf{1}\mathbf{1}^T,$$

with $\mathbf{1} = (1, 1, \ldots, 1)^T$, a vector of n ones.

To recover the coordinates from $\mathbf{B}$
The inner product matrix, $\mathbf{B}$, can be expressed as

$$\mathbf{B} = \mathbf{X}\mathbf{X}^T,$$

where $\mathbf{X} = [\mathbf{x}_1, \ldots, \mathbf{x}_n]^T$ is the $n \times p$ matrix of coordinates. The rank of $\mathbf{B}$, $r(\mathbf{B})$, is then

$$r(\mathbf{B}) = r(\mathbf{X}\mathbf{X}^T) = r(\mathbf{X}) = p.$$

Now $\mathbf{B}$ is symmetric, positive semi-definite and of rank p, and hence has p non-negative eigenvalues and $n - p$ zero eigenvalues.

Matrix $\mathbf{B}$ is now written in terms of its spectral decomposition,

$$\mathbf{B} = \mathbf{V}\boldsymbol{\Lambda}\mathbf{V}^T,$$

where $\boldsymbol{\Lambda} = \text{diag}(\lambda_1, \lambda_2, \ldots, \lambda_n)$, the diagonal matrix of eigenvalues $\{\lambda_i\}$ of $\mathbf{B}$, and $\mathbf{V} = [\mathbf{v}_1, \ \ldots, \mathbf{v}_n]$, the matrix of corresponding eigenvectors, normalized such that $\mathbf{v}_i^T\mathbf{v}_i = 1$. For convenience the eigenvalues of $\mathbf{B}$ are labelled such that $\lambda_1 \geq \lambda_2 \geq \ \ldots \geq \lambda_n \geq 0$.

Because of the $n - p$ zero eigenvalues, $\mathbf{B}$ can now be rewritten as

$$\mathbf{B} = \mathbf{V}_1\boldsymbol{\Lambda}_1\mathbf{V}_1^T,$$

where

$$\boldsymbol{\Lambda}_1 = \text{diag}(\lambda_1, \ldots, \lambda_p), \qquad \mathbf{V}_1 = [\mathbf{v}_1, \ldots, \mathbf{v}_p].$$

Hence as $\mathbf{B} = \mathbf{X}\mathbf{X}^T$, the coordinate matrix $\mathbf{X}$ is given by

$$\mathbf{X} = \mathbf{V}_1\boldsymbol{\Lambda}_1^{\frac{1}{2}},$$

where $\boldsymbol{\Lambda}_1^{\frac{1}{2}} = \text{diag}(\lambda_1^{\frac{1}{2}}, \ldots, \lambda_p^{\frac{1}{2}})$, and thus the coordinates of the points have been recovered from the distances between the points. The arbitrary sign of the eigenvectors $\{\mathbf{v}_i\}$ leads to invariance of the solution with respect to reflection in the origin.

2.2.2 Dissimilarities as Euclidean distances

To be of practical use, a configuration of points needs to be found for a set of dissimilarities $\{\delta_{rs}\}$ rather than simply for true Euclidean distances between points $\{d_{rs}\}$.

Suppose dissimilarities $\{\delta_{rs}\}$ are used instead of distances d_{rs} to define matrix $\mathbf{A}$, which is then doubly centred to produce matrix $\mathbf{B}$ as just described. Then it is interesting to ask under what circumstances $\mathbf{B}$ can give rise to a configuration of points in Euclidean space, using the spectral decomposition, so that the associated distances $\{d_{rs}\}$ are such that $d_{rs} = \delta_{rs}$ for all r, s. The answer is that if $\mathbf{B}$ is positive semi-definite of rank p, then a configuration in p dimensional Euclidean space can be found. Proofs are presented in de Leeuw and Heiser (1982) and Mardia *et al.* (1979).

Following Mardia *et al.*, if $\mathbf{B}$ is positive semi-definite of rank p, then

$$\mathbf{B} = \mathbf{V}\boldsymbol{\Lambda}\mathbf{V}^T = \mathbf{X}\mathbf{X}^T,$$

where

$$\boldsymbol{\Lambda} = \text{diag}(\lambda_1, \ldots, \lambda_p), \qquad \mathbf{X} = [\mathbf{x}_r]^T, \qquad \mathbf{x}_r = \lambda^{\frac{1}{2}}\mathbf{v}_r.$$

Now the distance between the rth and sth points of the configuration is given by $(\mathbf{x}_r - \mathbf{x}_s)^T(\mathbf{x}_r - \mathbf{x}_s)$, and hence

$$\begin{aligned}(\mathbf{x}_r - \mathbf{x}_s)^T(\mathbf{x}_r - \mathbf{x}_s) &= \mathbf{x}_r^T\mathbf{x}_r + \mathbf{x}_s^T\mathbf{x}_s - 2\mathbf{x}_r^T\mathbf{x}_s \\ &= b_{rr} + b_{ss} - 2b_{rs} \\ &= a_{rr} + a_{ss} - 2a_{rs} \\ &= -2a_{rs} = \delta_{rs}^2,\end{aligned}$$

by substituting for b_{rs} using equation (2.4). Thus the distance between the rth and sth points in the Euclidean space is equal to the original dissimilarity δ_{rs}.

Incidently the converse is also true that if $\mathbf{B}$ is formed from Euclidean distances then it is positive semi-definite. For when $d_{rs}^2 = (\mathbf{x}_r - \mathbf{x}_s)^T(\mathbf{x}_r - \mathbf{x}_s)$ is substituted into equation (2.4) then

$$b_{rs} = (\mathbf{x}_r - \hat{\mathbf{x}})^T(\mathbf{x}_s - \hat{\mathbf{x}})$$

where $\hat{\mathbf{x}} = n^{-1}\sum_r \mathbf{x}_r$. Hence

$$\mathbf{B} = (\mathbf{HX})(\mathbf{HX})^T$$

which implies that $\mathbf{B}$ is positive semi-definite.

The next question to be asked is how many dimensions are required in general for the configuration of points produced from a positive semi-definite matrix $\mathbf{B}$ of dissimilarities. It is easily shown that $\mathbf{B}$ has at least one zero eigenvalue, since $\mathbf{B1} = \mathbf{HAH1} = \mathbf{0}$. Thus a configuration of points in an $n-1$ dimensional Euclidean space can always be found whose associated distances are equal to the dissimilarities $\{\delta_{rs}\}$.

If the dissimilarities give rise to a matrix $\mathbf{B}$ which is not positive semi-definite, a constant can be added to all the dissimilarities (except the self-dissimilarities δ_{rr}) which will then make $\mathbf{B}$ positive semi-definite. Thus forming new dissimilarities, $\{\delta'_{rs}\}$ as $\delta'_{rs} = \delta_{rs} + c(1 - \delta^{rs})$, where c is an appropriate constant and δ^{rs} the Kronecker delta ($\delta^{rs} = 1$ if $r = s$ and zero otherwise; not to be confused with δ_{rs}), will make $\mathbf{B}$ positive semi-definite. This is the additive constant problem, see for example Cailliez (1983), which will be explored further in Section 2.2.8. Once $\mathbf{B}$ has been made positive semi-definite, a Euclidean space can be found as before where distances d_{rs} are exactly equal to dissimilaties δ'_{rs}.

2.2.3 Classical scaling in practice

It was shown in the previous section that a Euclidean space of, at most, $n-1$ dimensions could be found so that distances in the space equalled original dissimilarities, which were perhaps modified by the addition of a constant. Usually matrix $\mathbf{B}$ used in the procedure will be of rank $n-1$ and so the full $n-1$ dimensions are needed in the space, and hence little has been gained in dimension reduction of the data.

The configuration obtained could be rotated to its principal axes in the principal components sense; i.e. the projections of the points in the configuration onto the first principal axis have maximum variation possible, the projection of the points onto the second principle axis have maximum variation possible, but subject to this second axis being orthogonal to the first axis, etc.. Then only the first p, $(p < n-1)$ axes are chosen for representing the configuration. However this need not be undertaken since the procedure for finding $\mathbf{X}$ already has the points referred to their principal axes. This is easily seen since in searching for the principal axes,

$$\begin{aligned}\mathbf{X}^T\mathbf{X} &= (\mathbf{V}_1\boldsymbol{\Lambda}_1^{\frac{1}{2}})^T(\mathbf{V}_1\boldsymbol{\Lambda}_1^{\frac{1}{2}}) \\ &= \boldsymbol{\Lambda}^{\frac{1}{2}}\mathbf{V}_1^T\mathbf{V}_1\boldsymbol{\Lambda}^{\frac{1}{2}} = \boldsymbol{\Lambda},\end{aligned}$$

and $\boldsymbol{\Lambda}$ is a diagonal matrix.

Gower (1966) was the first to state clearly the formulation and the importance of the classical scaling technique, and from this selection of the first p "principal coordinates" for the configuration he coined the name "principal coordinates analysis" (PCO). Principal coordinates analysis is now synonymous with classical scaling, as also is the term metric scaling. However metric scaling encompasses more than this one technique.

Thus in the spectral decomposition of the matrix $\mathbf{B}$, the distances between the points in the $n-1$ dimensional Euclidean space are given by

$$d_{rs}^2 = \sum_{i=1}^{n-1} \lambda_i (x_{ri} - x_{si})^2,$$

and hence, if many of the eigenvalues are "small", then their contribution to the squared distance d_{rs}^2 can be neglected. If only p eigenvalues are retained as being significantly large, then the p dimensional Euclidean space formed for the first p eigenvalues and

with $\mathbf{x}_r$ truncated to the first p elements can be used to represent the objects. Hopefully, p will be small, preferably 2 or 3, for ease of graphical representation.

The selection of these first p principal coordinates is optimal in the following sense when $\{d_{rs}\}$ are Euclidean. If $\mathbf{x}_r^*$ is a projection of $\mathbf{x}_r$ onto a p' dimensional space with $p' \leq p$ and with associated distances between points $\{d_{rs}^*\}$, then it is precisely the projection given by using the first p' principal coordinates that minimises

$$\sum\sum(d_{rs}^2 - d_{rs}^{*2}).$$

For the non-Euclidean case, the above does not hold, but Mardia (1978) has given the following optimal property. For the matrix $\mathbf{B} = \mathbf{HAH}$ a positive semi-definite matrix $\mathbf{B}^* = [b_{rs}]$ of rank at most t is sought such that

$$\sum\sum(b_{rs} - b_{rs}^*)^2 = \text{tr}(\mathbf{B} - \mathbf{B}^*)^2 \tag{2.6}$$

is a minimum.

Let $\lambda_1^* \geq \ldots \geq \lambda_n^*$ be the eigenvalues of $\mathbf{B}^*$ and so at least $n - t$ of these must be zero, due to the rank constraint. Then it can be shown that

$$\min \text{tr}(\mathbf{B} - \mathbf{B}^*)^2 = \min \sum_{k=1}^{n}(\lambda_k - \lambda_k^*)^2.$$

For the minimum

$$\begin{aligned} \lambda_k^* &= \max(\lambda_k, 0) \qquad k = 1, \ldots, t \\ &= 0 \qquad k = t+1, \ldots, n. \end{aligned}$$

So if $\mathbf{B}$ has t or more positive eigenvalues then the first t principal coordinates derived from $\mathbf{B}$ are used for the projection. If $\mathbf{B}$ has fewer than t positive eigenvalues then the space of dimension less than t defined by the positive eigenvalues of $\mathbf{B}$ is used.

Hence, in practice, if it is found that $\mathbf{B}$ is not positive semi-definite (simply by noting whether there are any negative eigenvalues) then there is a choice of procedure. Either the dissimilarites are modified by adding an appropriate constant, or the negative eigenvalues are simply ignored. If the negative eigenvalues are small in magnitude then little is lost. If they are large then some argue that classical scaling is still appropriate as an exploratory data technique for dimension reduction.

2.2.4 How many dimensions?

As indicated previously, the eigenvalues $\{\lambda_i\}$ indicate how many dimensions are required for representing the dissimilarities $\{\delta_{rs}\}$. If $\mathbf{B}$ is positive semi-definite then the number of non-zero eigenvalues gives the number of dimensions required. If $\mathbf{B}$ is not positive semi-definite then the number of positive eigenvalues is the appropriate number of dimensions. These are the maximum dimensions of the space required. However, to be of practical value, the number of dimensions of the chosen space needs to be small. Since the coordinates recovered by the procedure are referred to their principal coordinates, then simply choosing the first p eigenvalues and eigenvectors of $\mathbf{B}$ ($p = 2$ or 3 say) will give a small dimensional space for the points.

The sum of squared distances between points in the full space is from (2.3)

$$\frac{1}{2}\sum_{r=1}^{n}\sum_{s=1}^{n} d_{rs}^2 = n\sum_{r=1}^{n}\mathbf{x}_r^T\mathbf{x}_r = n\mathrm{tr}\mathbf{B} = n\sum_{r=1}^{n-1}\lambda_i.$$

A measure of the proportion of variation explained by using only p dimensions is

$$\frac{\sum_{i=1}^{p}\lambda_i}{\sum_{i=1}^{n-1}\lambda_i}.$$

If $\mathbf{B}$ is not positive semi-definite this measure is modified to

$$\frac{\sum_{i=1}^{p}\lambda_i}{\sum_{i=1}^{n-1}|\lambda_i|} \quad \text{or} \quad \frac{\sum_{i=1}^{p}\lambda_i}{\sum(\text{positive eigenvalues})}.$$

Choice of p can then be assessed with this measure.

2.2.5 A practical algorithm for classical scaling

Although the various steps in the algorithm for classical scaling can be gleaned from the text in the previous sections, it is summarised here.

1. Obtain dissimilarities $\{\delta_{rs}\}$.
2. Find matrix $\mathbf{A} = [-\frac{1}{2}\delta_{rs}^2]$.
3. Find matrix $\mathbf{B} = [a_{rs} - a_{r.} - a_{.s} + a_{..}]$.
4. Find the eigenvalues $\lambda_1, \ldots, \lambda_{n-1}$ and associated eigenvectors $\mathbf{v}_1, \ldots, \mathbf{v}_{n-1}$, where the eigenvectors are normalized so that

$\mathbf{v}_i^T \mathbf{v}_i = \lambda_i$. If B is not positive semi-definite (some of the eigenvalues are negative), either (i) ignore the negative values and proceed, or (ii) add an appropriate constant c to the dissimilarities, $\delta'_{rs} = \delta_{rs} + c(1 - \delta^{rs})$ (see Section 2.2.8) and return to step 2.

5. Choose an appropriate number of dimensions p. Possibly use $\sum_1^p \lambda_i / \sum$ (positive eigenvalues) for this.
6. The coordinates of the n points in the p dimensional Euclidean space are given by $x_{ri} = v_{ir}$ $(r = 1, \ldots, n;\ i = 1, \ldots, p)$.

2.2.6 A grave example

There is a fascinating paper in the very first volume of *Biometrika*, published in 1901-1902, concerning cranial measurements on an ancient race of people from Egypt. The paper is by Cicely Fawcett (1901) who was assisted by Alice Lee and others, including the legendary K. Pearson and G.U. Yule. The paper is sixty pages long and gives an insight into the problems faced by statisticians of the time who had no access to modern computing facilities or advanced statistical methods.

Till that time, little statistical work had been done for, or by, craniologists on skull measurements, although several data sets had been collected. Karl Pearson had asked Professor Flinders Petrie to try to obtain one hundred skulls from a homogeneous race when he embarked on his Egyptian expedition in 1894. Professor Petrie managed to get four hundred skulls, together with their skeletons, sent back to University College in London. These were taken from cemeteries of the Naqada race in Upper Egypt, and were dated at about 8000 years old. Karl Pearson was credited as the first person to calculate correlations for length and breadth in skulls, studying modern German, modern French and the Naqada crania. The second study of the Naqada crania was started in 1895 by Karl Pearson's team, and the time taken to carry out extensive hand calculation of means, standard deviations, correlations, skewness, kurtosis, and probability density fitting, delayed publication until 1901-1902.

The Fawcett paper details the method of measuring the skulls, for which various measuring devices had been deployed, such as a craniometer, a goniometer and a Spengler's pointer. In all, forty-eight measurements and indices were taken and and were published at the end of the paper. The statistical analyses used on the data

Table 2.1 *The first five leading eigenvalues and eigenvectors of* **B** *giving principal coordinates of the skull data.*

Eigenvalue	Eigenvector
$\lambda_1 = 11.47$	(-1.16, -0.19, -0.07, 0.56, 1.01, -0.49, -0.71, -0.82, -0.42, -0.15, 0.26, -0.30, 0.40, -1.13, 0.02, -0.88, 0.45, 0.00, 0.11, -0.53, 0.79, -0.32, 0.37, -0.08, 0.09, 1.00, -0.41, 0.09, 0.47, 0.00, -0.01, -0.08, 0.60, 0.05, 0.60, 0.45, -0.23, -0.07, -0.24, 0.98)
$\lambda_2 = 4.98$	(0.11, -0.42, 0.21, -0.79, -0.14, -0.70, -0.26, -0.32, -0.03, -0.14, 0.00, 0.24, 0.14, 0.27, -0.64, 0.47, -0.51, -0.07, 0.36, -0.36, 0.31, 0.05, 0.28, -0.04, 0.38, -0.40, -0.33, 0.83, -0.19, -0.12, -0.01, -0.03, 0.26, 0.20, 0.22, 0.55, 0.16, 0.37, 0.40, 0.07)
$\lambda_3 = 4.56$	(-0.12, 0.15, -0.61, -0.10, -0.31, -0.07, -0.21, 0.33, -0.68, -0.01, 0.36, 0.56, -0.26, 0.07, -0.30, -0.16, -0.08, -0.02, -0.18, -0.30, -0.50, -0.69, -0.07, 0.06, 0.65, 0.34, 0.36, -0.25, 0.64, 0.49, 0.18, 0.30, -0.09, -0.02, 0.26, -0.20, 0.27, 0.45, -0.05, -0.19)
$\lambda_4 = 2.55$	(0.16, 0.04, -0.12, -0.12, 0.24, 0.15, 0.04, 0.20, 0.25, -0.16, -0.33, 0.39, 0.48, -0.20, -0.36, -0.07, 0.22, 0.53, -0.18, 0.02, 0.29, -0.55, 0.35, -0.15, -0.32, -0.19, 0.14, 0.10, 0.09, -0.27, 0.24, -0.05, 0.12, -0.09, 0.02, -0.15, -0.24, 0.17, -0.29, -0.44)
$\lambda_5 = 1.73$	(-0.03, -0.09, 0.23, 0.13, 0.07, -0.29, -0.11, 0.43, -0.08, -0.16, -0.04, -0.32, -0.18, 0.19, -0.37, -0.26, 0.32, 0.12, 0.17, 0.24, -0.20, -0.14, 0.11, 0.42, 0.15, -0.20, 0.05, 0.16, 0.06, 0.04, -0.25, -0.22, 0.40, 0.16, -0.25, -0.10, 0.09, -0.13, -0.10, 0.01)

would be classified as basic by modern standards, with means, standard deviations, correlations, etc. being compared in tables. Of course, no use could be made of hypothesis tests, confidence intervals, let alone multivariate methods such as cluster analysis, principal components or discriminant analysis.

The results obtained by Karl Pearson's team will not be generally discussed here, since they are rather long and of interest mainly to craniologists. However, to concentrate on one point, the team said it found it impossible to give diagrams of the forty-seven

variables, separated by sex. They chose twelve of these variables and constructed twenty-four histograms and fitted density functions, all calculated and plotted at considerable cost of time. The variables were: (i) greatest length, L; (ii) breadth, B; (iii) height, H; (iv) auricular height, OH; (v) circumference above the superciliary ridges, U; (vi) sagittal circumference, S; (vii) cross-circumference, Q; (viii) upper face height, G′H; (ix) nasal breadth, NB; (x) nasal height, NH; (xi) cephalic index, B/L; (xii) ratio of height to length, H/L. These twelve variables will be used for an analysis for 22 male and 18 female skulls. For clarity only a subset of the skulls were chosen and those used had no missing values.

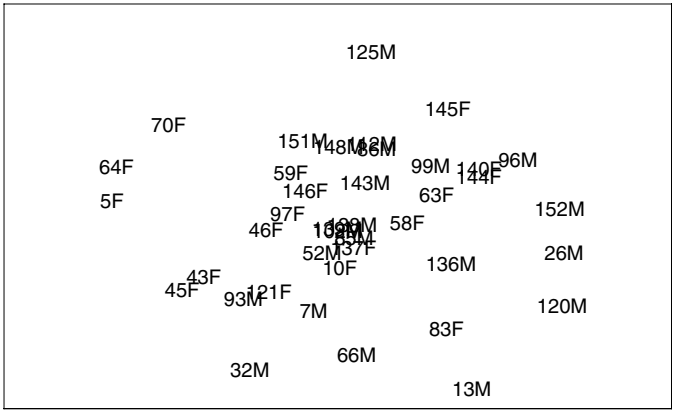

Figure 2.1(i) *Classical scaling of the skull data*

The twelve variables were standardized to have zero mean and standard deviation unity. Then dissimilarities between skulls were calculated using Euclidean distance and subjected to classical scaling.

Table 2.1 gives the five leading eigenvalues of $\mathbf{B}$ together with their associated eigenvectors. These are the first five principal coordinates. A two dimensional configuration is obtained by using the first two of these and is shown in Figure 2.1 (i) where male and female skulls are marked M and F respectively. For clarity, the points for males and females are plotted separately in Figures 2.1 (ii) and 2.1 (iii).

(ii)

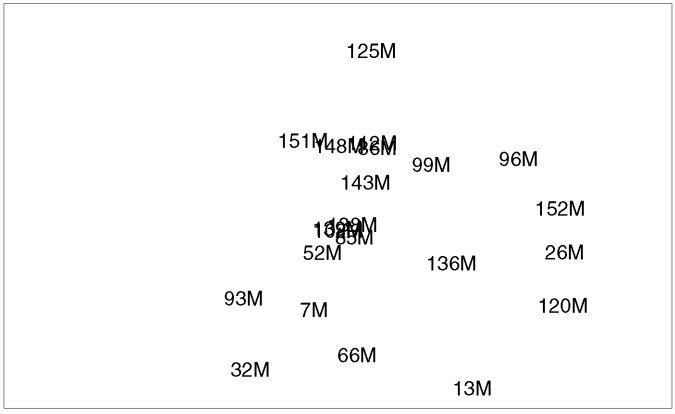

(iii)

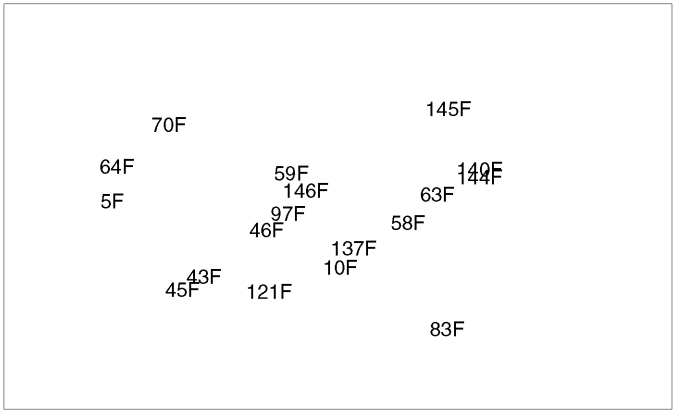

Figures 2.1(ii) and (iii) *Males and females plotted separately*

The most striking features are that the males tend towards the right of the plot and the females towards the left. The males {99M, 96M, 152M, 26M, 120M, 136M, 66M, 13M} towards the far right tended to have larger mean values for the twelve variables than the rest of the males. The three females {70F, 64F, 5F} to the extreme left of the configuration have mean values much less than those for

the other females. Size of skull seems to be the main interpretation horizontally across the configuration.

As a guide to the number of dimensions required for the configuration, the proportion of the variation ($\sum_{i=1}^{p} \lambda_i / \sum_{i=1}^{n} \lambda_i$) explained is 42%, 61%, 78%, 87% and 93% for 1, 2, 3, 4 and 5 dimensional spaces respectively. A three dimensional plot would have been somewhat superior to the two dimensional one shown.

Of course the classical scaling analysis is not the only analysis that could be done on these data. Cluster analysis, discriminant analysis and principal components analysis are all good candidates for such. A principal components analysis could have been carried out on the data – but the resulting configuration of skulls plotted on the first principal component against the second would have been exactly the same as that in Figure 2.1. This is because there is an equivalence between principal components analysis and classical scaling when dissimilarities for classical scaling are chosen to be Euclidean distances. This is explored further in the next section.

2.2.7 Classical scaling and principal components

Suppose $\mathbf{X}$ is a data matrix of dimension $n \times p$. The sample covariance matrix obtained from $\mathbf{X}$ is $\mathbf{S} = (n-1)^{-1}\mathbf{X}^T\mathbf{X}$, where it is assumed that the data have been mean corrected. Principal components are obtained by finding eigenvalues $\{\mu_i : i = 1, \ldots, p\}$ and right eigenvectors $\{\boldsymbol{\xi}_i : i = 1, \ldots, p\}$ of $\mathbf{S}$, and then the ith principal component is given by $y_i = \boldsymbol{\xi}_i^T\mathbf{x} \quad (i = 1, \ldots, p)$ (see for example, Chatfield and Collins, 1980 or Mardia *et al.*, 1979).

Suppose, on the other hand, Euclidean distance is used on the data matrix $\mathbf{X}$ to define dissimilarities among the n individuals or objects. The dissimilarities will be given by

$$\delta_{rs}^2 = (\mathbf{x}_r - \mathbf{x}_s)^T(\mathbf{x}_r - \mathbf{x}_s),$$

and hence when these dissimilarities are subjected to classical scaling, $b_{rs} = \mathbf{x}_r^T\mathbf{x}_s$ and $\mathbf{B} = \mathbf{X}\mathbf{X}^T$.

As before, let the eigenvalues of $\mathbf{B}$ be λ_i $(i = 1, \ldots, n)$ with associated eigenvectors $\mathbf{v}_i$ $(i = 1, \ldots, n)$.

It is a well known result that the eigenvalues of $\mathbf{X}\mathbf{X}^T$ are the

same as those for $\mathbf{X}^T\mathbf{X}$, together with an extra $n - p$ zero eigenvalues. This is easily shown. Let $\mathbf{v}_i$ be an eigenvector of $\mathbf{X}\mathbf{X}^T$ associated with a non-zero eigenvalue, and so

$$\mathbf{X}\mathbf{X}^T\mathbf{v}_i = \lambda_i\mathbf{v}_i.$$

Premultiplying by $\mathbf{X}^T$,

$$(\mathbf{X}^T\mathbf{X})(\mathbf{X}^T\mathbf{v}_i) = \lambda_i(\mathbf{X}^T\mathbf{v}_i).$$

But

$$\mathbf{X}^T\mathbf{X}\boldsymbol{\xi}_i = \mu_i\boldsymbol{\xi}_i,$$

and hence $\mu_i = \lambda_i$ and the eigenvectors are related by $\boldsymbol{\xi}_i = \mathbf{X}^T\mathbf{v}_i$. Thus there is a duality between a principal components analysis and PCO where dissimilarities are given by Euclidean distance. In fact, the coordinates obtained in p' dimensions for the n objects by PCO are simply the component scores for the n objects on the first p' principal components. Now $\boldsymbol{\xi}_i^T\boldsymbol{\xi}_i = \mathbf{v}_i^T\mathbf{X}\mathbf{X}^T\mathbf{v}_i = \lambda_i$. Normalizing $\boldsymbol{\xi}_i$, the first p' component scores are given by

$$\begin{aligned}\mathbf{X}[\lambda_1^{-1}\boldsymbol{\xi}_1, \lambda_2^{-1}\boldsymbol{\xi}_2, \ldots, \lambda_{p'}^{-1}\boldsymbol{\xi}_{p'}] &= \mathbf{X}[\lambda_1^{-1}\mathbf{X}^T\mathbf{v}_1, \ldots, \lambda_{p'}^{-1}\mathbf{X}^T\mathbf{v}_{p'}] \\ &= [\lambda_1^{-\frac{1}{2}}\mathbf{X}\mathbf{X}^T\mathbf{v}_1, \ldots, \lambda_{p'}^{-\frac{1}{2}}\mathbf{X}\mathbf{X}^T\mathbf{v}_{p'}] \\ &= [\lambda_1^{\frac{1}{2}}\mathbf{v}_1, \ldots, \lambda_{p'}^{\frac{1}{2}}\mathbf{v}_{p'}],\end{aligned}$$

which are the coordinates obtained from PCO in p' dimensions.

Optimal transformations of the variables

So far, the PCO space containing the points representing the objects or individuals has been a subspace of the original p dimensional space spanned by the columns of the data matrix $\mathbf{X}$. It will now be convenient to change notation so that $\mathbf{X}$ is the matrix of coordinates in the Euclidean space representing the objects or individuals and $\mathbf{Z}$ is the data matrix. The associated spaces can now be different.

Meulman (1993) considers optimal transformations of the variables in $\mathbf{Z}$. From equation (2.6), PCO can be considered as the search for $\mathbf{X}$ such that the loss function

$$\mathrm{tr}(\mathbf{Z}\mathbf{Z}^T - \mathbf{X}\mathbf{X}^T)^T(\mathbf{Z}\mathbf{Z}^T - \mathbf{X}\mathbf{X}^T) \tag{2.7}$$

is minimised with respect to $\mathbf{X}$ (remembering that $\mathbf{Z}$ is mean corrected). The term (2.7) is called STRAIN.

Following Meulman, let $\mathbf{X}$ be transformed into $\mathbf{Q} = [\mathbf{q}_i]$, $\mathbf{q}_i \in \Gamma$, where Γ is a set of admissable transformations, for example a set of spline transformations. The mean of $\mathbf{q}_i$ is set to be zero, $\mathbf{1}^T\mathbf{q}_i = 0$, and normalized so that $\mathbf{q}_i^T\mathbf{q}_i = 1$.

The loss function

$$\text{STRAIN}(\mathbf{Q};\mathbf{X}) = \text{tr}(\mathbf{Q}\mathbf{Q}^T - \mathbf{X}\mathbf{X}^T)^T(\mathbf{Q}\mathbf{Q}^T - \mathbf{X}\mathbf{X}^T)$$

is now minimised with respect to $\mathbf{X}$ and with respect to $\mathbf{Q}$. Meulman suggests using an alternating least squares technique where $\text{STRAIN}(\mathbf{Q};\mathbf{X})$ is minimised with respect to $\mathbf{X}$ for fixed $\mathbf{Q}$ and then with respect to $\mathbf{Q}$ for fixed $\mathbf{X}$. The minimisation process alternates between the two minimisation steps. The minimisation for fixed $\mathbf{Q}$ is straightforward and is based on the usual PCO analysis. The minimisation for fixed $\mathbf{X}$ is more difficult and an iterative majorization procedure is suggested (see Chapter 10).

2.2.8 The additive constant problem

In Chapter 1, various metric and Euclidean properties of dissimilarities were discussed. Here, one particular aspect is considered in more detail, that of the additive constant problem. There are two formulations of the problem. The first is simply the problem of finding an appropriate constant to be added to all the dissimilarities, apart from the self-dissimilarities, that makes the matrix $\mathbf{B}$ of Section 2.2 positive semi-definite. This then implies there is a configuration of points in a Euclidean space where the associated distances are equal to the adjusted dissimilarities. This problem has been referred to for many years, Messick and Abelson (1956) being an early reference.

The second formulation is more practically orientated. If dissimilarities are measured on a ratio scale, then there is a sympathy of the dissimilarities to the distances in the Euclidean space used to represent the objects. However if the dissimilarities are measured in an interval scale, where there is no natural origin, then there is not. The additive constant problem can then be stated as the need to estimate the constant c such that $\delta_{rs} + c(1 - \delta^{rs})$ may be taken as ratio data, and also possibly to minimise the dimensionality of the Euclidean space required for representing the objects. The first formulation is considered here.

The additive constant problem is easier to solve if a constant is

added to squared dissimilarities rather than dissimilarities themselves. For this case

$$\delta_{rs}^{2(c)} = \delta_{rs}^2 + c(1 - \delta^{rs}).$$

The smallest value of c that makes $\mathbf{B}$ positive semi-definite is $-2\lambda_n$, where λ_n is the smallest eigenvalue of $\mathbf{B}$ (see for example, Lingoes, 1971).

The solution for the case where a constant is to be added to δ_{rs} and not δ_{rs}^2, was given by Cailliez (1983). His results are summarised below. The smallest number $c^\star$ has to be found such that the dissimilarities defined by

$$\delta_{rs}^c = \delta_{rs} + c(1 - \delta^{rs}) \tag{2.8}$$

have a Euclidean representation for all $c \geq c^\star$, that is which makes the matrix $\mathbf{B}$ positive semi-definite. Let $\mathbf{B}_0(\delta_{rs}^2)$ be the doubly centred matrix based on $\mathbf{A} = [-\frac{1}{2}\delta_{rs}^2]$ for the original dissimilarities. Then substituting δ_{rs}^c for δ_{rs} in (2.8) gives

$$\mathbf{B}_c(\delta_{rs}^2) = \mathbf{B}_0(\delta_{rs}^2) + 2c\mathbf{B}_0(\delta_{rs}) + \tfrac{1}{2}c^2\mathbf{H},$$

noting that $\mathbf{B}_0(\delta_{rs})$ is equivalent to $\mathbf{B}_0(\delta_{rs}^2)$ except that the entries are based on δ_{rs} and not δ_{rs}^2.

It is now shown that there exists a constant $c^\star$ such that the dissimilarities $\{\delta_{rs}^c\}$ defined in (2.8) have a Euclidean representation for all $c \geq c^\star$. For $\mathbf{B}_c(\delta_{rs}^2)$ to be positive semi-definite it is required that $\mathbf{x}^T\mathbf{B}_c(\delta_{rs}^2)\mathbf{x} \geq 0$ for all $\mathbf{x}$. Now

$$\mathbf{x}^T\mathbf{B}_c(\delta_{rs}^2)\mathbf{x} = \mathbf{x}^T\mathbf{B}_0(\delta_{rs}^2)\mathbf{x} + 2c\mathbf{x}^T\mathbf{B}_0(\delta_{rs})\mathbf{x} + \tfrac{1}{2}c^2\mathbf{x}^T\mathbf{H}\mathbf{x},$$

and so for any $\mathbf{x}$ this gives $\mathbf{x}^T\mathbf{B}_c(\delta_{rs}^2)\mathbf{x}$ as a convex parabola. Therefore, to any $\mathbf{x}$ there corresponds a number $\alpha(\mathbf{x})$ such that $\mathbf{x}^T\mathbf{B}_c(\delta_{rs}^2)\mathbf{x} \geq 0$ if $c \geq \alpha(\mathbf{x})$. Because $\mathbf{B}_0(\delta_{rs}^2)$ is not positive semi-definite, there is at least one $\mathbf{x}$ such that $\mathbf{x}^T\mathbf{B}_0(\delta_{rs}^2)\mathbf{x} < 0$ and for which $\alpha(\mathbf{x})$ will be positive. Hence the number $c^\star = \sup_{\mathbf{x}} \alpha(\mathbf{x}) = \alpha(\mathbf{x}^\star)$ is positive and such that

$$\mathbf{x}^T\mathbf{B}_c(\delta_{rs}^2)\mathbf{x} \geq 0 \quad \text{for all } \mathbf{x} \text{ and all } c \geq c^\star$$

$$\mathbf{x}^{\star T}\mathbf{B}_{c^\star}(\delta_{rs}^2)\mathbf{x}^\star = 0.$$

Hence $\{\delta_{rs}^c\}$ has a Euclidean representation for all $c \geq c^\star$, and also it can be seen that when $c = c^\star$ a space of at most $n-2$ dimensions is needed since there are now two zero eigenvalues.

Cailliez goes on to find the actual value $c^\star$. He shows that $c^\star$ is given by the largest eigenvalue of the matrix.

$$\begin{bmatrix} \mathbf{0} & 2\mathbf{B}_0(\delta_{rs}^2) \\ -\mathbf{I} & -4\mathbf{B}_0(\delta_{rs}) \end{bmatrix}. \tag{2.9}$$

Cailliez also shows that a negative constant can be added to the original dissimilarities so that

$$\delta_{rs}^c = \mid \delta_{rs} + c(1 - \delta^{rs}) \mid,$$

and then a Euclidean representation of $\{\delta_{rs}^c\}$ can be found for all $c < c'$. The value of c' is the smallest eigenvalue of the matrix in (2.9). Going back in time, Messick and Abelson (1956) considered the effect of values of c in (2.8) on the resulting eigenvalues and eigenvectors. They suggested that for a "true" solution, there will be a few large eigenvalues and the rest will be zero or very close to zero. In practice, this will not usually be the case and they proposed a method which determined c by setting the mean of the smallest $n - p$ eigenvalues to zero. The largest p eigenvalues are taken as those required to define the Euclidean space. Problems could arise, however, if large negative eigenvalues occurred. Cooper (1972) included a 'discrepancy' term, η_{rs}, in the new dissimilarities, so that

$$\delta_{rs}^c = \delta_{rs} + c(1 - \delta^{rs}) + \eta_{rs},$$

and then c is found for given dimensionality by minimising $G = \frac{1}{2}\sum_r \sum_s \eta_{rs}^2$. Minimisation is done using a Fletcher-Powell routine. The number of dimensions required is then assessed by an index of goodness of fit, FIT:

$$\text{FIT} = 1 - \frac{\sum \eta_{rs}^2}{\sum (\delta_{rs}^c - \delta_{\cdot\cdot}^c)^2}.$$

For a perfect solution, FIT = 1. To assess the dimension required, FIT is plotted against dimension p. The dimension required is that value of p where there is no appreciable improvement in the increase of FIT with increase in p.

Saito (1978) introduced an index of fit, $P(c)$, defined by

$$P(c) = \frac{\sum_{i=1}^p \lambda_i^2(c)}{\sum_{i=1}^n \lambda_i^2(c)},$$

where λ_i is the ith eigenvalue of $B_c(\delta_{rs}^2)$. The constant to be added to the dissimilarities for given P, was then taken as that value

which maximises $P(c)$. Again a gradient method is used for the maximisation.

Bénasséni (1994) considered the case of adding a constant to only some of the squared dissimilarities, arguing that large discrepancies can occur when a constant has to be added to all of them. Suppose the n objects under consideration can be partitioned into two groups, G_1 and G_2, consisting of g_1 and g_2, $(g_1 + g_2 = n)$ objects respectively. For convenience label the objects so that the first g_1 are in group G_1 and the last g_2 are in group G_2. The dissimilarities within groups are assumed to be worthy of Euclidean representation without any addition of a constant, but dissimilarities between group members are assumed to be under estimated or over estimated by a quantity c. The quantity c is added to the between squared dissimilarities,

$$\begin{aligned}\delta_{rs}^{2(c)} &= \delta_{rs}^2 \qquad (r, s \in G_1 \text{ or } r, s \in G_2) \\ &= \delta_{rs}^2 + c(1 - \delta^{rs}) \qquad (r \in G_1,\ s \in G_2).\end{aligned}$$

Then Bénasséni shows that

$$\mathbf{B}_c(\delta_{rs}^2) = \mathbf{B}_0(\delta_{rs}^2) + \frac{c}{n^2}\mathbf{A},$$

where $\mathbf{A} = (g_2\mathbf{x} - g_1\mathbf{y})(g_2\mathbf{x} - g_1\mathbf{y})^T$, $\mathbf{x}^T = (1, \ldots, 1, 0, \ldots, 0)$, a vector of g_1 ones followed by g_2 zeros, $\mathbf{y}^T = (0, \ldots, 0, 1, \ldots, 1)$, a vector of g_1 zeros followed by g_2 ones. If there is only one negative eigenvalue, λ_n, of $\mathbf{B}_0$, then the required value of c is given by

$$c = -\lambda_n / f\left(\sum_{r \in G_1} u_{nr}\right),$$

where $f(t) = t^2 - |t|(g_1 g_2 n^{-1} - t^2)^{1/2}$ and $\mathbf{u}_n = (u_{n1}, \ldots, u_{nn})^T$ is the eigenvector corresponding to λ_n. For a solution, some conditions on the eigenvalues and eigenvectors have to be satisfied.

If group membership is not initially known, Bénasséni suggests looking at all possible groupings that satisfy $f(\sum_{r \in G_1} u_{nr}) > 0$ and choose G_1, G_2 which give the minimum value of c. This particular grouping will be the one that makes $|\sum_{r \in G_1} u_{nr}|$ a maximum.

If there are m negative eigenvalues of $\mathbf{B}_0$ initially, then $\mathbf{B}_c$ can be made positive semi-definite using m successive modifications with different groups G_1, G_2 and constants c at each step. Bénasséni goes on to consider the case of adding a constant c to all the squared dissimilarities within a group G_1, but to none other. The reader is referred to the paper for further details.

2.3 Robustness

Sibson (1979) studied the effect of perturbing the matrix $\mathbf{B}$ on the eigenvalues and eigenvectors of $\mathbf{B}$ and hence on the coordinate matrix $\mathbf{X}$. For small ϵ matrix $\mathbf{B}$ is perturbed to $\mathbf{B}(\epsilon)$, where

$$\mathbf{B}(\epsilon) = \mathbf{B} + \epsilon\mathbf{C} + \tfrac{1}{2}\epsilon^2\mathbf{D} + O(\epsilon^3),$$

where $\mathbf{C}$, $\mathbf{D}$ are symmetric matrices chosen for particular perturbations. The perturbation in $\mathbf{B}$ then causes a perturbation in the eigenvalues λ_i and associated eigenvectors $\mathbf{v}_i$ as follows:

$$\lambda_i(\epsilon) = \lambda_i + \epsilon\mu_i + \tfrac{1}{2}\epsilon^2\nu_i + O(\epsilon^3),$$

$$\mathbf{v}_i(\epsilon) = \mathbf{v}_i + \epsilon\mathbf{f}_i + \tfrac{1}{2}\epsilon^2\mathbf{g}_i + O(\epsilon^3).$$

Sibson shows that

$$\mu_i = \mathbf{v}_i^T\mathbf{C}\mathbf{v}_i, \qquad \mathbf{f}_i = -(\mathbf{B} - \lambda_i\mathbf{I})^T\mathbf{C}\mathbf{v}_i,$$

$$\nu_i = \mathbf{v}_i^T(\mathbf{D} - 2\mathbf{C}(\mathbf{B} - \lambda_i\mathbf{I})^+\mathbf{C})\mathbf{v}_i,$$

where $\mathbf{M}^+$ is the matrix $\sum \lambda_i^{-1}\mathbf{v}_i^T\mathbf{v}_i$.

If instead of $\mathbf{B}$ the matrix of squared distances $\mathbf{D}$ is perturbed to a matrix $\mathbf{D}(\epsilon)$

$$\mathbf{D}(\epsilon) = \mathbf{D} + \epsilon\mathbf{F} + O(\epsilon^2),$$

where $\mathbf{F}$ is a symmetric zero diagonal matrix, then the perturbations induced in λ_i and $\mathbf{v}_i$ are

$$\lambda_i(\epsilon) = \lambda_i + \epsilon\mu_i + O(\epsilon^2),$$

$$\mathbf{v}_i(\epsilon) = \mathbf{v}_i + \epsilon\mathbf{f}_i + O(\epsilon^2),$$

where

$$\mu_i = -\tfrac{1}{2}\mathbf{v}_i^T\mathbf{F}\mathbf{v}_i, \qquad \mathbf{f}_i = \tfrac{1}{2}(\mathbf{B} - \lambda_i\mathbf{I})^T\mathbf{F}\mathbf{v}_i + \tfrac{1}{2}(\lambda_i n)^{-1}(\mathbf{1}^T\mathbf{F}\mathbf{v}_i)\mathbf{1}.$$

Matrix $\mathbf{F}$ can be used to investigate various perturbations of the distances $\{d_{rs}\}$. Random errors to the distances can be modelled by assigning a distribution to $\mathbf{F}$ and the effect of these on μ_i and $\mathbf{f}_i$ can be studied.

2.4 Metric least squares scaling

Metric least squares scaling finds a configuration matching d_{rs} to δ_{rs} by minimising a loss function, S, with possibly a continuous

monotonic transformation of dissimilarity, $f(\delta_{rs})$. The configuration $\{x_{ri}\}$ is found in a p dimensional space but with typically $p = 2$. Sammon (1969), Spaeth and Guthery (1969), Chang and Lee (1973) and Bloxam (1978) are early references. Sammon (1969) suggested the loss function

$$S = \sum_{r<s} \delta_{rs}^{-1}(d_{rs} - \delta_{rs})^2 / \sum_{r<s} \delta_{rs}, \tag{2.10}$$

where d_{rs} is the Euclidean distance between points r and s.

In the numerator of S, the squared difference between the dissimilarity δ_{rs}, and its representative distance d_{rs} in the configuration, is weighted by δ_{rs}^{-1}. Hence smaller dissimilarities have more weight in the loss function than larger ones. The denominator, $\sum_{r<s} \delta_{rs}$ is a normalizing term making S scale free.

Now $d_{rs}^2 = \sum_{i=1}^{p}(x_{ri} - x_{si})^2$ and hence

$$\frac{\partial d_{rs}}{\partial x_{tk}} = \frac{1}{d_{rs}}(x_{rk} - x_{sk})(\delta^{rt} - \delta^{st}).$$

Differentiating S with respect to x_{tk},

$$\begin{aligned}\frac{\partial S}{\partial x_{tk}} &= \left(\frac{1}{\sum_{r<s}\delta_{rs}}\right)\sum_{r<s}\frac{2(d_{rs}-\delta_{rs})}{\delta_{rs}}\frac{1}{d_{rs}}(x_{rk}-x_{sk})(\delta^{rt}-\delta^{st}) \\ &= \left(\frac{2}{\sum_{r<s}\delta_{rs}}\right)\sum_{r=1}^{n}\frac{(d_{rt}-\delta_{rt})}{\delta_{rt}d_{rt}}(x_{rk}-x_{sk}).\end{aligned}$$

The equations

$$\frac{\partial S}{\partial x_{tk}} = 0 \ (t = 1, \ldots, n; k = 1, \ldots, p)$$

have to be solved numerically.

Sammon uses a steepest descent method, so that if $x_{tk}^{(m)}$ is the mth iteration in minimising S, then

$$x_{tk}^{(m+1)} = x_{tk}^{(m)} - \mathrm{MF}\frac{\partial S}{\partial x_{tk}} \Big/ \left|\frac{\partial^2 S}{\partial x_{tk}^2}\right|,$$

where MF is Sammon's magic factor to optimize convergence and was chosen as 0.3 or 0.4. Chang and Lee (1973) used a heuristic relaxation method to speed up the convergence to the minimum. Niemann and Weiss (1979) used an optimal step size calculated at each iteration instead of MF. Speed of convergence is not usually a

problem nowadays with modern computers. The resulting configurations are sometimes referred to as "Sammon maps". Two recent examples of their use are the indexing and mapping of proteins (Apostol and Szpankowski, 1999) and their use in neural networks (Lerner *et al.*, 1998).

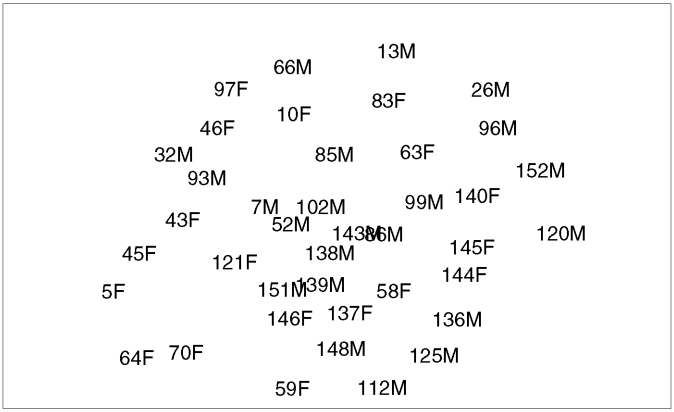

Figure 2.2 *Least squares scaling of the skull data*

Least squares scaling of the skulls

Figure 2.2 shows the least squares scaling of the skull data from Section 2.2.6. The loss function used is S defined in Equation (2.10). The configuration obtained is in reasonable agreement with that obtained from classical scaling.

Other loss functions have been considered by various authors. Shepard and Carroll (1966) and Calvert (1970) used

$$S = \sum \frac{\delta_{rs}^2}{d_{rs}^2} \Big/ \sum \frac{1}{d_{rs}^2}.$$

Niemann and Weiss (1979) used S in equation (2.10) but with weights δ_{rs}^q, with q to be chosen, instead of δ_{rs}^{-1}. Siedlecki *et al.* (1988) gave a summary of some MDS techniques involved in "mapping", where they considered discriminant analysis, principal components analysis, least squares scaling and projection pursuit and used these on various data sets. Dissimilarities can be transformed

using a continuous monotonic transformation, f, before a configuration is found. The loss function might then be

$$S = \frac{\sum_{r<s} w_{rs}(d_{rs} - f(\delta_{rs}))^2}{\sum_{r<s} d_{rs}^2},$$

where $\{w_{rs}\}$ are appropriately chosen weights.

In general, distances $\{d_{rs}\}$ do not have to be Euclidean.

Least absolute residuals

Heiser (1988) suggested minimising the absolute residual loss function defined by

$$\text{LAR} = \sum_{r<s} w_{rs}|d_{rs} - \delta_{rs}|$$

where w_{rs} are weights. The absolute residual loss function will not be influenced by outliers so much as a squared residual loss function. Heiser minimises LAR by a majorization algorithm (see Chapter 11).

Klein and Dubes (1989) used

$$S = \sum \frac{1}{\sqrt{\sum \delta_{rs}}} \sum \frac{|d_{rs} - \delta_{rs}|}{\delta_{rs}}$$

and minimised S using simulated annealing. The advantage of this method is that it seeks the global minimum of S trying to avoid local minima. The annealing algorithm uses a Markov chain where the minimum of S corresponds to the stable state of the Markov chain. The Markov chain is simulated and allowed to run until this stable state is found. In the process, whereas steepest descent methods always aim to decrease S at each step, the simulated annealing algorithm allows S to increase and then pass by a local minimum. See Klein and Dubes for further details.

2.5 Critchley's intermediate method

Critchley (1978) combines the idea of allowing a transformation of the dissimilarities as in least squares scaling and also the minimisation of a target function, with the methods of classical scaling. Firstly, the dissimilarities $\{\delta_{rs}\}$ are transformed using a continuous parametric function $f(\mu, \delta_{rs})$, where μ is possibly a vector-valued parameter. For example

$$f(\delta_{rs}) = \delta_{rs}^{\mu} \qquad \mu > 0.$$

Then, as for classical scaling

$$\mathbf{B} = \mathbf{HAH}, \quad [\mathbf{A}]_{rs} = -\tfrac{1}{2} f(\delta_{rs}).$$

Let the spectral decomposition of $\mathbf{B}$ be

$$\mathbf{B} = \mathbf{V}\boldsymbol{\Lambda}\mathbf{V}^T,$$

and then μ is estimated by $\hat{\mu}$, the value which minimises the function

$$T(\mu) = \frac{1}{n^2} \sum_{i=1}^{n} [\lambda_i(\mu)]^2,$$

subject to the constraints

a) $\lambda_n(\mu) = 0$, so that $\mathbf{B}$ is positive semi-definite, and

b) $\bar{\lambda} = n^{-1} \sum \lambda_i = 1$, a scale constraint.

See Critchley (1978) for further details.

2.6 Unidimensional scaling

When the space in which the points representing the objects or individuals has only one dimension, the scaling technique becomes that of unidimensional scaling. The loss function to be minimised is

$$S = \sum_{r<s} (\delta_{rs} - |x_r - x_s|)^2. \tag{2.11}$$

Some references are Guttman (1968), de Leeuw and Heiser (1977), Defays (1978), Olson (1984), Pliner (1984, 1986, 1988), Groenen (1993) and Hubert *et al.* (1997).

Minimising S is plagued by a large number of local minima. It can be shown that $\mathbf{x}$ is a local minimum of S if and only if

$$x_r = \frac{1}{n} \sum_{s=1}^{n} \delta_{rs} \text{sign}(x_r - x_s) \qquad (r = 1, \ldots, n), \tag{2.12}$$

(Guttman, 1968; Pliner, 1984).

Guttman (1968) devised an algorithm for finding a local minimum, not necessarily a global minimum. Let $x_r^{(m)}$ be the value of x_r at the mth iteration of the algorithm. The algorithm is

$$x_r^{(m+1)} = \frac{1}{n} \sum_{s=1}^{n} \delta_{rs} \text{sign}(x_r^{(m)} - x_s^{(m)}).$$

When $x_r^{(m)} = x_s^{(m)}$ $(r \neq s)$, $\text{sign}(x_r^{(m)} - x_s^{(m)})$ is replaced by $+1$ or -1 with the corresponding $\text{sign}(x_s^{(m)} - x_r^{(m)})$ replaced by -1 or $+1$ accordingly. The algorithm is started from several starting points and hopefully one of the local minima found will be a global minimum.

Hubert and Arabie (1986, 1988) consider the following dynamic programming approach to finding minima. Assume $x_1, \ldots, x_n$ satisfy (2.12) and let the rows and columns of the dissimilarity matrix, $\mathbf{D} = [\delta_{rs}]$, be reordered so that $x_1 \leq x_2 \leq \ldots \leq x_n$. Then $x_r = (\sum_{s=1}^{r-1} \delta_{rs} - \sum_{s=r+1}^{n} \delta_{rs})/n = t_r$ say. Thus a dissimilarity matrix with its rows and columns re-ordered to force $t_1 \leq t_2 \ldots \leq t_n$ can immediately give a set of coordinates $x_r = t_r$ to satisfy (2.12).

Now it is easily seen that, for fixed coordinates $x_1, \ldots, x_n$, minimising (2.11) is equivalent to maximising $S' = \sum_{r,s} \delta_{rs}|x_r - x_s|$.

Now

$$\begin{aligned} S' &= \sum_{r=1}^{n} \sum_{s=1}^{r-1} \delta_{rs}(x_r - x_s) + \sum_{r=1}^{n} \sum_{s=r+1}^{n} \delta_{rs}(x_s - x_r) \\ &= \sum_{r=1}^{n} x_r \left(\sum_{s=1}^{r-1} \delta_{rs} - \sum_{s=r+1}^{n} \delta_{rs} \right) + \sum_{s=1}^{n} x_s \left(\sum_{r=1}^{s-1} \delta_{rs} - \sum_{r=s+1}^{n} \delta_{rs} \right) \\ &= 2n \sum_{r=1}^{n} x_r t_r. \end{aligned}$$

Thus to maximise S', starting with a dissimilarity matrix $\mathbf{D}$, interchanges in rows and columns of the dissimilarity matrix are tried (for example pairwise). If $\sum_r x_r t_r$ is found to increase then the coordinates $x_1, \ldots, x_n$ are re-estimated as $t_1, \ldots, t_n$. The interchange procedure is repeated and $x_1, \ldots, x_n$ are updated again. This continues until $\sum_r x_r t_r$ reaches its maximum of $\sum_r t_r^2$. The whole process is restarted with other random orderings of rows and columns and hopefully a global maximum can be found.

A linear programming approach was suggested by Simanbiraki (1996). Lau *et al.* (1998) consider a nonlinear programming approach, as have other authors. They show that minimising S in (2.11) is equivalent to minimising

$$\sum_{r<s} \left\{ (\delta_{rs} - (x_r - x_s))^2,\ (\delta_{rs} - (x_s - x_r))^2 \right\}.$$

Let w_{1rs}, w_{2rs} be two binary variables taking values 0 and 1. Then the mathematical programming formulation is minimise

$$\sum_{r<s}\{w_{1rs}(e_{1rs}^2) + w_{2rs}(e_{2rs}^2)\},$$

subject to

$$\delta_{rs} = x_r - x_s + e_{1rs}$$

$$\delta_{rs} = x_s - x_r + e_{2rs}$$

$$w_{1rs} + w_{2rs} = 1$$

$$w_{1rs}, w_{2rs} \geq 0.$$

Here e_{1rs} is the error if $x_r > x_s$ and e_{2rs} is the error if $x_r < x_s$.

In fact, w_{1rs} and w_{2rs} can be considered continuous variables as a solution will force w_{1rs} and w_{2rs} to be either zero or one, and hence the problem becomes a nonlinear programming problem. See Lau *et al.* (1998) for the solution.

Hubert *et al.* (1997) consider minimising the loss function

$$\sum_{r<s}(\delta_{rs} + c - |x_r - x_s|)^2 = \sum_{r<s}(\delta_{rs} - \{|x_r - x_s| - c\})^2$$

where c is a constant.

The problem can be viewed as fitting $\{|x_r - x_s|\}$ to the translated dissimilarities $\{\delta_{rs} + c\}$, or fitting $\{|x_r - x_s| - c\}$ to the dissimilarities $\{\delta_{rs}\}$. Hubert *et al.* also consider circular unidimensional scaling where points representing the objects are placed around the circumference of a circle. The dissimilarities are represented by shortest paths around the circle.

2.6.1 A classic example

Cox and Brandwood (1959) use discriminant analysis to help establish the chronological order in which seven works of Plato were written. Of the seven works, it is known that *Republic (Rep.)* was writen first and *Laws* last. In between Plato wrote *Critias (Crit.), Philebus (Phil.), Politicus (Pol.), Sophist (Soph.)* and *Timaeus (Tim.)*. Classical scholars have different opinions as to the chronological order. For each work, data are available on the distribution of sentence endings. The last five syllables of each sentence are noted individually as being either short or long, giving thirty-two

possible sentence endings. Cox and Brandwood use the sentence endings for *Rep.* and *Laws* as samples from a multinomial distribution from which to find a sample discriminant function. This is used to find discriminant scores for the other five works which are then placed in chronological order according to the scores. The final ordering found by this method is *Rep., Tim., Soph., Crit., Pol., Phil., Laws.*

The same data are now analysed using unidimensional scaling. The sentence endings are transformed into percentage data and the dissimilarity between two works is measured as Euclidean distance. The dissimilarity matrix is

$$\begin{bmatrix} 0.00 & 12.28 & 10.72 & 12.65 & 11.55 & 8.59 & 8.89 \\ 12.28 & 0.00 & 11.80 & 6.44 & 8.58 & 10.58 & 13.02 \\ 10.72 & 11.80 & 0.00 & 11.75 & 11.96 & 9.38 & 9.52 \\ 12.65 & 6.44 & 11.75 & 0.00 & 6.99 & 10.08 & 12.26 \\ 11.55 & 8.58 & 11.96 & 6.99 & 0.00 & 7.72 & 11.23 \\ 8.59 & 10.58 & 9.38 & 10.08 & 7.72 & 0.00 & 6.10 \\ 8.89 & 13.02 & 9.52 & 12.26 & 11.23 & 6.10 & 0.00 \end{bmatrix}.$$

Using Guttman's algorithm with many random starts, the final configuration can be seen in Figure 2.3. Unidimensional scaling gives the ordering *Rep., Crit., Tim., Soph., Pol., Phil., Laws*, with a loss value of 290.2. This ordering is in agreement with that of Cox and Brandwood but with *Crit.* placed before *Tim.* However, the placement of *Crit.* is in accord with their results, too as they show that *Crit.* could be placed anywhere from before *Tim.* to before *Pol.*

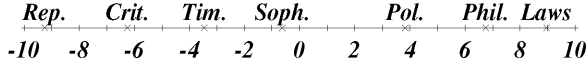

Figure 2.3 *Unidimensional scaling of seven works of Plato*

The "errors", $\delta_{rs} - d_{rs}$, are given in the matrix following. It can be seen that *Crit.* is involved with the two largest errors.

$$\begin{bmatrix} 0.00 & -5.92 & 7.72 & -3.35 & -1.53 & -0.03 & 3.11 \\ -5.92 & 0.00 & -3.40 & 4.24 & 3.47 & 1.01 & 0.60 \\ 7.72 & -3.40 & 0.00 & -1.25 & 1.88 & 3.75 & 6.73 \\ -3.35 & 4.24 & -1.25 & 0.00 & 4.08 & 2.71 & 2.05 \\ -1.53 & 3.47 & 1.88 & 4.08 & 0.00 & 3.26 & 3.93 \\ -0.03 & 1.01 & 3.75 & 2.71 & 3.26 & 0.00 & 3.26 \\ 3.11 & 0.60 & 6.73 & 2.05 & 3.93 & 3.26 & 0.00 \end{bmatrix}.$$

2.7 Grouped dissimilarities

Suppose objects are divided into g groups. Then the technique of Analysis of Distance (AOD) developed by Gower and Krzanowski (1999) can be used on the dissimilarities $\{\delta_{rs}\}$ to investigate the between and within group structure. Analysis of Distance is akin to Analysis of Variance (ANOVA). Dissimilarities, to be viewed as distances, are broken down into a within sum of squares component and a between sum of squares component ($T = W + B$).

Following Gower and Krzanowski (1999), let the group sizes be $n_1, n_2, \ldots, n_g$. Let group membership be given by $\mathbf{G} = [g_{ri}]$, where $g_{ri} = 1$ if the rth object belongs to the ith group, and zero otherwise. Let $\mathbf{n} = (n_1, \ldots n_g)$ and $\mathbf{N} = \text{diag}(n_1, \ldots, n_g)$. Let $\mathbf{D} = [\frac{1}{2}\delta_{rs}^2]$ ($= -\mathbf{A}$ of Section 2.2.1) and $\mathbf{X}$ be the coordinate matrix of points representing the objects. Then placing the centroid at the origin, from equation (2.5)

$$-\mathbf{HDH} = \mathbf{XX}^T. \tag{2.13}$$

The coordinates of the group means are given by $\bar{\mathbf{X}} = \mathbf{N}^{-1}\mathbf{G}^T\mathbf{X}$ and hence

$$\bar{\mathbf{X}}\bar{\mathbf{X}}^T = \mathbf{N}^{-1}\mathbf{G}^T\mathbf{XX}^T\mathbf{GN}^{-1}.$$

Substituting for $\mathbf{XX}^T$ from equation (2.13), it can be shown that the group mean distances, $\bar{d}_{ij}$, are given by

$$\bar{d}_{ij}^2 = 2f_{ij} - f_{ii} - f_{jj},$$

where $\mathbf{F} = [f_{ij}] = \mathbf{N}^{-1}\mathbf{G}^T\mathbf{DGN}^{-1}$.

Principal coordinate analysis can be used on $\mathbf{F}$ for finding a configuration of points representing the group means. Let $\mathbf{Y}$ be the coordinate matrix for the group means, and then

$$-\mathbf{HFH} = \mathbf{YY}^T.$$

If group size is to be taken into account then this equation is replaced by

$$-(\mathbf{I} - g^{-1}\mathbf{1}\mathbf{n}^T)\mathbf{F}(\mathbf{I} - g^{-1}\mathbf{1}\mathbf{n}^T) = \mathbf{Y}\mathbf{Y}^T.$$

Once a configuration of points representing the group means has been established, then points representing the individual objects can be placed around the group mean points by using the technique of adding points to plots devised by Gower (1968).

Let $\mathbf{D}$ be partitioned into g^2 submatrices, $\mathbf{D}_{ij}$ $(i, j = 1, \ldots g)$, where $\mathbf{D}_{ij}$ contains the squared dissimilarities divided by two, between each object in the ith group and each individual in the jth group. Let $\bar{\boldsymbol{\Delta}} = [\bar{d}_{ij}^2]$. Gower and Krzanowski go on to establish the fundamental AOD identity corresponding to that of ANOVA, $T = W + B$,

$$T = n^{-1}\mathbf{1}^T\mathbf{D}\mathbf{1} \qquad \text{(total sum of squares)}$$

$$W = \sum_{i=1}^{g} n_r^{-1}\mathbf{1}_i^T\mathbf{D}_{ii}\mathbf{1}_i \qquad \text{(within sum of squares)}$$

$$B = n^{-1}\mathbf{n}^T\bar{\boldsymbol{\Delta}}\mathbf{N} \qquad \text{(between sum of squares)}$$

where $\mathbf{1}_i$ is a vector of n_i ones. In ANOVA, F-tests can be used for hypothesis testing using the fundamental identity $T = W + B$. This is not so for AOD as distribution theory has not been established. Gower and Krzanowski do propose permutational tests in the interim.

2.8 Inverse scaling

DeLeeuw and Groenen (1997) consider the problem of inverse least squares scaling. That is, instead of finding the coordinate matrix, $\mathbf{X}$, of a configuration from the dissimilarities $\{\delta_{rs}\}$, the possible set of dissimilarities are found for a given coordinate matrix, and fixed set of weights.

For least squares scaling, consider minimising the loss function, S, where

$$S = \frac{1}{2}\sum_{r=1}^{n}\sum_{s=1}^{n} w_{rs}(\delta_{rs} - d_{rs})^2,$$

where $d_{rs}^2 = (\mathbf{x}_r - \mathbf{x}_s)^T(\mathbf{x}_r - \mathbf{x}_s)$. The half is used for convenience. There are usually many local minima and finding the global minimum cannot be guaranteed.

Inverse least squares scaling starts with fixed $\{\mathbf{x}_r\}$ and $\{w_{rs}\}$ and finds corresponding to stationary points of S and in particular the local and global minima.

Following de Leeuw and Groenen (1997) write

$$d_{rs}^2 = \mathrm{tr}(\mathbf{X}^T\mathbf{A}_{rs}\mathbf{X}),$$

where $\mathbf{X} = [\mathbf{x}_1, \mathbf{x}_2, \ldots, \mathbf{x}_n]^T$, $\mathbf{A}_{rs} = (\mathbf{e}_r - \mathbf{e}_s)(\mathbf{e}_r - \mathbf{e}_s)^T$, with $\mathbf{e}_r = (0, \ldots, 0, 1, 0, \ldots, 0)^T$, the unit vector for the rth dimension.

Now

$$\frac{\partial d_{rs}^2}{\partial \mathbf{X}} = \frac{\partial \mathrm{tr}(\mathbf{X}^T\mathbf{A}_{rs}\mathbf{X})}{\partial \mathbf{X}} = 2\mathbf{A}_{rs}\mathbf{X}.$$

Then

$$\frac{\partial S}{\partial \mathbf{X}} = \sum_{r=1}^{n}\sum_{s=1}^{n} 2w_{rs}\left(1 - \frac{\delta_{rs}}{d_{rs}}\right)\mathbf{A}_{rs}\mathbf{X}.$$

Thus for a stationary point of S,

$$\sum_{r=1}^{n}\sum_{s=1}^{n} w_{rs}\left(1 - \frac{\delta_{rs}}{d_{rs}}\right)\mathbf{A}_{rs}\mathbf{X} = \mathbf{0}. \tag{2.14}$$

Let $t_{rs} = w_{rs}(1 - \delta_{rs}/d_{rs})$ and so equation (2.14) can be written

$$\sum_{r=1}^{n}\sum_{s=1}^{n} t_{rs}\mathbf{A}_{rs}\mathbf{X} = \mathbf{0} \tag{2.15}$$

and is solved for $\{t_{rs}\}$.

Now $\{A_{rs}\}$ are a basis for any n dimensional symmetric doubly centred matrix and so equation (2.15) reduces to

$$\mathbf{TX} = \mathbf{0}$$

where $\mathbf{T}$ has to be a symmetric doubly centred matrix.

Now let $\mathbf{K}$ be an orthonormal, column centred, matrix such that $\mathbf{K}^T\mathbf{X} = \mathbf{0}$, and let $\mathbf{M}$ be an arbitrary symmetric matrix. Thus $\mathbf{T}$ is found as $\mathbf{T} = \mathbf{KMK}^T$, and hence

$$\delta_{rs} = d_{rs}\left(1 - \frac{t_{rs}}{w_{rs}}\right),$$

noting that the condition $t_{rs} \leq w_{rs}$ must be met.

De Leeuw and Groenen (1997) show that the set of dissimilarity matrices $\mathbf{D} = [\delta_{rs}]$ which give rise to $\mathbf{X}$ as a stationary point is a closed bounded convex polyhedron. To compute possible $\mathbf{D}$, let $\{\mathbf{P}_l\}$ be a basis for the symmetric matrices of order $n - r - 1$. Let

$\mathbf{Q}_l = \mathbf{K}\mathbf{P}_l\mathbf{K}^T$ and then $\mathbf{T}$ can be written as a weighted sum of the basis $\{\mathbf{Q}_l\}$, $\mathbf{T} = \sum \theta_l \mathbf{Q}_l$. Not every $\{\theta_l\}$ gives an admissible $\mathbf{T}$ since the condition $t_{rs} \leq w_{rs}$ must be met. One of the examples given by de Leeuw and Groenen (1997) is as follows.

Let four points form the corners of a square, with coordinate matrix

$$\mathbf{X} = \begin{bmatrix} -\frac{1}{2} & -\frac{1}{2} \\ \frac{1}{2} & -\frac{1}{2} \\ \frac{1}{2} & \frac{1}{2} \\ -\frac{1}{2} & \frac{1}{2} \end{bmatrix}.$$

The corresponding distances are

$$\mathbf{D} = \begin{bmatrix} 0 & 1 & \sqrt{2} & 1 \\ 1 & 0 & 1 & \sqrt{2} \\ \sqrt{2} & 1 & 0 & 1 \\ 1 & \sqrt{2} & 1 & 0 \end{bmatrix}.$$

The matrix $\mathbf{T}$ is of rank 1 and so the basis $\{P_l\}$ is trivially 1.

Now

$$\mathbf{K} = \begin{bmatrix} -\frac{1}{2} \\ \frac{1}{2} \\ -\frac{1}{2} \\ \frac{1}{2} \end{bmatrix}$$

and so

$$\mathbf{T} = \theta\mathbf{K}\mathbf{K}^T = \frac{\theta}{4}\begin{bmatrix} 1 & -1 & 1 & -1 \\ -1 & 1 & -1 & 1 \\ 1 & -1 & 1 & -1 \\ -1 & 1 & -1 & 1 \end{bmatrix}.$$

For weights all unity ($w_{rs} = 1$), $\delta_{rs} = d_{rs}(1 - t_{rs})$ and hence

$$\mathbf{D} = \begin{bmatrix} 0 & a & b & a \\ a & 0 & a & b \\ b & a & 0 & a \\ a & b & a & 0 \end{bmatrix},$$

where $a = 1 + \theta/4$, $b = \sqrt{2}(1 - \theta/4)$ and $-4 \leq \theta \leq 4$ to satisfy $t_{rs} \leq 1$. The minimum of S will occur when $\theta = 0$, with $S = 0$, with other values of θ giving rise to other stationary points. De Leeuw and Groenen (1997) give further examples.

CHAPTER 3

Nonmetric multidimensional scaling

3.1 Introduction

This chapter presents the underlying theory of nonmetric multidimensional scaling developed in the 1960s. The theory is given for two-way, one-mode data, essentially for dissimilarity data collected on one set of objects.

Suppose there are n objects with dissimilarities $\{\delta_{rs}\}$. The procedure is to find a configuration of n points in a space, which is usually chosen to be Euclidean, so that each object is represented by a point in the space. A configuration is sought so that distances between pairs of points $\{d_{rs}\}$ in the space match "as well as possible" the original dissimilarities $\{\delta_{rs}\}$.

Mathematically, let the objects comprise a set O. Let the dissimilarity, defined on $\mathrm{O} \times \mathrm{O}$, between objects r and s be δ_{rs} $(r, s \in \mathrm{O})$. Let ϕ be an arbitrary mapping from O onto a set of points X, where X is a subset of the space which is being used to represent the objects. Let the distance between points x_r, x_s in X be given by the real-valued function $d_{x_r x_s}$. Then a disparity, $\hat{d}$, is defined on $\mathrm{O} \times \mathrm{O}$, which is a measure of how well the distance $d_{\phi(r)\phi(s)}$ "matches" dissimilarity δ_{rs}. The aim is to find a mapping ϕ, for which $d_{\phi(r)\phi(s)}$ is approximately equal to $\hat{d}_{rs}$, and is usually found by means of some loss function. The points in X together with their associated distances will be referred to as a configuration of points.

The choice of dissimilarity measure was discussed in Chapter 1, and it is assumed that dissimilarities $\{\delta_{rs}\}$ have been calculated for the set of objects. The set X is often taken as R^2 and d as Euclidean distance, although others are sometimes used, for example R^3, and the Minkowski metric. Once these are chosen, together with the method for calculating disparities, the nonmetric multidimensional

scaling problem becomes one of finding an appropriate algorithm for minimising a loss function.

A simple example

As a trivial but illustrative example, consider the following. Suppose O consists of just three objects labelled $\{1, 2, 3\}$ with dissimilarities given by

$$\delta_{11} = \delta_{22} = \delta_{33} = 0, \delta_{12} = 4, \delta_{13} = 1, \delta_{23} = 3.$$

Let C be a space with just two points $\{a, b\}$, which is used for representing the objects, and so X will be a subset of C. A mapping ϕ then maps each of the three objects in O to one of the two points in C. Thus there must be at least one coincident point. Let the distance function on C be defined as $d_{aa} = d_{bb} = 0, d_{ab} = 1$. Now suppose the disparity function is defined as follows: if the rank order of $\{d_{rs}\}$ is the same as the rank order of $\{\delta_{rs}\}$ then $\hat{d}_{rs} = d_{rs}$, otherwise $\hat{d}_{rs} = 1 - d_{rs}$ for all r, s. Note that the "self-dissimilarities" $\delta_{11}, \delta_{22}, \delta_{33}$ will not be used, as is usually the case. The loss function is taken as

$$S = \min_{\phi}\{ \sum_{r,s} |d_{rs} - \hat{d}_{rs}|\}.$$

There are only eight possible mappings ϕ:

$$\begin{aligned}
\phi_1 &: \ \phi_1(1) = a, \ \phi_1(2) = a, \ \phi_1(3) = a \\
\phi_2 &: \ \phi_2(1) = a, \ \phi_2(2) = a, \ \phi_2(3) = b \\
\phi_3 &: \ \phi_3(1) = a, \ \phi_3(2) = b, \ \phi_3(3) = a \\
\phi_4 &: \ \phi_4(1) = b, \ \phi_4(2) = a, \ \phi_4(3) = a \\
\phi_5 &: \ \phi_5(1) = a, \ \phi_5(2) = b, \ \phi_5(3) = b \\
\phi_6 &: \ \phi_6(1) = b, \ \phi_6(2) = a, \ \phi_6(3) = b \\
\phi_7 &: \ \phi_7(1) = b, \ \phi_7(2) = b, \ \phi_7(3) = a \\
\phi_8 &: \ \phi_8(1) = b, \ \phi_8(2) = b, \ \phi_8(3) = b
\end{aligned}$$

although only four need to be considered since $\phi_i \equiv \phi_{9-i}$. The rank order of the dissimilarities is $\delta_{13}, \delta_{23}, \delta_{12}$. The possible rank orders of the distances under ϕ_3 for example are d_{13}, d_{12}, d_{23} and d_{13}, d_{23}, d_{12}, giving disparities $\hat{d}_{13} = 1, \ \hat{d}_{12} = \hat{d}_{23} = 0$ and $\hat{d}_{13} = 0, \ \hat{d}_{23} = \hat{d}_{12} = 1$ respectively. The corresponding value of S is 0.0.

The eight values of S under the different mappings are 0.0, 3.0, 0.0, 3.0, 3.0, 0.0, 3.0, and 0.0. So the mappings giving minimum loss are ϕ_1 and ϕ_3 (or ϕ_8 and ϕ_6). The mapping ϕ_1 maps all three objects to a, while ϕ_3 maps objects 1 and 3 to a and 2 to b. In effect, the ϕ's carry out a trivial cluster analysis of the three points, ϕ_1 producing only one cluster, and ϕ_3 two clusters.

3.1.1 R^p space and the Minkowski metric

Although nonmetric MDS can be carried out in abstruse spaces, the majority of MDS analyses are carried out with X a subset of R^p, and with $p = 2$ in particular. A configuration of points is sought in R^p which represent the original objects, such that the distances between the points $\{d_{rs}\}$ match orderwise, as well as possible, the original dissimilarities $\{\delta_{rs}\}$.

Let the rth point in X have coordinates $\mathbf{x}_r = (x_{r1}, \ldots, x_{rp})^T$.

Let the distance measure for X be the Minkowski metric, and so for points r and s in X,

$$d_{rs} = \left[\sum_{i=1}^{p} |x_{ri} - x_{si}|^{\lambda} \right]^{1/\lambda} \qquad (\lambda > 0). \tag{3.1}$$

Define disparities $\{\hat{d}_{rs}\}$, viewed as a function of the distances $\{d_{rs}\}$, by

$$\hat{d}_{rs} = f(d_{rs}),$$

where f is a monotonic function such that

$$\hat{d}_{rs} \leq \hat{d}_{tu} \quad \text{whenever} \quad \delta_{rs} < \delta_{tu} \quad (\text{Condition } C_1).$$

Thus the disparities "preserve" the order of the original dissimilarities but allow possible ties in disparities. Ties in the dissimilarities will be discussed in Section 3.2.5.

Let the loss function be L, where for example

$$L = \left\{ \frac{\sum_{r,s} (d_{rs} - \hat{d}_{rs})^2}{\sum_{r,s} d_{rs}^2} \right\}^{\frac{1}{2}}. \tag{3.2}$$

Note the original dissimilarities $\{\delta_{rs}\}$ only enter into the loss function by defining an ordering for the disparities $\{\hat{d}_{rs}\}$. The loss function defined above is very commonly used, although there are

others which will be discussed later. The aim is to find a configuration which attains minimum loss. The loss function can be written in terms of the coordinates $\{x_{ri}\}$ by using equation (3.1) to replace the distances $\{d_{rs}\}$, and can hence be partially differentiated with respect to $\{x_{ri}\}$ in order to seek a minimum. The disparities $\{\hat{d}_{rs}\}$ will usually be a very complicated non-differentiable function of the distances $\{d_{rs}\}$ and hence of the coordinates $\{x_{ri}\}$. This means that the loss function cannot be fully differentiated with respect to the coordinates $\{x_{ri}\}$ when searching for the minimum. Instead, various algorithms have been suggested that minimise L with respect to $\{x_{ri}\}$ and also with respect to $\{\hat{d}_{rs}\}$.

Shepard (1962a, 1962b) was the first to produce an algorithm for nonmetric MDS, although he did not use loss functions. His method was first to rank and standardize the dissimilarities such that the minimum and maximum dissimilarities were 0 and 1 respectively. Then n points representing the objects are placed at the vertices of a regular simplex in R^{n-1} Euclidean space. Distances $\{d_{rs}\}$ between the n points are then calculated and ranked. The measure of the departure from monotonicity of the distances to the dissimilarities by distance d_{rs} is given by $\delta_{rs} - \delta_{[rs]}$, where $\delta_{[rs]}$ is the dissimilarity of rank equal to the rank of d_{rs}. Shepard's method then moves the points along vectors that will decrease the departure from monotonicity, also stretching larger distances and shrinking smaller distances. The points are repeatedly moved in this manner until adjustments become negligible – however there is no formulation of a proper loss function. After the last iteration, the coordinate system is rotated to principal axes and the first p principal axes are used to give the final configuration in p dimensional space.

It was Kruskal (1964a, 1964b) who improved upon the ideas of Shepard and put nonmetric MDS on a sounder footing by introducing a loss function to be minimised.

3.2 Kruskal's approach

Let the loss function (3.2) be relabelled as S and let

$$S = \sqrt{\frac{S^*}{T^*}}, \tag{3.3}$$

where $S^* = \sum_{r,s}(d_{rs} - \hat{d}_{rs})^2$, and $T^* = \sum_{r,s} d_{rs}^2$. Note that the summations in the loss function are taken over $1 = r < s = n$ since

$\delta_{sr} = \delta_{rs}$ for all r, s. The loss function is minimised with respect to $\{d_{rs}\}$, i.e. with respect to $\{x_{ri}\}$, the coordinates of the configuration, and also with respect to $\{\hat{d}_{rs}\}$ using isotonic regression.

3.2.1 Minimising S with respect to the disparities

For convenience, let the dissimilarities $\{\delta_{rs}\}$ be relabelled $\{\delta_i : i = 1, \ldots, N\}$ and assume they have been placed in numerical order and that there are no ties. Also, relabel the distances $\{d_{rs}\}$ as $\{d_i : i = 1, \ldots, N\}$ where d_i corresponds to the dissimilarity δ_i. To illuminate the proof that follows an example will be employed.

Example
Suppose there are only four objects with dissimilarities

$$\delta_{12} = 2.1,\ \delta_{13} = 3.0,\ \delta_{14} = 2.4,\ \delta_{23} = 1.7,\ \delta_{24} = 3.9,\ \delta_{34} = 3.2$$

and a configuration of points representing the four objects with distances

$$d_{12} = 3.3,\ d_{13} = 4.5,\ d_{14} = 5.7,\ d_{23} = 3.3,\ d_{24} = 4.3,\ d_{34} = 1.3.$$

Then the ordered dissimilarities with the new notation, together with their associated distances, are,

$$\delta_1 = 1.7,\ \delta_2 = 2.1,\ \delta_3 = 2.4,\ \delta_4 = 3.0,\ \delta_5 = 3.2,\ \delta_6 = 3.9$$

$$d_1 = 3.3,\ d_2 = 3.3,\ d_3 = 5.7,\ d_4 = 4.5,\ d_5 = 1.3,\ d_6 = 4.3.$$

Minimisation of S is equivalent to minimisation of $S' = \sum_i (d_i - \hat{d}_i)^2$, again using the new suffix notation. Let the cumulative sums of $\{d_i\}$ be

$$D_i = \sum_{j=1}^{i} d_j \quad (i = 1, \ldots, N),$$

and consider a plot of D_i against i, giving points $P_0, P_1, \ldots, P_N$ where the origin is labelled P_0. Figure 3.1 shows the plot for the example. Note that the slope of the line joining P_{i-1} and P_i is just d_i. The greatest convex minorant of the cumulative sums is the graph of the supremum of all convex functions whose graphs lie below the graph of the cumulative sums. (Holding a piece of taut string at P_0 and P_N would give the greatest convex minorant). The greatest convex minorant for the example is also shown in

the figure. The $\{\hat{d}_i\}$ which minimises S' is given by the greatest convex minorant, where $\hat{d}_i$ is the value of the minorant at abscissa i. From Figure 3.1, it is seen that some of the values $\hat{d}_i$ are actually equal to d_i, and obviously $S' = 0$ if $\hat{d}_i = d_i$, for all i. Note that $\hat{d}_i = \hat{D}_i - \hat{D}_{i-1}$ and is the slope of the line. Thus if $\hat{D}_i < D_i$ then $\hat{d}_i = \hat{d}_{i+1}$.

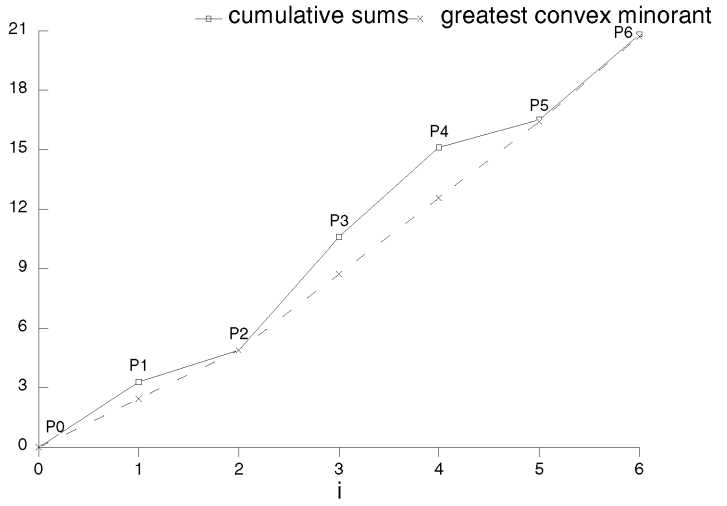

Figure 3.1 *Isotonic regression for the data in the example: solid line – the cumulative sums* $\{D_i\}$*, dashed line – the greatest convex minorant.*

In order to show that this $\{\hat{d}_i\}$ does indeed minimise S', let $\{d_i^*\}$ be an arbitrary set of real values that satisfy condition C_1. It simply has to be shown that

$$\sum_{i=1}^{N}(d_i - d_i^*)^2 \geq \sum_{i=1}^{N}(d_i - \hat{d}_i)^2.$$

Let

$$D_i^* = \sum_{j=1}^{i} d_j^*, \qquad \hat{D}_i = \sum_{j=1}^{i} \hat{d}_j.$$

Abel's formula, that $\sum_{i=1}^{N} a_i b_i = \sum_{i=1}^{N-1} A_i(b_i - b_{i+1}) + A_N b_N$,

where $A_i = \sum_{j=1}^{i} a_j$ are partial sums, will be needed in the following.

Write

$$\sum_{i=1}^{N}(d_i - d_i^*)^2 = \sum_{i=1}^{N}\{(d_i - \hat{d}_i) + (\hat{d}_i - d_i^*)\}^2$$

$$= \sum_{i=1}^{N}(d_i - \hat{d}_i)^2 + \sum_{i=1}^{N}(\hat{d}_i - d_i^*)^2 + 2\sum_{i=1}^{N}(d_i - \hat{d}_i)(\hat{d}_i - d_i^*).$$

Now

$$\sum_{i=1}^{N}(d_i - \hat{d}_i)(\hat{d}_i - d_i^*) = \sum_{i=1}^{N-1}(D_i - \hat{D}_i)(\hat{d}_i - \hat{d}_{i+1})$$

$$- \sum_{i=1}^{N-1}(D_i - \hat{D}_i)(d_i^* - d_{i+1}^*) + (D_N - \hat{D}_N)(\hat{d}_N - d_N^*). \quad (3.4)$$

Now $D_N - \hat{D}_N = 0$ since the last point of the greatest convex minorant and P_N are coincident. Consider $(D_i - \hat{D}_i)(\hat{d}_i - \hat{d}_{i+1})$. If the ith point on the greatest convex minorant is coincident with P_i then $D_i = \hat{D}_i$ and so the term is zero. On the other hand, if $\hat{D}_i < D_i$ then $\hat{d}_i = \hat{d}_{i+1}$ and so the term is again zero. Hence, since $D_i - \hat{D}_i \geq 0$ and because of the condition C_1, $d_i^* < d_{i+1}^*$ the final term left in (3.4), $-\sum_{i=1}^{N-1}(D_i - \hat{D}_i)(d_i^* - d_{i+1}^*)$, is positive. Hence

$$\sum_{i=1}^{N}(d_i - d_i^*)^2 \geq \sum_{i=1}^{N}(d_i - \hat{d}_i)^2 + \sum_{i=1}^{N}(\hat{d}_i - d_i^*)^2,$$

and so

$$\sum_{i=1}^{N}(d_i - d_i^*)^2 \geq \sum_{i=1}^{N}(d_i - \hat{d}_i)^2.$$

These $\{\hat{d}_{rs}\}$ giving S', and hence S, as a minimum, is the isotonic regression of $\{d_{rs}\}$ (using equal weights) with respect to the simple ordering of $\{\delta_{rs}\}$. Barlow *et al.* (1972) discuss the use of isotonic regression in a variety of situations and illustrate its use in the case of nonmetric MDS. In the MDS literature, isotonic regression is referred to as primary monotone least squares regression of $\{d_{rs}\}$ on $\{\delta_{rs}\}$.

So for the illustrative example

$$d_1 = d_2 = 2.45,\ d_3 = d_4 = d_5 = 3.83,\ d_6 = 4.3,$$

noting that $\hat{d}_1, \hat{d}_2$ are the mean of d_1 and d_2; $\hat{d}_3, \hat{d}_4, \hat{d}_5$ are the mean of d_3, d_4 and d_5; $\hat{d}_6$ is equal to d_6. The value of S is 0.14.

3.2.2 A configuration with minimum stress

With $\{\hat{d}_{rs}\}$ defined as the monotone least squares regression of $\{d_{rs}\}$ on $\{\delta_{rs}\}$, S is then termed the stress of the configuration; S^* is called the raw stress. The numerator T^* in the formula for stress is used as a normalizing factor allowing the stress to be dimension free.

A configuration is now sought that minimises the stress S. Minimisation of S is not a particularly easy task. The first step is to place all the coordinates of the points in X in a vector $\mathbf{x} = (x_{11}, \ldots, x_{1p}, \ldots, x_{np})^T$, a vector with np elements. The stress S is then regarded as a function of $\mathbf{x}$, and is minimised with respect to $\mathbf{x}$ in an iterative manner. The method of steepest descent is used, so that if $\mathbf{x}_m$ is the vector of coordinates after the mth iteration

$$\mathbf{x}_{m+1} = \mathbf{x}_m - \frac{\frac{\partial S}{\partial \mathbf{x}} \times sl}{|\frac{\partial S}{\partial \mathbf{x}}|},$$

where sl is the step length discussed later.

Now

$$\begin{aligned}
\frac{\partial S}{\partial x_{ui}} &= \frac{1}{2}\sqrt{\frac{T^*}{S^*}}\frac{(T^*\frac{\partial S^*}{\partial x_{ui}} - S^*\frac{\partial T^*}{\partial x_{ui}})}{T^{*2}} \\
&= \frac{1}{2}S\left(\frac{1}{S^*}\frac{\partial S^*}{\partial x_{ui}} - \frac{1}{T^*}\frac{\partial T^*}{\partial x_{ui}}\right) \\
\frac{\partial S^*}{\partial x_{ui}} &= 2\sum_{r,s}(d_{rs} - \hat{d}_{rs})\frac{\partial d_{rs}}{\partial x_{ui}} \\
\frac{\partial T^*}{\partial x_{ui}} &= 2\sum_{r,s} d_{rs}\frac{\partial d_{rs}}{\partial x_{ui}}.
\end{aligned}$$

For the Minkowski metric

$$\frac{\partial d_{rs}}{\partial x_{ui}} = d_{rs}^{1-\lambda}\sum_{r,s}(x_{ri} - x_{si})^{\lambda-1}(\delta^{ru} - \delta^{su})\text{signum}(x_{ri} - x_{si})$$

and hence

$$\frac{\partial S}{\partial x_{ui}} = S \sum_{r,s} (\delta^{ru} - \delta^{su}) \left[\frac{d_{rs} - \hat{d}_{rs}}{S^*} - \frac{d_{rs}}{T^*} \right] \times \frac{|x_{ri} - x_{si}|^{\lambda - 1}}{d_{rs}^{\lambda - 1}} \text{signum}(x_{ri} - x_{si})$$

as given by Kruskal (1964b).

A starting configuration giving $\mathbf{x}_0$ needs to be chosen. One possibility is to generate n points according to a Poisson process in a region of R^p. In its simplest form, this means simulating each individual coordinate for each point, independently from a uniform distribution on $[0, 1]$. There are several other suggested methods for choosing a starting configuration and these will be discussed in Section 3.6.

Once $\mathbf{x}_0$ has been chosen the method of steepest descent can then be employed to find a configuration with minimum stress using the following algorithm, which is summarised from Kruskal (1964b).

3.2.3 Kruskal's iterative technique

The following summarises the iterative technique used to find a configuration with minimum stress.

1. Choose an initial configuration.
2. Normalize the configuration to have its centroid at the origin and unit mean square distance from the origin. This is done since stress is invariant to translation, uniform dilation, and otherwise successive iterations of the procedure might have the configurations continually expanding or wandering around the plane.
3. Find $\{d_{rs}\}$ from the normalized configuration.
4. Fit $\{\hat{d}_{rs}\}$. It was seen that the monotonic least squares regression of $\{d_{rs}\}$ on $\{\delta_{rs}\}$ partitioned $\{\delta_{rs}\}$ into blocks in which the values of $\hat{d}_{rs}$ were constant, and equal to the mean of the corresponding d_{rs} values. In order to find the appropriate partition of $\{\delta_{rs}\}$, first the finest partition is used which has N blocks each containing a single δ_i, using the alternative notation. If this initial partition has $d_1 \leq d_2 \leq \ldots \leq d_N$, then $\hat{d}_i = d_i$ and this partition is the final one. Otherwise two consecutive blocks are amalgamated where $\delta_i > \delta_{i+1}$, and then

$\hat{d}_i = \hat{d}_{i+1} = (d_i + d_{i+1})/2$. Blocks are continually amalgamated and new $\hat{d}_i$'s found until the required partition is reached. Full details can be found in Kruskal (1964a) and Barlow *et al.* (1972). The required partition can also be found by considering the graph of the cumulative sums, D_i, and finding the greatest convex minorant. The slope, s_i, of D_i from the origin is D_i/i. The point with the smallest slope must be on the greatest convex minorant. All the points preceding this point are not on the minorant and their slopes can be removed from further consideration. The point with the next smallest slope is then found from those slopes remaining. This point is on the minorant, but the points between the preceding minorant point and this, are not. Their slopes are discarded. This procedure continues until the Nth point is reached. Once the greatest convex minorant has been established it is then an easy task to find $\{\hat{d}_i\}$.

5. Find the gradient $\frac{\partial S}{\partial \mathbf{x}}$. If $|\frac{\partial S}{\partial \mathbf{x}}| < \epsilon$, where ϵ is a preselected very small number, then a configuration with minimum stress has been found and the iterative process can stop. Note that this configuration could be giving a local minimum for the stress, and not the global minimum.
6. Find the new step length sl. Kruskal recommends the *ad hoc* rule that sl is changed at every step according to

$$\begin{aligned} sl_{\text{present}} = sl_{\text{previous}} &\times (\text{angle factor}) \\ &\times (\text{relaxation factor}) \\ &\times (\text{good luck factor}) \end{aligned}$$

where

$$\text{angle factor} = 4.0^{\cos^3 \theta},$$

θ = angle between the present and previous gradients,

$$\text{relaxation factor} = \frac{1.3}{1 + (5 \text{ step ratio})^5},$$

$$5 \text{ step ratio} = \min\left[1, \left(\frac{\text{present stress}}{\text{stress 5 iterations ago}}\right)\right],$$

$$\text{good luck factor} = \min\left[1, \frac{\text{present stress}}{\text{previous stress}}\right].$$

7. Find the new configuration

$$\mathbf{x}_{n+1} = \mathbf{x}_n - sl\frac{\frac{\partial S}{\partial \mathbf{x}}}{|\frac{\partial S}{\partial \mathbf{x}}|}$$

8. Go to step 2.

3.2.4 Nonmetric scaling of breakfast cereals

The 1993 Statistical Graphics Exposition organized by the American Statistical Association contained a data set on breakfast cereals, analyses of which by interested people could be presented at the Annual Meeting of the Association. Originally, observations on eleven variables were collected for seventy-seven different breakfast cereals. For clarity of graphical illustration, only those breakfast cereals manufactured by Kellogg are analysed here, reducing the number of cereals to twenty-three. The variables measured were: type (hot or cold); number of calories; protein (g); fat (g); sodium (mg); dietry fibre (g); complex carbohydrates (g); sugars (g); display shelf (1,2,3, counting from the floor); potassium (mg); vitamins and minerals (0, 25, or 100, respectively indicating none added; enriched up to 25% of the recommended daily amount; 100% of the recommended daily amount). Two dimensional nonmetric scaling was carried out on the Kellogg breakfast cereals, first measuring dissimilarity by Euclidean distance on the variables standardized to have zero mean and unit variance. The stress was 14%. Then using Gower's general dissimilarity coefficient, a configuration was found with a 15% stress value. Table 3.1 lists the twenty-three cereals, and Figure 3.2 shows the final configuration. Connoisseurs of breakfast cereals may wish to interpret the configuration. One interesting feature is the spatial pattern of fibre content of the cereals when this is plotted for each cereal at its position in the configuration. Figure 3.3 shows this. Low fibre content is to the lower left of the configuration, high fibre content to the upper right.

Table 3.1 *The twenty-three breakfast cereals*

Cereal		**Cereal**	
All Bran	AllB	Just Right Fruit and Nut	JRFN
All Bran with extra fibre	AllF	Meuslix Crispy Blend	MuCB
Apple Jacks	AppJ	Nut and Honey Crunch	Nut&
Cornflakes	CorF	Nutri Grain Almond Raisin	NGAR
Corn Pops	CorP	Nutri Grain Wheat	NutW
Cracklin Oat Bran	Crac	Product 19	Prod
Crispix	Cris	Raisin Bran	RaBr
Froot Loops	Froo	Raisin Squares	Rais
Frosted Flakes	FroF	Rice Crispies	RiKr
Frosted Mini Wheats	FrMW	Smacks	Smac
Fruitful Bran	FruB	Special K	Spec
Just Right Crunch Nuggets	JRCN		

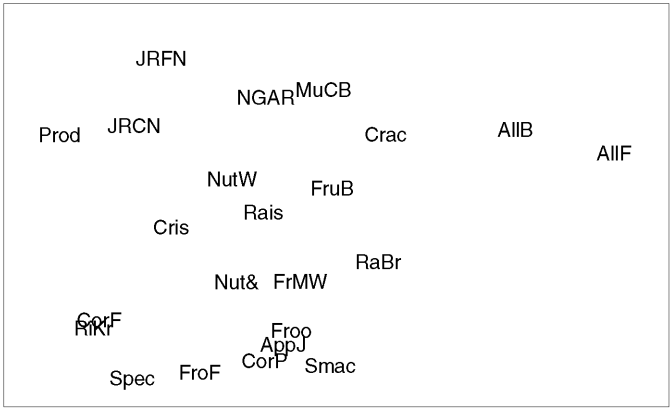

Figure 3.2 *Nonmetric scaling of Kellog breakfast cereals.*

Figure 3.4 shows a plot of the dissimilarities $\{\delta_{rs}\}$ against distances $\{d_{rs}\}$ for the configuration together with the isotonic regression of $\{d_{rs}\}$ on $\{\delta_{rs}\}$, i.e. the disparities. This is known as the Shepard diagram and is useful in assessing the fit. Note that the Shepard diagram is usually plotted with the axes of Figure 3.4 reversed in accordance with usual regression practice. Preference depends on how the figure is to be viewed, either the isotonic regression of $\{d_{rs}\}$ on $\{\delta_{rs}\}$, or disparities plotted against $\{d_{rs}\}$.

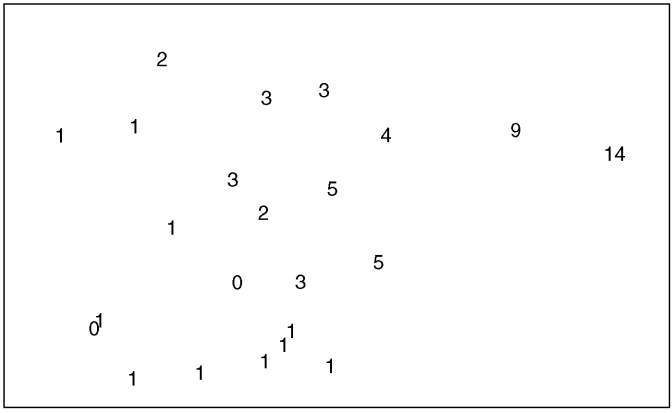

Figure 3.3 *Fibre content of the cereals.*

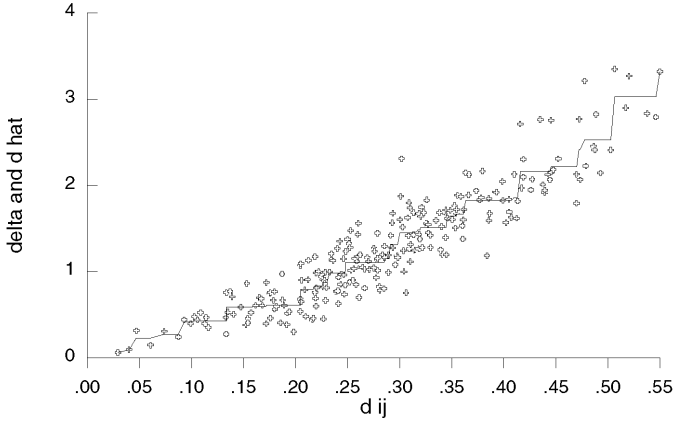

Figure 3.4 *Shepard diagram for the breakfast cereal data.*

3.2.5 STRESS1/2, monotonicity, ties and missing data

The stress function (3.3) used by Kruskal is often referred to as

STRESS1. An alternative stress function is sometimes employed in nonmetric MDS, given by

$$S = \left\{ \frac{\sum_{r,s}(d_{rs} - \hat{d}_{rs})^2}{\sum_{r,s}(d_{rs} - d_{..})^2} \right\}^{\frac{1}{2}},$$

where $d_{..}$ is the mean of the distances $\{d_{rs}\}$ over $1 \leq r < s \leq n$. This is referred to as STRESS2. Only the normalizing factor differs in the two definitions of stress.

Recall condition C_1 that

$$\hat{d}_{rs} \leq \hat{d}_{tu} \quad \text{whenever} \quad \delta_{rs} < \delta_{tu}.$$

This is referred to as the weak monotonicity condition and the fitted $\{\hat{d}_{rs}\}$ are weakly monotone with the data. This condition can be replaced by condition C_2 that

$$\hat{d}_{rs} < \hat{d}_{tu} \quad \text{whenever} \quad \delta_{rs} < \delta_{tu} \quad \text{(Condition } C_2\text{)}.$$

This is the strong monotonicity condition and the fitted $\{\hat{d}_{rs}\}$ are strongly monotone with the data. This latter case will give larger stress values since more restriction is placed on the configuration.

There are two ways that ties in the dissimilarities can be treated. The primary approach is:

$$\text{If } \delta_{rs} = \delta_{tu} \text{ then } \hat{d}_{rs} \text{ is not necessarily equal to } \hat{d}_{tu}.$$

The secondary approach is:

$$\text{If } \delta_{rs} = \delta_{tu} \text{ then } \hat{d}_{rs} = \hat{d}_{tu}.$$

The secondary approach is very restrictive and has been shown by many authors, for example Kendall (1971) and Lingoes and Roskam (1973), to be less satisfactory than the primary approach. Kendall (1977), in an appendix to Rivett (1977), introduces a tertiary approach to ties which is a hybrid between the primary and secondary approaches.

One desirable aspect of nonmetric MDS is that if some of the dissimilarities are missing then they are simply left out of the formula for stress, and the fitting algorithm proceeds without them.

3.3 The Guttman approach

Guttman (1968) took a different approach to Kruskal (1964a, b) in setting up nonmetric MDS. He defined a loss function called the coefficient of alienation which was basically equivalent to the stress function of Kruskal, but which led to a different algorithm for minimisation. His approach will only be described briefly.

Let the rank ordered dissimilarities $\{\delta_{rs}\}$ be placed in a vector $\boldsymbol{\delta}$ with elements δ_r $(r = 1, \ldots, N)$. Let the distances $\{d_{rs}\}$ from a configuration be placed in a vector $\mathbf{d}$ in order corresponding to $\{\delta_r\}$. Let $\mathbf{E}$ be an $N \times N$ permutation matrix which places the elements of $\mathbf{d}$ into ascending order. Disparities are then defined by the rank-image $\mathbf{d}^*$ of $\mathbf{d}$, given by

$$\mathbf{d}^* = \mathbf{E}\mathbf{d}$$

The coefficient of continuity, μ, for the configuration is given by

$$\mu = \sqrt{\frac{(\sum d_r d_r^*)^2}{\sum d_r^2 \sum d_r^{*2}}}$$

which has the value unity for a perfect fit. In order to find a best fitting configuration, the coefficient of alienation, K, given by

$$K = \sqrt{1 - \mu^2}$$

is minimised using the method of steepest descent.

Example
Suppose there are only three objects, with dissimilarities

$$\delta_{12} = 4,\ \delta_{13} = 1,\ \delta_{23} = 3,$$

with "self-dissimilarities" zero. Let a particular configuration have distances between its points

$$d_{12} = 2,\ d_{13} = 4,\ d_{23} = 5.$$

Then in the single suffix notation, and ordering the dissimilarities,

$$\begin{array}{lcccc} \delta_i & : & 1, & 3, & 4 \\ d_i & : & 4, & 5, & 2. \end{array}$$

The permutation matrix $\mathbf{E}$ is

$$\mathbf{E} = \begin{bmatrix} 0 & 0 & 1 \\ 1 & 0 & 0 \\ 0 & 1 & 0 \end{bmatrix}$$

giving $\mathbf{d}^* = (2, 4, 5)^T$.

The coefficient of continuity, μ is then 0.84, and the coefficient of alienation K is 0.54.

Guttman's paper is much more detailed than this simple exposition, dealing with strong and weak monotonicity and ties in the data. It can be shown that minimising K is equivalent to minimising stress S. Guttman and Lingoes produced a series of computer programs for nonmetric MDS based on the Guttman approach, and these are included in their SSA-I (smallest space analysis) series of programs.

They use two main strategies for minimisation. Their single phase G-L algorithm minimises

$$\phi^* = \sum (d_{rs} - d^*_{rs})^2,$$

using the method of steepest descent. For brevity the various derivatives similar to those for the Kruskal algorithm are not written down here, but can be found in Lingoes and Roskam (1973), or Davies and Coxon (1983). Their double-phase G-L algorithm first minimises ϕ^* with respect to $\{d_{rs}\}$ as its first phase, i.e. finds the configuration that best fits the current values $\{d^*_{rs}\}$. The second phase then finds new values $\{d^*_{rs}\}$ which best fit the new configuration.

3.4 A further look at stress

Several authors have studied stress in more detail. We report on some of their results.

Differentiability of stress

Because of the complicated nature of stress through the involvement of least squares monotone regression, continuity and differentiability of stress and its gradient could cause concern when seeking a minimum. However Kruskal (1971) shows that $\sum(d_i - \hat{d}_i)^2$ has gradient vector with ith element $2(d_i - \hat{d}_i)$ and that the gradient exists and is continuous everywhere.

De Leeuw (1977a) noted that the Euclidean distance between

two points, $d_{rs} = \{\sum_i (x_{ri} - x_{si})^2\}^{\frac{1}{2}}$ is not differentiable in a configuration if points x_r and x_s are coincident. De Leeuw (1977b) shows that gradient algorithms can be modified to cope with the problem. De Leeuw (1984) shows that when stress is minimised coincident points cannot occur.

Limits for stress

The minimum possible value of Kruskal's stress is zero, implying a perfect fit. However, a zero stress value can imply that the final configuration is highly clustered with a few tight clusters of points.

De Leeuw and Stoop (1984) give upper bounds for stress. Let STRESS1 be denoted by $S(n, p)$, where the number of points, n, and the dimension, p, of the configuration are fixed. They show that

$$S(n, p) \leq \kappa(n, p),$$

where

$$\kappa(n, p) = \min_{x_{ri}} \left\{ \sqrt{\frac{\sum_{r,s}(d_{rs} - d_{..})^2}{\sum_{r,s} d_{rs}^2}} \right\},$$

with $d_{..}$ the usual mean of $\{d_{rs}\}$ over r, s.

This result is easily seen as

$$\sum_{r,s}(d_{rs} - \hat{d}_{rs})^2 \quad \leq \quad \sum_{r,s}(d_{rs} - d_{..})^2,$$

since disparities defined as $\hat{d}_{rs} = d_{..}$ for all r, s satisfy the monotonicity requirement, but obviously do not minimise the stress or raw stress over the disparities, since this is achieved by $\{\hat{d}_{rs}\}$, the isotonic regression of $\{d_{rs}\}$ on $\{\delta_{rs}\}$. Dividing by $\sum_{r,s} d_{rs}^2$, taking square roots and minimising over the configuration $\{x_{ri}\}$ proves the result.

De Leeuw and Stoop (1984) then go on to show that

$$\kappa(n, p) \leq \kappa(n, 1) = \sqrt{\frac{n-2}{3n}} \leq \frac{1}{\sqrt{3}} = 0.5774.$$

It is easily seen that $\kappa(n, p) \leq \kappa(n, 1)$ since in minimising

$$\sqrt{\frac{\sum_{r,s}(d_{rs} - d_{..})^2}{\sum_{r,s} d_{rs}^2}} \tag{3.5}$$

over the p dimensional configuration $\{x_{ri}\}$, it is always possible to

take the configuraton as the projection onto the single axis used for $\kappa(n,1)$ (or any other subspace of dimension less than p).

To calculate $\kappa(n,1)$, assume without loss of generality $\sum x_r = 0$, and $\sum x_r^2 = 1$. Then

$$\sum_{r,s} d_{rs}^2 = \frac{1}{2}\sum_{r=1}^{n}\sum_{s=1}^{n} d_{rs}^2 = \frac{1}{2}\sum_{r=1}^{n}\sum_{s=1}^{n}(x_r - x_s)^2 = n,$$

and hence minimising (3.5) is equivalent to minimising

$$\sqrt{1 - \frac{(n-1)}{2} d_{..}^2},$$

which in turn is equivalent to maximising $d_{..}$.

Reordering the points $\{x_r\}$ such that $x_1 \leq x_2 \leq \ldots \leq x_n$, it is seen that $d_{..}$ is given by

$$d_{..} = \frac{2}{n(n-1)}\sum_{r=1}^{n}(2r - n - 1)x_r.$$

Now $d_{..}$ is maximised when $\{x_r\}$ are equally spaced along the axis. Let $x_r = a + br$. Hence

$$\sum(a + br) = na + \tfrac{1}{2}n(n+1)b = 0,$$

and

$$\sum(a + br) = na^2 + n(n+1)ab + \tfrac{1}{6}n(n+1)(2n+1)b^2 = 1.$$

Solving gives

$$x_r = \sqrt{\frac{12}{n(n^2-1)}}\left\{r - \frac{(n+1)}{2}\right\}.$$

Hence $\kappa(n,1) = (\frac{n-2}{3n})^{\frac{1}{2}}$ after some algebra, and it is easily seen that $\kappa(n,1)$ tends to $1/\sqrt{3}$ as n tends to infinity.

De Leeuw and Stoop also give an upper bound for $\kappa(n,2)$ and show

$$\kappa(n,2) \leq \kappa^*(n,2) = \left\{1 - \frac{2\cot^2(\pi/2n)}{n(n-1)}\right\}^{\frac{1}{2}} \leq \left\{1 - \frac{8}{\pi^2}\right\}^{\frac{1}{2}} = 0.4352.$$

The value of $\kappa^*(n,2)$ is the value of (3.5) if $\{x_{ri}\}$ consists of n equally spaced points on a circle. Note that $\kappa(n,2)$ is not necessarily equal to $\kappa^*(n,2)$.

For STRESS2 it can easily be seen from (3.5) that the upper limit for STRESS2 is unity.

3.4.1 Interpretation of stress

Since Kruskal's 1964 papers in *Psychometrika* there have been many investigations of stress using Monte Carlo methods. Various findings are reported below.

Stenson and Knoll (1969) suggested that in order to assess dimensionality and fit of the final configuration, stress values for a set of dissimilarity data should be compared with those obtained using random permutations of the first $\binom{n}{2}$ integers as dissimilarities. They used n=10(10)60, p=1(1)10 in a Monte Carlo study, using three random permutations for each combination of n and p. They plotted mean stress against dimension p, for a fixed number of objects n. They managed with only three random permutations since the variability of stress was small. Spence and Ogilvie (1973) carried out a more thorough Monte Carlo study using fifteen replications for each n, p combination. De Leeuw and Stoop (1984) carried out a similar exercise using one hundred random rankings. Spence and Ogilvie's results for mean and standard deviation of stress are shown in Figure 3.5. The mean stress is useful since it gives a guide as to whether the stress obtained in a study is too large or not for a reasonably fitting final configuration. Levine (1978) carried out a similar exercise using Kruskal's STRESS2 in place of STRESS1.

Klahr (1969) generated $\binom{n}{2}$ dissimilarities $\{\delta_{rs}\}$ independently from a uniform distribution on [0,1], choosing n as 6,7,8,10,12 and 16, p=1(1)5, and subjected them to nonmetric MDS. This was done one hundred times for smaller values of n and fifty times for larger values, for each value of p. The sample distribution function for stress was plotted, as well as a plot of mean stress. Klahr noted that it was often possible to obtain a well-fitting final configuration of points for small values of n even when the dissimilarities were randomly generated in this manner.

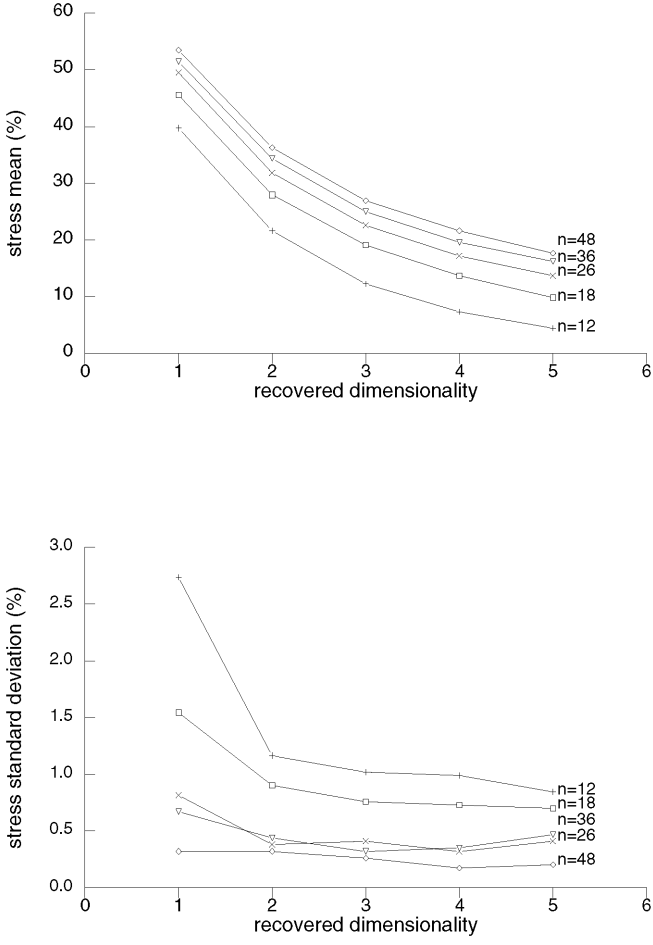

Figure 3.5 *Percentage mean stress and standard deviation obtained from random rankings.*

Spence (1970) generated configurations of points according to a p dimensional Poisson process within a unit hypersphere. To each individual coordinate an independent normally distributed random "error" was added. Dissimilarities were then taken as the Euclidean

distances between the pairs of points and these were subjected to nonmetric MDS. The stress values obtained in attempting to retrieve the original configurations were used to compare the frequency with which the three MDS programs, TORSCA, MDSCAL and SSA-1 got stuck in local minimum solutions. Spence (1972) went on to compare the three programs in more depth. Wagenaar and Padmos (1971) carried out a simulation study of stress in a similar manner to that of Spence using a realization of a p dimensional Poisson process. However their dissimilarities were taken as the Euclidean distance between pairs of points in the configuration, together with multiplicative error, introduced by multiplying the distances by an independent random number generated from a normal distribution. They used their stress results in a method to assess the required dimensionality of the configuration. This method is explained in Section 3.5.

Sherman (1972) used the p dimensional Poisson process to generate configurations, choosing n=6, 8, 10, 15, 30, p=1, 2, 3. An independent normal error was added to each coordinate and dissimilarities were generated using the Minkowski metric with $\lambda = 1, 2, 3$. Sherman used analysis of variance to investigate the factors most affecting nonmetric MDS results, and concluded with basic common sense suggestions, such as that the hypothesized structure should be of low dimension, measurement errors should be minimised, and various dimensions should be tried for the configuration with varying λ in the Minkowski metric.

Sibson *et al.* (1981) consider more sophisticated models for producing dissimilarities from distances obtained from a configuration of points before attempting to recover the orginal configuration using nonmetric MDS. Their first model is based on binary data and the Hamming distance. Suppose there are k binary variables measured on each of the objects. Then the Hamming distance between objects r and s is simply the number of variables in which the two objects differ, and thus is very closely related to the dissimilarity coefficients of Chapter 1. Consider two points r and s in a p dimensional Euclidean space together with a Poisson hyperplane process where random hyperplanes cut the space into two half spaces. The two half spaces are denoted zero and one arbitrarily. Figure 3.6 shows Euclidean space with p=2, and three hyperplanes, with associated zeros and ones allocated.

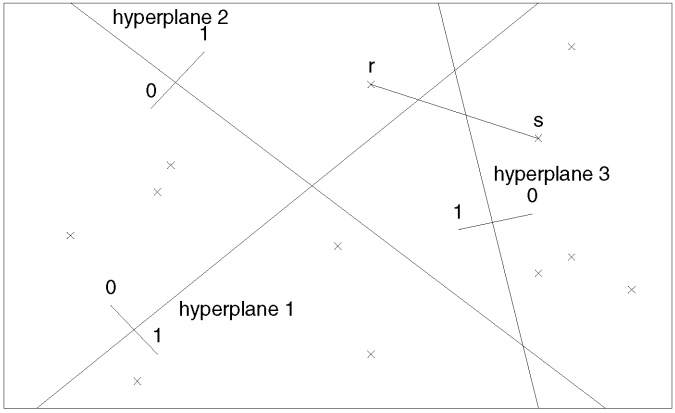

Figure 3.6 *Points r and s in two dimensional Euclidean space with three random hyperplanes*

The binary data associated with the point r is (0,1,1) and that with point s (1,0,1). The Hamming distance is 2. In general, the Hamming distance is equal to the number of hyperplanes crossed in going from one point to another, and can be randomly generated by randomly locating these hyperplanes. From Figure 3.6, the number of hyperplanes crossing the line between points r and s is two, in agreement with the data. The number of hyperplanes crossing the line between point r and point s follows a Poisson distribution with parameter equal to λd_{rs} where λ is the intensity of the process. Conditioned upon the total number of hyperplanes the distribution of the Hamming distance is a binomial distribution. Thus for their first model, Sibson *et al.* generate a realization from a p dimensional Poisson process and then split the space with Poisson hyperplanes. The dissimilarity between points r and s is then taken as the Hamming distance between these points.

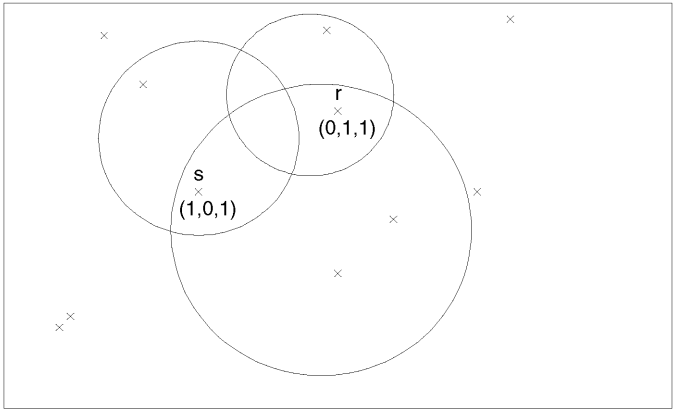

Figure 3.7 *Model for binary data and the Jaccard coefficients*

Their second model is similar to the first model but has dependence between points removed. The dissimilarity δ_{rs} is taken as a random number from a Poisson distribution with parameter λd_{rs}.

Sibson *et al.*'s third model generates random Jaccard coefficients. Each binary variable is considered to measure presence (1), or absence (0). A realization of a p dimensional Poisson process again starts off the model. Then for each variable a p dimensional hypersphere is generated with radius randomly chosen from some distribution, and centre a point in another realization of a Poisson process. Inside each hypersphere, the variable assumes the value unity, and outside the hypersphere the value zero. For example, Figure 3.7 shows ten points and three variables for a two dimensional space. The point r has binary data associated with it (0,1,1) and point s has (1,0,1), and hence $\delta_{rs} = 1/3$. If r and s were both to lie outside all the spheres, the dissimilarity would be unity.

For their fourth model, points are again generated from a p dimensional Poisson process, but then Dirichelet tessellations are found; see Green and Sibson (1978). Figure 3.8 shows a two dimensional example. Dirichelet tessellations are found for each point r, a surrounding polygon where all points of the space within the polygon are closer to r than any other. The Wilkinson metric for points r and s is then the minimum number of boundaries crossed

to get from one point to the other. The dissimilarity δ_{rs} is then taken as this Wilkinson distance.

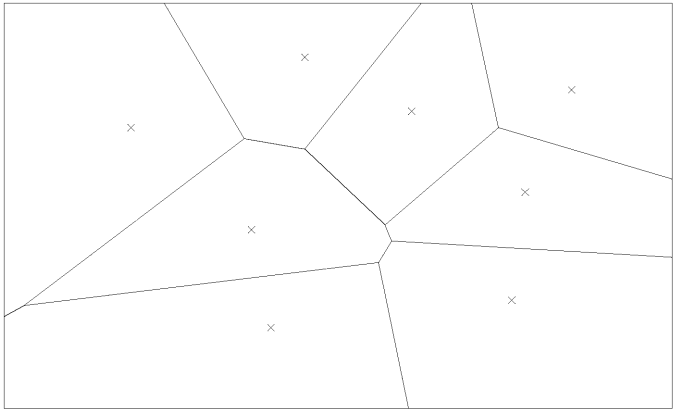

Figure 3.8 *Dirichelet tessellation model*

Sibson *et al.* (1981) use the Procrustes statistic (see Chapter 5) to compare recovered configurations using nonmetric MDS with the original configurations. They use three scaling methods: classical MDS, Kruskal's nonmetric MDS, and least squares scaling. Among their conclusions, they maintain that classical MDS compares well with nonmetric MDS for most "Euclidean-like" models, but not for "non-Euclidean-like" models. Least squares scaling is slightly superior to nonmetric MDS for the Euclidean-like models, but inferior for the Jaccard coefficient model. Nonmetric MDS is never significantly worse than the other methods if it is given a reasonable starting configuration.

The models in Sibson *et al.* (1981) have been described in detail here, even though their investigation does not deal directly with stress, because they use models which generate dissimilarities of an interesting nature. Most other Monte Carlo investigations mundanely have additive or multiplicative noise applied to coordinates or distances in order to produce dissimilarities.

All the stress studies have shown that stress decreases with increase of dimension p, increases with the number of points n, and that there is not a simple relationship between stress, n and p. By using a different model for error, Cox and Cox (1990), and Cox

and Cox (1992) found a simple relationship between stress, n and p. Up till then, most Monte Carlo investigations started with a configuration of points generated according to a Poisson process. Cox and Cox considered configurations covering a wide range of spatial patterns; see for example, Ripley (1981), Diggle (1983) or Cressie (1991) for full discussion of spatial stochastic models.

At one extreme was the highly regular process of a rectangular grid. For a pattern with less regularity, this rectangular grid had its points independently radially displaced by an amount (R, Θ) where R has a Rayleigh distribution (pdf $r\sigma^{-2}\exp(-\frac{1}{2}r^2/\sigma^2)$) and Θ a uniform distribution on $[0, 2\pi]$. The further the average displacement the less regular the process becomes, and in the limit the process tends to a Poisson process. At the other extreme, points were generated according to a Poisson cluster process. Here cluster centres are generated according to a Poisson process and then a fixed number of cluster members are positioned at radial points (R, Θ) from the cluster centre, where R, Θ are as above. As the points in a cluster are moved further and further away from their cluster centres, the process tends towards a Poisson process again. Thus a very wide range of spatial patterns were considered ranging from extreme regularity on one hand, through complete spatial randomness (i.e. the Poisson process), to extreme aggregation on the other. Figure 3.9 shows realizations for the three models.

For each configuration generated, dissimilarities were defined as

$$\delta_{rs} = d_{rs}(1 - \epsilon_{rs}),$$

where d_{rs} is the usual Euclidean distance and $\{\epsilon_{rs}\}$ are independent uniformly distributed random variables on the interval $[0, l]$. The value of l can be considered as the noise level. Several values of n and l were chosen. The number of dimensions, p, was chosen as only $p = 2$ in Cox and Cox (1990), but results were extended for other values of p in Cox and Cox (1992). Nonmetric MDS was used on the dissimilarities generated for each configuration and the stress recorded. Each model was replicated ten times and the average stress found. In keeping with other authors' results, the variability in stress for fixed n, p and l was extremely small. For two dimensional initial configurations, together with a derived configuration also in two dimensions, the following results were observed.

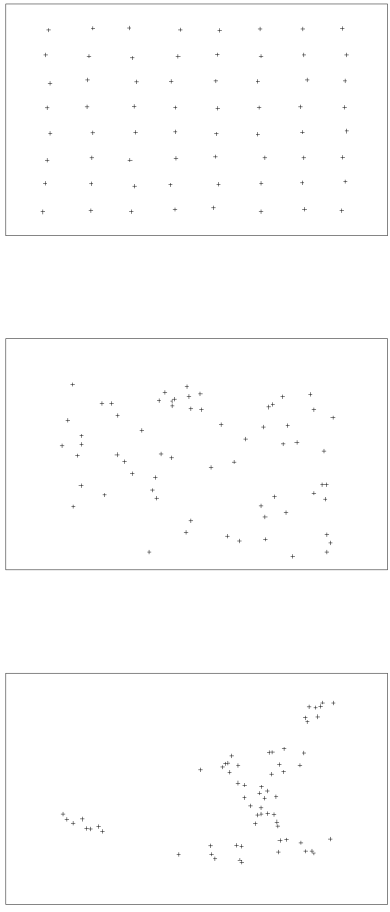

Figure 3.9 *Realizations of the three models considered by Cox and Cox: regular process; Poisson process; Poisson cluster process.*

Figure 3.10 shows average stress plotted against the "noise level" l for (i) a Poisson process, $n = 36$; (ii) a Poisson process, $n = 64$; (iii) a rectangular grid, $n = 36$; (iv) a regular process, $n = 64$, $\sigma^2 = 0.25$; (v) a Poisson cluster process, 16 clusters of size 4,

$\sigma^2 = 0.1$, and (vi) a Poisson cluster process, 4 clusters of size 16, $\sigma^2 = 0.1$.

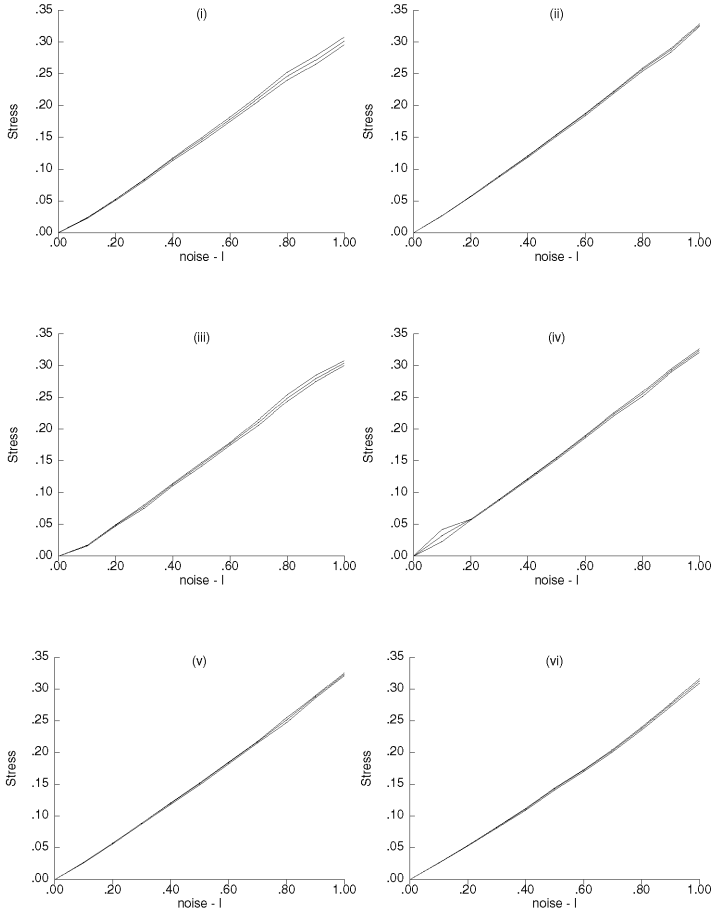

Figure 3.10 *Stress plotted against noise l for various spatial models*

The remarkable result is that with this noise model, stress is proportional to noise level l ($l \doteq 3 \times$ stress) whatever the value of n and for all reasonable spatial patterns of points (i.e. ones which

are not comprised of a few very tight clusters). This means that if the model is reasonable then stress levels for different sets of dissimilarities can be directly compared for any differing number of objects and for any spatial pattern formed by the final configuration of points. For dimensions other than two, similar results were found by Cox and Cox (1992), but with not such a strong linear relationship between stress and l. It should be noted that these results only hold when the dimension of the configuration derived by MDS is the same as that of the original configuration used to generate the dissimilarities.

3.5 How many dimensions?

For illustrative purposes, the obviously preferred number of dimensions to be chosen for nonmetric MDS is two. Configurations in three dimensions can be illustrated using three dimensional plotting procedures from various statistical packages, such as SAS, SOLO and STATISTICA. However, a less well-fitting configuration in two dimensions may be preferable to one in several dimensions where only projections of points can be graphically displayed.

To choose an appropriate number of dimensions, Kruskal (1964a) suggests that several values of p, the number of dimensions, are tried and the stress of the final configuration plotted against p. Stress always decreases as p increases. Kruskal suggests that p is chosen where the "legendary statistical elbow" is seen in the graph. For the breakfast cereal data of Section 3.2.4 this was done and results are shown in Figure 3.11.

The "elbow" appears to be at $p = 4$. However it has been noted that often there is no sharp flattening of stress in these diagrams and that an elbow is hard to discern.

Wagenaar and Padmos (1971) suggested the following method for choosing the appropriate number of dimensions. Dissimilarities are subjected to nonmetric MDS in 1, 2, 3,... dimensions, and the values of stress noted in each case, say S_1, S_2, S_3,... . These are then compared to the stress results from Monte Carlo simulations where dissimilarities are generated from distances in spatial configurations of points, together with random noise. The level of noise, σ_1 needed in one dimension to give stress S_1 is noted. Then for two dimensions, S_2 is compared with S_2^E, the "expected stress" for two dimensions with noise level σ_1. If S_2 is significantly less than S_2^E then the second dimension is definitely needed. The noise level

σ_2, needed to produce a stress level S_2 in two dimensions, is found, and then the "expected stress" S_3^E, for three dimensions with this noise level, σ_2. The stress S_3 for three dimensions is then compared with S_3^E. This process continues until stress is comparable to the expected stress, implying that there is no gain to be made in increasing the number of dimensions beyond that point.

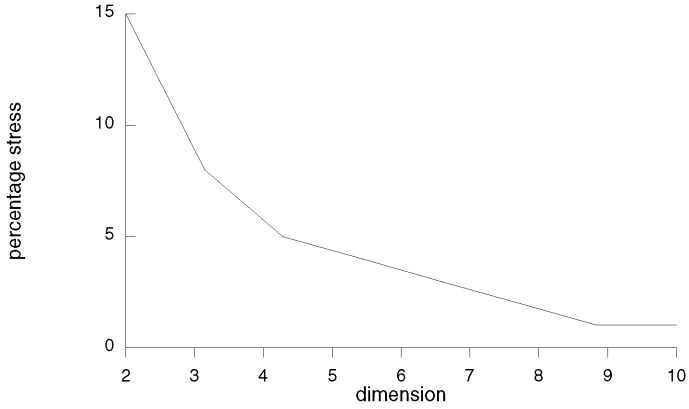

Figure 3.11 *Stress plotted against dimension for the breakfast cereal data*

3.6 Starting configurations

One possibility for a starting configuration for nonmetric MDS algorithms is simply to use an arbitrary one. Points can be placed at the vertices of a regular p dimensional lattice for instance, or could be generated as a realization of a p dimensional Poisson process. This latter case simply requires all coordinates to be independently generated from a uniform distribution on $[-1, 1]$ say, and the configuration is then normalized in the usual manner to have centroid at the origin and mean squared distance of the points from the origin, unity. It is always recommended that several different starting configurations are tried in order to avoid local minimum solutions.

If metric MDS is used on the data initially, the resulting configuration can be used as a starting configuration for nonmetric MDS.

Guttman (1968) and Lingoes and Roskam (1973) suggested the

following for finding a starting configuration. Let matrix $\mathbf{C}$ be defined by $[\mathbf{C}]_{rs} = c_{rs}$, where

$$\begin{aligned} c_{rs} &= 1 + \sum_s \rho_{rs}/N \quad (r = s) \\ &= 1 - \rho_{rs}/N \quad (r \neq s), \end{aligned}$$

where N is the total number of dissimilarities $\{\delta_{rs}\}$, and ρ_{rs} is the rank of δ_{rs} in the numerical ordering of $\{\delta_{rs}\}$. The principal components of $\mathbf{C}$ are found and the initial configuration is given by the eigenvectors of the first p principal components, but ignoring the one with constant eigenvector.

3.7 Interesting axes in the configuration

A simple method for finding meaningful directions or axes within the final configuration is to use multiple linear regression. The method is explained in Kruskal and Wish (1978). An axis is found for a variable, y, related to the objects, or even one of the original variables used in defining the dissimilarities. This variable is taken as the dependent variable. The independent variables are the coordinates of the points in the final configuration.

The regression model is then

$$\mathbf{y} = \mathbf{X}\boldsymbol{\beta} + \boldsymbol{\epsilon},$$

where $\mathbf{y}$ is the vector of observations $\{y_i\}$ $(i = 1, \ldots, n)$, $\mathbf{X}$ is the $n \times (p + 1)$ matrix consisting of a column of ones followed by the coordinates of the points in the final configuration, $\boldsymbol{\beta}$ is the parameter vector, and $\boldsymbol{\epsilon}$ the "error" vector.

The least squares estimate of $\boldsymbol{\beta}$ is given by

$$\hat{\boldsymbol{\beta}} = (\mathbf{X}^T\mathbf{X})^{-1}\mathbf{X}^T\mathbf{y}.$$

As long as the regression has a reasonable fit, tested either by an analysis of variance or by the multiple correlation coefficient, then an axis for the variable can be defined through the origin of the configuration and using the direction cosines

$$\hat{\beta}_i / \sqrt{\sum \hat{\beta}_i^2} \quad (i = 1, \ldots, p).$$

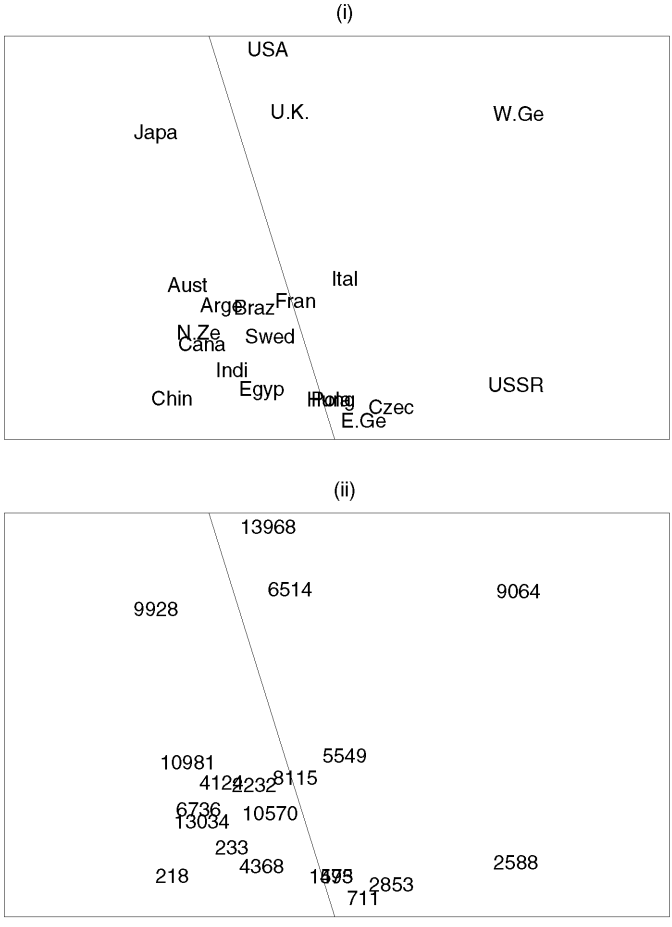

Figure 3.12 (i) *Nonmetric MDS of the trading data, together with Figure 3.12 (ii) the gross domestic product per capita axis.*

Example

Data were taken from the *New Geographical Digest* (1986) on which countries traded with which other countries. Twenty countries were chosen and their main trading partners were noted. If significant trade occurred between country r and country s, then x_{rs} was put equal to unity, and zero otherwise. From these binary data, dissimilarities were calculated using the Jaccard coefficient. Also recorded for the various countries was the gross national product

per capita (gnp/cap). The dissimilarities were then subjected to two dimensional nonmetric MDS. Figure 3.12 (i) shows the final configuration, the stress for which was 11%, implying a reasonable fit. From the figure, Japan, the USA and the UK can be seen to be separated from the bulk of the countries, while West Germany (as it was then) and USSR (also now changed) are also singled out.

The variable gnp/cap was regressed on the coordinates of the points in the final MDS configuration giving an adjusted coefficient of multiple determination of 42%. Although the fit of gnp/cap is not particularly good, a meaningful axis arises using the regression coefficients to define its direction. This is also shown in Figure 3.12 (i) Shown in Figure 3.12 (ii) is the same plot but with gnp/cap replacing country names. There are interesting positions taken up by some of the countries, for example Sweden, Canada and the UK. The reader is invited to delve further into the plots.

CHAPTER 4

Further aspects of multidimensional scaling

4.1 Other formulations of MDS

Schneider (1992) formulates MDS as a continuum that has metric MDS at one end of the continuum and nonmetric MDS at the other. Let f_μ be the logistic function

$$f_\mu(y) = \frac{1}{1 + e^{-\mu y}}$$

where μ is the continuum parameter, $(0 < \mu < \infty)$. Schneider uses the loss function

$$L_\mu = \sum_{\substack{r \le s, r' \le s' \\ (r,s) \ll (r's')}} \left[f_\mu(d_{rs}^2 - d_{r's'}^2) - f_\mu(\delta_{rs}^2 - \delta_{r's'}^2) \right]^2,$$

which is minimised for given μ. Here $(r, s) \ll (r', s')$ means $r < r'$ or if $r = r'$ then $s < s'$.

For $\mu = 0$ the loss function to be minimised is

$$L_0 = \sum_{\substack{r \le s, r' \le s' \\ (r,s) \ll (r's')}} \left[(d_{rs}^2 - d_{r's'}^2) - (\delta_{rs}^2 - \delta_{r's'}^2) \right]^2,$$

For $\mu = \infty$ the loss function is

$$L_\infty = \sum_{r,s,r',s'} X_{rsr's'}$$

where

$$X_{rsr's'} = \begin{cases} 1 & \text{if } d_{rs} > d_{r's'} \text{ but } \delta_{rs} < \delta_{r's'} \\ 1 & \text{if } d_{rs} < d_{r's'} \text{ but } \delta_{rs} > \delta_{r's'} \\ 0.25 & \text{if } d_{rs} \neq d_{r's'} \text{ but } \delta_{rs} = \delta_{r's'} \\ 0.25 & \text{if } d_{rs} = d_{r's'} \text{ but } \delta_{rs} \neq \delta_{r's'} \\ 0 & \text{if otherwise.} \end{cases}$$

As $\mu \to 0$, L_0 is essentially minimised leading to a metric MDS

formulation. As $\mu \to \infty$, L_∞ is minimised leading to a nonmetric formulation. A general μ gives a formulation between the two.

Trosset (1998) gives a different formulation for nonmetric scaling. Let $\mathbf{B} = [b_{rs}]$ where $b_{rs} = -\frac{1}{2}(\delta_{rs} - \delta_{r.} - \delta_{.s} + \delta_{..})$. Let $\hat{\mathbf{D}} = [\hat{\delta}_{rs}]$ be a matrix of "disparities". Let $\hat{b}_{rs} = -\frac{1}{2}(\hat{\delta}_{rs} - \hat{\delta}_{r.} - \hat{\delta}_{.s} + \hat{\delta}_{..})$. Trosset's formulation is to find $\mathbf{B}$ that minimises the loss function

$$\sum_r \sum_s (b_{rs} - \hat{b}_{rs})^2,$$

subject to $\mathbf{B}$ being a symmetric positive semi-definite matrix of rank less than or equal to p, and $\hat{\mathbf{D}}$ the matrix of disparaties such that the rank order of $\{\hat{\delta}_{rs}\}$ is the same as the rank order of the original dissimilarities $\{\delta_{rs}\}$, and $\sum_r \sum_s \hat{\delta}_{rs}^2 \geq \sum_r \sum_s \delta_{rs}^2$. Trosset suggests a gradient projection method for the minimisation. From $\mathbf{B}$ the coordinate matrix, $\mathbf{X}$, for the points in the MDS configuration can be found in the usual manner. From the formulation, the mix of metric and nonmetric scaling can be seen.

In Chapter 3, Kruskal's steepest descent algorithm for minimising STRESS was described in detail. It is the algorithm used in the nonmetric scaling program on the enclosed CD-ROM. The algorithm could be viewed as rather old fashioned now, as more up to date algorithms have been proposed by various authors. Some algorithms have already been referred to in Sections 2.4 and 2.6 on least squares scaling and unidimensional scaling. This monograph is not the place to describe these algorithms fully, since a collection of such algorithms with their descriptions and properties could easily form the content of a monograph in their own right. Takane *et al.* (1977) developed an alternating least squares algorithm for multidimensional scaling (ALSCAL). This algorithm is discussed in Chapter 11 along with SMACOF, developed by de Leeuw (1977b). Kearsley *et al.* (1994) review some of the algorithms for MDS and suggest one of their own. Klock and Buhmann (1997) consider MDS using a deterministic annealing algorithm.

4.2 MDS Diagnostics

Very little work has been carried out on diagnostics for MDS configurations as to goodness of fit, outliers, etc. To date, the two main diagnostics for nonmetric scaling have been the value of STRESS

and the Shepard diagram. For classical scaling the "amount of variation explained", based on eigenvalues is used, and for least squares scaling the value of the loss function.

Chen (1996) and Chen and Chen (2000) discuss interactive diagnostic plots for MDS. They have written a computer program that links the dissimilarities, distances and disparaties to the plot of the MDS configuration. Any point can be highlighted by the analyst in the configuration, which then causes all its associated dissimilarities, distances and disparaties to be highlighted in other plots, such as the Shepard plot. Colour linkage is also used, so for example, the dissimilarities can be mapped to a colour spectrum ranging from deep blue for the largest dissimilarities through to bright red for the smallest dissimilarities. If the point $\mathbf{x}_r$ is chosen in the configuration (using the computer mouse) then this causes the sth point in the configuration to adopt the appropriate colour in the spectrum according to the value of δ_{rs}. The coloured points then indicate "goodness of fit" for the rth point – for a good fit, close points should be mainly coloured red, distant points blue. Chen and Chen also allow for colour smearing of this plot by estimating the colour at all points within the configuration space (not only those marked as representing the original objects or observations). The colour smearing is carried out using a kernel density estimation approach, so that at point $\mathbf{x}$, the estimate of proximity (based on the rth object) is

$$\hat{\delta}_r(\mathbf{x}) = \frac{n^{-1}\sum_{s=1}^{n}\delta_{rs}\kappa(\mathbf{x}-\mathbf{x}_s)}{n^{-1}\sum_{s=1}^{n}\kappa(\mathbf{x}-\mathbf{x}_s)},$$

where κ is an appropriately chosen kernel. The point $\mathbf{x}$ is then coloured according to the value of $\hat{\delta}_r(\mathbf{x})$. Thus when this is done for many points within the configuration space, the colours of the original configuration points are smeared into the "empty" space between them.

A configuration where $\mathbf{x}_r$ has a small contribution to STRESS (i.e. $\sum_s(\delta_{rs}-\hat{d}_{rs})^2$ is small) will have a peak of bright red centred at $\mathbf{x}_r$ and then moving away from $\mathbf{x}_r$, colour smoothly descends the spectrum. For x_r having a large contribution to stress, the plot will either be a twisted colour pattern, or smooth but with colours not as expected. By viewing these plots and the Shepard type plots in turn for each point in the configuration, abnormalities and other special features are shown up.

In line with regression diagnostics for regression analysis there is future scope for work in the diagnostic area for MDS. For instance, residuals, e_{rs}, can be defined: $e_{rs} = |d_{rs} - \delta_{rs}|$ for metric MDS; $e_{rs} = |d_{rs} - \hat{d}_{rs}|$ for nonmetric MDS. For the stochastic approach to MDS in Section 4.7, residuals are naturally defined. The residuals could then be analysed globally or within observations. For the rth observation the mean residual is $e_{r.} = n^{-1} \sum_s e_{rs}$. Then $\{e_{r.}\}$ could be plotted against position in the MDS configuration. The mean residuals could also be plotted against each variable in the data matrix (if there is one) from which the dissimilarities were constructed.

Outliers could be sought in terms of large residuals or mean residuals. Influential observations could be sought by systematically leaving out (i) one of the dissimilarities, (ii) all dissimilarities associated with one of the observations, and then noting the effect on the MDS analysis. The effect could be measured in various ways, for example the reduction in STRESS, or the Procrustes statistic (Chapter 5) when configurations are matched, one based on the full data and one based on the reduced data.

4.3 Robust MDS

Spence and Lewandowsky (1989) consider the effect of outliers in multidimensional scaling. They illustrate the potentially disastrous effects of outliers by using as dissimilarities the forty-five Euclidean distances obtained from nine points in a two dimensional Euclidean space. One of the distances, however, is multiplied by a factor of ten. The resulting configuration using classical scaling has the two points associated with the outlying distance forced well away from their true positions. To overcome the effects of outliers, Spence and Lewandowsky suggest a method of robust parameter estimation and a robust index of fit, described briefly below.

Robust parameter estimation

Suppose a configuration of n points is sought in a p dimensional Euclidean space with associated distances $\{d_{rs}\}$ representing dissimilarities $\{\delta_{rs}\}$. As usual, let the coordinates of the points in the

space be denoted by $\{x_{ri}\}$. Consider the distance between the rth and sth points,

$$d_{rs}^2 = \sum_{i=1}^{p} (x_{ri} - x_{si})^2.$$

Concentrating on the coordinate x_{rk}, this enters into $n-1$ distances, and $n-1$ discrepancies, $f(x_{rk})$, between dissimilarity and distance,

$$f_s(x_{rk}) = \delta_{rs} - \left\{ \sum_{i=1}^{p} (x_{ri} - x_{si})^2 \right\}^{\frac{1}{2}} \qquad (s \neq r,\ s = 1, \ldots, n).$$

Obviously, $f_s(x_{r1}) \equiv f_s(x_{r2}) \equiv \ldots \equiv f_s(x_{rn})$.

Let $\{x_{ri}^t\}$ be the coordinates at the tth iteration in the search for the optimum configuration, and let $\{d_{rs}^t\}$ be the associated distances. The Newton-Raphson method for finding roots of equations leads to

$$\begin{aligned} x_{rk}^{t+1} &= x_{rk}^t - \frac{f_s(x_{rk}^t)}{f_s'(x_{rk}^t)} \qquad (s \neq r,\ s = 1, \ldots, n) \\ &= x_{rk}^t + \frac{(\delta_{rs} - d_{rs}^t) d_{rs}^t}{x_{rk}^t - x_{sk}^t} \\ &= x_{rk}^t + {}_s g_{rk}^t. \end{aligned}$$

The corrections ${}_s g_{rk}^t$ to x_{rk}^t can be greatly influenced by outliers and hence Spence and Lewandowsky suggest using their median. Thus

$$x_{rk}^{t+1} = x_{rk}^t + {}_M g_{rk}^t,$$

where ${}_M g_{rk}^t = \text{median}_{r \neq s}({}_s g_{rk}^t)$.

They also suggest a modification to step size, giving

$$x_{rk}^{t+1} = x_{rk}^t + \beta^t {}_M g_{rk}^t,$$

where

$$\begin{aligned} \beta^t &= \frac{\alpha^t}{g^t}, \\ \alpha^{t+1} &= \alpha^t \left\{ \frac{\sum_{r,j} (x_{rj}^{t-1} - x_{rj}^{t-2})^2}{\sum_{r,j} (x_{rj}^t - 2x_{rj}^{t-1} + x_{rj}^{t-2})^2} \right\}^{\frac{1}{2}}, \\ g^t &= \left\{ \frac{\sum_{r,j} ({}_M g_{rj}^t)^2}{\sum_{r,j} (x_{rj}^t)^2} \right\}^{\frac{1}{2}}. \end{aligned}$$

The above is easily modified to incorporate transformations of distances, dissimilarities or both.

Care has to be taken over the starting configuration. It is suggested that a starting configuration is found by replacing the dissimilarities by their ranks and using classical scaling on these; the configuration is then suitably scaled.

Robust index of fit

Spence and Lewandowsky suggest TUF as an index of fit where

$$\text{TUF} = \text{median}_r \text{median}_{s \neq r} \left| \frac{\delta_{rs} - d_{rs}}{\delta_{rs}} \right|,$$

which, when multiplied by 100, can be interpreted as the median percentage discrepancy between the dissimilarities and the fitted distances.

Spence and Lewandowsky carried out simulation exercises to compare several MDS programs in their ability to cope with outliers. They showed that nonmetric methods were more resistant to outliers than metric methods, as expected, but that their method (TUFSCAL) was the most resistant.

4.4 Interactive MDS

In an experiment where a subject is presented with pairs of stimuli in order to elicit a dissimilarity/similarity measurement, the number of possible pairs that have to be judged soon becomes overwhelmingly large. An experimental design using just a subset of the possible pairs can be attempted. Spence and Domoney (1974) carried out a Monte Carlo simulation study to show that up to two-thirds of the full set of dissimilarities can be discarded without a disastrous effect on the MDS results.

Young and Cliff (1972) introduce an interactive classical scaling method, where an initial number, n_1, of stimuli are presented for paired comparison. From the resulting scaled dissimilarities the pair of stimuli furthest apart are used to start the definition of a "frame". The frame starts in one dimension as a line passing through two points representing these two stimuli. The distance between the points represents the associated dissimilarity. The rest of the stimuli in the initial set are considered in turn. If the two dissimilarities between a particular stimulus and the two existing frame stimuli can be represented by the distances from the two

points to another collinear point, then the stimulus is in the same dimension as the other two. If not a new dimension is required for the frame. The stimulus giving the lowest "residual" distance is used to define another dimension and increases the frame. This process is continued, looking at distances of new stimuli to frame points in terms of projections onto the frame dimensions until a frame of r dimensions is found. Those original stimuli of the n_1 not in the frame are set aside.

More stimuli are added to the ones in the frame and the process is repeated, updating the frame. This continues until all the stimuli have been considered and a final frame settled upon. Dissimilarities are then found between those stimuli outside the frame and those within it. Some of these will already have been found, however, as the frame was being constructed.

Girard and Cliff (1976) carried out a Monte Carlo study to investigate the accuracy of the interactive scaling method by comparing results with a solution based on all the possible dissimilarities, and also with solutions based on subsets of the dissimilarities. They concluded that interactive scaling was superior to simply using a subset of the dissimilarities. Interactive MDS was further developed by Cliff *et al.* (1977) and improved by Green and Bentler (1979).

4.5 Dynamic MDS

Ambrosi and Hansohm (1987) describe a dynamic MDS method for analysing proximity data for a set of objects where dissimilarities are measured at each of T successive time periods. Let these dissimilarities be denoted by $\{\delta_{rs}^t\}$, $(r, s = 1, \ldots, n; t = 1, \ldots, T)$. The aim is to produce a configuration of nT points in a space, where each object is represented T times, once for each of the time periods. The T points for each object are, hopefully, not too distant from one another, and by plotting their path over time, insight into the changing nature of the relationship among the objects with respect to time can be found.

One possibility for coping with the T sets of dissimilarities is to place them into a super-dissimilarity matrix, $\mathbf{D}$,

$$\mathbf{D} = \begin{bmatrix} \mathbf{D}_{11} & \mathbf{D}_{12} & \ldots & \mathbf{D}_{1T} \\ \vdots & \vdots & \ddots & \vdots \\ \mathbf{D}_{T1} & \mathbf{D}_{T2} & \ldots & \mathbf{D}_{TT} \end{bmatrix},$$

where $\mathbf{D}_{tt} = [\delta_{rs}^t]$, the dissimilarity matrix formed from the dissimilarities collected at the tth time period. The matrix $\mathbf{D}_{tt'} = [\delta_{rs}^{t,t'}]$ has to be specified where $\delta_{rs}^{t,t'}$ is the dissimilarity of object r at the tth time period with object s at the t'th time period ($t \neq t'$). Some information may be available from which these cross time period dissimilarities can be found. For example if data matrices were available for the objects, with one for each time period, these dissimilarities could be found using the observations on object r at time period t and those on object s at time period t' to define $\delta_{rs}^{t,t'}$ by the Jaccard coefficient for instance. Usually $\delta_{rs}^{t,t'} \neq \delta_{rs}^{t',t}$ ($r \neq s$). However, the super-dissimilarity matrix will still be symmetric. If the dissimilarities $\delta_{rs}^{t,t'}$ cannot be found, it may be that they can be constructed from $\{\delta_{rs}^t\}$. One possibility is

$$\delta_{rs}^{t,t'} = \tfrac{1}{2}(\delta_{rs}^t + \delta_{rs}^{t'}).$$

Another possibility is to assume all $\delta_{rs}^{t,t'}$ ($t \neq t'$) are missing. A third is to define $\delta_{rr}^{t,t'} = 0$, with all $\delta_{rs}^{t,t'}$ ($r \neq s$) missing.

Once the super-dissimilarity matrix has been constructed, it can be subjected to metric or nonmetric multidimensional scaling in the usual manner.

A different approach is suggested by Ambrosi and Hansohm. They use stress for nonmetric MDS based on the dissimilarities for the tth time period defined by

$$S^t = \frac{\sum_{r<s}(\delta_{rs}^t - \hat{d}_{rs}^t)^2}{\sum_{r<s}(\hat{d}_{rs}^t - \bar{d}^t)^2},$$

where

$$\bar{d} = \frac{2}{n(n-1)} \sum_{r<s} \hat{d}_{rs}^t.$$

The combined stress for the T time periods can be chosen as either

$$S = \frac{\sum_{t=1}^T \sum_{r<s}(\delta_{rs}^t - \hat{d}_{rs}^t)^2}{\sum_{t=1}^T \sum_{r<s}(\hat{d}_{rs}^t - \bar{d}^t)^2}$$

or

$$S = \sum_{t=1}^T S^t.$$

This overall stress is to be minimised, but subject to the constraint that, in the resulting configuration, the T points that represent

each object tend to be close to each other. This is achieved by using a penalty function, for example

$$U = \sum_{t=1}^{T-1} \sum_{r=1}^{n} \sum_{i=1}^{p} (x_{ri}^{t+1} - x_{ri}^{t})^2,$$

where $\mathbf{x}_r^t = (x_{ri}^t, \ldots, x_{rp}^t)$ are the coordinates representing object r at the tth time period.

A configuration is then found that minimises

$$S_\epsilon = S + \epsilon U, \qquad \epsilon > 0,$$

where ϵ is a chosen constant $<<1$.

Minimising the stress S and also minimising the penalty function U is then a compromise which will depend on the value of ϵ, which in turn will depend on the importance placed on the requirement that the T points representing an object are near to each other.

A further restriction can be added that the T points representing each object lie on a straight line. This is achieved by insisting

$$\mathbf{x}_r^t = \mathbf{x}_r^1 + \boldsymbol{\alpha}_r^T y_r^t \qquad (r = 1, \ldots, n; t = 2, \ldots, T),$$

where $\boldsymbol{\alpha}_r$ (note in the equation above the superscript T is transpose) gives the direction of the line for the rth object, $\mathbf{x}_r^1$ the starting point of the line, and y_r^t the distance along of the point $\mathbf{x}_r^t$. These new parameters are estimated in the course of minimising S_ϵ.

An example

Hansohm (1987) describes a computer package DMDS which carries out dynamic MDS. It also includes programs for ordinary MDS, and FACALS, a principal component analysis program.

Hansohm illustrates DMDS using data collected by Schobert (1979) on fifteen cars, where each is described by fifteen variables. Data are collected yearly for the period 1970-1973. Hansohm gives a two dimensional configuration showing the fifteen cars at the four time points with the points for each car lying on a straight line.

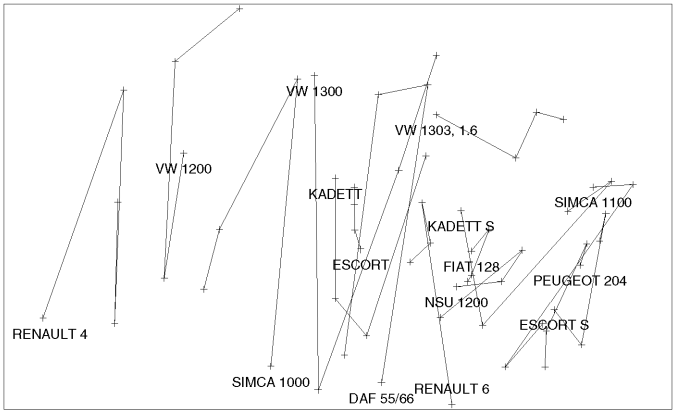

Figure 4.1 *Dynamic MDS for cars using DMDS*

The same data have been used without this restriction and the resulting two dimensional configuration is shown in Figure 4.1. The value of ϵ was chosen as 0.001, the final penalized stress value was 11%. The Renault 4, the VW1200, the Simca 1000 and the VW1300 are on the left of the configuration. The Simca 1100, the Peugeot 204 and the Escort S are on the right. The cars on the left can be seen to change their positions much more drastically than those on the right.

A different approach can be taken to dynamic MDS, by simply carrying out an MDS analysis for each time period separately, and then matching the resulting configurations using a Procrustes analysis. This was done for the car data resulting in the configuration given in Figure 4.2. The stresses for the four initial configurations were 8%, 7%, 9% and 8%. The configurations for the second, third and fourth time periods were matched to that of the first. The values of the Procrustes statistic were 0.09, 0.20 and 0.12 respectively. Alternatively the second configuration could have been matched to the first, the third to the second, and the fourth to the third. The length of the trajectories are shorter for this method, but cannot be controlled as they can for the previous method by choice of ϵ.

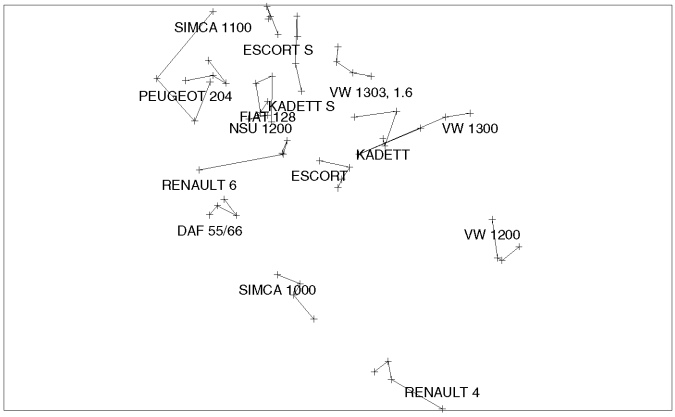

Figure 4.2 *Dynamic MDS for cars using Procrustes analysis*

4.6 Constrained MDS

Sometimes it is desirable to place restrictions on the configuration obtained from an MDS analysis, either through parameters or on the distances in the resulting configurations. For example, a particular set of stimuli may fall into ten subsets, and it is required that all the projections of stimuli points in a subset onto a particular axis are coincident. Bentler and Weeks (1978) describe a situation involving nine Munsell colours of the same red hue, but of differing brightness and saturation, the data coming from Torgerson (1958). The MDS configuration can be constrained so that the first two axes give the true brightness and saturation values for the nine colours.

Another colour example is the data of Ekman (1954) consisting of similarities for fourteen colours. A two-dimensional MDS analysis of the data gives the colours lying close to the circumference of a circle – the colour circle. Constrained MDS methods can ensure that the colours actually lie on the circumference.

In order to constrain an MDS configuration, Bentler and Weeks (1978) use least squares scaling with the configuration in a Euclidean space and simply incorporate the required equality constraints in the least squares loss function. Bloxom (1978) has the same approach but allows for non-orthogonal axes. Lee and Bentler

(1980) also constrain configurations using least squares scaling incorporating Lagrange multipliers. Lee (1984) uses least squares scaling to allow not only for equality constraints, but also inequality constraints. Borg and Lingoes (1980) constrain configurations using the following approach, which covers the metric and nonmetric methods.

Let $\{\delta_{rs}\}$, $\{d_{rs}\}$ be the usual dissimilarities and distances within a configuration. Let $\{\delta_{rs}^R\}$ be pseudo-dissimilarities which reflect the constraints required. Many of the pseudo-dissimilarities may be missing if they are not involved with constraints. Let $\{\hat{d}_{rs}\}$ be disparities for $\{\delta_{rs}\}$ and $\{\hat{\delta}_{rs}^R\}$ disparities for $\{\delta_{rs}^R\}$ where "disparities" can be the disparities from nonmetric MDS or actual dissimilarities for metric MDS. This allows both cases to be covered simultaneously. Then the constrained solution is found by minimising the loss function

$$L = (1-\alpha)L_U + \alpha L_R \qquad (0 \leq \alpha \leq 1),$$

with

$$L_U = \sum_{r,s}(d_{rs} - \hat{\delta}_{rs})^2,$$

$$L_R = \sum_{r,s}(d_{rs} - \hat{\delta}_{rs}^R)^2.$$

The loss functions L_U and L_R can be Kruskal's STRESS or just a least squares loss function. The loss function L is minimised iteratively with α^t, the value of α at the tth iteration. By ensuring that $\lim_{t\to\infty}\alpha^t = 1$, a configuration with the required restrictions is found. Note: minimising L is not the same as minimising L_R, since L_R will contain many missing values while L_U will be complete. Like many other authors Borg and Lingoes use their method on Ekman's colour data and constrain the colours to lie on a circle.

Ter Braak (1992) considers constraining MDS models with regression models, so that coordinates of the configuration are regressed on external variables. He gives as an example a PCO analysis of twenty-one colonies of butterflies where coordinates are regressed on eleven environmental variables. One further constrained MDS model, CANDELINC, will be covered in Chapter 12. Other references to constrained MDS are de Leeuw and Heiser (1980), Weeks and Bentler (1982), Mather (1988, 1990), Takane *et al.* (1995) and Winsberg and De Soete (1997).

4.6.1 Spherical MDS

Cox and Cox (1991) show how points of a configuration from nonmetric MDS can be forced to lie on the surface of a sphere. In a sense, this is not constrained MDS since the space representing the objects is simply taken to be the two-dimensional surface of a sphere. The advantage of using the surface of a sphere as a space in which to represent the objects is that the configuration need not have any "edge points", whereas in a Euclidean space, there always have to be points at the edge of the configuration. These could be defined as those points lying in the convex hull of the configuration, for instance.

The metric methods of constrained MDS of Bloxom (1978), Bentler and Weeks (1978), Lee and Bentler (1980) and Lee (1984) can produce configurations of points lying on the surface of a sphere as particular cases. The nonmetric method of Borg and Lingoes (1980) can also produce points on a sphere, but is much more awkward than starting with the sphere's surface as space within which to work, as with Cox and Cox.

Let the coordinates of the points in the spherical configuration be given by

$$(1, \theta_{1r}, \theta_{2r}) \qquad (r = 1, \ldots, n).$$

Transforming to Cartesian coordinates, these are

$$(\cos\theta_{1r} \sin\theta_{2r}, \sin\theta_{1r} \sin\theta_{2r}, \cos\theta_{1r}).$$

The distance between points r and s, d_{rs}, is defined as the shortest arc length along the great circle which passes through the two points. This arc length is monotonically related to the Euclidean distance between the two points (i.e. passing through the interior of the sphere). Since only the rank order of the dissimilarities is important, and hence the rank order of the distances, using the more convenient Euclidean distance rather than the arc length makes very little difference to the resulting configuration. The Euclidean distance is

$$d_{rs} = \{2 - 2\sin\theta_{2r}\sin\theta_{2s}\cos(\theta_{1r} - \theta_{1s}) - 2\cos\theta_{2r}\cos\theta_{2s}\}^{\frac{1}{2}}.$$

Kruskal's stress is defined in the usual manner and then minimised with respect to $\{\theta_{1r}\}$ and $\{\theta_{2r}\}$. The gradient term can be found in Cox and Cox (1991).

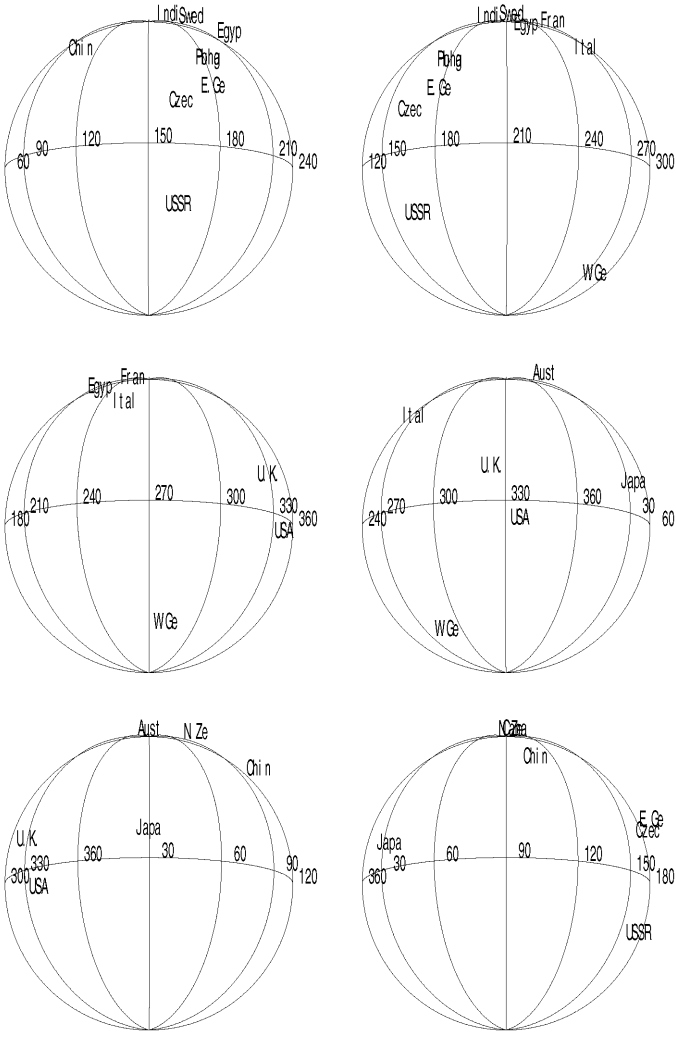

Figure 4.3 *Spherical MDS of the nations' trading data*

The resulting configuration is not unique, since an arbitrary rotation of the points or negating one of θ_1 or θ_2 will preserve distances on the sphere, and hence give another solution with minimum stress. In passing, note that d_{rs} is invariant to the addition

of an arbitrary angle α to each θ_{1r}, but not to the addition of an arbitrary angle β to each θ_{2r}. To find the mapping for an arbitrary rotation, first rotate about the z-axis and then the y-axis. This gives

$$(\cos\theta_{1r}\sin\theta_{2r}, \sin\theta_{1r}\sin\theta_{2r}, \cos\theta_{2r}) \rightarrow$$
$$(\cos(\theta_{1r}+\alpha)\sin\theta_{2r}\cos\beta - \cos\theta_{2r}\sin\beta, \sin(\theta_{1r}+\alpha)\sin\theta_{2r},$$
$$\cos(\theta_{1r}+\alpha)\sin\theta_{2r}\sin\beta + \cos\theta_{2r}\cos\beta).$$

An example

The trading data described in the previous chapter were subjected to spherical MDS. The stress for the configuration was 7%, which is 4% less than that for conventional MDS of the data. Figure 4.3 shows the results of subjecting the dissimilarities to spherical MDS. Six views of the sphere are given. Various clusters of countries can just about be seen, noting, of course, that there have been political changes since the data were collected. The clusters are {Czechoslovakia, East Germany, Hungary, Poland}, {China, Italy}, {Japan, USA, UK}, {Argentina, Australia, Brazil, Canada, Egypt, France, India, New Zealand, Sweden}, {West Germany}, and {USSR}.

4.7 Statistical inference for MDS

Ramsay (1982) read a paper to the Royal Statistical Society entitled "Some Statistical Approaches to Multidimensional Scaling Data". The content of the paper was the culmination of research into the modelling of dissimilarities incorporating an error structure which leads onto inferential procedures for multidimensional scaling; see Ramsay (1977, 1978a, 1978b, 1980, 1982). There followed an interesting discussion with protagonists for and against the use of inference in multidimensional scaling. For instance C. Chatfield said

> ...and I suggest that this is one area of Statistics [MDS] where the emphasis should remain with data-analytic, exploratory techniques.

B.W. Silverman said

> I must say that I am in agreement with Dr. Chatfield in being a little uneasy about the use of multidimensional scaling as a model-based inferential technique, rather than just an exploratory or presentational method.

On the other hand E.E. Roskam said

> For a long time, there has been a serious need for some error theory,...

and D.R. Cox said

> Efforts to discuss some probabilistic aspects of methods that are primarily descriptive are to be welcomed,...

Since 1982, some inferential research has been applied to multidimensional scaling, but to date, has not made a large impact on the subject. A brief description of some of the inferential ideas is given.

Suppose there is an underlying configuration of points in a Euclidean space that represent objects. As usual, let the Euclidean distances between pairs of points be $\{d_{rs}\}$. Let the observed dissimilarity between objects r and s, conditioned on d_{rs}, have probability density function $p(\delta_{rs}|d_{rs})$. It is assumed that these conditioned observations are independent and identically distributed, and hence the log-likelihood is

$$l = \sum_r \sum_s \ln p(\delta_{rs}|d_{rs}).$$

The distances can be written in terms of the coordinates of the points, $d_{rs}^2 = (\mathbf{x}_r - \mathbf{x}_s)^T(\mathbf{x}_r - \mathbf{x}_s)$, and hence the log-likelihood can be minimised with respect to $\mathbf{x}_r$ and any parameters of the probability density function p. This gives the maximum likelihood estimates of the coordinates, $\hat{\mathbf{x}}_r$.

Two possible distributions for $\delta_{rs}|d_{rs}$ are the normal and log-normal. For the normal distribution

$$\delta_{rs} \sim \mathrm{N}(d_{rs}, d_{rs}^2\sigma^2),$$

having constant coefficient of variation. There is a non-zero probability of negative δ_{rs} with this model. For the log-normal distribution

$$\ln \delta_{rs} \sim \mathrm{N}(\ln d_{rs}, \sigma^2).$$

It is possible that a transformation of the dissimilarities is desirable before applying the error structure, such as a power law. Ramsay (1982) suggests a transformation based on monotone splines. However, the overall resulting model is rather complicated, and this was one of the main reasons it attracted criticism from the discussants of Ramsay's paper.

For further illustration consider the log-normal model for dissimilarities and Euclidean distance between points in the MDS space. The log-likelihood is

$$l = -\frac{1}{2\sigma^2}\sum_{r<s}\ln^2\left(\frac{\delta_{rs}}{d_{rs}}\right) - \sum_{r<s}\ln\delta_{rs} - \frac{n(n-1)}{4}\ln(2\pi\sigma^2),$$

where $d_{rs}^2 = \sum_{i=1}^{p}(x_{ri} - x_{si})^2$.

The parameters to be estimated are $\{x_{ri}\}$ and σ^2. Differentiating l with respect to σ^2 gives the maximum likelihood estimate of σ^2 as

$$\hat{\sigma}^2 = \frac{2}{n(n-1)}\sum_{r<s}\ln^2\left(\frac{\delta_{rs}}{d_{rs}}\right).$$

Then substituting $\hat{\sigma}^2$ back into the log-likelihood, the log-likelihood becomes

$$l = -\frac{n(n-1)}{4}\ln\left\{\sum_{r<s}\ln^2\left(\frac{\delta_{rs}}{d_{rs}}\right)\right\} - \sum_{r<s}\ln\delta_{rs} + \text{constant}.$$

The estimates of $\{x_{ri}\}$ have to be found by maximising l numerically. A fast efficient algorithm is recommended, since there can be many parameters. Also, a good starting configuration is desirable, such as the coordinates in the classical scaling MDS configuration. It is recommended that this initial configuration is scaled by the factor $\sum_{i=1}^{n-1}\lambda_i / \sum_{i=1}^{p}\lambda_i$ (from Section 2.2.4) in order to account for the loss of "size" when using classical scaling. Once the coordinates $\{x_{ri}\}$ have been estimated, these form the maximum likelihood configuration, and as with many other MDS techniques, this configuration can be arbitrarily translated, rotated and reflected to give another maximum likelihood solution. Ramsay (1991) has written a comprehensive program called MULTISCALE to carry out maximum likelihood MDS (MLMDS). The program allows choices of: a normal or log-normal error structure; scale, power or spline transformations of the dissimilarities; linking with auxiliary variables; weighting of objects; object-specific variances.

Example

Several subjects were asked to score, from zero to twenty, the dissimilarities between thirteen crimes. The data for one subject are

Table 4.1 *Dissimilarities for thirteen crimes*

Crime	*1*	*2*	*3*	*4*	*5*	*6*	*7*	*8*	*9*	*10*	*11*	*12*
2	2											
3	15	13										
4	15	14	6									
5	15	14	3	3								
6	6	4	3	10	12							
7	4	2	14	14	15	13						
8	15	6	5	11	10	6	10					
9	15	10	12	2	2	12	14	7				
10	2	2	15	15	15	14	4	11	15			
11	14	12	2	11	11	6	15	11	12	14		
12	14	15	8	4	3	12	14	11	3	15	11	
13	9	13	6	14	9	5	10	11	7	13	7	11

1-Murder, 2-Manslaughter, 3-Burglary, 4-Possessing illegal drugs, 5-Shoplifting, 6-Drunk Driving, 7-Arson, 8-Actual Bodily Harm, 9-Drunk & Disorderly, 10-Rape, 11-Car Theft, 12-Trespassing, 13-Tax Evasion

given in Table 4.1. These were analysed using MULTISCALE giving rise to the configuration in Figure 4.4.

From the maximum likelihood configuration, it can be seen that *Arson, Rape, Murder* and *Manslaughter* are grouped together and most likely thought of as serious crimes. A group of perceived less serious crimes *Trespass, Drunk and Disorderly, Shoplifting* and *Possession of illegal drugs* occurs. *Actual Bodily Harm* is an isolated point. *Tax Evasion, Drunk Driving, Burglary* and *Car Theft* also form a group. There is a perceived East-West axis of "seriousness of the crime".

Asymptotic confidence regions

Since the likelihood has been used to estimate the coordinates in the MDS configuration, it should be possible to obtain the estimated asymptotic covariance matrix of the coordinate estimators, and hence lead to asymptotic confidence regions for the points in the configuration. However, this is not a straightforward procedure.

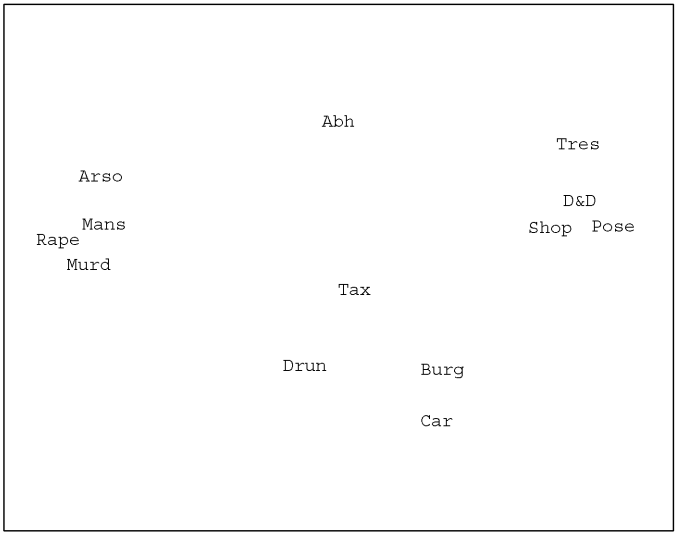

Figure 4.4 *The maximum likelihood configuration for the crime data*

Suppose all the coordinate estimators are placed in a vector $\hat{\mathbf{x}}$. The asymptotic distribution of $\hat{\mathbf{x}}$ is multivariate normal. Now concentrating on the rth point, its coordinate estimators $\hat{\mathbf{x}}_r = (\hat{x}_{r1}, \ldots, \hat{x}_{rp})^T$ are asymptotically unbiased and have marginally an asymptotic multivariate normal distribution. Hopefully, from this, an asymptotic confidence region can be formed using

$$\Pr\{(\hat{\mathbf{x}}_r - \mathbf{x}_r)^T \boldsymbol{\Sigma}^{-1} (\hat{\mathbf{x}}_r - \mathbf{x}) < \chi^2_{p,\alpha}\} = 1 - \alpha, \qquad (4.1)$$

where $\chi^2_{p,\alpha}$ is the upper $100\alpha\%$ point of the chi-square distribution on p degrees of freedom.

The problem occurs in that the maximum likelihood configuration can be arbitrarily translated, rotated and reflected. This affects the covariance matrix of the coordinate estimators. For instance, suppose every maximum likelihood configuration were to be translated so that the first point was always placed at the origin, then the variation for that point would always be zero – it is always at the origin!

Ramsay (1978a, 1982) considers this problem in detail. The expected information matrix, $E[\frac{\partial^2 l}{\partial \mathbf{x} \partial \mathbf{x}^T}]$ is singular, and hence cannot

be inverted to give the asymptotic covariance matrix for $\mathbf{x}$. Ramsay suggests constraining the maximum likelihood configuration so that it is in principal axis orientation, i.e. its centroid is at the origin and if $\mathbf{X}$ is the matrix of coordinates, then $\mathbf{X}^T\mathbf{X}$ is diagonal. To find this particular maximum likelihood configuration, the augmented log-likelihood $l(\mathbf{X}) + q(\mathbf{X})$ is maximised where

$$q(\mathbf{X}) = -\frac{1}{2}\sum_{i=1}^{p}\left(\sum_{r=1}^{n} x_{ri}\right)^2 - \frac{1}{2}\sum_{i=1}^{p}\sum_{i'=1}^{p}\left(\sum_{r=1}^{n} x_{ti}x_{ri'}\right)^2.$$

At the maximum, both terms in the expression for $q(\mathbf{X})$ will have the value zero. The first ensures that the centroid is at the origin and the second that $\mathbf{X}^T\mathbf{X}$ is diagonal, and hence principal axis orientation. The expected information matrix is no longer singular, and after negation, can be inverted to give the asymptotic covariance matrix.

Another possibility to constrain the maximum likelihood configuration is to simply use the Moore-Penrose generalized inverse of the negated expected information matrix. It is unclear as to the exact nature of the implied constraints using this method. Abe (1998) suggests fixing an appropriate number of coordinates in the configuration, for example, in a two-dimensional space, the first point could be placed at the origin and the second along the positive x-axis. This would be enough to tie down the configuration.

Asymptotic covariance matrices for the points in the maximum likelihood configuration for the crime data were found using MULTISCALE. These were based on the Moore-Penrose generalized inverse. Replacing $\boldsymbol{\Sigma}$ by the estimated covariance matrices for the points gives approximate confidence regions, which will be ellipsoidal in shape. Figure 4.5 shows these approximate confidence regions. In general, the method of constraining the maximum likelihood configuration will have a significant effect on the asymptotic covariance matrices and any subsequent confidence region calculated for points in the configuration.

Bell and Cox (1998) use a bootstrapping technique and Procrustes analysis (see Chapter 5) to measure variability in maximum likelihood configurations. This is taken further in Bell and Cox (2000), bringing the ideas of shape analysis to bear on the problem.

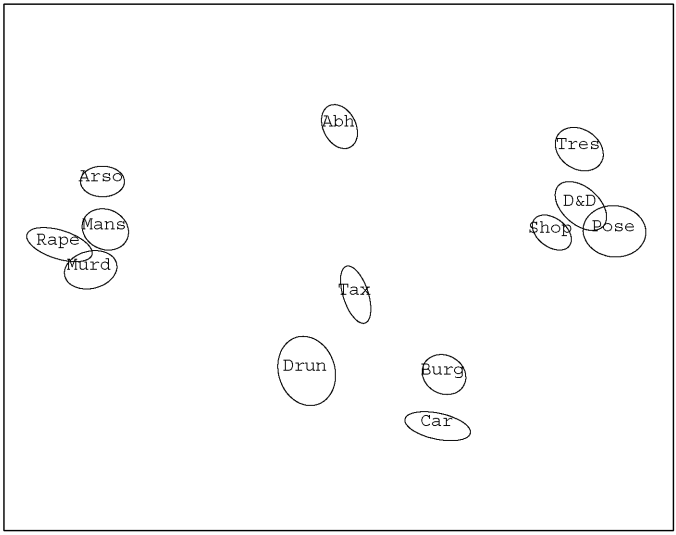

Figure 4.5 *Approximate confidence regions for the points in the maximum likelihood configuration for the crime data*

In general, once the likelihood has been formulated for multidimensional scaling, further inferences can ensue, such as the testing of hypotheses and the formation of confidence regions. For example, if l_k is the maximum value of the log-likelihood when a k dimensional space is used for the configuration of points, then the quantity

$$2(l_k - l_{k-1}),$$

has an asymptotic χ^2 distribution with $n - k$ degrees of freedom, where n is the number of points in the configuration. This can be used to assess the required number of dimensions needed.

Takane (1978a,b) introduces a maximum likelihood method for nonmetric scaling. Let there be an underlying configuration of points representing the objects with coordinates $\{\mathbf{x}_r\}$ and distances between points $\{d_{rs}\}$. For an additive error model, let there be a latent variable λ_{rs} so that

$$\lambda_{rs} = d_{rs} + \epsilon_{rs}, \qquad \epsilon_{rs} \sim \mathrm{N}(0, \sigma_{rs}^2).$$

Then if $\lambda_{rs} \geq \lambda_{r's'}$, for the observed dissimilarities $\delta_{rs} \succ \delta_{r's'}$ where $\succ$ represents ordering of the dissimilarities, define

$$\begin{aligned} Y_{rsr's'} &= 1 \qquad \text{if } \delta_{rs} \succ \delta_{r's'} \\ &= 0 \qquad \text{if } \delta_{rs} \prec \delta_{r's'}. \end{aligned}$$

Then

$$\begin{aligned} \Pr(Y_{rsr's'} = 1) &= \Pr(\lambda_{rs} - \lambda_{r's'} \geq 0) \\ &= \Phi\left(\frac{d_{rs} - d_{r's'}}{(\sigma_{rs}^2 + \sigma_{r's'}^2)^{\frac{1}{2}}}\right) \qquad (= \Phi_{rsr's'} \text{ say}), \end{aligned}$$

and hence the likelihood is given by

$$L = \prod \Phi_{rsr's'}^{Y_{rsr's'}} (1 - \Phi_{rsr's'})^{1 - Y_{rsr's'}},$$

assuming independence of $\{\epsilon_{rs}\}$.

Writing d_{rs} in terms of the coordinates $\mathbf{x}_r$ allows the likelihood or log-likelihood to be maximised with respect to these, giving $\hat{\mathbf{x}}_r$ as the maximum likelihood configuration.

In a similar manner Takane (1981) gives a maximum likelihood approach to multidimensional successive categories scaling. Successive categories scaling is a special case where dissimilarities are ordered categorical variables. So for the whisky tasting experiment of Chapter 1, the possible categories for comparison of two whiskies might be: very similar; similar; neutral (neither similar nor dissimilar); dissimilar; and very dissimilar. The categories could be assigned scores 0, 1, 2, 3, 4, and hence the dissimilarities $\{\delta_{rs}\}$ can each take one of only five possible values. The dissimilarities could then be subjected to metric or nonmetric MDS in the usual manner. Takane suggests the following model, assuming a single set of dissimilarities. Again, let there be an underlying configuration of points representing the objects, with coordinates $\mathbf{x}_r$ and distances between points d_{rs}, an additive error. Let there be a latent variable λ_{rs} as above. The successive categories are represented by a set of ordered intervals

$$-\infty = b_0 \leq b_1 \leq \ldots \leq b_M = \infty,$$

where the number of possible categories is M. So the interval $(b_{i-1}, b_i]$ represents the ith category. If the value of the latent variable λ_{rs} lies in the interval $(b_{i-1}, b_i]$ then δ_{rs} is observed as being in the ith category.

Let p_{rsi} be the probability that δ_{rs} is observed as being in the ith category. Then

$$p_{rsi} = \Phi\left(\frac{b_i - d_{rs}}{\sigma}\right) - \Phi\left(\frac{b_{i-1} - d_{rs}}{\sigma}\right).$$

Let the indicator variable Z_{rsi} be defined as

$$\begin{array}{rl} Z_{rsi} = 1 & \text{if } \delta_{rs} \text{ falls in the } i\text{th category} \\ 0 & \text{otherwise} \end{array}.$$

Assuming independence, the likelihood of $\{Z_{rsi}\}$ is then given by

$$L = \prod_r \prod_s \prod_i p_{rsi}^{z_{rsi}}$$

and hence the log-likelihood is

$$l = \sum_r \sum_s \sum_i z_{rsi} \ln p_{rsi}.$$

The log-likelihood is then maximised with respect to the category boundaries $\{b_i\}$, the coordinates $\{\mathbf{x}_r\}$ and the error variance σ^2. This then gives the maximum likelihood configuration $\{\hat{\mathbf{x}}_r\}$. The procedure can easily be generalized to the cases of replications and several judges.

Zinnes and MacKay (1983) report on a different approach for introducing probabilistic errors, using the Hefner model (Hefner, 1958). Here, each stimulus (conceptually it is easier to think of stimuli rather than objects) is represented by a p dimensional random vector $\mathbf{X}_r = (X_{r1}, \ldots, X_{rp})^T$. All components, X_{ri}, of $\mathbf{X}_r$ are assumed independently normally distributed with mean μ_r and variance σ_r^2. These distributions then induce a distribution on the Euclidean distance $(\mathbf{X}_r - \mathbf{X}_s)^T(\mathbf{X}_r - \mathbf{X}_s)$, and it is assumed that the observed dissimilarity is this Euclidean distance. Thus

$$\delta_{rs} = \{(\mathbf{X}_r - \mathbf{X}_s)^T(\mathbf{X}_r - \mathbf{X}_s)\}^{\frac{1}{2}}.$$

It is also assumed that the "true" distance between points r and s is given by

$$d_{rs}^2 = (\boldsymbol{\mu}_r - \boldsymbol{\mu}_s)^T(\boldsymbol{\mu}_r - \boldsymbol{\mu}_s),$$

where $\boldsymbol{\mu} = (\mu_{r1}, \ldots, \mu_{rp})^T$, $(r = 1, \ldots, n)$.

Hefner (1958) has shown that $\delta_{rs}^2/(\sigma_r^2 + \sigma_s^2)$ has a non-central chi-squared distribution, $\chi'^2(p, d_{rs}^2/(\sigma_r^2 + \sigma_s^2))$. From this it is possible

to find the distribution of δ_{rs}. Zinnes and MacKay give approximations to the probability density functions. For $(d_{rs}\delta_{rs})/(\sigma_r^2+\sigma_s^2) \geq 2.55$ the density function can be approximated by

$$2\delta_{rs}^{-1} z\phi\left[\left(\frac{z}{p+\lambda}\right)^h\right](p+\lambda)^{-h}(hz^{h-1}),$$

where $z = \delta_{rs}^2/(\sigma_r^2+\sigma_s^2)$, $\lambda = d_{rs}^2/(\sigma_r^2+\sigma_s^2)$, $h = 1-\frac{2}{3}(p+\lambda)(p+3\lambda)/(p+2\lambda)^2$.

For $(d_{rs}\delta_{rs})/(\sigma_r^2+\sigma_s^2) < 2.55$ an approximation based on beta functions is used,

$$2\delta_{rs}^{-1}\exp\{-\tfrac{1}{2}(z^2+\lambda)\}(\tfrac{1}{2}z)^{p/2}\sum_{k=0}^{\infty} A_k,$$

$$A_0 = \frac{1}{\Gamma}\frac{p}{2}, \quad A_k = \frac{\lambda z}{4k(k+\frac{1}{2}p-1)}A_{k-1},$$

with five terms in the summation usually giving sufficient accuracy.

Zinnes and MacKay maximise the sum of the logarithms of the approximating density functions, one for each dissimilarity, with respect to $\{\boldsymbol{\mu}_r\}$ and $\{\sigma_r^2\}$. The values $\{\boldsymbol{\mu}_r\}$ give the coordinates of the points in the configuration.

Brady (1985) considered in detail consistency and hypothesis testing for nonmetric MDS. Brady's work is very general and he uses his own special notation. Bennett (1987) considers influential observations in multidimensional scaling. Cox and Ferry (1993) use multidimensional scaling for discriminant analysis. Storms (1995) looks at robustness of maximum likelihood scaling.

4.8 Asymmetric dissimilarities

Metric and nonmetric MDS methods so far described have been for one-mode, two-way symmetric data, where the symmetry in dissimilarities (similarities) $\delta_{rs} = \delta_{sr}$ is reflected in the symmetry in distances within the MDS configuration $d_{rs} = d_{sr}$. Some situations give rise to asymmetric proximities. For example, within a school class, each child is asked to score the friendship he/she feels for each of the other members of the class. Results are unlikely to be symmetric.

In the early days of MDS, Kruskal (1964a) suggested two approaches that could be taken with asymmetric dissimilarities. The first was to average δ_{rs} and δ_{sr} and proceed as usual. The other

was to let the summations in STRESS extend over all $r \neq s$ rather than $r < s$. Another possibility is to represent every object twice with new dissimilarities $\delta'_{ni+r,nj+s}$ $(i, j = 0, 1)$, where both r and $n + r$ represent the rth object. Let

$$\begin{aligned}
\delta'_{r,s} &= \delta'_{s,r} = \delta_{rs} \\
\delta'_{n+r,n+s} &= \delta'_{n+s,n+r} = \delta_{sr} \\
\delta'_{r,n+r} &= \delta'_{n+r,r} = 0
\end{aligned}$$

and treat dissimilarities $\delta'_{r,n+s}$ and $\delta_{n+r,s}$ $(r \neq s)$ as missing.

The above methods attempt to overcome the problem of asymmetric dissimilarities using techniques designed for symmetric dissimilarities. It is more satisfactory to model the asymmetry. Gower (1977) does this in several ways. Let the dissimilarities be placed in matrix $\mathbf{D}$. His first method is to use the singular value decomposition of $\mathbf{D}$,

$$\mathbf{D} = \mathbf{U}\boldsymbol{\Lambda}\mathbf{V}^T,$$

whereupon

$$\begin{aligned}
\mathbf{V}\mathbf{U}^T\mathbf{D} &= \mathbf{V}\boldsymbol{\Lambda}\mathbf{V}^T \\
\mathbf{D}\mathbf{V}\mathbf{U}^T &= \mathbf{U}\boldsymbol{\Lambda}\mathbf{U}^T
\end{aligned}$$

are both symmetric and the orthogonal matrix $\mathbf{A} = \mathbf{U}^T\mathbf{V}$ can be regarded as a measure of symmetry, since if $\mathbf{D}$ is symmetric, $\mathbf{A} = \mathbf{I}$.

His second method is as follows. Define matrix $\mathbf{A}$ as $[\mathbf{A}]_{rs} = -\frac{1}{2}d^2_{rs}$. Centre its rows and columns as for classical scaling. Express $\mathbf{A}$ as

$$\mathbf{A} = \mathbf{U}\boldsymbol{\Lambda}\mathbf{U}^{-1},$$

where $\boldsymbol{\Lambda}$ is the diagonal matrix of eigenvalues of $\mathbf{A}$, some of which could be complex. Matrix $\mathbf{U}$ consists of the left eigenvectors of $\mathbf{A}$, and matrix $\mathbf{U}^{-1}$ the right eigenvectors. Use $\mathbf{U}\boldsymbol{\Lambda}^{\frac{1}{2}}$, $(\mathbf{U}^{-1})^T\boldsymbol{\Lambda}^{\frac{1}{2}}$ to plot two configurations of points. If $\mathbf{A}$ was symmetric the configurations would coincide.

The third method works on the rows and columns of $\mathbf{D}$ expressed in terms of the upper and lower triangular matrices of $\mathbf{D}$, $\mathbf{D} = (\mathbf{L}\backslash\mathbf{U})$. The rows and columns are permuted so that

$$\left| \sum [\mathbf{U}]_{rs} - \sum [\mathbf{L}]_{rs} \right|$$

is a maximum. Then make $\mathbf{U}$ and $\mathbf{L}$ symmetric and subject both

to an MDS analysis. The results can be regarded as the worst situation for the asymmetry of $\mathbf{D}$. This approach was further investigated by Rodgers and Thompson (1992).

Gower's fourth method is simply to use multidimensional unfolding or correspondence analysis on $\mathbf{D}$. See Chapters 8 and 9.

Gower's fifth method considers the best rank 1 and rank 2 matrices that, when added to $\mathbf{D}$, make it the most symmetric. Ten Berge (1997) investigated this idea further and showed that results depend upon how departures from symmetry are measured, whether by the squared distance between a matrix and its transpose, $||\mathbf{D} - \mathbf{D}^T||^2 = \sum(\delta_{rs} - \delta_{sr})^2$, or from the squared distance between $\mathbf{D}$ and its symmetric part, $||\mathbf{D} - (\mathbf{D} + \mathbf{D}^T)/2||^2$. These quantities look the same, but differences will occur when a matrix of low rank, $\mathbf{H}$, is added to $\mathbf{D}$ to bring it closer to symmetry, i.e. the quantities will be $||(\mathbf{D} - \mathbf{H}) - (\mathbf{D}^T - \mathbf{H}^T)||^2$ and $||(\mathbf{D} - \mathbf{H}) - (\mathbf{D} + \mathbf{D}^T)/2||^2$ respectively.

The matrix $\mathbf{D}$ can be expressed as the sum of asymmetric matrix $\mathbf{A}$ and a skew-symmetric matrix $\mathbf{B}$, so that $\mathbf{D} = \mathbf{A} + \mathbf{B}$, where $\mathbf{A} = \frac{1}{2}(\mathbf{D} + \mathbf{D}^T)$, and $\mathbf{B} = \frac{1}{2}(\mathbf{D} - \mathbf{D}^T)$. Gower (1977) and Constantine and Gower (1978) suggest analysing $\mathbf{A}$ using techniques designed for symmetric matrices, e.g. classical scaling, and to decompose $\mathbf{B}$ into a sum of rank 2 skew-symmetric matrices

$$\mathbf{B} = \sum_{i=1}^{[n/2]} \lambda_i(\mathbf{u}_i\mathbf{v}_i^T - \mathbf{v}_i\mathbf{u}_i^T) \tag{4.2}$$

where $\{\lambda_i^2\}$ are the ordered eigenvalues of $\mathbf{B}\mathbf{B}^T$ with associated eigenvalues $\{\mathbf{u}_i, \mathbf{v}_i\}$, noting that the eigenvalues occur in pairs and $\mathbf{u}_i, \mathbf{v}_i$ are two eigenvalues for λ_i^2.

To approximate $\mathbf{B}$ use the first eigenvalue only and then

$$\mathbf{B} \approx \lambda_1(\mathbf{u}_1\mathbf{v}_1^T - \mathbf{v}_1\mathbf{u}_1^2).$$

If points representing the objects are plotted at (u_{1r}, v_{1r}), then $[B]_{rs}$ is approximately given by twice the area of the triangle formed by the origin and the points r and s.

Weeks and Bentler (1982) suggested that the symmetric and skew-symmetric parts of $\mathbf{D}$ could be modelled by

$$\delta_{rs} = \alpha d_{rs} + \beta + c_r - c_s + \epsilon_{rs},$$

where d_{rs} is Euclidean distance; α, β are parameters; c_r, c_s represent the skew-symmetric component; and ϵ_{rs} an error component.

Constraints are placed to make the model identifiable, and then the various parameters, components and coordinates are estimated using least squares.

Zielman and Heiser (1993) develop the slide-vector model for asymmetry which was first suggested by Kruskal. The dissimilarities $\{\delta_{rs}\}$ are modelled by the quantities

$$d_{rs} = \{\sum_{i=1}^{p}(x_{ri} - x_{si} + z_i)^2\}^{\frac{1}{2}},$$

where $\mathbf{X} = [x_{ri}]$ is the usual coordinate matrix of points representing the objects, and $\mathbf{z} = (z_1, \ldots, z_p)^T$ is the slide-vector which distorts the Euclidean distances between points to model the asymmetry. Clearly $d_{rs} \neq d_{sr}$ unless $\mathbf{Z} = \mathbf{0}$. Letting $y_{si} = x_{si} - z_{si}$, $d_{rs} = \{\sum_{i=1}^{p}(x_{ri} - y_{si})^2\}^{\frac{1}{2}}$ which links the slide-vector model to the unfolding models of Chapter 8.

Two other MDS models for asymmetric dissimilarities are DEDICOM and GIPSCAL which are described in Chapter 12. Other papers on modelling asymmetric dissimilarities are Levin and Brown (1979), DeSarbo *et al.* (1987) and Gower and Zielman (1998).

Example

Okada and Imaizumi (1997) analyse some occupational mobility data using a two-mode, three-way asymmetric model, described in Chapter 12. Data are available for several years, "years" being one of the modes. The data concern the occupations of sons compared with the occupations of their fathers. Occupations are divided into the eight categories: *1- Professional, 2- Nonmanual large enterprises, 3- Nonmanual small enterprises, 4- Nonmanual self-employed, 5- Manual large enterprises, 6- Manual small enterprises, 7- Manual self-employed, 8- Farm occupations.* Here only data for the year 1985 are analysed. The data to be used are in the form of a two-way table, $\mathbf{X}$, where the $[\mathbf{X}]_{rs}$ is the percentage of sons of the fathers in occupation group r who have occupations in occupation group s. These data were transformed to matrix $\mathbf{D}$

where $d_{rs} = |x_{rr} - x_{rs}|$,

$$\mathbf{D} = \begin{bmatrix} 0.0 & 25.3 & 19.5 & 40.1 & 40.5 & 38.1 & 43.1 & 43.8 \\ 10.9 & 0.0 & 9.5 & 21.7 & 18.1 & 22.8 & 26.4 & 29.0 \\ 26.5 & 17.4 & 0.0 & 28.1 & 26.3 & 13.9 & 30.1 & 34.6 \\ 19.5 & 21.9 & 13.3 & 0.0 & 24.3 & 25.4 & 26.7 & 32.1 \\ 13.2 & 17.6 & 16.1 & 29.9 & 0.0 & 20.0 & 26.5 & 31.9 \\ 20.6 & 15.4 & 7.5 & 24.0 & 10.9 & 0.0 & 19.6 & 26.1 \\ 25.5 & 20.1 & 19.4 & 23.5 & 21.3 & 12.7 & 0.0 & 30.3 \\ 1.7 & 2.3 & 0.9 & 3.4 & 3.9 & 10.7 & 2.6 & 0.0 \end{bmatrix}.$$

The symmetric matrix $\frac{1}{2}(\mathbf{D} + \mathbf{D}^T)$ can be analysed using one of the techniques for symmetric matrices. Figure 4.6 shows the configuration obtained by nonmetric scaling. The STRESS value was 9%.

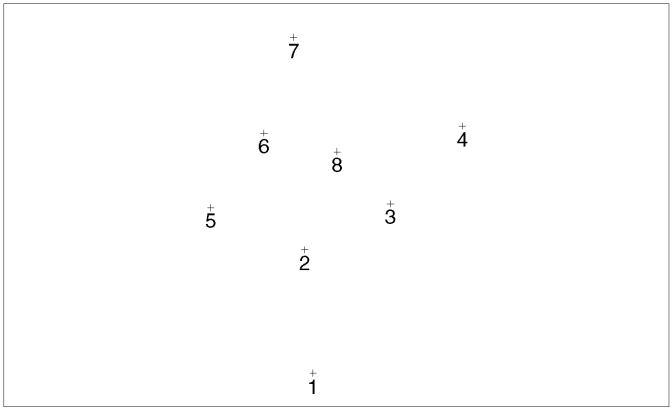

Figure 4.6 *Nonmetric scaling of the symmetric occupational mobility data*

The manual occupations (5, 6, 7) form a group. The professional occupations (1) are distanced from the other groups. Self-employed (4) also stands out. The nonmanual occupations (2, 3) are together. The farm occupations (8) are in the centre. The sons of these fathers tend to leave the farming industry for other occupations.

The skew-symmetric matrix $\frac{1}{2}(\mathbf{D} - \mathbf{D}^T)$ can be decomposed into four rank two canonical matrices according to equation (4.2). Figure 4.7 shows a plot for the first canonical matrix, i.e. a plot of the

points (u_{1i}, u_{2i}) together with the origin (+). The area of the triangle formed by the origin and the rth and sth points approximates the (r, s)th entry in the skew-symmetric matrix. The occupations that feature highly in the skew-symmetry are the professions (1), the nonmanual small enterprises (3), and the farm occupations (8).

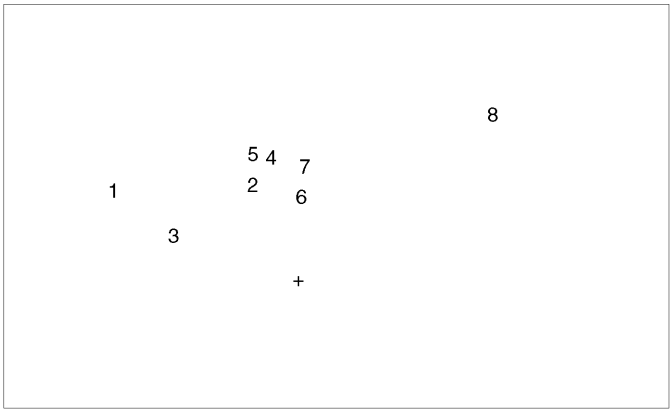

Figure 4.7 *Skew-symmetric analysis of the occupational mobility data*

CHAPTER 5

Procrustes analysis

5.1 Introduction

It is often necessary to compare one configuration of points in a Euclidean space with another where there is a one-to-one mapping from one set of points to the other. For instance, the configuration of points obtained from an MDS analysis on a set of objects might need to be compared with a configuration obtained from a different analysis, or perhaps with an underlying configuration, such as physical location.

The technique of matching one configuration to another and producing a measure of the match is called Procrustes analysis. This particular technique is probably the only statistical method to be named after a villain. Any traveller on the road from Eleusis to Athens in ancient Greece was in for a surprise if he accepted the kind hospitality and a bed for the night from a man named Damastes, who lived by the roadside. If his guests did not fit the bed, Damastes would either stretch them on a rack to make them fit if they were too short, or chop off their extremities if they were too long. Damastes earned the nickname Procrustes meaning "stretcher". Procrustes eventually experienced the same fate as that of his guests at the hands of Theseus – all this, of course, according to Greek mythology.

Procrustes analysis seeks the isotropic dilation and the rigid translation, reflection and rotation needed to best match one configuration to the other. Solutions to the problem of finding these motions have been given by Green (1952), Schönemann (1966), Schönemann and Carroll (1970). Sibson (1978) gives a short review of Procrustes analysis and sets out the solution. Hurley and Cattell (1962) were the first to use the term "Procrustes analysis".

Procrustes analysis has been used in many practical situations. For example, Richman and Vermette (1993) use it to discriminate dominant source regions of fine sulphur in the U.S.A. Pastor *et*

al. (1996) use Procrustes analysis on the sensory profiles of peach nectars. Sinesio and Moneta (1996) use it similarly on the sensory evaluation of walnut fruit. Gower and Dijksterhuis (1994) and de Jong *et al.* (1998) use Procrustes analysis in the study of coffee. Faller *et al.* (1998) use it for the classification of corn-soy breakfast cereals. An important use of Procrustes analysis is in the statistical analysis of shape, where configurations of points formed by "landmarks" placed on objects in order to define them, are translated and rotated to match each other. The reader is referred to Dryden and Mardia (1998) for an introduction to this area. See also Kendall (1984), Goodall (1991), Dryden *et al.* (1997) and Kendall *et al.* (1999).

5.2 Procrustes analysis

Suppose a configuration of n points in a q dimensional Euclidean space, with coordinates given by the $n \times q$ matrix $\mathbf{X}$, needs to be optimally matched to another configuration of n points in a $p \quad (p \geq q)$ dimensional Euclidean space with coordinate matrix $\mathbf{Y}$. It is assumed that the rth point in the first configuration is in a one-to-one correspondence with the rth point in the second configuration. The points in the two configurations could be representing objects, cities, stimuli, etc. Firstly, $p - q$ columns of zeros are placed at the end of matrix $\mathbf{X}$ so that both configurations are placed in p dimensional space. The sum of the squared distances between the points in the $\mathbf{Y}$ space and the corresponding points in the $\mathbf{X}$ space is given by

$$R^2 = \sum_{r=1}^{n} (\mathbf{y}_r - \mathbf{x}_r)^T (\mathbf{y}_r - \mathbf{x}_r)$$

where $\mathbf{X} = [\mathbf{x}_1, \ldots, \mathbf{x}_n]^T$, $\mathbf{Y} = [\mathbf{y}_1, \ldots, \mathbf{y}_n]^T$, and $\mathbf{x}_r$ and $\mathbf{y}_r$ are the coordinate vectors of the rth point in the two spaces.

Let the points in the $\mathbf{X}$ space be dilated, translated, rotated, reflected to new coordinates $\mathbf{x}'_r$, where

$$\mathbf{x}'_r = \rho \mathbf{A}^T \mathbf{x}_r + \mathbf{b}.$$

The matrix $\mathbf{A}$ is orthogonal, giving a rotation and possibly a reflection, vector $\mathbf{b}$ is a rigid translation vector and ρ is the dilation.

The motions are sought that minimize the new sum of squared distances between points,

$$R^2 = \sum_{r=1}^{n} (\mathbf{y}_r - \rho \mathbf{A}^T \mathbf{x}_r - \mathbf{b})^T (\mathbf{y}_r - \rho \mathbf{A}^T \mathbf{x}_r - \mathbf{b}). \tag{5.1}$$

Optimal translation
Let $\mathbf{x}_0$, $\mathbf{y}_0$ be the centroids of the two configurations,

$$\mathbf{x}_0 = \frac{1}{n} \sum_{r=1}^{n} \mathbf{x}_r, \quad \mathbf{y}_0 = \frac{1}{n} \sum_{r=1}^{n} \mathbf{y}_r.$$

Measuring $\mathbf{x}_r$ and $\mathbf{y}_r$ relative to these centroids in (5.1) gives

$$R^2 = \sum_{r=1}^{n} \Big((\mathbf{y}_r - \mathbf{y}_0) - \rho \mathbf{A}^T (\mathbf{x}_r - \mathbf{x}_0) + \mathbf{y}_0 - \rho \mathbf{A}^T \mathbf{x}_0 - \mathbf{b} \Big)^T$$
$$\Big((\mathbf{y}_r - \mathbf{y}_0) - \rho \mathbf{A}^T (\mathbf{x}_r - \mathbf{x}_0) + \mathbf{y}_0 - \rho \mathbf{A}^T \mathbf{x}_0 - \mathbf{b} \Big).$$

On expanding

$$R^2 = \sum_{r=1}^{n} \Big((\mathbf{y}_r - \mathbf{y}_0) - \rho \mathbf{A}^T (\mathbf{x}_r - \mathbf{x}_0) \Big)^T$$
$$\Big((\mathbf{y}_r - \mathbf{y}_0) - \rho \mathbf{A}^T (\mathbf{x}_r - \mathbf{x}_0) \Big)$$
$$+ n \Big(\mathbf{y}_0 - \rho \mathbf{A}^T \mathbf{x}_0 - \mathbf{b} \Big)^T \Big(\mathbf{y}_0 - \rho \mathbf{A}^T \mathbf{x}_0 - \mathbf{b} \Big). \tag{5.2}$$

Since the last term in (5.2) is non-negative, and $\mathbf{b}$ only occurs in this term, in order that R^2 be a minimum,

$$\mathbf{b} = \mathbf{y}_0 - \rho \mathbf{A}^T \mathbf{x}_0.$$

Hence

$$\mathbf{x}'_r = \rho \mathbf{A}^T (\mathbf{x}_r - \mathbf{x}_0) + \mathbf{y}_0,$$

which implies the centroid in the $\mathbf{X}'$ space is coincident with the centroid in the Y space. The most convenient way of ensuring this is initially to translate the configurations in the $\mathbf{X}$ space and $\mathbf{Y}$ space so that they both have their centroids at the origin.

Optimal dilation
Now assuming $\mathbf{x}_0 = \mathbf{y}_0 = \mathbf{0}$, then

$$\begin{aligned} R^2 &= \sum_{r=1}^{n} (\mathbf{y}_r - \rho \mathbf{A}^T \mathbf{x}_r)^T (\mathbf{y}_r - \rho \mathbf{A}^T \mathbf{x}_r) \\ &= \sum_{r=1}^{n} \mathbf{y}_r^T \mathbf{y}_r + \rho^2 \sum_{r=1}^{n} \mathbf{x}_r^T \mathbf{x}_r - 2\rho \sum_{r=1}^{n} \mathbf{x}_r^T \mathbf{A} \mathbf{y}_r \\ &= \mathrm{tr}(\mathbf{Y}\mathbf{Y}^T) + \rho^2 \mathrm{tr}(\mathbf{X}\mathbf{X}^T) - 2\rho \mathrm{tr}(\mathbf{X}\mathbf{A}\mathbf{Y}^T). \end{aligned} \tag{5.3}$$

Differentiating with respect to ρ gives $\hat{\rho}$, the value of ρ giving R^2 as a minimum,

$$\begin{aligned} \hat{\rho} &= \mathrm{tr}(\mathbf{X}\mathbf{A}\mathbf{Y}^T)/\mathrm{tr}(\mathbf{X}\mathbf{X}^T), \\ &= \mathrm{tr}(\mathbf{A}\mathbf{Y}^T\mathbf{X})/\mathrm{tr}(\mathbf{X}\mathbf{X}^T). \end{aligned}$$

The rotation matrix, $\mathbf{A}$, is still unknown and needs to be considered next.

Optimal rotation
Ten Berge (1977) derives the optimal rotation matrix with an elegant proof not requiring matrix differentiation of R^2. The derivation is repeated in Sibson (1978).The following is based on their work. For the alternative approach, using matrix differentiation, see for example ten Berge (1977) and Mardia *et al.* (1979).

The value of R^2 in (5.3) will be a minimum if $\mathrm{tr}(\mathbf{X}\mathbf{A}\mathbf{Y}^T) = \mathrm{tr}(\mathbf{A}\mathbf{Y}^T\mathbf{X})$ is a maximum. Let $\mathbf{C} = \mathbf{Y}^T\mathbf{X}$, and let $\mathbf{C}$ have the singular value decomposition

$$\mathbf{C} = \mathbf{U}\boldsymbol{\Lambda}\mathbf{V}^T,$$

where $\mathbf{U}$ and $\mathbf{V}$ are orthonormal matrices and $\boldsymbol{\Lambda}$ is a diagonal matrix of singular values. Then

$$\mathrm{tr}(\mathbf{A}\mathbf{C}) = \mathrm{tr}(\mathbf{A}\mathbf{U}\boldsymbol{\Lambda}\mathbf{V}^T) = \mathrm{tr}(\mathbf{V}^T\mathbf{A}\mathbf{U}\boldsymbol{\Lambda}).$$

Now $\mathbf{V}$, $\mathbf{A}$ and $\mathbf{U}$ are all orthonormal matrices; and hence so is $\mathbf{V}^T\mathbf{A}\mathbf{U}$. Since $\boldsymbol{\Lambda}$ is diagonal and an orthogonal matrix cannot have any element greater than unity,

$$\mathrm{tr}(\mathbf{A}\mathbf{C}) = \mathrm{tr}(\mathbf{V}^T\mathbf{A}\mathbf{U}\boldsymbol{\Lambda}) \leq \mathrm{tr}(\boldsymbol{\Lambda}).$$

Thus R^2 is minimised when $\mathrm{tr}(\mathbf{A}\mathbf{C}) = \mathrm{tr}(\boldsymbol{\Lambda})$, implying

$$\mathbf{V}^T\mathbf{A}\mathbf{U}\boldsymbol{\Lambda} = \boldsymbol{\Lambda}. \tag{5.4}$$

Equation (5.4) has solution $\mathbf{A} = \mathbf{V}\mathbf{U}^T$, giving the optimal rotation matrix as the product of the orthonormal matrices in the SVD of $\mathbf{Y}^T\mathbf{X}$.

The solution can be taken further. Pre-multiplying and post-multiplying (5.4) by $\mathbf{V}$ and $\mathbf{V}^T$ respectively,

$$\mathbf{A}\mathbf{U}\boldsymbol{\Lambda}\mathbf{V}^T = \mathbf{V}\boldsymbol{\Lambda}\mathbf{V}^T.$$

Hence

$$\mathbf{A}\mathbf{C} = \mathbf{V}\boldsymbol{\Lambda}\mathbf{V}^T = (\mathbf{V}\boldsymbol{\Lambda}^2\mathbf{V}^T)^{\frac{1}{2}} = (\mathbf{V}\boldsymbol{\Lambda}\mathbf{U}\mathbf{U}^T\boldsymbol{\Lambda}\mathbf{V}^T)^{\frac{1}{2}}$$

$$= (\mathbf{C}^T\mathbf{C})^{\frac{1}{2}}.$$

Thus the optimal rotation matrix is given by

$$(\mathbf{C}^T\mathbf{C})^{\frac{1}{2}}\mathbf{C}^{-1} = (\mathbf{X}^T\mathbf{Y}\mathbf{Y}^T\mathbf{X})^{\frac{1}{2}}(\mathbf{Y}^T\mathbf{X})^{-1},$$

if $\mathbf{Y}^T\mathbf{X}$ is nonsingular, and by a solution of

$$\mathbf{A}\mathbf{C} = (\mathbf{C}^T\mathbf{C})^{\frac{1}{2}}$$

otherwise. Note that the solution no longer requires the SVD of $\mathbf{Y}^T\mathbf{X}$, which was only needed in the proof of (5.4).

Returning to the optimal dilation, it is now seen that

$$\hat{\rho} = \mathrm{tr}(\mathbf{X}^T\mathbf{Y}\mathbf{Y}^T\mathbf{X})^{\frac{1}{2}}/\mathrm{tr}(\mathbf{X}^T\mathbf{X}).$$

Assessing the match of the two configurations can be done using the minimised value of R^2, which is

$$R^2 = \mathrm{tr}(\mathbf{Y}\mathbf{Y}^T) - \{\mathrm{tr}(\mathbf{X}^T\mathbf{Y}\mathbf{Y}^T\mathbf{X})^{\frac{1}{2}}\}^2/\mathrm{tr}(\mathbf{X}^T\mathbf{X}).$$

The value of R^2 can now be scaled, for example, by dividing by $\mathrm{tr}(\mathbf{Y}^T\mathbf{Y})$ to give

$$R^2 = 1 - \{\mathrm{tr}(\mathbf{X}^T\mathbf{Y}\mathbf{Y}^T\mathbf{X})^{\frac{1}{2}}\}^2/\{\mathrm{tr}(\mathbf{X}^T\mathbf{X})\mathrm{tr}(\mathbf{Y}^T\mathbf{Y})\}.$$

This is known as the Procrustes statistic.

5.2.1 Procrustes analysis in practice

Summarizing the steps in a Procrustes analysis where configuration Y is to be matched to configuration X:

1. Subtract the mean vectors for the configurations from each of the respective points in order to have the centroids at the origin.

2. Find the rotation matrix $\mathbf{A} = (\mathbf{X}^T\mathbf{Y}\mathbf{Y}^T\mathbf{X})^{\frac{1}{2}}(\mathbf{Y}^T\mathbf{X})^{-1}$ and rotate the $\mathbf{X}$ configuration to $\mathbf{XA}$.
3. Scale the $\mathbf{X}$ configuration by multiplying each coordinate by ρ, where $\rho = \mathrm{tr}(\mathbf{X}^T\mathbf{Y}\mathbf{Y}^T\mathbf{X})^{\frac{1}{2}}/\mathrm{tr}(\mathbf{X}^T\mathbf{X})$.
4. Calculate the minimised and scaled value of

$$R^2 = 1 - \{\mathrm{tr}(\mathbf{X}^T\mathbf{Y}\mathbf{Y}^T\mathbf{X})^{\frac{1}{2}}\}^2/\{\mathrm{tr}(\mathbf{X}^T\mathbf{X})\mathrm{tr}(\mathbf{Y}^T\mathbf{Y})\}.$$

An example

Figure 5.1(i) shows the two dimensional classical scaling configuration of the breakfast cereal data analysed in Section 3.2.4. Again, Euclidean distance has been used to generate the dissimilarities after scaling each variable to have range [0, 1]. The first two eigenvalues of $\mathbf{B}$ are 5.487 and 4.205 and give an adequacy measure of 54% when compared with the sum of all the eigenvalues.

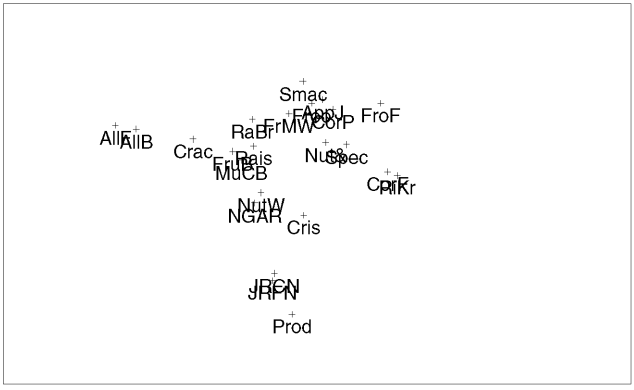

Figure 5.1(i) *Classical scaling of the breakfast cereals*

Figure 5.1(ii) shows the nonmetric MDS configuration, noting that this is different to that of Chapter 3 where a different scaling of the variables was used. The STRESS this time was 14%. Figure 5.1(iii) shows the nonmetric MDS configuration matched to the classical scaling configuration using Procrustes analysis. The Procrustes statistic had the value 0.102.

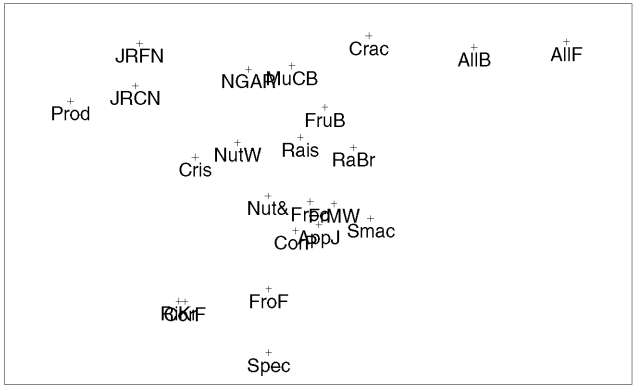

Figure 5.1(ii) *Nonmetric scaling of the breakfast cereals*

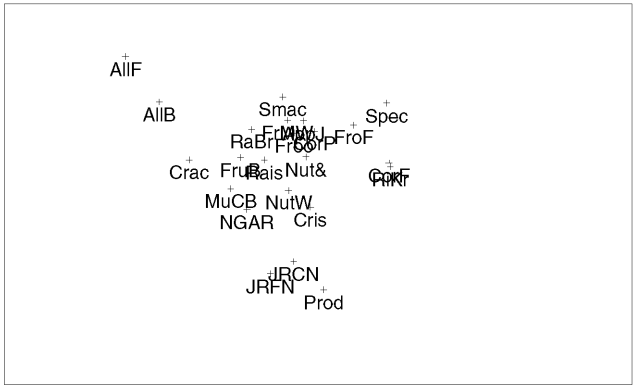

Figure 5.1(iii) *The nonmetric MDS configuration matched to the classical scaling configuration using Procrustes analysis*

5.2.2 The projection case

Gower (1994) considers the case $p > q$. The matrix $\mathbf{A}$ is required so that

$$r^2 = \text{tr}(\mathbf{Y} - \mathbf{XA})(\mathbf{Y} - \mathbf{XA})^T$$

is minimised as before, but $\mathbf{A}$ is now a $p \times q$ projection matrix.

Green and Gower (1979) and Gower (1994) propose the following algorithm for the solution. See also Gower and Hand (1996).

1. Add $p - q$ columns of zeros to $\mathbf{Y}$.
2. Match $\mathbf{X}$ to $\mathbf{Y}$ in the usual Procrustes manner, giving a $p \times p$ rotation matrix $\mathbf{A}^*$. Rotate $\mathbf{X}$ to $\mathbf{X}\mathbf{A}^*$.
3. Replace the final $p-q$ columns of $\mathbf{Y}$ by the final $p-q$ columns of $\mathbf{X}\mathbf{A}^*$. Calculate the value of R^2.
4. Stop if the value of R^2 has reached a minimum. Otherwise, return to step 2 using the current $\mathbf{Y}$ and $\mathbf{X}$.

The matrix $\mathbf{A}$ is then given by the first q columns of $\mathbf{A}^*$.

5.3 Historic maps

The construction of maps centuries ago was clearly not an easy task, where only crude measuring instruments could be used, in contrast to the satellite positioning available today. John Speed's County Atlas, the *Theatre of the Empire of Great Britain*, was first engraved and printed in Amsterdam by Jodous Hondius in 1611-1612. A copy of his map of Worcestershire appears in Bricker *et al.* (1976). Twenty towns and villages were chosen from the map and the coordinates were found for each by measuring from the lower left-hand corner of the map. The corresponding places were also

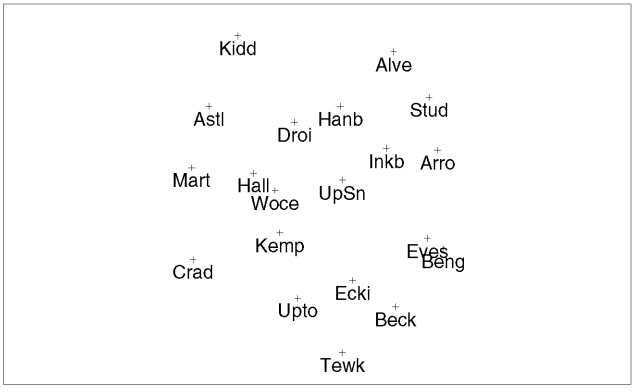

Figure 5.2(i) *Location of villages and towns from Speed's map: Alvechurch, Arrow, Astley, Beckford, Bengeworth, Cradley, Droitwich, Eckington, Evesham, Hallow, Hanbury, Inkberrow, Kempsey, Kidderminster, Martley, Studley, Tewkesbury, Upper Snodsbury, Upton, Worcester.*

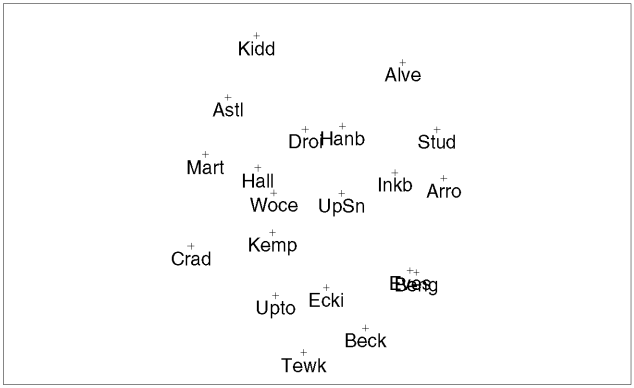

Figure 5.2(ii) *The locations of the villages and towns from Ordnance Survey maps*

found on the Landranger Series of Ordnance Survey Maps (numbers 150, 139, 138) and their coordinates noted. Since the area covered was relatively small, any projection from the earth's sphere onto a two dimensional plane was ignored. Historic buildings like churches were taken as the point locations of the towns and villages. A Procrustes analysis for the two configurations of places should give some insight into the accuracy of the early map. Figure 5.2 (i) shows the locations of the various villages and towns from Speed's map. Figure 5.2 (ii) shows the same places according to Ordnance Survey maps. The configuration of points in Speed's map was subjected to Procrustes analysis, giving rise to the rotated, dilated and translated set of points in Figure 5.2 (iii). The points did not have to move very far as indicated by the value of the Procrustes statistic, 0.004, indicating that Speed's map was fairly accurate. The root mean squared distance between corresponding points was equivalent to a distance of about 8 miles; a possible measure of the accuracy of the early map.

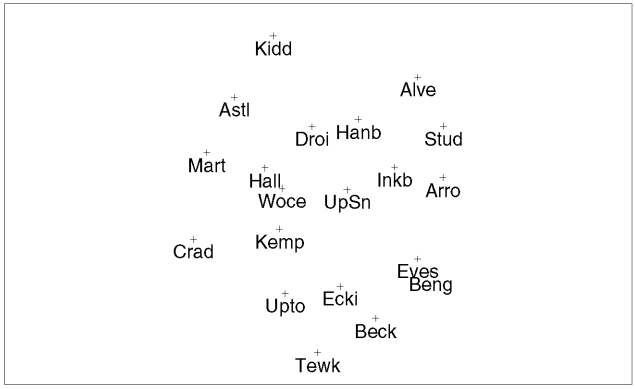

Figure 5.2(iii) *Speed's map after Procrustes analysis to match it to the Ordnance Survey map*

5.4 Some generalizations

Once the configurations of points have been translated to have centroids at the origin, the "Procrustes analysis" or the "Procrustes rotation" described in the previous section can be simply described as the rotation of a matrix $\mathbf{X}$ so that it matches matrix $\mathbf{Y}$ as best as possible. This was achieved by essentially minimising

$$R^2 = \text{tr}(\mathbf{Y} - \mathbf{XA})^T(\mathbf{Y} - \mathbf{XA}).$$

The technique can be described as the unweighted orthogonal Procrustes rotation. Some generalizations of the method are briefly explained.

5.4.1 Weighted Procrustes rotation

Suppose the contribution to R^2 by point r is to be weighted by an amount ω_r^2 $(r = 1, \ldots, n)$. Then the rotation $\mathbf{A}$ is sought that minimises

$$R^2 = \text{tr}(\mathbf{Y} - \mathbf{XA})^T\mathbf{W}_n^2(\mathbf{Y} - \mathbf{XA}), \tag{5.5}$$

where $\mathbf{W}_n = \text{diag}(\omega_1, \ldots, \omega_n)$.

Now R^2 can be rewritten as

$$R^2 = \text{tr}(\mathbf{W}_n\mathbf{Y} - \mathbf{W}_n\mathbf{XA})^T(\mathbf{W}_n\mathbf{Y} - \mathbf{W}_n\mathbf{XA}),$$

and hence the solution for the unweighted case can be used, but using $\mathbf{W}_n\mathbf{X}$ and $\mathbf{W}_n\mathbf{Y}$ instead of $\mathbf{X}$ and $\mathbf{Y}$. Lissitz *et al.* (1976) is an early reference to the problem. See also Gower (1984).

If, instead of weighting the points in the configuration, the dimensions are weighted in matrix $\mathbf{Y}$, then the appropriate quantity to minimise is now

$$R^2 = \text{tr}(\mathbf{Y} - \mathbf{XA})\mathbf{W}_p^2(\mathbf{Y} - \mathbf{XA})^T,$$

where $\mathbf{W}_p = \text{diag}(\omega_1, \ldots, \omega_p)$. This case is much more difficult to solve since $\mathbf{X}$ and $\mathbf{Y}$ cannot simply be replaced by $\mathbf{XW}_p$ and $\mathbf{YW}_p$. Lissitz *et al.* (1976) show that R^2 can be minimised if the condition $\mathbf{AA}^T = \mathbf{I}$, is replaced by $\mathbf{AW}_p^2\mathbf{A}^T = \mathbf{I}$, but, as noted by Gower (1984) and Koschat and Swayne (1991), this may be convenient mathematically, but does not solve the original problem.

Mooijaart and Commandeur (1990) and Koschat and Swayne (1991) give a solution to the problem. Following the latter, suppose the column vectors in $\mathbf{X}$ are pairwise orthogonal and each of length ρ, so that $\mathbf{X}^T\mathbf{X} = \rho\mathbf{I}$. Then

$$\begin{aligned} R^2 &= \text{tr}(\mathbf{Y} - \mathbf{XA})\mathbf{W}_p^2(\mathbf{Y} - \mathbf{XA})^T \\ &= \text{tr}(\mathbf{YW}_p^2\mathbf{Y}^T) - 2\text{tr}(\mathbf{W}_p^2\mathbf{Y}^T\mathbf{XA}) + \rho^2\text{tr}(\mathbf{W}_p^2), \end{aligned}$$

and hence, minimisation of R^2 is equivalent to the maximisation of

$$\text{tr}(\mathbf{W}_p^2\mathbf{Y}^T\mathbf{XA}) = \text{tr}(\mathbf{XAW}_p^2\mathbf{Y}^T)$$

and can be achieved in the same manner as the unweighted case with $\mathbf{Y}^T$ replaced by $\mathbf{W}_p^2\mathbf{Y}^T$. This result can now be used for general $\mathbf{X}$ as follows.

Enlarge $\mathbf{X}$ and $\mathbf{Y}$ to $(n + p) \times p$ matrices

$$\mathbf{X}^* = \begin{bmatrix} \mathbf{X} \\ \mathbf{X}_a \end{bmatrix}, \qquad \mathbf{Y}_1^* = \begin{bmatrix} \mathbf{Y} \\ \mathbf{Y}_1 \end{bmatrix}$$

with $\mathbf{X}_a$ chosen so that $\mathbf{X}^{*T}\mathbf{X}^* = \rho^2\mathbf{I}$ for some ρ. Thus $\mathbf{X}_a$ is chosen so that

$$\mathbf{X}_a^T\mathbf{X}_a = \rho^2\mathbf{I} - \mathbf{X}^T\mathbf{X}.$$

Koschat and Swayne (1991) suggest using $\rho = 1.1$ times the largest eigenvalue of $\mathbf{X}^T\mathbf{X}$, and chosing $\mathbf{X}_a$ as the Cholesky decomposition of $\rho^2\mathbf{I} - \mathbf{X}^T\mathbf{X}$. The matrix $\mathbf{Y}_1$ is arbitrary, and is used as a starting point, although careful choice might be desirable. Koschat

and Swayne's algorithm for finding an $\mathbf{A}$ which minimises R^2 is as follows:

1. Set the starting matrices $\mathbf{X}^*, \mathbf{Y}_1^*$.
2. For $i = 1, 2, \ldots$, find $\mathbf{H}_i$, the orthogonal rotation that minimises
$$R^2 = \text{tr}(\mathbf{Y}_i^* - \mathbf{X}^*\mathbf{H}_i)\mathbf{W}_p^2(\mathbf{Y}_i^* - \mathbf{X}^*\mathbf{H}_i)^T,$$
using results for the unweighted case, since $\mathbf{X}^{*T}\mathbf{X}^* = \rho^2\mathbf{I}$. Stop if convergence has been achieved.
3. Compute the updated $\mathbf{Y}^*$ matrix
$$\mathbf{Y}_{i+1}^* = \begin{bmatrix} \mathbf{Y} \\ \mathbf{X}_a\mathbf{H}_i \end{bmatrix}$$
4. Go to step 2.

Koschat and Swayne show that the values of R^2 form a non-increasing sequence, and hence, converge, and also that $\mathbf{H}_i$ converges if there are only finitely many extrema or saddle points for R^2.

Chu and Trendafilov (1998) give an alternative algorithm based on a matrix differential equation aproach. They also allow for a more general $\mathbf{W}_p$. Briefly the algorithm is as follows.

Let the function $F(\mathbf{Z})$ be defined as
$$F(\mathbf{Z}) = \frac{1}{2}\text{tr}(\mathbf{Y}\mathbf{W}_p - \mathbf{X}\mathbf{Z}\mathbf{W}_p)(\mathbf{Y}\mathbf{W}_p - \mathbf{X}\mathbf{Z}\mathbf{W}_p)^T.$$
The gradient $\nabla F(\mathbf{Z})$ is given by
$$\nabla F(\mathbf{Z}) = \mathbf{X}^T(\mathbf{Y}\mathbf{W}_p - \mathbf{X}\mathbf{Z}\mathbf{W}_p)\mathbf{W}_p^T.$$
The function F is minimised with respect to $\mathbf{Z}$, but with $\mathbf{Z}$ constrained to be orthogonal. Then the required matrix $\mathbf{A}$ is the $\mathbf{Z}$ giving rise to the minimum.

Moving along the gradient $\nabla F(\mathbf{Z})$ as in gradient descent algorithms for finding minima, would violate the condition that $\mathbf{Z}$ has to be orthogonal. To overcome this, $\nabla F(\mathbf{Z})$ is projected onto the tangent space of the topology for all $p \times p$ orthogonal matrices. Let this projection be $g(\mathbf{Z})$ and so the algorithm moves $\mathbf{Z}$ along this projection towards the solution. Chu and Trendafilov show the projection is given by
$$g(\mathbf{Z}) = \frac{1}{2}\mathbf{Z}(\mathbf{Z}^T\mathbf{X}^T(\mathbf{X}\mathbf{Z} - \mathbf{Y})\mathbf{W}_p^2 - \mathbf{W}_p^2(\mathbf{X}\mathbf{Z} - \mathbf{Y})^T\mathbf{X}\mathbf{Z}).$$

Chu and Trendafilov numerically compare their algorithm with that of Koschat and Swayne. They show that the two algorithms behave similarly in the proportion of global minima they find, as opposed to local minima, but concede that their algorithm is slower. However, they have brought a powerful numerical analysis method to bear in the multivariate data analysis arena, and further developments in this area should ensue.

5.4.2 Generalized Procrustes analysis

Instead of two configurations to be matched, suppose there are m configurations that need to be matched simultaneously. Procrustes analysis can be modified to allow for this, and is termed generalized Procrustes analysis. Let the configurations be given by matrices $\mathbf{X}_i$ $(i = 1, \ldots, m)$ (assuming centroids are at the origin), and let $\mathbf{A}_i$ be the orthogonal rotation applied to the ith configuration. Then

$$R^2 = \sum_{i<j} \mathrm{tr}(\mathbf{X}_i\mathbf{A}_i - \mathbf{X}_j\mathbf{A}_j)^T(\mathbf{X}_i\mathbf{A}_i - \mathbf{X}_j\mathbf{A}_j)$$

needs to be minimised.

Kristof and Wingersky (1971) and Gower (1975) give a method for solving this generalized Procrustes problem. Firstly, the configurations $\mathbf{X}_i$ are centred at the origin, and scaled uniformly so that $\sum_{i=1}^{m} \mathrm{tr}(\mathbf{X}_i\mathbf{X}_i^T) = m$. The configurations $\mathbf{X}_i$ are rotated in turn to $\mathbf{Y}$, the mean matrix, $\mathbf{Y} = m^{-1}\sum \mathbf{X}_i$, using the usual two configuration Procrustes rotation. The mean matrix is then updated after every rotation. The iterations will converge to a minimum for R^2. If scaling of the matrices is required, a further step in the algorithm is needed. Ten Berge (1977) considered the algorithm of Kristof and Wingersky in detail and suggested a modification to Gower's method, arguing that better results are obtained if $\mathbf{X}_i$ is not rotated to the current mean matrix $\mathbf{Y}$, but to the mean matrix, $\mathbf{Y}_{(i)}$, of the remaining $m - 1$ matrices. He also suggested a different method for updating the scaling factor. Ten Berge and Bekker (1993) give more evidence as to why their scaling procedure should be used rather than that of Gower.

Peay (1988) gives a good summary of the problem and suggests a method for rotating configurations which maximises the matching among subspaces of the configurations, the essentials of which had been given by ten Berge and Knol (1984).

Ten Berge *et al.* (1993) consider the case of missing data in

the matrices $\mathbf{X}_i$. For instance, they argue that it would not be uncommon for data to be missing in "Free Choice Profiling", where $\mathbf{X}_i$ a matrix of scores for n objects on p idiosyncratic concepts obtained from judge i. These matrices are to be rotated to maximal agreement. It is conceivable that certain columns of data could be missing, certain rows could be missing, or single elements could be missing.

Missing columns can be replaced by columns of zeros. For missing rows Commandeur (1991) minimises the loss function R^2, given by

$$R^2 = \sum_{i=1}^{m} \text{tr}(\mathbf{M}_i(\mathbf{X}_i\mathbf{A}_i - \mathbf{Y})^T\mathbf{M}_i(\mathbf{X}_i\mathbf{A}_i - \mathbf{Y}))$$

where $\mathbf{M}_i$ is a diagonal $n \times n$ matrix with jth diagonal element equal to unity if the data in row j is present and zero if it is missing. The centroid matrix $\mathbf{Y}$ is $\mathbf{Y} = (\sum_i \mathbf{M}_i)^{-1} \sum_i \mathbf{M}_i\mathbf{X}_i\mathbf{A}_i$.

Ten Berge *et al.* (1993) consider missing data in arbitrary places in the matrices. They minimise the usual R^2 not only over orthogonal rotations (and translations, dilations), but also over parameters that replace the missing values. This is shown to give the same results for the missing rows case of Commandeur. Accordingly, the parameter values giving rise to the minimum R^2 are estimates of the missing values. The reader is referred to the papers for further details.

Verboon and Gabriel (1995) consider the case of generalized Procrustes analysis with weights that are not fixed, but are estimated. The intention is to have a Procrustes procedure which is resistant to outliers. This is an extension to the case of only two configurations given earlier by Verboon and Heiser (1992). The loss function to be minimised is

$$\sum_{i=1}^{m}\sum_{r=1}^{n}\sum_{j=1}^{p} w_{rj,i}(y_{rj} - \mathbf{x}_{r,i}^T\mathbf{a}_{j,i})^2$$

where $\mathbf{W}_i = [w_{rj,i}]$ is the weight matrix for the ith configuration $\mathbf{X}_i = [\mathbf{x}_1, \ldots, \mathbf{x}_n]^T$, $\mathbf{Y} = [y_{rj}]$ is the centroid matrix $m^{-1} \sum_i \mathbf{X}_i\mathbf{A}_i$, $\mathbf{A}_i = [\mathbf{a}_1, \ldots, \mathbf{a}_p]^T$.

The weights are chosen as some decreasing function of the Euclidean distances between the points in the configurations, $\mathbf{X}_i$ and

the corresponding point in the centroid matrix. For the rth point in the ith configuration the distance is

$$d_{r,i} = \left(\sum_{j=1}^{p} (y_{rj} - \mathbf{x}_{r,i}^T \mathbf{a}_{j,i})^2 \right)^{\frac{1}{2}}.$$

Then the resistant weight function could be chosen as the Huber function

$$\begin{aligned} w_{rj,i} &= 1 \quad \text{if } d_{r,i} < c \\ &= \frac{c}{d_{r,i}} \quad \text{if } d_{r,i} \geq c \end{aligned}$$

where c is a tuning constant. Other functions are possible. See Verboon and Gabriel for further details.

5.4.3 The coefficient of congruence

Tucker (1951) introduced the coefficient of congruence between two vectors $\mathbf{x}$ and $\mathbf{y}$ as

$$\boldsymbol{\Gamma}(\mathbf{x}, \mathbf{y}) = \mathbf{x}^T\mathbf{y} / \{(\mathbf{x}^T\mathbf{x})(\mathbf{y}^T\mathbf{y})\}^{\frac{1}{2}}.$$

The maximum value of $\boldsymbol{\Gamma}$ is unity when $\mathbf{x} = \lambda\mathbf{y}$, λ a positive constant. Instead of using R^2, the sum of the distances between corresponding points in the two configurations, Brokken (1983) has suggested using the sum of the coefficients of congruence, g, between the corresponding points. This can be written as

$$g(\mathbf{A}) = \text{tr}\{[\text{diag}(\mathbf{A}^T\mathbf{X}^T\mathbf{X}\mathbf{A})]^{-\frac{1}{2}}\mathbf{A}^T\mathbf{X}^T\mathbf{Y}[\text{diag}(\mathbf{Y}^T\mathbf{Y})]^{-\frac{1}{2}}\}.$$

Now $g(\mathbf{A})$ has to be minimised with respect to $\mathbf{A}$ with the constraint $\mathbf{A}\mathbf{A}^T - \mathbf{I} = \mathbf{0}$. Using the matrix $\boldsymbol{\Theta}$ of Lagrange multipliers, consider minimising

$$h(\mathbf{A}, \boldsymbol{\Theta}) = g(\mathbf{A}) + \text{tr}[\boldsymbol{\Theta}(\mathbf{A}\mathbf{A}^T - \mathbf{I})].$$

After some algebra, Brokken shows that

$$\begin{aligned} \frac{\partial h}{\partial \mathbf{A}} &= (\boldsymbol{\Theta} + \boldsymbol{\Theta}^T)\mathbf{A} + \mathbf{X}^T\mathbf{Y}^*(\text{diag}(\mathbf{A}^T\mathbf{X}^T\mathbf{X}\mathbf{A}))^{-\frac{1}{2}} \\ &\quad -\mathbf{X}^T\mathbf{X}\mathbf{A}\text{diag}(\mathbf{A}^T\mathbf{X}^T\mathbf{Y}^*)(\text{diag}(\mathbf{A}^T\mathbf{X}^T\mathbf{X}\mathbf{A}))^{-\frac{3}{2}}, \end{aligned}$$

where $\mathbf{Y}^* = \mathbf{Y}[\text{diag}(\mathbf{Y}^T\mathbf{Y})]^{-\frac{1}{2}}$.

Using these first partial derivatives, and possibly the more complicated second partial derivatives, h, and hence g, can be minimised numerically using an appropriate algorithm.

Kiers and Groenen (1996) offer a majorization algorithm (see Chapter 10) to maximise congruence. Theirs is easier to program and is guaranteed to converge from every starting point, unlike that of Brokken.

Using Tucker's coefficients of congruence in the matching of matrices is useful in factor analysis (see for example Mardia *et al.* (1979), Chapter 9), where factor loadings given by matrices $\mathbf{X}$ and $\mathbf{Y}$ are to be compared. Also useful in factor analysis is the use of oblique rotations of factor matrices. This gives rise to the oblique Procrustes problem.

5.4.4 Oblique Procrustes problem

The oblique Procrustes problem is to find a non-orthogonal rotation matrix $\mathbf{A}$ such that

$$R^2 = \text{tr}(\mathbf{Y} - \mathbf{XA})^T(\mathbf{Y} - \mathbf{XA})$$

is a minimum and subject only to $\text{diag}(\mathbf{A}^T\mathbf{A}) = \mathbf{I}$.

Browne (1967) gave a numerical solution using Lagrange multipliers. No constraints are imposed between columns of $\mathbf{A}$, and hence each column can be considered separately. Let $\mathbf{y}$ be a column of $\mathbf{Y}$. A vector $\mathbf{a}$ has to be found such that

$$(\mathbf{y} - \mathbf{Xa})^T(\mathbf{y} - \mathbf{Xa})$$

is a minimum subject to $\mathbf{a}^T\mathbf{a} = 1$.

Let

$$g = (\mathbf{y} - \mathbf{Xa})^T(\mathbf{y} - \mathbf{Xa}) - \mu(\mathbf{a}^T\mathbf{a} - 1),$$

where μ is a Lagrange multiplier. Differentiating with respect to $\mathbf{a}$ and setting equal to $\mathbf{0}$ gives

$$\mathbf{X}^T\mathbf{Xa} - \mu\mathbf{a} = \mathbf{X}^T\mathbf{y}. \tag{5.6}$$

This equation can be simplified by using the spectral decomposition of $\mathbf{X}^T\mathbf{X}$ ($= \mathbf{U}\boldsymbol{\Lambda}\mathbf{U}^T$ say).

Equation (5.6) becomes

$$\mathbf{U}\boldsymbol{\Lambda}\mathbf{U}^T\mathbf{a} - \mu\mathbf{a} = \mathbf{X}^T\mathbf{y}.$$

Pre-multiply by $\mathbf{U}^T$, let $\mathbf{U}^T\mathbf{a} = \mathbf{b}$ and $\mathbf{U}^T\mathbf{X}^T\mathbf{y} = \mathbf{w}$, then

$$\boldsymbol{\Lambda}\mathbf{b} - \mu\mathbf{b} = \mathbf{w}. \tag{5.7}$$

Now $\mathbf{a}^T\mathbf{a} = 1$, and hence the equation now to be solved can be written

$$b_i = \frac{w_i}{\lambda_i - \mu}, \qquad \sum b_i^2 = 1,$$

and hence the roots of $z(\mu) = 0$ are required, where

$$z(\mu) = \sum \frac{w_i^2}{(\lambda_i - \mu)^2} - 1,$$

giving the stationary points of R^2.

Browne goes on to show that the minimum value of R^2 corresponds to the smallest real root of $z(\mu)$. He uses the Newton-Raphson method to solve for the roots.

Cramer (1974) pointed out that if $\mathbf{X}^T\mathbf{y}$ is orthogonal to the eigenvector corresponding to the smallest eigenvalue λ_p then there may be a solution to (5.7) which is not a solution of $z(\mu) = 0$. Ten Berge and Nevels (1977) give a general solution to the problem which covers this case noted by Cramer, and also takes care of the case where $\mathbf{X}$ is not of full rank. They derived a general algorithm for the solution. The reader is referred to their paper for further details.

Korth and Tucker (1976) consider the maximum congruence approach for finding $\mathbf{A}$. The congruence coefficient for column i of $\mathbf{X}$ and $\mathbf{Y}$ is

$$g_i = \frac{(\mathbf{X}\mathbf{A}_i)^T\mathbf{Y}_i}{((\mathbf{X}\mathbf{A}_i)^T(\mathbf{X}\mathbf{A}_i))^{\frac{1}{2}}(\mathbf{Y}_i^T\mathbf{Y}_i)^{\frac{1}{2}}}$$

where $\mathbf{A}_i$ and $\mathbf{Y}_i$ are the ith columns of $\mathbf{A}$ and $\mathbf{Y}$ respectively. It is easy to show that g_i is maximised when $\mathbf{A}_i = (\mathbf{X}^T\mathbf{X})-1\mathbf{Y}_i$, and hence the regression type solution

$$\mathbf{A} = (\mathbf{X}^T\mathbf{X})^{-1}\mathbf{X}^T\mathbf{Y}.$$

5.4.5 Perturbation analysis

Sibson (1979) investigated the distribution of R^2 when a configuration matrix $\mathbf{X}$ is perturbed with random errors added to its elements, $\mathbf{X} + \epsilon\mathbf{Z}$, and then matched back to the original $\mathbf{X}$.

Let $\mathbf{X}^T\mathbf{X}$ have eigenvalues $\lambda_1 > \ldots > \lambda_n > 0$ and corresponding eigenvectors $\mathbf{v}_1, \ldots, \mathbf{v}_n$. Sibson shows that if dilation is not included

$$R^2 = \frac{1}{2}\epsilon^2 \Bigg\{ \sum_{i=1}^{p}\sum_{j=1}^{p} \frac{(\mathbf{v}_i^T(\mathbf{X}^T\mathbf{Z} + \mathbf{Z}^T\mathbf{X})\mathbf{v}_j)^2}{\lambda_i + \lambda_j} + 2\sum_{i=p+1}^{n-1} \mathbf{v}_i^T\mathbf{Z}\mathbf{Z}^T\mathbf{v}_i \Bigg\}. \tag{5.8}$$

Thus it can be shown that if the elements of $\mathbf{Z}$ are independent N(0,1) random variables, then approximately

$$R^2 \sim \epsilon^2 \chi^2_{np-\frac{1}{2}p(p+1)}.$$

If dilation of a configuration is included the term

$$-2\frac{(\mathrm{tr}\mathbf{X}^T\mathbf{Z})^2}{\mathrm{tr}\mathbf{X}^T\mathbf{X}}$$

has to be included in (5.8) and approximately

$$R^2 \sim \epsilon^2 \chi^2_{np-\frac{1}{2}p(p+1)-1}.$$

Langron and Collins (1985) extend the work of Sibson to the generalized case of several configuration matrices. They consider the two configuration situations with errors in both configuration matrices and show

$$R^2 \sim 2\epsilon^2 \chi^2_{np-\frac{1}{2}p(p+1)}, \qquad R^2 \sim 2\epsilon^2 \chi^2_{np-\frac{1}{2}p(p+1)-1},$$

approximately for the cases of no dilation allowed and dilation allowed respectively. They generalize this to the situation of m configurations. They also show how an ANOVA can be carried out to investigate the significance of the different parts of the Procrustes analysis, translation, rotation/reflection and dilation. The reader is referred to their paper for further details.

Söderkvist (1993) considers the perturbation problem of Procrustes matching (but not allowing reflections) $\mathbf{X}+\Delta\mathbf{X}$ to $\mathbf{Y}+\Delta\mathbf{Y}$ where $\Delta\mathbf{X}$ and $\Delta\mathbf{Y}$ are perturbation matrices. Let $\mathbf{A}$ be the Procrustes rotation matrix that optimally rotates $\mathbf{X}$ to $\mathbf{Y}$. Söderkvist investigates how the Procrustes rotation matrix $\mathbf{A} + \Delta\mathbf{A}$ that optimally rotates $\mathbf{X} + \Delta\mathbf{X}$ to $\mathbf{Y} + \Delta\mathbf{Y}$ depends on $\Delta\mathbf{X}$ and $\Delta\mathbf{Y}$.

CHAPTER 6

Monkeys, whisky and other applications

6.1 Introduction

Metric and nonmetric multidimensional scaling is currently being used for data analysis in a multitude of disciplines. Some relatively recent examples are: biometrics – Lawson and Ogg (1989), counselling psychology – Fitzgerald and Hubert (1987), ecology – Tong (1989), ergonomics – Coury (1987), forestry – Smith and Iles (1988), lexicography – Tijssen and Van Raan (1989), marketing – Büyükkurt and Büyükkurt (1990), tourism – Fenton and Pearce (1988), and brain connectivity – Goodhill *et al.* (1995) and Young *et al.* (1995).

In this chapter, five applications of multidimensional scaling are reported. The examples come from the areas of animal behaviour, defence, food science and biological cybernetics.

6.2 Monkeys

Corradino (1990) used MDS to study the proximity structure in a colony of Japanese monkeys. Observations were made on a social group of 14 Japanese monkeys over a period of a year. The fourteen monkeys are named and described in Table 6.1.

Proximity relations every 60 seconds were observed. If two monkeys were within 1.5 m of each other, and were tolerating each other, then they were said to be "close". Dissimilarities were calculated for each pair of monkeys based on the amount of time the pair were in proximity to one another. The dissimilarities were then subjected to nonmetric MDS, proximities in the breeding season and non-breeding season being treated separately.

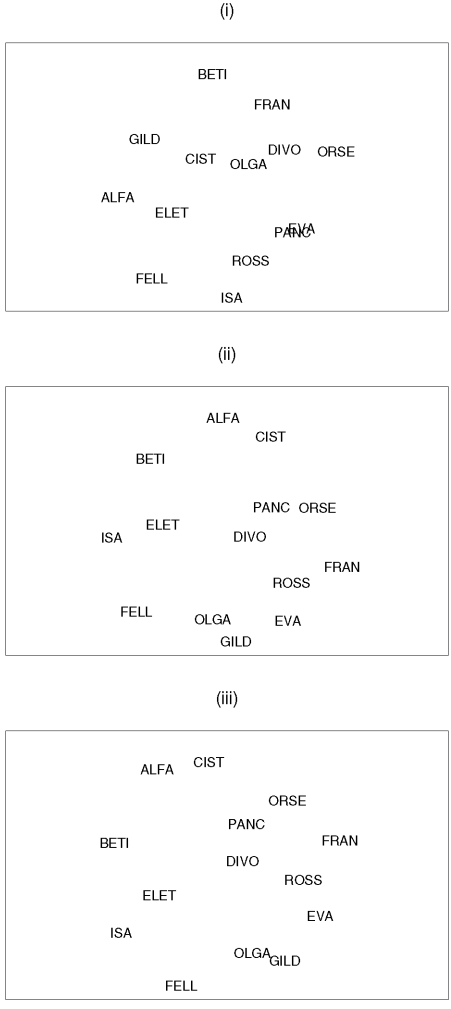

Figure 6.1 *Two dimensional configurations obtained from nonmetric MDS of the monkey data: (i) non-breeding season; (ii) breeding season; (iii) breeding season mathched to the non-breeding season using Procrustes analysis*

Table 6.1 *The colony of Japanese monkeys.*

Monkey	age/sex	Monkey	age/sex
Alfa (ALFA)	Adult male	Olga (OLGA)	Adult female
Francesca (FRAN)	Adult female	Orsetta (ORSE)	Inf/juv female
Fello (FELL)	Inf/juv male	Rossella (ROSS)	Adult female
Pancia (PANC)	Adult female	Divo (DIVO)	Subadult male
Isa (ISA)	Adult female	Cisto (CIST)	Subadult male
Gilda (GILD)	Adolescent female	Elettra (ELET)	Adult female
Betino (BETI)	Subadult male	Eva (EVA)	Inf/juv female

Figure 6.1 (i) shows the two dimensional configuration for the non-breeding season, and Figure 6.1 (ii) for the breeding season. The two configurations have been aligned using Procrustes analysis in Figure 6.1 (iii). The stress was 25% for the non-breeding season and 25% for the breeding season. These values are very high, indicating a poor fit. The latter value agrees with that of Corradino, but not the first. Although the stress is high, some interpretation can be placed on the configurations. Firstly, the three infant/juveniles (FELL, ORSE, EVA) maintain their relative positions in the configurations for the non-breeding and breeding seasons and are towards the edges of the configurations. The males (BETI, DIVO, CIST, ALFA) become closer to each other in the breeding season than in the non-breeding season. Likewise the females (GILD, ROSS, OLGA, PANC, ISA, FRAN, ELET) "move away" from the males in the breeding season.

6.3 Whisky

In the spirit of Lapointe and Legendre (1994) properties of the nose and taste of nineteen whiskies were analysed using nonmetric multidimensional scaling. The whiskies chosen came from distilleries established before 1820. The data were gleaned from the descriptions given about the whiskies in Milroy (1998). Table 6.2 gives the presence/absence of eleven nose characteristics, "1" indicating presence and blank otherwise. Table 6.3 is a similar table for the taste characteristics.

The data in the two tables were combined and dissimilarities between all pairs of whiskies were found using the Jaccard coefficient. These dissimilarities were then subjected to nonmetric MDS

Table 6.2 *Nose characteristics of nineteen whiskies.*

	Characteristics											
Whisky	1	2	3	4	5	6	7	8	9	10	11	12
Glenburgie	1	1			1							
Strathisla	1											
Balblair						1	1					
Clynelish	1							1				
Royal Brackla		1				1	1	1				
Teaninich	1					1	1					
Glen Garioch						1	1					
Glenturret				1		1			1			
Oban						1		1				
Bladnoch	1		1						1			
Littlemill	1		1	1								
Ardbeg						1		1				
Bowmore		1					1	1				
Lagavulin							1	1			1	
Laphroaig							1	1		1		
Highland Park				1			1					
Isle of Jura								1				1
Tobermory	1		1			1						
Bushmills						1	1				1	

Key: (1)-fruit, (2)-floral, (3)-light, (4)-delicate, (5)-fragrant, (6)-sweetness, (7)-smoke, (8)-peaty, (9)-aromatic, (10)-medicinal, (11)-sherry, (12)-tart

with resulting STRESS of 15%. Figure 6.2 shows the MDS configuration. The whiskies can be grouped into the following regions of Scotland and these are reflected in the MDS configuration.

Speyside: Glenburgie, Strathisla
Northern Highlands: Balblair, Clynelish, Royal Brackla, Teaninich
Eastern Highlands: Glen Garioch
Southern Highlands: Glenturret
Western Highlands: Oban
The Lowlands: Bladnoch, Littlemill
Islay: Ardbeg, Bowmore, Lagavulin, Laphroaig
The Islands: Highland Park, Isle of Jura, Tobermory
Northern Ireland: Bushmills

This last whisky is obviously not from Scotland. It is interesting

Table 6.3 *Taste characteristics of nineteen whiskies.*

	Characteristics													
Whisky	1	2	3	4	5	6	7	8	9	10	11	12	13	14
Glenburgie	1			1										
Strathisla		1										1	1	
Balblair												1	1	
Clynelish		1												1
Royal Brackla							1	1				1	1	
Teaninich					1								1	
Glen Garioch										1				
Glenturret														1
Oban												1		
Bladnoch									1			1		
Littlemill				1										
Ardbeg						1				1				
Bowmore					1					1				
Lagavulin						1		1	1					
Laphroaig										1		1		
Highland Park					1		1				1			
Isle of Jura			1										1	
Tobermory				1							1	1		
Bushmills									1					

Key: (1)-delicate, (2)-fruit, (3)-floral, (4)-light, (5)-medium bodied, (6)-full bodied, (7)-dry, (8)-sherry, (9)-smooth, (10)-peaty, (11)-smoke, (12)-sweetness, (13)-lingering, (14)-full

to see that in the MDS configuration, it is in with The Islands group of Scotch whisky.

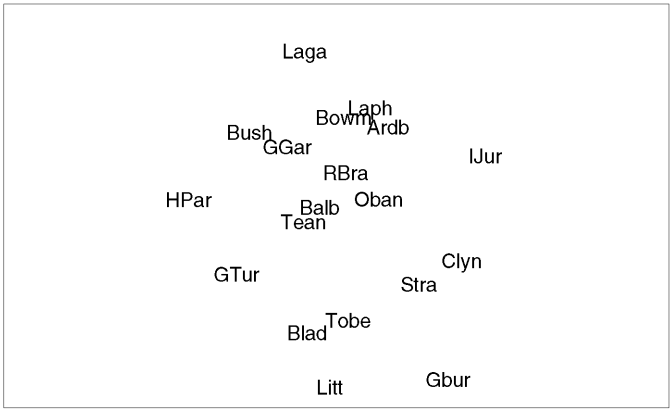

Figure 6.2 *Nonmetric MDS of the whisky data*

6.4 Aeroplanes

Polzella and Reid (1989) used nonmetric MDS on performance data from simulated air combat maneuvering, collected by Kelly *et al.* (1979). Data were collected for experienced and novice pilots. The variables measured included aircraft system variables, engagement outcomes and events, air combat performance variables, and automatically recorded aircraft variables, e.g. position, altitude. Polzella and Reid used the correlation matrix for thirteen variables measuring pilot performance as similarities for nonmetric scaling, using the SPSS program ALSCAL to perform the analysis.

Figure 6.3 (i) shows their two dimensional output for expert pilots, and Figure 6.3 (ii) for novice pilots. Stress for the two cases was 6% and 8% respectively.

Their conclusions were that the cluster of variables on the left of Figure 6.3 (i) are all energy related, indicating that the expert "pilots' performance" was characterized by frequent throttle activity. The cluster of variables on the right are related to air combat maneuverability, indicating that mission success was associated primarily with offensive and defensive maneuverability. The configuration for the novice pilots is markedly different from that for the expert pilots. "Gun kill" was isolated from the other variables,

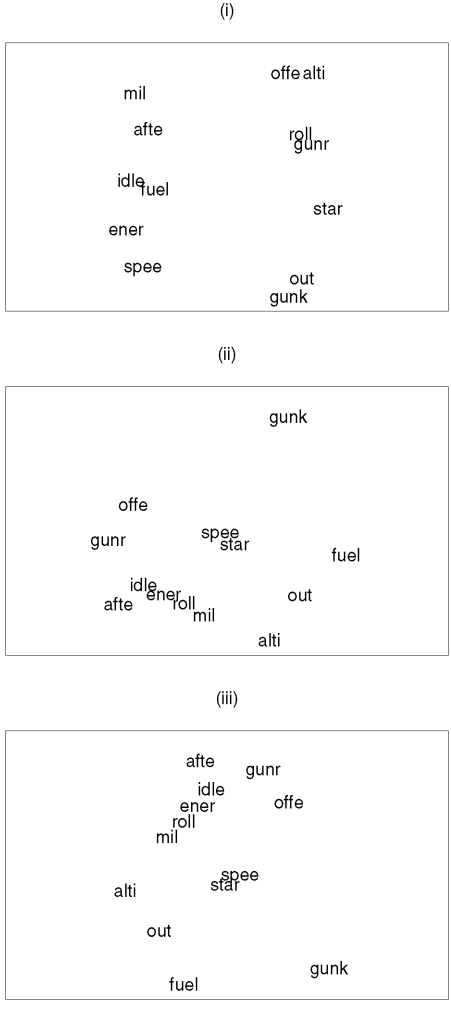

Figure 6.3 *MDS configurations for pilots: (i) experienced pilots; (ii) novice pilots; (iii) the configuration for novice pilots aligned with that for the expert pilots using Procrustes analysis.*

indicating mission success was not related to efficient energy management or skillful flying. The variable "fuel flow" being close to the variables "out of view" and "altitude rate" suggests defensive

action for novice pilots requires excessive fuel consumption compared to the expert pilots. Also with "offense", "gun range" and "roll rate" within a cluster of energy related variables, novice pilots made more use of throttle activity for offensive flying than did the expert pilots.

A Procrustes analysis was not carried out by Polzella and Reid in order to allign the two configurations. When this is done, the Procrustes statistic has the value 0.88, indicating a substantial difference in the configurations. Figure 6.3 (iii) shows the resulting rotated, reflected, dilated configuration for the novice pilots matched to that of the expert pilots.

6.5 Yoghurts

Poste and Patterson (1988) carried out metric and nonmetric MDS analyses on yoghurts. Twelve commercially available yoghurts (four firm, eight Swiss style) were evaluated by ten judges on nine variables. Strawberry yoghurts were presented in pairs to the panelists, who were asked to evaluate how similar the two samples were on a 15 cm descriptive line scale. Panelists were asked about the following attributes: colour, amount of fruit present, flavour, sweetness, acidity, lumpiness, graininess, set viscosity, aftertaste. Numerical scores were obtained from the scales, which were then used to compute a correlation matrix for the nine attributes. Metric and nonmetric scaling were used. Unfortunately, their results give the stress in two dimensions as 31% and in three dimensions as 22%. From Figure 3.5 of Chapter 3 it can be seen that for twelve points the mean stress for a random ranking of dissimilarities is about 22% for two dimensions and about 12% for three dimensions. A mistake is indicated somewhere in their analysis. Also, the configuration they obtained has ten points forming a circle with two points enclosed within the circle. All the points are straining to be as far away from each other as possible, but subject to the normalizing constraint. This could have happened if similarities were accidently used as dissimilarities.

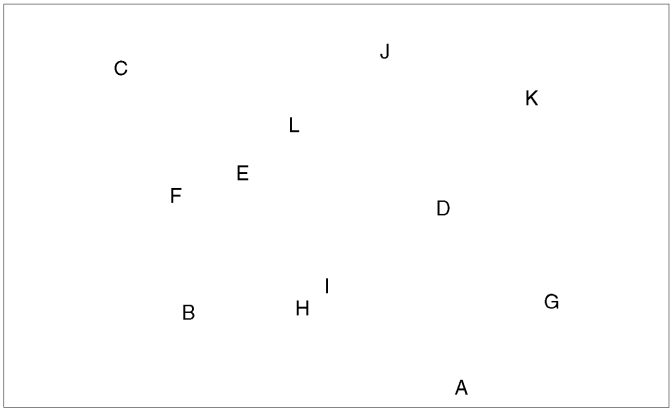

Figure 6.4 *Nonmetric MDS configuration for yoghurts. Swiss style: A, B, C, E, F, H, I, L. Firm: D, G, J, K.*

Included in the paper are mean scores for the nine variables for each of the yoghurts. Measuring dissimilarity by Euclidean distance, a configuration of points representing the yoghurts was found using nonmetric scaling. The stress was 9% which is rather high for only twelve points. The configuration is shown in Figure 6.4. The firm yoghurts, D, G, J, K, are towards the right of the configuration. The Swiss style yoghurts can be "imaginatively" ordered by projecting the points representing them onto a line at 45° to the configuration. The order is A, I, H, B, E, L, F, C. This agrees well with the configuration obtained by Poste and Patterson when they used metric scaling on the data.

6.6 Bees

Bees have been used in many experiments designed to study their colour vision. Bees' colour perception is investigated by analysing frequency data of the choice made between various colours when they search for food. For example, a bee can first be trained to the colour green by always supplying it with food from a green container. Later, the bee has to seek food having a choice of blue and green containers to visit, but where the food is only placed in the green container. The bee has to search for food several times

and the frequency with which it visits a green container first is recorded.

Backhaus *et al.* (1987) report on an experiment where multidimensional scaling was used on colour similarity data for bees. Firstly, each bee was trained to one of twelve colour stimuli by rewarding it with food. Then each bee was tested by giving it a choice of colour in its search for food. Some bees were given a choice of two colours, others a choice of all twelve colours. Multiple choice data were converted to dual choice data as follows.

Let ${}_tf_r$ be the frequency with which bees trained to colour stimulus t mistakenly choose colour stimulus r. Then ${}_t\hat{p}_{rs} = {}_tf_r/({}_tf_r + {}_tf_s)$ is the proportion of times colour stimulus r was judged more similar to the training colour t than colour stimulus s was so judged. As dual choice proportions obtained from the multiple choice tests were not significantly different from those for dual choice tests, the multiple choice data were included in the MDS analysis.

Define ${}_tz_{rs}$ by ${}_tz_{rs} = \Phi^{-1}({}_t\hat{p}_{rs})$, the inverse of the standard normal distribution function, for which the approximation can be made

$${}_tz_{rs} = \frac{1}{(8\pi)^{\frac{1}{2}}} \ln\left\{\frac{{}_t\hat{p}_{rs}}{(1 - {}_t\hat{p}_{rs})}\right\}.$$

The dissimilarities between the colours $\{\delta_{rs}\}$ are assumed to satisfy

$${}_tz_{rs} = \delta_{tr} - \delta_{ts}.$$

Let $\delta_{rs} = h_{rs} + c$, where c is an unknown additive constant. Then h_{rs} can be estimated by

$$h_{rs} = \tfrac{1}{2}({}_rh_{.s} + {}_.z_{r.} + {}_sz_{r.} + {}_.z_{.s}).$$

Backhaus *et al.* subjected the derived dissimilarities to metric and nonmetric scaling in a thorough investigation. The Minkowski metric was used with various values of the exponent λ. The city block metric ($\lambda = 1$) and the dominance metric ($\lambda \to \infty$) gave the smallest stress values. Euclidean distance ($\lambda = 2$) gave the highest stress values. This was true for two, three and four dimensinal solutions.

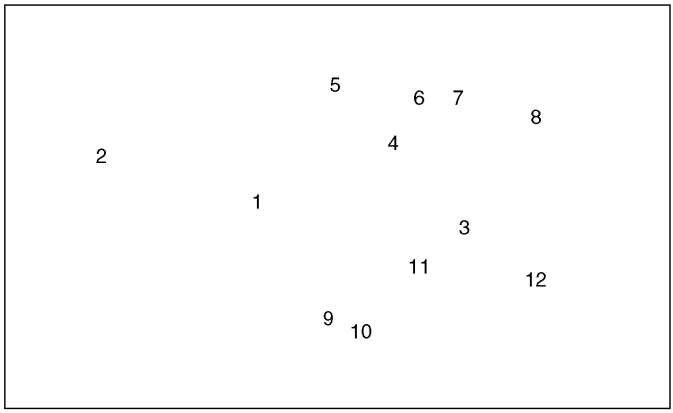

Figure 6.5 *Two dimensional MDS configuration for colour stimuli for bees.*

Figure 6.5 shows their two dimensional solution using the city block metric. The twelve colour stimuli are: 1. aluminium + foil, 2. grey, 3. BV1, 4. BV2, 5. BV3, 6. BV3 + foil, 7. BV3 + double foil, 8. BG18, 9. GR4, 10. GR4 + foil, 11. GR4 + double foil, 12. VG6. The stimuli 3 to 12 are varying shades of blue-green with or without foils which decreased reflection. In the configuration, the aluminium and grey stimuli are well to the left, the more blue than green stimuli are towards the top right, and the more green than blue are towards the bottom right. From all their analyses, Backhaus *et al.* conclude that bees main perceptual parameters are hue (blue/green) and saturation (UV/blue-greenness), and that brightness is ignored by bees.

CHAPTER 7

Biplots

7.1 Introduction

Biplots are plots in two or more dimensions which illustrate observations (individuals, objects) and variables of a data matrix simultaneously. Thus "bi" of biplot refers to the two modes (observations, variables) and not to the dimension of the display space. Biplots were introduced by Gabriel (1971) and subsequently developed by Gabriel (1981), Bradu and Gabriel (1978), Gabriel and Zamir (1979) and more latterly by Gower and Harding (1988), Gower (1990, 1992). This chapter follows the authoritative monograph on biplots by Gower and Hand (1996).

Biplots can be constructed for a variety of MDS techniques where data involves variables and not just dissimilarities. Both continuous and categorical variables can be included. In each case, the aim is to find a space in which points representing objects are plotted, and upon which a "framework" is overlaid representing the variables. For continuous variables, the framework is a set of axes, each axis representing one of the variables. The axes do not need to be linear. A categorical variable can be represented by a simplex of points in the space with one point for each category. The original and most popular biplots are those based on principal components analysis, where objects are represented by points in a sub-space of the original space spanned by the variables of the data matrix. The original variables are represented by vectors plotted in this subspace. From this beginning, the concept of a biplot can be extended to a variety of other situations, for example to nonmetric scaling, correspondence analysis, multiple correspondence analysis and biadditive models.

7.2 The classic biplot

The classic biplot represents the rows and columns of a matrix

Table 7.1 *Scores by Roger de Piles for Renaissance Painters*

	Composition	Drawing	Colour	Expression
Del Sarto	12	16	9	8
Del Piombo	8	13	16	7
Da Udine	10	8	16	3
Giulio Romano	15	16	4	14
Da Vinci	15	16	4	14
Michelangelo	8	17	4	8
Fr. Penni	0	15	8	0
Perino del Vaga	15	16	7	6
Perugino	4	12	10	4
Raphael	17	18	12	18

as vectors in a two dimensional space. Let data be collected for p variables on n objects and placed in an $n \times p$ data matrix $\mathbf{X}$. Let the SVD of $\mathbf{X}$ be given by $\mathbf{X} = \mathbf{U}\boldsymbol{\Lambda}\mathbf{V}^T$. Now let $\mathbf{X}$ be approximated using the first two singular values and corresponding right and left singular vectors,

$$\mathbf{X} \approx \mathbf{U}_2\boldsymbol{\Lambda}_2\mathbf{V}_2^T = (\mathbf{U}_2\boldsymbol{\Lambda}_2^{\alpha})(\mathbf{V}_2\boldsymbol{\Lambda}_2^{1-\alpha})^T,$$

where α is a chosen constant with $0 \leq \alpha \leq 1$. Different choices of α give rise to different biplots.

The $n \times 2$ matrix $\mathbf{U}_2\boldsymbol{\Lambda}^{\alpha}$ consists of n row vectors representing the rows of the matrix $\mathbf{X}$. The $p \times 2$ matrix $(\mathbf{V}_2\boldsymbol{\Lambda}^{1-\alpha})^T$ consists of p column vectors representing the columns of $\mathbf{X}$. A biplot is a plot of these two sets of vectors. Biplots are usually plotted in two dimensions for ease of display, and hence only the first two singular values and their associated vectors are used in the approximation of $\mathbf{X}$. However, biplots can be constructed in three or more dimensions by using more singular values in the approximation.

7.2.1 An example

Table 7.1 shows the scores on a scale zero to twenty for ten Renaissance painters for *composition, drawing, colour* and *expression.* These scores are a subset of those made by Roger de Piles in the seventeenth century on fifty-six painters and which have been used to illustrate statistical analyses by various authors; see, for example, Davenport and Studdert-Kennedy (1972) and Jolliffe (1986).

These scores were mean corrected and placed in matrix $\mathbf{X}$. The SVD of $\mathbf{X}$ is given by the matrices

$$\mathbf{U} = \begin{bmatrix} 0.05 & -0.01 & 0.09 & 0.33 \\ -0.19 & -0.41 & -0.32 & 0.12 \\ -0.31 & -0.54 & 0.42 & -0.32 \\ 0.36 & 0.18 & 0.09 & -0.37 \\ 0.36 & 0.18 & 0.09 & -0.37 \\ 0.01 & 0.43 & -0.10 & -0.00 \\ -0.51 & 0.39 & -0.24 & 0.21 \\ 0.09 & 0.07 & 0.60 & 0.53 \\ -0.34 & 0.06 & -0.14 & -0.36 \\ 0.47 & -0.35 & -0.49 & 0.23 \end{bmatrix}$$

$$\boldsymbol{\Lambda} = \begin{bmatrix} 23.41 & 0 & 0 & 0 \\ 0 & 13.94 & 0 & 0 \\ 0 & 0 & 7.34 & 0 \\ 0 & 0 & 0 & 4.66 \end{bmatrix}$$

$$\mathbf{V} = \begin{bmatrix} 0.64 & 0.25 & -0.25 & 0.68 \\ -0.33 & 0.33 & -0.87 & -0.12 \\ 0.65 & -0.37 & -0.31 & -0.59 \\ 0.22 & 0.83 & 0.29 & -0.41 \end{bmatrix}.$$

First α is chosen as unity. Then $\mathbf{U}_2\boldsymbol{\Lambda}_2$ gives the coordinates for the painters and $\mathbf{V}_2^T$ gives the coordinates for the four descriptions of the painters. The biplot for the painters and their descriptions are shown in Figure 7.1. The "primary" axis refers to the first singular vectors and the "secondary" axis to the second singular vectors. Let the ith row of $\mathbf{U}_2$ be $\mathbf{u}_{2i}$, the jth row of $\mathbf{V}$ be $\mathbf{v}_{2j}$ and the ith diagonal element of $\boldsymbol{\Lambda}$ be λ_i. Then $x_{ij} \approx (\mathbf{u}_{2i}\lambda_i)^T(\mathbf{v}_{2j})$. Hence x_{ij} is given approximately by the inner product of the two vectors $\mathbf{u}_{2i}\lambda_i$ and $\mathbf{v}_{2j}$. This quantity can be gleaned from the biplot as the product of the projection of $\mathbf{u}_{2i}\lambda_i$ onto $\mathbf{v}_{2j}$ and the length of $\mathbf{v}_{2j}$. Or alternatively, as the product of the projection of $\mathbf{v}_{2j}$ onto $\mathbf{u}_{2i}\lambda_i$ and the length of $\mathbf{u}_{2j}\lambda_i$. For clarity in the plot, the lengths of the vectors $\{\mathbf{v}_{2j}\}$ have been scaled by a factor of 10.

From the biplot, it can be seen that the vectors representing *composition* and *expression* are linked, as are those for *drawing* and *colour* to some extent. But note that the positive and negative directions for drawing and colour are opposite to each other. Also, *composition* is nearly orthogonal to *drawing*, as is *expression*

to *colour*. Now looking at the positions of the painters in the biplot, Fr. Penni can be seen to score very low in expression and composition, in contrast to Raphael at the other end of the axes. Da Udine scores high in colour and low in drawing, in contrast to Michelangelo. Da Vinci and Guilio Romano score exactly the same on all four variables.

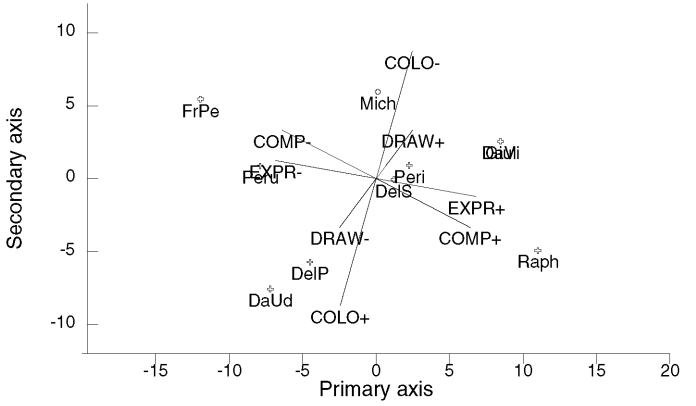

Fig. 7.1 *Biplot for Renaissance painters and their descriptions* ($\alpha = 1$)

To assess the "goodness of fit" of a biplot as a representation of $\mathbf{X}$, the residual at each point is measured as $x_{ij} - \lambda_i \mathbf{u}_{2i}\mathbf{v}_{2j}$. The residual matrix $\mathbf{R}$ is given by

$$\begin{aligned}\mathbf{R} &= \mathbf{U}\boldsymbol{\Lambda}\mathbf{V}^T - \mathbf{U}_2\boldsymbol{\Lambda}_2\mathbf{V}_2^T \\ &= \sum_{i=3}^{p} \lambda_i \mathbf{u}_i \mathbf{v}_i^T.\end{aligned}$$

Hence the sum of squared residuals is $\mathrm{tr}(\mathbf{R}^T\mathbf{R}) = \sum_{i=3}^{p} \lambda_i^2$ giving a measure of the goodness of fit as

$$\frac{\sum_{i=3}^{p} \lambda_i^2}{\sum_{i=1}^{p} \lambda_i^2}.$$

Of course, if the dimension of the biplot is more than two, then this formula is adjusted accordingly. For the biplot of the painters, the goodness of fit is 76%.

Now α is chosen to be zero. Figure 7.2 shows the biplot for

the painters and their descriptions for this case. This choice of α places more emphasis on variables than individuals and is sometimes called a $\mathbf{J}^T\mathbf{K}$ plot. The interpretation is basically the same as for the previous case. The lengths of the vectors for the variables are approximately equal to their standard deviations.

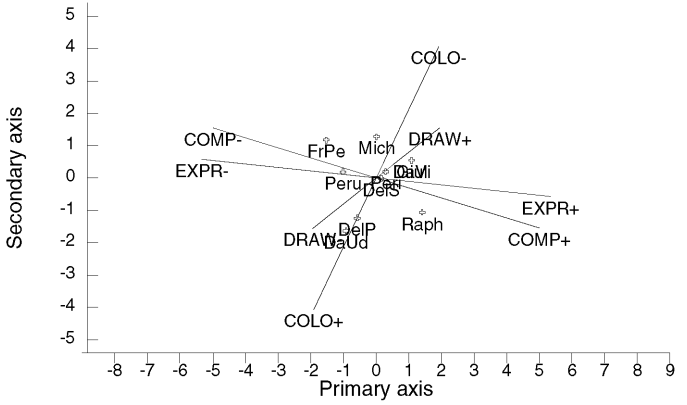

Fig. 7.2 *Biplot for Renaissance painters and their descriptions ($\alpha = 0$)*

7.2.2 Principal component biplots

Let $\mathbf{X}$ be mean corrected. The sample covariance matrix $\mathbf{S}$ is given by $(n-1)\mathbf{S} = \mathbf{X}^T\mathbf{X} = \mathbf{V}\boldsymbol{\Lambda}\mathbf{U}^T\mathbf{U}\boldsymbol{\Lambda}\mathbf{V}^T = \mathbf{V}\boldsymbol{\Lambda}^2\mathbf{V}^T$. This gives the spectral decomposition of $\mathbf{S}$ with eigenvalues of $(n-1)\mathbf{S}$ being the squares of the singular values of $\mathbf{X}$. The eigenvector matrix $\mathbf{V}$ gives the principal components (PCs) and is identical to the $\mathbf{V}$ in the SVD of $\mathbf{X}$. The component scores are given by $\mathbf{XV} = \mathbf{U}\boldsymbol{\Lambda}$. If only the first two PCs are used, or equivalently $(n-1)\mathbf{S}$ is approximated by $\mathbf{V}_2\boldsymbol{\Lambda}_2\mathbf{V}_2^T$, a PC biplot is constructed by plotting the component scores $\mathbf{U}\boldsymbol{\Lambda}$ and the PC coefficients, $\mathbf{V}$. Thus the biplot of the data matrix with α chosen to be unity, is equivalent to the PC biplot. Also, as PCA (principal components analysis) is equivalent to PCO (principal coordinates analysis) when Euclidean distance is used to measure dissimilarity, the distances between the points representing the observations in the biplot approximate the equivalent Euclidean distances between the original observations.

For example, the Euclidean distance between Da Vinci and Michelangelo based on the original scores is 9.27 and the corresponding distance in the biplot is 9.00.

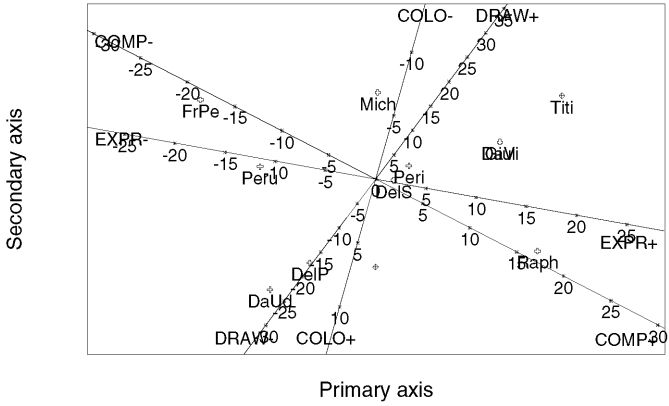

Fig. 7.3 *Principal component biplot for Renaissance painters and their descriptions ($\alpha = 0$)*

The column vectors of $\mathbf{V}$ are the principal component coefficients. Matrix $\mathbf{V}$ represents the rotation of the original coordinate axes (variables) to the principal component axes, i.e. $\mathbf{XV} = \mathbf{U\Lambda}$, and $\mathbf{V}^T$ represents the inverse rotation of the principal component axes to the original axes, i.e. $(\mathbf{U\Lambda})\mathbf{V}^T = \mathbf{X}$. The biplot shows this rotation, but projected onto the first two dimensions. If the plot could be in the full p dimensions, these axes would appear orthogonal. These vectors (axes) only indicate direction, and not any particular length. Gower and Hand (1996) encourage the analyst to treat these "variable" vectors as true axes and draw them through the entire biplot, together with appropriate scale marks. The axis for the ith variable in the original space can be defined by the locus of points mapped out by the vector $\mathbf{v} = (0, \ldots, 0, \gamma, 0 \ldots, 0)$ as γ varies. The vector has zeros for every element except the ith. Let the unit vector in the direction of the ith axis be $\mathbf{e}_i$, and so $\mathbf{v} = \gamma\mathbf{e}_i$. This axis is projected onto the biplot as $\gamma\mathbf{e}_i\mathbf{V}_2$. Markers are placed on the axis at the points given by $\gamma = 0, \pm 1, \pm 2, \ldots$, or for some other suitable graduations.

Figure 7.3 shows the principal component biplot for the Renaissance painters together with the four axes for composition, drawing, colour and expression and is marked accordingly. These axes can be used for interpolation. For example, a painter with scores given by (18, 13, 17, 17) and mean corrected to (7.6, -1.7, 8, 8.8) is placed at the vector sum of the vectors (7.6, 0, 0, 0), (0, -1.7, 0, 0), (0, 0, 8, 0) and (0, 0, 0, 8.8) in the biplot. This painter is indicated by *Titi* and is in fact Titian, who was not a Renaissance painter.

It is possible to use these axes, but with different markers for prediction, i.e. the prediction of composition, drawing, colour and expression for a painter represented by a particular point in the biplot. These prediction marks are given by $\gamma \mathbf{e}_i \mathbf{V}_2 / \mathbf{e}_i \mathbf{V}_2 \mathbf{V}_2^T \mathbf{e}_i^T$. See Gower and Hand for further details.

7.3 Another approach

The distance between points in the biplots so far considered is Euclidean. Gower and Harding (1988) extended the early work on biplots by allowing different distance measures between points. This gives rise to non-linear biplots.

Consider the data matrix $\mathbf{X}$ as a set of points in a p dimensional space, R_p, each variable being represented by a Cartesian axis. A two dimensional (or other low number of dimensions) space, S, is sought so that points in S represent the original set of points. This is essentially the MDS problem and several methods of finding such a space have already been discussed, for example, least squares scaling and nonmetric scaling. Indeed, as another example, in the previous section PCA refers $\mathbf{X}$ to its principal axes and then S is a subspace of R_p, which is spanned by the first two principal components. A plot of the points in this two dimensional subspace is the plot of the component scores for the first two principal components, and this constitutes the points in the PCA biplot.

The aim now is to define axes within S, each one representing one of the original variables. Suppose from $\mathbf{X}$ dissimilarities $\{\delta_{rs}\}$ are constructed and from these an MDS configuration and biplot are sought. Following Gower and Hand (1996) two cases are considered, where (i) $\{\delta_{rs}\}$ are embeddable in a Euclidean space and (ii) where they are not.

$\{\delta_{rs}\}$ embeddable

From $\mathbf{X}$ the matrix of dissimilarities, $\mathbf{D}$, is calculated. From the results of classical scaling (Chapter 2), the Euclidean space in which to embed the objects is $n-1$ dimensional with the coordinates of the points representing the objects given by $\mathbf{Y} = \mathbf{V}\boldsymbol{\Lambda}^{\frac{1}{2}}$, where

$$\mathbf{A} = [-\frac{1}{2}\delta_{rs}]$$
$$\mathbf{B} = \mathbf{HAH}$$
$$\mathbf{V}\boldsymbol{\Lambda}\mathbf{V}^T = \mathbf{B}.$$

Now consider the representation of the ith variable in this Euclidean space. The axis for the ith variable in the original space of $\mathbf{X}$ is the locus of $\gamma\mathbf{e}_i = (0, \ldots, 0, \gamma, 0, \ldots, 0)^T$. This $\gamma\mathbf{e}_i$ is termed a pseudosample for the ith variable. Consider this pseudosample as the $(n+1)$th object added to the n original objects. The point $\gamma\mathbf{e}_i$ has coordinates

$$\mathbf{y}(\gamma) = \boldsymbol{\Lambda}^{-1}\mathbf{Y}^T(\mathbf{d}_{n+1} - \frac{1}{n}\mathbf{D1})$$

where $\mathbf{d}_{n+1} = (d^2_{1,n+1}, \ldots, d^2_{n,n+1})^T$ and $d_{r,n+1}$ is the distance from the new point to the rth original point (Gower, 1968; Gower and Hand, 1996, p252).

In fact, as there are now $n+1$ points to consider overall, an extra dimension is needed to accommodate the extra point in the Euclidean space. The original points will have coordinate value zero in this extra dimension, while the new point will have value

$$y_n = \left(\frac{1}{n}\mathbf{1}^T\mathbf{D1} - \frac{2}{n}\mathbf{1}^T\mathbf{d}_{n+1} - \mathbf{y}^T\mathbf{y}\right)^{\frac{1}{2}}.$$

Now as γ varies, a locus in the Euclidean space will be mapped out; label this ξ_i and as it will usually be non-linear, it is termed a trajectory rather than an axis. Markers can be placed on the trajectory by marking the points corresponding to specific values of γ such as $\gamma = 0, \pm 1, \pm 2, \ldots$. This procedure is carried out for each variable. The set of trajectories $\{\xi_i\}$ forms the framework representing the variables.

So far, the space within which we are working is high dimensional; $n-1$ (or n if the extra dimension is included). The next

step is to consider how the trajectories impact on S, the low dimensional MDS space in which the configuration of points representing the objects has already been found. The simplest method is to embed S in the n dimensional Euclidean space using Procrustes analysis. This is the projection Procrustes problem where $||\mathbf{Z} - \mathbf{XP}||$ is minimised giving $\mathbf{P}$ as an $n \times 2$ projection matrix. This projection matrix can then be used to project $\{\xi_i\}$ onto S.

An example
For comparison with the case of linear biplot axes, the same Renaissance painter data are used. The distance between painters is measured by

$$\delta_{rs} = \left\{ \sum_{i=1}^{p} |x_{ri} - x_{si}| \right\}^{\frac{1}{2}},$$

and the method of MDS is chosen to be classical scaling.

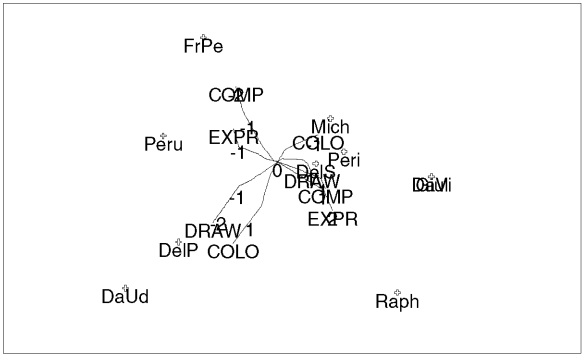

Fig. 7.4 *Non-linear biplot of Renaissance painters*

Figure 7.4 shows the configuration of the painters together with the trajectories of the four variables. These trajectories are highly non-linear, but their similarity to the linear axes can be seen. They tend to follow roughly the directions of the linear axes, although the trajectory in the positive direction for *drawing* bends dramatically towards those of *expression* and *composition*. The configuration of the painters is similar to that in the linear biplots.

$\{\delta_{rs}\}$ not embeddable

The $n-1$ dimensional Euclidean space in which $\{\delta_{rs}\}$ is embedded is no longer available. However, the idea of a pseudosample, $\gamma \mathbf{e}_i$ can be still be used. The chosen procedure for finding S and the configuration of points therein can be extended to include the pseudosample. Suppose the coordinates of the point in S that is to represent $\gamma \mathbf{e}_i$ is $\mathbf{z}_\gamma$. The loss function used in finding S can be used for the loss for $\mathbf{z}_\gamma$. For example, in nonmetric MDS the loss (STRESS) is

$$S(\mathbf{z}_\gamma) = \sqrt{\frac{S^*}{T^*}},$$

where

$$S^* = \sum_{r=1}^{n} (d_{r,n+1} - \hat{d}_{r,n+1})^2, \qquad T^* = \sum_{r=1}^{n} d_{r,n+1}^2,$$

and $d_{r,n+1}$ is the distance from the rth point in the configuration to the new point $\mathbf{z}_\gamma$, and $\{\hat{d}_{r,n+1}\}$ is the monotone least squares regression of $\{d_{r,n+1}\}$ on $\{\delta_{r,n+1}\}$. This loss function is then minimised to find the optimal point for defining the trajectory at this particular γ. Varying γ traces out the trajectory for the ith variable. This procedure is repeated for all the variables.

7.4 Categorical variables

So far, variables have been assumed to be continuous. Gower (1992) introduced generalized biplots so that categorical variables could be incorporated. This is done by the use of pseudosamples applied to each variable in turn.

Let the observation on the ith variable be replaced by the value γ for all the n observations. These are considered as n pseudosamples for the ith variable,

$$\mathbf{x}_r(\gamma) = (x_{r1}, \ldots, x_{ri-1}, \gamma, x_{ri+1}, \ldots, x_{r,p})^T \qquad (r = 1, \ldots n).$$

For continuous variables, γ can take any value in a range of values. For categorical variables, γ can only take one of the possible category levels. These pseudosamples are superimposed as points onto the space containing the configuration representing the original observations (objects). The centroid of these points, as γ varies, leads to the "axis" representing the ith variable.

To be more explicit, consider the following example. Suppose Gower's general dissimilarity coefficient has been used to measure dissimilarity between the observations (objects) (Gower, 1971) where the data may consist of a mixture of continuous and categorical variables. Suppose further, a configuration of points in S which represents the original observations has been found by nonmetric scaling. Then as in the previous section, dissimilarities between each of the original observations and the rth pseudosample are found, again using Gower's general dissimilarity coefficient and for a particular value of γ. These are used to find a point in S representing the rth pseudosample by minimising $S(\mathbf{x}_r(\gamma))$. This is repeated for all n pseudosamples and then the centroid of these n points is found. The process is repeated for various values of γ. As γ varies, a trajectory will emerge in S for a continuous variable, and give rise to a set of points for a categorical variable. For the latter, these are called category-level-points. The procedure is carried out in turn for all the variables, leading to a framework representing the variables.

If the dissimilarity measure used was embeddable in Euclidean space, then the same procedure is essentially carried out, but is easier to implement because of available algebraic results. The reader is referred to Gower (1992) or Gower and Hand (1996, Chapter 7) for further details.

CHAPTER 8

Unfolding

8.1 Introduction

Models for "unfolding" can be categorized into unidimensional or multidimensional models, and also metric or nonmetric models. Coombs (1950) first introduced unfolding as the following unidimensional nonmetric model. Suppose n judges consider a set of m objects (stimuli) and individually rank them. Coombs suggested that the judges and objects could be represented by points on a straight line (scale), where for each judge, the rank order of the distances from his point to the points representing the m objects is the same as his original rank ordering of the objects. For example, suppose there are two judges (1, 2) and five essays (A, B, C, D, E) to be judged and ranked in order to allocate prizes. Suppose the judges rank the essays as follows

	1st	2nd	3rd	4th	5th
Judge 1	B	C	A	E	D
Judge 2	A	B	C	E	D

Then the seven points in Figure 8.1 (top line) represent the judges and the five essays. It can be seen that the distances from judge 1 to the five essays have the same ranking as his original ranking of the essays. Similarly for judge 2. The term "unfolding" was coined since, for each judge, the line can be folded together at the judge's point and his original rankings are observed. These unfoldings can be seen in Figure 8.1 for the two judges. Alternatively, looking at the situation in reverse, the judges' rankings when placed on a line can be "unfolded" to obtain the "common" ordering of the objects.

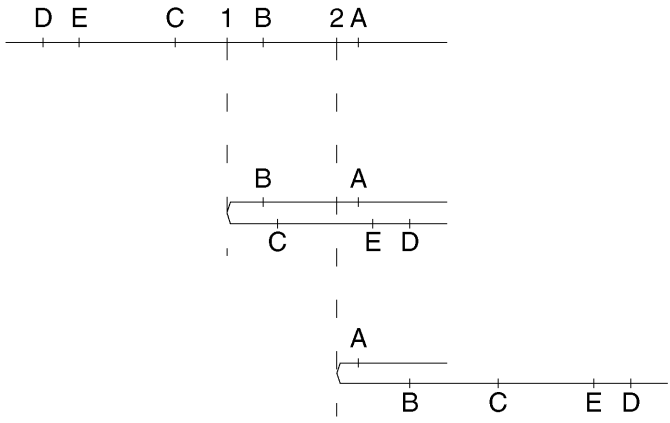

Figure 8.1 *Five essays (A, B, C, D, E) ranked by two judges (1, 2), together with their unfoldings.*

This unidimensional model can be extended to p dimensions simply by placing the $m + n$ points for judges and objects in a p dimensional space and then using distances, Euclidean or otherwise, in this p dimensional space to determine the rankings for the individual judges. For the "folding" of the space, Coombs used the simile of picking up a handkerchief (p dimensional) at a judge's point, and letting the ends fall together to determine the rankings for that judge. The metric unfolding model is very similar to the nonmetric model, but dissimilarities replace the rankings by the judges, and distances from a judge's point in the folding space to the objects are to match the original dissimilarities. Of course, the matching of distances to dissimilarities or ranks to ranks can never be guaranteed, and so compromises have to be made.

8.2 Nonmetric unidimensional unfolding

Coombs (1950, 1964) introduced the J scale and I scale. The line upon which points are placed for the n judges or individuals together with the m stimuli is called the J scale. Each individual's preference ordering is called an I scale. Consider just four stimuli A, B, C and D. Figure 8.2 shows these on a J scale.

Table 8.1 *Preference orderings for the J scale.*

Interval:	I_1	I_2	I_3	I_4	I_5	I_6	I_7
Ordering:	ABCD	BACD	BCAD	CBAD	CBDA	CDBA	DCBA

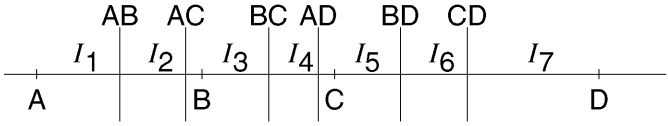

Figure 8.2 *Four stimuli (A, B, C, D) placed on a J scale together with intervals for I scales.*

Also shown are all the midpoints between pairs of stimuli where, for instance, AB denotes the midpoint between A and B. The J scale can be seen to be split into seven intervals. Any judge represented by a point in a particular interval will have the same I scale as any other judge in that interval. For example, a point in interval I_5 has the preference ordering CBDA. Table 8.1 gives the preference ordering for the seven intervals.

Of course, not all preference orderings can be accommodated. For instance, DABC in this example is impossible to achieve. For a given J scale it is easy to generate the possible I scales. However, the more challenging task is to generate the J scale from a set of I scales.

When a J scale is folded to produce an I scale, the I scale must end with either of the two end stimuli of the J scale. Hence the end stimuli for the J scale will be known by simply looking at the end stimuli for all the I scales. There will be only two I scales starting and ending with the two end points of J, and these two I scales will be mirror images of each other. There will be no other I scales which are mirror images of each other. The rank order of the J scale can be taken as the rank order of either of the mirror image I scales. Next, the order of the midpoints as in Figure 8.2 needs to be determined. This is done by determining the order of the I scales. Note that in Table 8.1, as the intervals are read from left to right, an adjacent pair of stimuli are interchanged at each step.

For example, the first interval corresponds to the ordering ABCD, whereupon interchanging A and B gives the ordering BACD of the second interval. Then interchanging A and C gives the third, etc. The interchanging of a pair of stimuli corresponds to the crossing of the midpoint of that pair. Hence for given preference orderings, to order the midpoints, the I scales are ordered accordingly, starting with one of the mirror image I scales and ending with the other. In practice, further geometrical considerations have to be taken into account. The reader is referred to Coombs (1964) for further details, and also for details of applications of the technique to sets of psychological data.

The main problem with this unfolding technique is that, for a given set of I scales, it is unlikely that a single J scale can be found. Hettmansperger and Thomas (1973) attempt to overcome this problem by using a probability model. For a given number of stimuli, the probabilities of the various possible I scales for a given J scale are taken to be constant, i.e. $P(I_i|J_j) = c$. Then $P(I_i) = \sum_j P(I_i|J_j)P(J_j) = c\sum_j P(J_j)$ is used to form the likelihood for a sample of N I scales. From the likelihood, the various $P(J_j)$ are estimated.

Zinnes and Griggs (1974) use a probabilistic model for metric unfolding. Firstly, consider the univariate case. They assume that each individual, r, is placed independently on a point X_r on the J scale, where $X_r \sim \mathrm{N}(\mu_r, \sigma_r^2)$. The jth stimulus is placed independently at the point Y_j, where $Y_j \sim \mathrm{N}(\xi_j, \nu_j^2)$. Then the probability that individual r prefers stimulus i to stimulus j is $p_{ij} = \Pr(|X_r - Y_i| < |X_r - Y_j|)$. For the case $\sigma_r^2 = \nu_i^2 = \frac{1}{2}$ for all i, Zinnes and Griggs show that

$$p_{ij} = 1 - \Phi(a_{ij}) - \Phi(b_{ij}) + 2\Phi(a_{ij})\Phi(b_{ij}),$$

where

$$a_{ij} = (2\mu_r - \xi_i - \xi_j)/\sqrt{3}, \quad b_{ij} = \xi_i - \xi_j,$$

with similar results under different assumptions regarding the variances. Data collected from individuals are then used to find maximum likelihood estimates of $\{\xi_i\}$ and $\{\mu_r\}$ in order to draw up a J scale. The data for an individual can be in the form of preference data for pairs, or can be extracted in this form from the individual's preference ranking.

8.3 Nonmetric multidimensional unfolding

Bennett and Hays (1960) and Hays and Bennett (1961) generalized Coombs' unidimensional unfolding model to several dimensions. Their work is also reported in Coombs (1964). Great detail is not gone into here, since the theory is similar to that for the unidimensional case, except that the geometrical structure is much more complicated. Some of their results are summarised below.

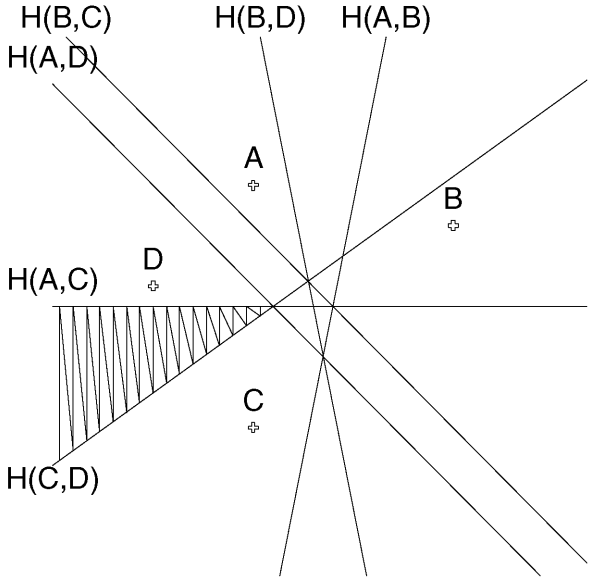

Figure 8.3 *Isotonic regions for four stimuli in a two dimensional space*

Consider points representing individuals and stimuli placed in a space of p dimensions. The locus of points, equidistant from stimuli A and B, is a hyperplane, $H(A,B)$ of dimension $p-1$. Similarly, the locus of points equidistant from m stimuli (assuming none of the stimuli are coplanar) is a hyperplane, $H(A,B,...)$ of dimension $p-m+1$. The hyperplane $H(A,B)$ splits the space into two half spaces, where an individual placed in one half space prefers A to B, and if placed in the other, prefers B to A. Bennett and Hays call these half spaces or zones, the isotonic regions AB and BA,

indicating the preferred orderings. The space can be divided up into isotonic regions by the hyperplanes defined by each pair of stimuli. Figure 8.3 shows the case for $p = 2$ and $n = 4$. The hyperplanes are straight lines. The isotonic regions are labelled according to the preferred order for the points in a particular isotonic region. For example, all points in the shaded isotonic region have the preferred ordering D, C, A, B.

As in the unidimensional case, certain preferred orderings cannot occur. This will happen when there are more than $p+2$ stimuli in a p dimensional space. Again, it is a relatively easy task to divide a p dimensional space, with stimuli in fixed positions (J scale), into the various isotonic regions, although for high dimensional space, the lack of a graphical illustration will detract from the interpretation. The more difficult task is to construct a configuration of points in p dimensions, representing the stimuli from a set of experimentally obtained I scales.

Bennett and Hays tackle the problem of determining the required dimension of the space in three ways. It is, of course, always possible to place the points in a space of $n-1$ dimensions to recover all possible rankings of the n stimuli. However, to be useful, a space of a much lower dimension is required. Their first method for determining dimension is based on the bounding of isotonic regions and can only be used for $p = 1$ or 2. Their second method is based on the number of isotonic regions that can be generated from m stimuli in p dimensions, $c(m, p)$ say. They give the recurrence relation

$$c(m, p) = c(m-1, p) + (m-1)c(m-1, p-1)$$

and a corresponding table of values of $c(m, p)$ for $m = 1(1)20$, $p = 1(1)5$. It is not surprising that $c(m, p)$ is much less than the total number of possible rankings, $m!$, for reasonably large m and small dimension p. For example, for $m = 9$, $p = 3$, $m! = 362\,880$ and $c(m, p) = 5119$. From experimental data, the total number of rankings of the m stimuli by the individuals is obtained and then dimensionality is assessed by comparing this with values of $c(m, p)$.

Bennett and Hays' third method for determining dimension is based on the result that the minimum dimension of the space in which a complete solution may be realized must be one less than the number of elements in the largest transposition group of stimuli present in the experimental data. The reader is referred to the papers by Bennett and Hayes for further details.

McElwain and Keats (1961) considered the case of four stimuli in two dimensions in detail. They looked at the I scales generated by all possible geometric configurations of stimuli, and then were able to characterize a set of I scales to determine the type of geometrical configuration required. For more than four stimuli or more than two dimensions, this would appear to be an impossible task.

Davidson (1972, 1973) gives further geometric results for nonmetric multidimensional unfolding. He derives necessary and sufficient conditions for a configuration of points representing stimuli to give rise to a particular set of I scales. Also he gives the necessary and sufficient geometric constraints that determine the subset of pairs of orders and opposites of the stimuli, contained in the particular set of I scales.

Zinnes and Griggs (1974) and MacKay and Zinnes (1995) extend the unidimensional probabilistic model of Zinnes and Griggs previously discussed, to the multidimensional case, so that now $\mathbf{X}_r = (X_{r1}, \ldots, X_{rp})$ and $\mathbf{Y}_i = (Y_{i1}, \ldots, Y_{ip})$ have multivariate normal distributions, $\mathbf{X}_r \sim \mathrm{N}_p(\boldsymbol{\mu}_r, \boldsymbol{\Sigma}_r)$, $\mathbf{Y}_i \sim \mathrm{N}_p(\boldsymbol{\xi}_i, \mathbf{V}_i)$, with $\boldsymbol{\mu}_r = (\mu_{r1}, \ldots, \mu_{rp})^T$, $\boldsymbol{\xi}_i = (\xi_{i1}, \ldots, \xi_{ip})^T$, $[\boldsymbol{\Sigma}_r]_{kl} = \sigma_{rkl}$ and $[\mathbf{V}_i]_{kl} = \nu_{ikl}$.

Let $d_{ri}^2 = \sum_{k=1}^{p}(X_{rk} - Y_{ik})^2$ be the Euclidean distance in the p dimensional space containing the points, from individual r to stimulus i and let $d_{rik} = (X_{rk} - Y_{ik})$. Define $\mathbf{D}_{ri} = (d_{ri1}, \ldots, d_{rip})^T$ which has a multivariate normal distribution, $\mathrm{N}_p(\boldsymbol{\mu}_r - \boldsymbol{\xi}_i, \boldsymbol{\Sigma}_r + \mathbf{V}_i)$. Then the squared distance d_{ri}^2 can be expressed as the quadratic form, $d_{ri}^2 = \mathbf{D}_{ri}^T \mathbf{D}_{ri} = Q(\mathbf{D}_{ri})$ say.

Now let $\boldsymbol{\Sigma}_{ri} = \boldsymbol{\Sigma}_r + \mathbf{V}_i$ and express $\boldsymbol{\Sigma}_{ri}$ in terms of its spectral decomposition, but dropping some of the subscripts for convenience, and so $\boldsymbol{\Sigma}_{ri} = \mathbf{U}\boldsymbol{\Lambda}\mathbf{U}^T$ where $\boldsymbol{\Lambda}$ is the diagonal matrix of eigenvalues of $\boldsymbol{\Sigma}_{ri}$ and $\mathbf{U}$ is the matrix of eigenvectors. Also express $\boldsymbol{\Sigma}_{ri}$ in terms of the lower triangular matrix $\mathbf{L}$, $\boldsymbol{\Sigma}_{ri} = \mathbf{L}\mathbf{L}^T$. Define $\mathbf{E}_{ri} = \mathbf{U}^T\mathbf{L}^{-1}\mathbf{D}_{ri}$ and then the canonical form for $Q(\mathbf{D}_{ri})$ is

$$Q(\mathbf{D}_{ri}) = Q(\mathbf{E}_{ri}) = \mathbf{E}_{ri}^T \boldsymbol{\Lambda} \mathbf{E}_{ri} = \sum_{k=1}^{p} \lambda_k E_k^2,$$

where $\{E_k\}$ are the elements of $\mathbf{E}_{ri}$. Now $\{E_k\}$ are independent with $\mathrm{E}(\mathbf{E}_{ri}) = \mathbf{V}^T\mathbf{L}^{-1}(\boldsymbol{\mu}_r - \boldsymbol{\xi}_i)$ and $\mathrm{var}(\mathbf{E}_{ri}) = \mathbf{I}$. Thus d_{ri}^2 can be expressed as the weighted sum of one degree of freedom noncentral chi-square variables.

Next is needed

$$\Pr(d_{ri}^2 < d_{rj}^2) = \Pr(R_{rij}^2 < 1)$$

where $R_{rij}^2 = d_{ri}^2/d_{rj}^2$. Combine $\mathbf{D}_{ri}$ and $\mathbf{D}_{rj}$ into a single vector random variable, $\mathbf{D}^T = (\mathbf{D}_{ri}^T, \mathbf{D}_{rj}^T)$. Define the $p \times p$ matrices $\mathbf{A}$ and $\mathbf{B}$ by

$$\mathbf{A} = \begin{bmatrix} \mathbf{I}_{p\times p} & \mathbf{0} \\ \mathbf{0} & \mathbf{0} \end{bmatrix} \qquad \mathbf{B} = \begin{bmatrix} \mathbf{0} & \mathbf{0} \\ \mathbf{0} & \mathbf{I}_{p\times p} \end{bmatrix}.$$

Then

$$R_{rij}^2 = \frac{\mathbf{D}^T\mathbf{A}\mathbf{D}}{\mathbf{D}^T\mathbf{B}\mathbf{D}}$$

and $\Pr(R_{rij}^2 < 1)$ is determined from the distribution of the ratio of these two quadratic forms.

Independent sampling for individuals implies

$$\mathrm{var}(\mathbf{D}) = \begin{bmatrix} \boldsymbol{\Sigma}_r + \mathbf{V}_i & \mathbf{0} \\ \mathbf{0} & \boldsymbol{\Sigma}_r + \mathbf{V}_j \end{bmatrix},$$

but this has an indeterminancy, namely $\boldsymbol{\Sigma}_r + \mathbf{V}_i = (\boldsymbol{\Sigma}_r + \mathbf{C}) + (\mathbf{V}_i - \mathbf{C})$ where $\mathbf{C}$ is arbitrary.

A dependent sampling model overcomes this indeterminancy with

$$\mathrm{var}(\mathbf{D}) = \begin{bmatrix} \boldsymbol{\Sigma}_r + \mathbf{V}_i & \boldsymbol{\Sigma}_r \\ \boldsymbol{\Sigma}_r & \boldsymbol{\Sigma}_r + \mathbf{V}_j \end{bmatrix}.$$

The cumulative distribution function of the ratio of the quadratic forms is given by

$$F(r^2) = \Pr\left(\frac{\mathbf{D}^T\mathbf{A}\mathbf{D}}{\mathbf{D}^T\mathbf{B}\mathbf{D}} \le r^2\right) = \Pr(\mathbf{D}^T(\mathbf{A} - \mathbf{B}r^2)\mathbf{D} \le 0).$$

The quadratic form $\mathbf{D}^T(\mathbf{A}-\mathbf{B}r^2)\mathbf{D}$ can be put into canonical form and then $F(r^2)$ can be estimated by one of several methods, e.g. inverting the characteristic function. The density function can then be obtained by numerically differentiating $F(r^2)$, whence the value of the log-likelihood can be found. This is then maximised in order to find the maximum likelihood estimates of $\boldsymbol{\mu}_r$, $\boldsymbol{\xi}_i$, $\boldsymbol{\Sigma}_r$ and $\mathbf{V}_i$. These are then plotted to give the unfolding. See Zinnes and Griggs (1974) and MacKay and Zinnes (1995) for further details.

For another slant on stochastic unfolding, see DeSarbo *et al.* (1996) where an unfolding approach is used to represent phased decision outcomes.

8.4 Metric multidimensional unfolding

The case of metric unidimensional unfolding will be subsumed in the multidimensional case. Coombs and Kao (1960) and Coombs (1964) started to look at a metric method for unfolding by using a principal components analysis on the correlation matrix obtained from the correlations between pairs of I scales. Ross and Cliff (1964) took the method further. Schönemann (1970) found an algebraic solution for metric unfolding.

As before, let there be n individuals or judges, and suppose the rth individual produces dissimilarities $\{\delta_{ri}\}$ for m stimuli. Suppose $m+n$ points are placed in a p dimensional Euclidean space where each individual and each stimulus is represented by one of the points. Let the coordinates of the points representing the individuals be $\mathbf{x}_r$ $(r = 1, \ldots, n)$ and the coordinates of the points representing the stimuli be $\mathbf{y}_i$ $(i = 1, \ldots, m)$. Let the distance between the points representing the rth individual and the ith stimulus be d_{ri}. The metric unfolding problem is to find a configuration such that the distances $\{d_{ri}\}$ best represent the dissimilarities $\{\delta_{ri}\}$.

Schönemann (1970) gave an algorithm to find $\{\mathbf{x}_r\}$, $\{\mathbf{y}_i\}$ from the distances $\{d_{ri}\}$. Gold (1973) clarified Schönemann's work; the following is a brief summary.

Let $\mathbf{X} = [\mathbf{x}_1, \ldots, \mathbf{x}_n]^T$, $\mathbf{Y} = [\mathbf{y}_1, \ldots, \mathbf{y}_m]^T$. Let the matrix of squared distances between the points representing the individuals and the points representing the objects be $\mathbf{D}(\mathbf{X}, \mathbf{Y})$. Hence

$$[\mathbf{D}(\mathbf{X}, \mathbf{Y})]_{ri} = (\mathbf{x}_r - \mathbf{y}_i)^T(\mathbf{x}_r - \mathbf{y}_i).$$

Let the matrix of squared dissimilarities be $\mathbf{D} = [\delta_{ri}^2]$. The metric unfolding problem is to find $(\mathbf{X}, \mathbf{Y})$ such that $\mathbf{D}(\mathbf{X}, \mathbf{Y}) = \mathbf{D}$.

The matrices $\mathbf{D}$ and $\mathbf{D}(\mathbf{X}, \mathbf{Y})$ are now doubly centred to give $\mathbf{C} = \mathbf{HDH}$, and $\mathbf{C}(\mathbf{X}, \mathbf{Y}) = \mathbf{HD}(\mathbf{X}, \mathbf{Y})\mathbf{H}$, where $\mathbf{H}$ is the centring matrix.

Then the unfolding problem can be rewritten as

$$\mathbf{C}(\mathbf{X}, \mathbf{Y}) = \mathbf{C} \tag{8.1}$$

$$\mathbf{D}(\mathbf{X}, \mathbf{Y})_{r\cdot} = \mathbf{D}_{r\cdot} \quad (r = 1, \ldots, n) \tag{8.2}$$

$$\mathbf{D}(\mathbf{X}, \mathbf{Y})_{\cdot i} = \mathbf{D}_{\cdot i} \quad (i = 1, \ldots, m). \tag{8.3}$$

The matrices $(\mathbf{X}, \mathbf{Y})$ satisfying these equations are called an unfolding. Schönemann's algorithm requires two steps. Step 1 is to find those unfoldings $(\mathbf{X}, \mathbf{Y})$ which satisfy (8.1), Step 2 is then to

find which unfoldings of Step 1 satisfy (8.2) and (8.3). For further details see Schönemann (1970) and Gold (1973).

A more useful approach is the introduction of a loss function as in Greenacre and Browne (1986). They proposed an efficient alternating least squares algorithm for metric unfolding. It is the one used in this book to analyse example data and the program for it is included on the accompanying CD-ROM. A brief description is given. The algorithm uses squared Euclidean distances $\{d_{ij}^2\}$ to approximate to the squared dissimilarities $\{\delta_{ij}^2\}$. This leads to a simplification over the use of non-squared distances and dissimilarities. Using the previous notation, the model which incorporates residuals $\{\epsilon_{ri}\}$ is

$$\delta_{ri}^2 = d_{ri}^2 + \epsilon_{ri},$$

or

$$\delta_{ri}^2 = (\mathbf{x}_r - \mathbf{y}_i)^T(\mathbf{x}_r - \mathbf{y}_i) + \epsilon_{ri}.$$

An unfolding $(\mathbf{X}, \mathbf{Y})$ is then found that minimises

$$\sum_r \sum_i \epsilon_{ri}^2 = \mathrm{tr}(\mathbf{R}\mathbf{R}^T),$$

where $[\mathbf{R}]_{ri} = \epsilon_{ri}$.

Following Greenacre and Browne, let

$$f(\mathbf{X}, \mathbf{Y}; \mathbf{D}^{(2)}) = \sum_{r=1}^{n} \sum_{i=1}^{m} \{\delta_{ri}^2 - (\mathbf{x}_r - \mathbf{y}_i)^T(\mathbf{x}_r - \mathbf{y}_i)\}^2 \qquad (8.4)$$

where $[\mathbf{D}^{(2)}]_{ri} = \delta_{ri}^2$.

Then

$$\frac{\partial f}{\partial \mathbf{x}_r} = 4 \sum_{i=1}^{m} \{\delta_{ri}^2 - (\mathbf{x}_r - \mathbf{y}_i)^T(\mathbf{x}_r - \mathbf{y}_i)\}(\mathbf{x}_r - \mathbf{y}_i),$$

and equating to $\mathbf{0}$ gives

$$\sum_{i=1}^{m} \{\delta_{ri}^2 - (\mathbf{x}_r - \mathbf{y}_i)^T(\mathbf{x}_r - \mathbf{y}_i)\}\mathbf{y}_i = \sum_{i=1}^{m} \{\delta_{ri}^2 - (\mathbf{x}_r - \mathbf{y}_i)^T(\mathbf{x}_r - \mathbf{y}_i)\}\mathbf{x}_r.$$

This can be written as

$$\sum_{i=1}^{m} [\mathbf{R}]_{ri}\mathbf{y}_i = \sum_{i=1}^{m} [\mathbf{R}]_{ri}\mathbf{x}_r.$$

Combining these equations gives

$$\mathbf{RY} = \text{diag}(\mathbf{RJ}^T)\mathbf{X} \tag{8.5}$$

where $\mathbf{J}$ is an $n \times m$ matrix of ones, and diag($\mathbf{M}$) is the diagonal matrix formed from the diagonal of a matrix $\mathbf{M}$. Similarly,

$$\mathbf{R}^T\mathbf{X} = \text{diag}(\mathbf{R}^T\mathbf{J})\mathbf{Y}. \tag{8.6}$$

Equations (8.5) and (8.6) need to be solved numerically to find an unfolding $(\mathbf{X}, \mathbf{Y})$ giving the minimum sum of squared residuals.

Greenacre and Browne use an alternating least squares procedure to minimise (8.4). Their iterative scheme first holds $\mathbf{Y}$ fixed and minimises (8.4) with respect to $\mathbf{X}$, and then holds $\mathbf{X}$ fixed and minimises (8.4) with respect to $\mathbf{Y}$. Convergence is guaranteed but can be very slow. A brief description of the derivation of the algorithm is given.

Consider $\mathbf{Y}$ fixed, and write $f(\mathbf{X}, \mathbf{Y})$ as $\sum_{r=1}^{n} f_r$, where

$$f_r = \sum_{i=1}^{m} \{\delta_{ri}^2 - (\mathbf{x}_r - \mathbf{y}_i)^T(\mathbf{x}_r - \mathbf{y}_i)\}^2.$$

Minimising $f(\mathbf{X}, \mathbf{Y})$ with respect to $\mathbf{X}$ for fixed $\mathbf{Y}$ can be done by minimising each f_r with respect to $\mathbf{x}_r$ separately.

Differentiating f_r with respect to $\mathbf{x}_r$ and setting equal to $\mathbf{0}$, gives

$$\sum_{i=1}^{m} (\delta_{ri}^2 - \mathbf{x}_r^T\mathbf{x}_r - \mathbf{y}_i^T\mathbf{y}_i + 2\mathbf{x}_r^T\mathbf{y}_i)(\mathbf{x}_r - \mathbf{y}_i) = \mathbf{0}. \tag{8.7}$$

Greenacre and Browne introduce notation similar to

$$\mathbf{d}_r^{(2)} = [\delta_{r1}^2, \ldots, \delta_{rm}^2]^T$$

$$\mathbf{h} = [\mathbf{y}_1^T\mathbf{y}_1, \ldots, \mathbf{y}_m^T\mathbf{y}_m]^T$$

$$\mathbf{w}_r = \mathbf{Y}^T[\mathbf{d}_r^{(2)} - \mathbf{h}]$$

$$c_r = \mathbf{1}^T[\mathbf{d}_r^{(2)} - \mathbf{h}],$$

and then (8.7) can be written as

$$(c_r - m\mathbf{x}_r^T\mathbf{x}_r - 2\mathbf{1}^T\mathbf{Y}\mathbf{x}_r)\mathbf{x}_r = \mathbf{w}_r - \mathbf{Y}^T\mathbf{1}(\mathbf{x}_r^T\mathbf{x}_r) + 2\mathbf{Y}^T\mathbf{Y}\mathbf{x}_r.$$

They argue that, although $\mathbf{Y}$ is fixed, the origin and orientation can be chosen. So the choice is made to place the centroid of $\mathbf{Y}$ at the origin and to refer $\mathbf{Y}$ to its principal axes. Thus $\mathbf{Y}^T\mathbf{1} = \mathbf{0}$

and $\mathbf{Y}^T\mathbf{Y} = \mathbf{D}_\lambda$, where $\mathbf{D}_\lambda$ is a diagonal matrix of nonnegative numbers, $\lambda_1 \geq \lambda_2 \geq \ldots \geq \lambda_p$. Obviously if $\mathbf{Y}$ is not in principal axes form, it can be made so by a principal coordinates analysis (PCO) as in Chapter 2. Equation (8.7) becomes

$$(c_r - m\mathbf{x}_r^T\mathbf{x}_r)\mathbf{x}_r - 2\mathbf{D}_\lambda\mathbf{x}_r = \mathbf{w}_r,$$

and hence

$$x_{rk} = \frac{w_{rk}}{c_r - m\mathbf{x}^T\mathbf{x} - 2\lambda_k} \quad (k = 1, \ldots, p). \tag{8.8}$$

A variable, ϕ_r, is introduced, where

$$\phi_r = c_r - m\mathbf{x}_r^T\mathbf{x}_r = c_r - m\sum_{k=1}^{p} x_{rk}^2. \tag{8.9}$$

Hence (8.8) becomes

$$x_{rk} = \frac{w_{rk}}{\phi_r - 2\lambda_k} \quad (k = 1, \ldots, p). \tag{8.10}$$

Substituting (8.10) back into (8.9) gives

$$0 = \phi_r - c_r + m\sum_{k=1}^{p} \frac{w_{rk}^2}{(\phi_r - 2\lambda_k)^2} = g(\phi_r).$$

The function $g(\phi_r)$ can then be used to find the required stationary points. If $\phi_r^\star$ is a stationary point of $g(\phi_r)$, then substituting $\phi_r^\star$ into (8.10) gives the stationary point $\mathbf{x}_r^\star$. Greenacre and Browne show that the smallest root of $g(\phi_r) = 0$ is actually the required root to give the global minimum of f_r. (In a footnote to their paper they attribute the proof of this result to Alexander Shapiro.) Thus the minimisation problem for this stage has been reduced to one of finding the smallest root of the equation $g(\phi_r) = 0$. This has to be done for each $\mathbf{x}_r$.

The second stage of the procedure is carried out in a similar manner to the first stage, except that $\mathbf{X}$ is fixed this time. Iterations between the two stages are carried out until convergence is reached.

A starting value for $\mathbf{Y}$ needs to be chosen. Greenacre and Browne suggest using the algorithm of Schönemann (1970) for this. The matrix $-\frac{1}{2}\mathbf{D}^{(2)}$ formed from $\mathbf{d}_r^{(2)}$, is doubly centred to give

$$\mathbf{C} = -\tfrac{1}{2}\mathbf{H}\mathbf{D}^{(2)}\mathbf{H}.$$

The singular value decomposition of $\mathbf{C}$ is found, $\mathbf{C} = \mathbf{U}\mathbf{D}_\alpha\mathbf{V}^T$, where $\mathbf{D}_\alpha = \text{diag}(\alpha_1, \ldots, \alpha_p)$. The starting value for $\mathbf{Y}$ is then taken as $\mathbf{Y}_0 = [\alpha_1\mathbf{v}_1, \ldots, \alpha_p\mathbf{v}_p]$.

8.4.1 The rating of nations

Wish *et al.* (1972) report on a study of the ways that people perceive nations. Students were asked to judge the similarity between pairs of nations. They were each given only a subset of all the possible pairs of nations to judge, since there were 21 nations and hence 210 possible pairs in total. The nations are given in Table 8.2. The students were then asked to score each nation on 18 variables on a scale 1 to 9. These variables are given in Table 8.3.

Given in the report are the mean scores of the nations for each of the variables. Wish *et al.* concentrate on using dissimilarities in an individual differences model (INDSCAL) which is described in Chapter 9. Here the mean scores for the nations are subjected to unfolding analysis in a two dimensional space, the nations being treated as "individuals" and the variables as "stimuli". The mean scores were converted to "distances" using the transformation $(9 - \text{mean score})^{\frac{1}{2}}$. Figure 8.4 shows the resulting configuration, which shows some interesting features. The nations split into various groups {UK, USA, Japan, West Germany}, {Greece, Mexico, Ethiopia, Spain}, {Congo, Brazil, Poland, India, Cuba, Indonesia, Yugoslavia, South Africa}, {France, Israel}, {USSR}, and {China}. The 18 variables form a horseshoe. A possible ordering is approximately the same as their numerical order. Indeed, looking at the list of variables, a scale can be envisaged starting from the second variable. The first few variables relate to individuals, the middle to the nation viewed as a population, and the last of the variables to the nation seen as a non-human entity. It is interesting to note the positions of the various nations, realizing of course that the world has progressed since the data were collected in 1968.

Table 8.2 *The 21 nations.*

Nation		Nation	
Brazil	(BRA)	Israel	(ISR)
China	(CHI)	Japan	(JAP)
Congo	(CON)	Mexico	(MEX)
Cuba	(CUB)	Poland	(POL)
Egypt	(EGY)	USSR	(USSR)
UK	(UK)	South Africa	(SA)
Ethiopia	(ETH)	Spain	(SPA)
France	(FRA)	USA	(USA)
Greece	(GRE)	West Germany	(WG)
India	(INDI)	Yugoslavia	(YUG)
Indonesia	(INDO)		

Table 8.3 *The variables scored for the nations.*

Variable	Variable
1 Aligned with USA	10 Population satisfied
2 Individualistic	11 Internally united
3 Peaceful	12 Cultural influence
4 Many rights	13 Educated population
5 I like	14 Rich
6 Good	15 Industrialized
7 Similarity to ideal	16 Powerful
8 Can change status	17 Progressing
9 Stable	18 Large

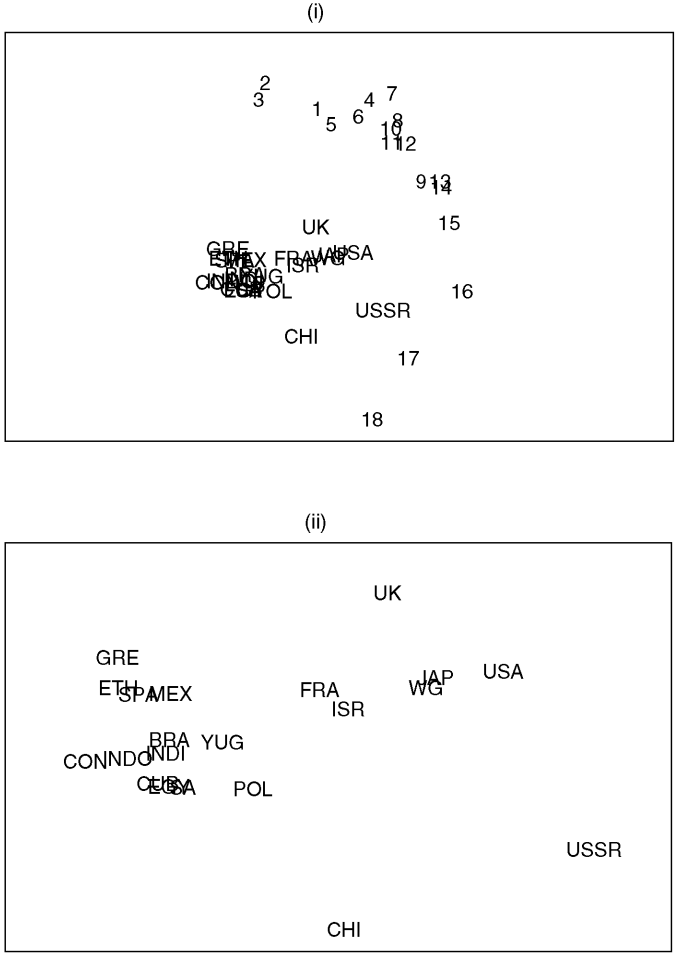

Figure 8.4(i) *Unfolding analysis of the rating of nations.* *Figure 8.4(ii) magnifies the region occupied by the countries.*

CHAPTER 9

Correspondence analysis

9.1 Introduction

Correspondence analysis represents the rows and columns of a data matrix as points in a space of low dimension, and is particularly suited to two-way contingency tables. The method has been discovered and rediscovered several times over the last sixty years, and has gone under several different names. Now the most widely accepted name for this particular technique is correspondence analysis, but it is also referred to as "reciprocal averaging" and "dual scaling". Nishisato (1980) and Greenacre (1984) give brief historical accounts of the development. They trace the origins of the method back to Richardson and Kuder (1933), Hirschfeld (1935), Horst (1935), Fisher (1940) and Guttman (1941). Gower and Hand (1996) give a good summary of correspondence analysis in their monograph on biplots.

Much of correspondence analysis was developed in France in the 1960s by Benzécri. Benzécri originally called the technique "analyse factorielle des correspondances" but later shortened this to "analyse des correspondances", and hence the English translation. Because correspondence analysis can be related to several other statistical procedures, such as canonical correlation analysis, principal components analysis, dual scaling, etc., there are potentially hundreds of references to the subject. Here the method is simply viewed as a metric multidimensional scaling method on the rows and columns of a contingency table or data matrix with non-negative entries.

9.2 Analysis of two-way contingency tables

Suppose data have been collected in the form of an $r \times s$ contingency table. Correspondence analysis finds two vector spaces, one for the rows and one for the columns of the contingency table. These vector

Table 9.1 *Malignant melanoma data*

Histological type	Site of tumour: Head, neck (h)	Trunk (t)	Extremities (e)
Hutchison's melanotic freckle (H)	22	2	10
Superficial spreading melanoma (S)	16	54	115
Nodular (N)	19	33	73
Interminate (I)	11	17	28

spaces give rise to a graphical display of the data. The theory developed will be illustrated by the following example.

Example
Roberts *et al.* (1981) carried out a study of malignant melanoma, a dangerous type of skin cancer, recording the site of the tumour, and also its histological type, for four hundred patients. Results are shown in Table 9.1. These data could be analysed by various more common categorical data methods such as the fitting of log-linear models, see for example Dobson (1983).

These data will be placed in a 4×3 matrix $\mathbf{X}$ and subjected to correspondence analysis. However, first the SVD of $\mathbf{X}$ is found for comparison with results from correspondence analysis. The matrix $\mathbf{X}$ can be viewed as a coordinate matrix of four histological types (rows) in three dimensional space with each dimension given by a tumour site (columns). Alternatively, it can be viewed as a coordinate matrix for three tumour sites in four dimensional space with each dimension given by a histological type. Euclidean distance could be used to measure distance between histological types, with for example, the distance between (H) and (S) being 116.9. Similarly, for distances between tumour sites, with the distance between (h) and (t) being 45.6.

Following Section 1.4.2, the SVD of $\mathbf{X}$ is given by

$$\mathbf{X} = \begin{bmatrix} 0.087 & 0.906 & 0.221 \\ 0.818 & -0.292 & 0.109 \\ 0.526 & 0.215 & 0.187 \\ 0.217 & 0.219 & -0.951 \end{bmatrix} \begin{bmatrix} 156.369 & 0 & 0 \\ 0 & 22.140 & 0 \\ 0 & 0 & 4.083 \end{bmatrix} \times \begin{bmatrix} 0.175 & 0.418 & 0.891 \\ 0.982 & -0.144 & -0.125 \\ -0.075 & -0.897 & 0.436 \end{bmatrix},$$

or equivalently by

$$\begin{aligned} \mathbf{X} = 156.369 & \begin{bmatrix} 0.015 & 0.036 & 0.078 \\ 0.143 & 0.342 & 0.729 \\ 0.092 & 0.220 & 0.469 \\ 0.038 & 0.091 & 0.194 \end{bmatrix} \\ + 22.140 & \begin{bmatrix} 0.889 & -0.130 & -0.114 \\ -0.287 & 0.042 & 0.037 \\ 0.211 & -0.031 & -0.027 \\ 0.215 & -0.031 & -0.027 \end{bmatrix} \\ + 4.083 & \begin{bmatrix} -0.017 & -0.198 & 0.096 \\ -0.008 & -0.098 & 0.048 \\ -0.014 & -0.167 & 0.081 \\ 0.072 & 0.853 & -0.414 \end{bmatrix}. \end{aligned}$$

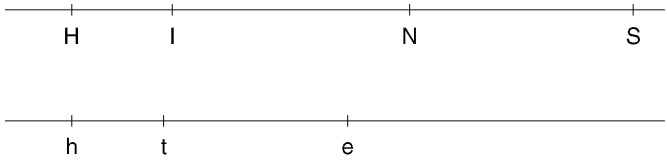

Figure 9.1 *The SVD of the tumour data approximated in one dimension. First space – histological type, second space – site of tumour.*

Since the first singular value is seven times as large as the second, a one dimensional space could be used to represent the tumour type and also for the site. From the first left singular vector, the coordinates in this one dimensional space for histological types (H, S, N, I) are given by $(13.6,\ 127.9,\ 82.3,\ 33.9)^T$. Similarly, the coordinates for tumour sites (h, t, e) are obtained from the first right

singular vector, as $(27.4,\ 65.4,\ 139.3)^T$. Figure 9.1 shows plots of the points. In the first space, the ordering H, I, N, S for the type of tumour can be seen, and in the second space, the ordering h, t, e for the site of the tumour. The distances between histological types in this one dimensional space approximate those in the original three dimensional space, and similarly for the one dimensional space of tumour sites. For instance, the distance between (H) and (S) is now 114.3 and the distance between (h) and (t) is now 38.0.

9.2.1 Distances between rows (columns) in a contingency table

The above use of Euclidean distance to measure distance between rows of a contingency table or the distance between columns will usually not be appropriate. The distances will be greatly affected by marginal totals in the contingency table which, in turn, will depend on the sampling methods being used to collect the data. A more common distance measure used is the χ^2-distance.

Firstly, the matrix $\mathbf{X}$ is normalized so that $\sum_i \sum_j x_{ij} = 1$, i.e. each element of $\mathbf{X}$ is divided by the total sum of all the elements. The ith row profile of matrix $\mathbf{X}$ is the ith row of $\mathbf{X}$ standardized so the row sum is unity. Let r_i be the ith row sum of $\mathbf{X}$. The matrix of row profiles is given by $\mathbf{D}_r^{-1}\mathbf{X}$ where $\mathbf{D}_r = \text{diag}(r_1, \ldots, r_n)$.

Similarly, the jth column profile of $\mathbf{X}$ is defined as the standardized jth column of $\mathbf{X}$. Let the jth column sum be c_j and then the matrix of column profiles is given by $\mathbf{D}_c^{-1}\mathbf{X}$, where $\mathbf{D}_c = \text{diag}(c_1, \ldots, c_p)$.

Distances between rows in $\mathbf{X}$ are based on the row profiles, the distance between the ith and i'th rows being given by

$$d_{ii'}^2 = \sum_{j=1}^{p} \frac{1}{c_j} \left(\frac{x_{ij}}{r_i} - \frac{x_{i'j}}{r_{i'}} \right)^2. \tag{9.1}$$

This weighted Euclidean distance is called χ^2-distance.

The χ^2-distance between columns j and j' is similarly defined as

$$d_{jj'}^2 = \sum_{i=1}^{n} \frac{1}{r_i} \left(\frac{x_{ij}}{c_j} - \frac{x_{ij'}}{c_{j'}} \right)^2.$$

Note that distance is not defined between a row and a column.

For the cancer data, the matrix of χ^2-distances between rows is

$$\begin{bmatrix} 0 & 1.498 & 1.323 & 1.223 \\ 1.498 & 0 & 0.175 & 0.313 \\ 1.323 & 0.175 & 0 & 0.173 \\ 1.223 & 0.313 & 0.173 & 0 \end{bmatrix}.$$

The matrix of χ^2-distances between columns is

$$\begin{bmatrix} 0 & 1.122 & 1.047 \\ 1.122 & 0 & 0.132 \\ 1.047 & 0.132 & 0 \end{bmatrix}.$$

9.3 The theory of correspondence analysis

Having introduced the idea of χ^2-distance between rows and between columns of a contingency table $\mathbf{X}$ the theory of correspondence analysis is explored in the style of Greenacre (1984). Two vector spaces are found, one representing the rows of matrix $\mathbf{X}$ and one representing its columns, and in such a way that the rows and columns are similarly treated. The row and column profiles are represented in vector spaces which are based on the generalized SVD of $\mathbf{X}$.

Let the generalized SVD of $\mathbf{X}$ be given by

$$\mathbf{X} = \mathbf{A}\mathbf{D}_\lambda\mathbf{B}^T, \tag{9.2}$$

where

$$\mathbf{A}^T\mathbf{D}_r^{-1}\mathbf{A} = \mathbf{B}^T\mathbf{D}_c^{-1}\mathbf{B} = \mathbf{I}. \tag{9.3}$$

The matrix $\mathbf{A}$ is an orthonormal basis for the columns of $\mathbf{X}$, normalized with respect to $\mathbf{D}_r^{-1}$, which allows for the differing row profile weights $\{r_i\}$. Similarly $\mathbf{B}$ is an orthonormal basis for the rows of $\mathbf{X}$, normalized with respect to $\mathbf{D}_c^{-1}$, allowing for the column profile weights $\{c_j\}$.

Using equation (9.2) the row profiles can then be expressed as

$$\mathbf{D}_r^{-1}\mathbf{X} = \mathbf{D}_r^{-1}\mathbf{A}\mathbf{D}_\lambda\mathbf{B}^T,$$

and equation (9.3) can be written as

$$(\mathbf{D}_r^{-1}\mathbf{A})^T\mathbf{D}_r(\mathbf{D}_r^{-1}\mathbf{A}) = \mathbf{B}^T\mathbf{D}_c^{-1}\mathbf{B} = \mathbf{I}.$$

Letting $\mathbf{U} = \mathbf{D}_r^{-1}\mathbf{A}$,

$$\mathbf{D}_r^{-1}\mathbf{X} = \mathbf{U}\mathbf{D}_\lambda\mathbf{B}^T, \quad \mathbf{U}^T\mathbf{D}_r\mathbf{U} = \mathbf{B}^T\mathbf{D}_c^{-1}\mathbf{B} = \mathbf{I}. \tag{9.4}$$

Equation (9.4) shows the rows of $\mathbf{X}$ can be represented as points in the $\mathbf{UD}_\lambda$ space, with $\mathbf{B}$ the rotation matrix which transforms the points in this space to the row profiles. The χ^2-distances between row profiles are equal to the Euclidean distances between points representing the rows in the $\mathbf{UD}_\lambda$ space. To see this, consider the following.

Let $\mathbf{e}_i$ be a vector of zeros, except for the ith element which has the value unity. Then, in general, if $\mathbf{Y}$ is an $n \times p$ matrix of coordinates, $\mathbf{e}_i^T\mathbf{Y}$ is the row vector of coordinates for the ith point. From equation (9.2) the χ^2-distance $d_{ii'}$ between the ith and i'th row profiles can be written as

$$\begin{aligned} d_{ii'}^2 &= \left((\mathbf{e}_i^T - \mathbf{e}_{i'}^T)\mathbf{D}_r^{-1}\mathbf{X}\mathbf{D}_c^{-\frac{1}{2}}\right)\left((\mathbf{e}_i^T - \mathbf{e}_{i'}^T)\mathbf{D}_r^{-1}\mathbf{X}\mathbf{D}_c^{-\frac{1}{2}}\right)^T \\ &= (\mathbf{e}_i^T - \mathbf{e}_{i'}^T)\mathbf{D}_r^{-1}\mathbf{X}\mathbf{D}_c^{-1}\mathbf{X}^T\mathbf{D}_r^{-1}(\mathbf{e}_i - \mathbf{e}_{i'}) \\ &= (\mathbf{e}_i^T - \mathbf{e}_{i'}^T)(\mathbf{UD}_\lambda)\mathbf{B}^T\mathbf{D}_c^{-1}\mathbf{B}(\mathbf{UD}_\lambda)^T(\mathbf{e}_i - \mathbf{e}_{i'}) \\ &= (\mathbf{e}_i^T - \mathbf{e}_{i'}^T)(\mathbf{UD}_\lambda)(\mathbf{UD}_\lambda)^T(\mathbf{e}_i - \mathbf{e}_{i'}). \end{aligned}$$

The last term is the Euclidean distance between the ith and i'th points in the $\mathbf{UD}_\lambda$ space.

In like manner, the column profiles can be expressed as

$$\mathbf{D}_c^{-1}\mathbf{X}^T = \mathbf{D}_c^{-1}\mathbf{B}\mathbf{D}_\lambda\mathbf{A}^T,$$

with

$$\mathbf{A}^T\mathbf{D}_r^{-1}\mathbf{A} = (\mathbf{D}_c^{-1}\mathbf{B})^T\mathbf{D}_c(\mathbf{D}_c^{-1}\mathbf{B}) = \mathbf{I},$$

and letting $\mathbf{V} = \mathbf{D}_c^{-1}\mathbf{B}$,

$$\mathbf{D}_c^{-1}\mathbf{X}^T = \mathbf{V}\mathbf{D}_\lambda\mathbf{A}^T, \quad \mathbf{A}^T\mathbf{D}_r^{-1}\mathbf{A} = \mathbf{V}^T\mathbf{D}_c\mathbf{V} = \mathbf{I}. \tag{9.5}$$

Equation (9.5) shows the columns can be represented as points in the $\mathbf{VD}_\lambda$ space, with $\mathbf{A}$ the necessary rotation matrix to the column profiles. Again, Euclidean distances between points in the $\mathbf{VD}_\lambda$ space are equal to the χ^2-distances between column profiles.

For a low dimensional representation of the row and column profiles, the generalized SVD allows the first k columns of $\mathbf{UD}_\lambda$ and the first k columns of $\mathbf{VD}_\lambda$ to be taken as approximating spaces.

9.3.1 The cancer example

The normalized data matrix $\mathbf{X}$ and the other relevant matrices are:

$$\mathbf{X} = \begin{bmatrix} 0.055 & 0.005 & 0.025 \\ 0.040 & 0.135 & 0.288 \\ 0.048 & 0.083 & 0.183 \\ 0.028 & 0.043 & 0.070 \end{bmatrix}$$

$$\mathbf{D}_r = \text{diag}[0.085, \quad 0.463, \quad 0.314, \quad 0.141]$$

$$\mathbf{D}_c = \text{diag}[0.171, \quad 0.266, \quad 0.566]$$

$$\mathbf{D}_r^{-1}\mathbf{X} = \begin{bmatrix} 0.647 & 0.059 & 0.294 \\ 0.086 & 0.292 & 0.622 \\ 0.152 & 0.264 & 0.584 \\ 0.196 & 0.304 & 0.500 \end{bmatrix}$$

$$\mathbf{D}_c^{-1}\mathbf{X}^T = \begin{bmatrix} 0.324 & 0.235 & 0.279 & 0.162 \\ 0.019 & 0.509 & 0.311 & 0.160 \\ 0.044 & 0.509 & 0.323 & 0.124 \end{bmatrix}.$$

The generalized SVD of $\mathbf{X}$ is given by

$$\mathbf{X} = \begin{bmatrix} 0.085 & 0.269 & -0.050 \\ 0.463 & -0.255 & -0.166 \\ 0.313 & -0.036 & -0.131 \\ 0.140 & 0.021 & 0.346 \end{bmatrix} \begin{bmatrix} 1.0 & 0 & 0 \\ 0 & 0.403 & 0 \\ 0 & 0 & 0.047 \end{bmatrix}$$

$$\times \begin{bmatrix} 0.170 & 0.265 & 0.565 \\ 0.374 & -0.153 & -0.222 \\ 0.029 & 0.414 & -0.443 \end{bmatrix}$$

$$\mathbf{U} = \begin{bmatrix} 1 & 3.167 & -0.591 \\ 1 & -0.550 & -0.358 \\ 1 & -0.116 & -0.418 \\ 1 & 0.153 & 2.474 \end{bmatrix}$$

$$\mathbf{V} = \begin{bmatrix} 1 & 2.203 & 0.172 \\ 1 & -0.576 & 1.563 \\ 1 & -0.393 & -0.785 \end{bmatrix}$$

$$\mathbf{U}\mathbf{D}_\lambda = \begin{bmatrix} 1 & 1.276 & -0.023 \\ 1 & -0.222 & -0.017 \\ 1 & -0.047 & -0.020 \\ 1 & 0.062 & 0.116 \end{bmatrix}$$

$$\mathbf{V}\mathbf{D}_\lambda = \begin{bmatrix} 1 & 0.888 & 0.008 \\ 1 & -0.232 & 0.073 \\ 1 & -0.158 & -0.037 \end{bmatrix}.$$

There is always a singular value of unity with associated eigenvector $\mathbf{1}$. This is easily seen since $\mathbf{D}_r^{-1}\mathbf{X}\mathbf{1} = \mathbf{1}$, $\mathbf{D}_c^{-1}\mathbf{X}^T\mathbf{1} = \mathbf{1}$, noting the $\mathbf{1}$ vectors have differing lengths. From Section 1.4.2 the singular values in $\mathbf{D}_\lambda$ are given by the square roots of the non-zero eigenvalues of

$$(\mathbf{D}_r^{-\frac{1}{2}}\mathbf{X}\mathbf{D}_c^{-\frac{1}{2}})(\mathbf{D}_r^{-\frac{1}{2}}\mathbf{X}\mathbf{D}_c^{-\frac{1}{2}})^T = \mathbf{D}_r^{-\frac{1}{2}}\mathbf{X}\mathbf{D}_c^{-1}\mathbf{X}^T\mathbf{D}_r^{-\frac{1}{2}}. \qquad (9.6)$$

These eigenvalues are the same as those of $\mathbf{D}_r^{-1}\mathbf{X}\mathbf{D}_c^{-1}\mathbf{X}^T$. So

$$\mathbf{D}_r^{-1}\mathbf{X}\mathbf{D}_c^{-1}\mathbf{X}^T\mathbf{1} = \mathbf{D}_r^{-1}\mathbf{X}\mathbf{1} = \mathbf{1}.$$

Hence unity is an eigenvalue and also a singular value and $\mathbf{1}$ will be the corresponding singular vector of $\mathbf{U}$. A similar argument also shows that $\mathbf{1}$ is the corresponding singular vector for $\mathbf{V}$.

The singular value of unity and its associated singular vector $\mathbf{1}$ give rise to the so called trivial dimension and can be omitted from calculations by removal from row and column profile matrices. Thus the matrices submitted to correspondence analysis are $\mathbf{D}_r^{-1}\mathbf{X} - \mathbf{1}\mathbf{c}^T$ and $\mathbf{D}_c^{-1}\mathbf{X}^T - \mathbf{1}\mathbf{r}^T$, where $\mathbf{r}$ and $\mathbf{c}$ are vectors of row and column sums.

Ignoring the trivial dimension, Figure 9.2 uses the singular vectors of $\mathbf{U}\mathbf{D}_\lambda$ to plot points representing the histological type of tumour, and the singular vectors of $\mathbf{V}\mathbf{D}_\lambda$ for points representing the site of the tumours. One dimensional spaces for type of tumour and site of tumour can easily be gleaned from the figure by simply ignoring the second axis. Since the first singular value is nearly nine times as large as the second, one dimensional spaces adequately represent the types and sites of tumour.

The figure shows that Hutchinson's melanotic freckle stands well away from the other types of tumour, and the head and neck away from the other two sites. The row profile matrix confirms that this should be so with 65% of Hutchinson's melanotic freckle occurring on the head and neck, while the other three tumour types each have over 50% of their occurrences at the extremities.

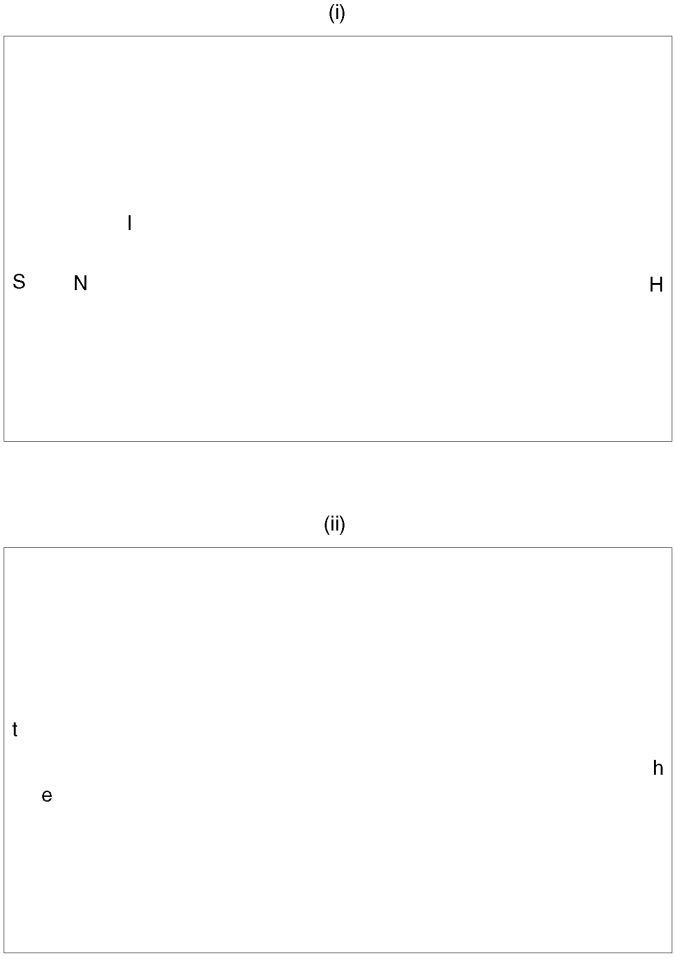

Figure 9.2 *Correspondence analysis of the cancer data.*
First space, 9.2(i)– histological type, second space, 9.2(ii)– site of tumour.

The column profiles show that the head and neck is a common site for all four types of tumour, while the trunk and the extremities rarely have Hutchinson's melanotic freckle and with 50% of their occurrences being superficial spreading melanoma.

The distances between row points in the $\mathbf{UD}_\lambda$ space can be found and are equal to the χ^2-distances already calculated in Section 9.2.

If a one dimensional space is used to represent the row points the distances between points in this space are

$$\begin{bmatrix} 0 & 1.498 & 1.323 & 1.214 \\ 1.498 & 0 & 0.175 & 0.284 \\ 1.323 & 0.175 & 0 & 0.109 \\ 1.214 & 0.284 & 0.109 & 0 \end{bmatrix}.$$

Similarly, the distances between column points in a one dimensional space are

$$\begin{bmatrix} 0 & 1.120 & 1.046 \\ 1.120 & 0 & 0.074 \\ 1.046 & 0.074 & 0 \end{bmatrix}.$$

The largest discrepancies between these distances and those from Section 9.2 are for (S) and (N), for (S) and (I) and for (t) and (e).

These results from correspondence analysis can be compared with those using the SVD of $\mathbf{X}$. For tumour type, the same ordering in one dimension is obtained, although the direction of the axis has been reversed non-consequentially. However, the results for the site of tumour are very different for those from the SVD analysis.

A single plot

Since the $\mathbf{UD}_\lambda$ and the $\mathbf{VD}_\lambda$ spaces have arisen from the singular value decomposition of $\mathbf{X}$ and share the same singular values, it is possible to plot the points representing the rows and the points representing the columns of $\mathbf{X}$ together, and to transform from the $\mathbf{UD}_\lambda$ space to the $\mathbf{VD}_\lambda$ space and vice versa. Consider $(\mathbf{UD}_\lambda)$ multiplied by $\mathbf{B}^T\mathbf{D}_c^{-1}\mathbf{B}$ $(= \mathbf{I})$.

$$\begin{aligned}(\mathbf{UD}_\lambda) &= (\mathbf{UD}_\lambda)(\mathbf{B}^T\mathbf{D}_c^{-1}\mathbf{B}) = (\mathbf{UD}_\lambda)\mathbf{B}^T\mathbf{V} = (\mathbf{D}_r^{-1}\mathbf{X})\mathbf{V} \\ &= (\mathbf{D}_r^{-1}\mathbf{X})(\mathbf{VD}_\lambda)\mathbf{D}_\lambda^{-1}.\end{aligned}$$

and similarly

$$(\mathbf{VD}_\lambda) = (\mathbf{D}_c^{-1}\mathbf{X})(\mathbf{UD}_\lambda)\mathbf{D}_\lambda^{-1}.$$

The relationships between $\mathbf{UD}_\lambda$ and $\mathbf{VD}_\lambda$ in these equations are known as the transition formulae.

Figure 9.3 shows the rows and columns of the cancer matrix plotted together. It must be remembered that distances between columns and rows are not defined, but from the plot it can be seen

that row points tend to be closer to those column points for which the row profile values are highest, and vice versa.

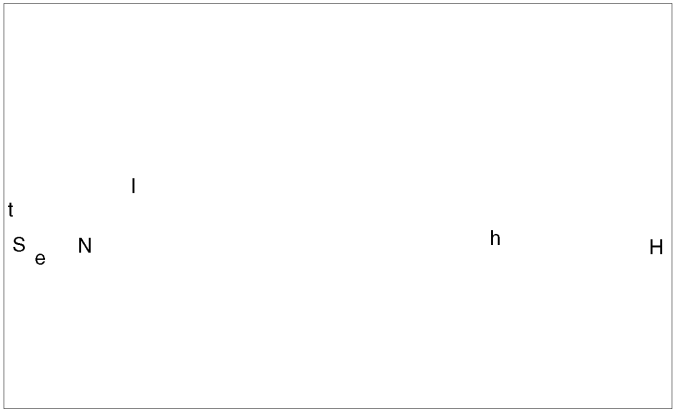

Figure 9.3 *Combined space for correspondence analysis of the cancer data*

9.3.2 Inertia

A measure of the dispersion of the points representing the rows is given by the "total inertia", a term taken from its physical counterpart. The total inertia is the weighted sum of χ^2-distances of row points to their centroid. Let $\mathbf{r} = (r_1, \ldots, r_n)^T$ be the vector of row sums and let $\mathbf{c} = (c_1, \ldots, c_p)^T$ be the vector of column sums. The row point centroid is given by $\mathbf{r}^T\mathbf{D}_r^{-1}\mathbf{X}/\mathbf{r}^T\mathbf{1}$. Now $\mathbf{r}^T\mathbf{1} = 1$ and $\mathbf{r}^T\mathbf{D}_r = \mathbf{1}^T$ and hence the row centroid is given by $\mathbf{1}^T\mathbf{X} = \mathbf{c}$. Similarly, the column centroid is given by $\mathbf{X1} = \mathbf{r}$. The total inertia, I, is defined by

$$I = \sum_i r_i(\mathbf{r}_i - \mathbf{c})^T\mathbf{D}_c^{-1}(\mathbf{r}_i - \mathbf{c}).$$

To see the connection of I with the usual X^2 quantity calculated for a contingency table under the assumption of independent rows and columns, consider

$$n^{-1}X^2 = n^{-1}\sum_i\sum_j \frac{\left(x_{ij} - \frac{x_{i+}x_{+j}}{n}\right)^2}{\frac{x_{i+}x_{+j}}{n}},$$

where x_{i+} and x_{+j} are row and column sums using the more traditional notation for contingency tables here.

This can be written

$$n^{-1}X^2 = \sum_i \left\{ x_{i+} \sum_j \frac{\left(\frac{x_{ij}}{x_{i+}} - \frac{x_{+j}}{n}\right)^2}{x_{+j}} \right\},$$
$$= \sum_i r_i(\mathbf{r}_i - \mathbf{c})^T \mathbf{D}_c^{-1}(\mathbf{r}_i - \mathbf{c}) = I,$$

transferring back to the other notation, and hence the connection.

Interchanging rows and columns gives the total inertia for the column points as

$$\sum_j c_j(\mathbf{c}_j - \mathbf{r})^T \mathbf{D}_r^{-1}(\mathbf{c}_j - \mathbf{r}),$$

and by symmetry of X^2 is equal to the total inertia for the row points.

Now I can be written as

$$I = \mathrm{tr}(\mathbf{D}_r(\mathbf{D}_r^{-1}\mathbf{x} - \mathbf{1}\mathbf{c}^T)\mathbf{D}_c^{-1}(\mathbf{D}_r^{-1}\mathbf{X} - \mathbf{1}\mathbf{c}^T)^T),$$

where $\mathbf{D}_r^{-1}\mathbf{X} - \mathbf{1}\mathbf{c}^T$ is the matrix of row profiles with the trivial dimension removed. Replace $\mathbf{D}_r^{-1}\mathbf{X} - \mathbf{1}\mathbf{c}^T$ by $\mathbf{D}_r^{-1}\mathbf{X}$ assuming this trivial dimension has been removed, then

$$\begin{aligned} I &= \mathrm{tr}(\mathbf{D}_r(\mathbf{D}_r^{-1}\mathbf{X})\mathbf{D}_c^{-1}(\mathbf{D}_r^{-1}\mathbf{X})^T) \\ &= \mathrm{tr}((\mathbf{A}\mathbf{D}_\lambda\mathbf{B}^T)\mathbf{D}_c^{-1}(\mathbf{B}\mathbf{D}_\lambda\mathbf{A}^T)\mathbf{D}_r^{-1}) \\ &= \mathrm{tr}(\mathbf{A}\mathbf{D}_\lambda^2\mathbf{A}^T\mathbf{D}_r^{-1}) = \mathrm{tr}(\mathbf{D}_\lambda^2\mathbf{A}^T\mathbf{D}_r^{-1}\mathbf{A}) \\ &= \mathrm{tr}(\mathbf{D}_\lambda^2). \end{aligned}$$

Hence the total inertia is equal to the sum of the squared singular values. The required dimension of the row and column profile spaces can be judged by the contribution to the total inertia by the various dimensions. Thus, if k dimensional spaces are chosen the contribution to total inertia is

$$\sum_1^k \lambda_i^2 / \sum_1^n \lambda_i^2,$$

where n is the total number of non-unit singular values. For the cancer example, the total inertia was 0.1645 and the first dimension contributed 98.6% of this.

9.4 Reciprocal averaging

Reciprocal averaging, like dual scaling, is essentially the same as correspondence analysis, although Greenacre (1984) maintains that there are differences, especially in the geometric framework of the various models. The term reciprocal averaging was first used by Hill (1973, 1974) and has since become very popular with plant ecologists. It is within this area that the theory can be well illustrated.

Suppose n different species of plants are investigated at p different sites, and to fix ideas, suppose the sites are chosen for their varying exposure to extreme weather conditions, while the species of plant are chosen for their various levels of hardiness. Let $\mathbf{X} = [x_{ij}]$, where x_{ij} is the response of species i at site j. For example the ecologist may simply be interested in presence/absence ($x_{ij} = 1/0$) of the ith species at the jth site.

Let u_i be a hardiness score for the ith species. Let v_j be an exposure score for the jth site. It is assumed that the exposure score at the jth site is proportional to the mean hardiness score of the species at that site. Thus

$$v_j \propto \sum_i u_i x_{ij} / \sum_i x_{ij}.$$

Correspondingly, it is assumed that the hardiness score of species i is proportional to the mean exposure score of the sites occupied by that species. Thus

$$u_i \propto \sum_j v_j x_{ij} / \sum_j x_{ij}.$$

Reciprocal averaging then solves the two equations

$$\rho u_i = \sum_j v_j x_{ij} / r_i \quad (i = 1, \ldots, n) \tag{9.7}$$

$$\rho v_j = \sum_i u_i x_{ij} / c_j \quad (j = 1, \ldots, p), \tag{9.8}$$

where $r_i = \sum_j x_{ij}$, $c_j = \sum_i x_{ij}$, and ρ is a scaling parameter.

9.4.1 Algorithm for solution

A trivial solution is $\rho = 1$, $u_i = 1$, $(i = 1, \ldots, n)$, $v_j = 1$, $(j = 1, \ldots, p)$ (cf. the trivial dimension of the theory of correspondence

analysis, with singular value unity, and singular vectors **1**). This trivial solution is removed from the data by transforming to $x_{ij} - r_i c_j / x_{..}$, and then solving equations (9.7) and (9.8) iteratively.

Hill (1973) gives an algorithm for the solution. Choose an initial set of exposure scores placed in a vector $\mathbf{v}_0$. The scores are scaled so that the smallest is zero and the largest unity, say. Let $\rho = 1$ and calculate hardiness scores $\mathbf{u}_1$ from (9.7). Use these in (9.8) to obtain updated exposure scores $\mathbf{v}_1$ which are then scaled again to have minimum zero and maximum unity. This process is continued until convergence. The value of ρ is calculated as the factor required for the scaling of the final scores. The value of ρ and the two sets of scores give rise to a first axis. This first axis can be "subtracted" from the incidence matrix, and then the whole procedure repeated to find a second axis, and so forth. However, since reciprocal averaging is related to correspondence analysis, the axes are more easily found as eigenvalues and eigenvectors of various matrices, as discussed below.

9.4.2 An example: the Münsingen data

Hodson's Münsingen data have been a popular candidate for reciprocal averaging. The contents of various ancient graves at La Tène cemetery at Münsingen-Rain in Switzerland were recorded. From this, an incidence matrix, $\mathbf{X}$, is formed where each row represents a grave and each column an artefact - pottery, jewellery, etc. Then $[\mathbf{X}]_{ij} = 1$ if the ith grave contains an example of the jth artefact, and zero otherwise. Kendall (1971) gives the data and an analysis.

Figure 9.4 shows a plot of the grave scores and the artefact scores recovered as the first two axes from reciprocal averaging. The grave scores form a "horseshoe", as do the artefacts, a phenomenon discussed by Kendall. It is possible that taking the graves and artefacts in order around their horseshoes will give an age ordering to the graves and artefacts.

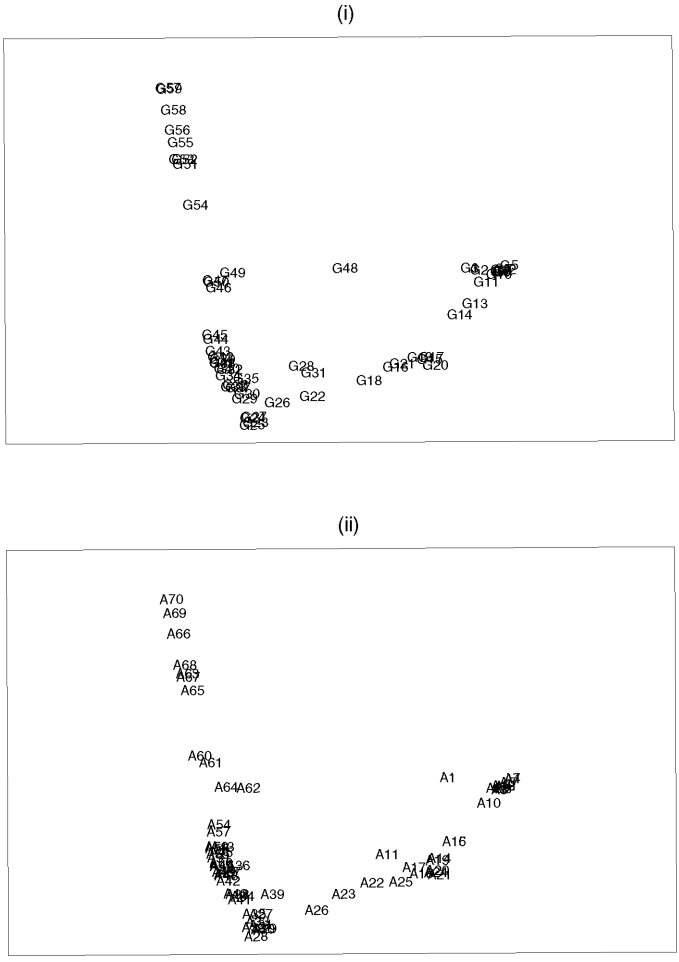

Figure 9.4 *Reciprocal averaging of the Münsingen data. Upper* figure, 9.4 (i) *graves, lower* figure, 9.4 (ii) *artefacts*

9.4.3 The whisky data

Data on the nose and taste of nineteen whiskies were subjected to nonmetric MDS in Chapter 6. Here, the same data are subjected

to reciprocal averaging. Let $[X]_{ij} = 1$ if the ith whisky has the jth nose/taste property.

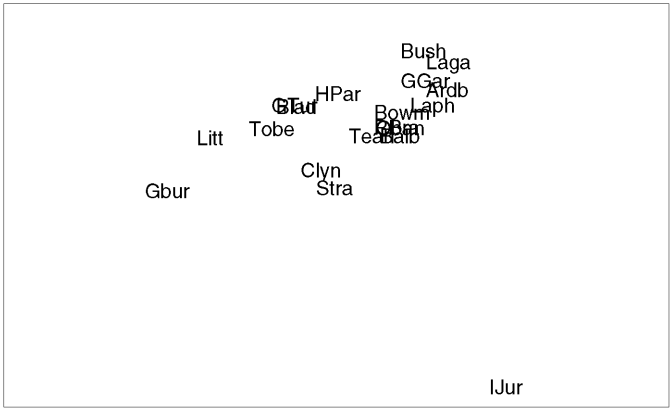

Figure 9.5 *Reciprocal averaging of whisky data*

Figure 9.5 shows the whiskies plotted on the first two axes from reciprocal averaging. Figure 9.6 shows similar plots for the nose and taste characteristics, noting that these have been plotted separately for clarity. Groupings of the whiskies according to region (see page 144) can be seen in the first plot. The Speyside pair are at the bottom left of the main cluster of whiskies. The Islay group are at the top left of the cluster. There is a tight group of Northern Highland whiskies (Balblair, Royal Brackla, Teaninich together with the Oban). The Isle of Jura is a singleton. The Irish Bushmills is close to the Islay group.

The nose characteristics have sherry, smoke and medicinal at one end of the cluster of characteristics and fragrance at the other end. Tart stands well apart from the other characteristics. Similarly, the taste characteristics have full bodied, sherry and peaty at one end and delicate and light at the other. Floral is the characteristic that stands apart. The outlying points of Isle of Jura, tart and floral can be explained by the fact that the Isle of Jura whisky is the only one to have these as characteristics.

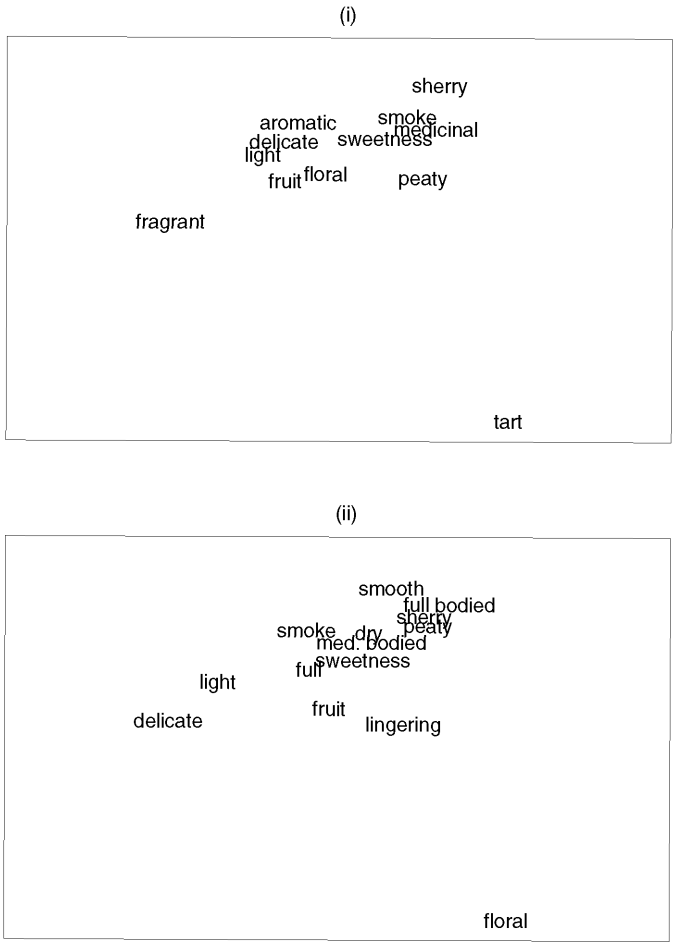

Figure 9.6 *Reciprocal averaging of whisky data. Upper figure, 9.6 (i)– nose characteristics, lower figure, 9.6 (ii)– taste characteristics*

9.4.4 The correspondence analysis connection

If all the dimensions found by reciprocal averaging are considered

simultaneously, then the method is seen to be equivalent to correspondence analysis. Equations (9.7) and (9.8) can be written as

$$\rho \mathbf{u} = \mathbf{D}_r^{-1}\ \mathbf{X}\mathbf{v}$$
$$\rho \mathbf{v} = \mathbf{D}_c^{-1}\mathbf{X}^T\mathbf{u},$$

where $\mathbf{D}_r = \text{diag}(\sum_j x_{ij})$, and $\mathbf{D}_c = \text{diag}(\sum_i x_{ij})$. Then

$$\rho \mathbf{D}_r^{\frac{1}{2}}\mathbf{u} = (\mathbf{D}_r^{-\frac{1}{2}}\mathbf{X}\mathbf{D}_c^{-\frac{1}{2}})\mathbf{D}_c^{\frac{1}{2}}\mathbf{v}, \tag{9.9}$$
$$\rho \mathbf{D}_c^{\frac{1}{2}}\mathbf{v} = (\mathbf{D}_r^{-\frac{1}{2}}\mathbf{X}\mathbf{D}_c^{-\frac{1}{2}})^T\mathbf{D}_r^{\frac{1}{2}}\mathbf{u}. \tag{9.10}$$

Substituting equation (9.10) into equation (9.9) gives

$$\rho^2(\mathbf{D}_r^{\frac{1}{2}}\mathbf{u}) = (\mathbf{D}_r^{-\frac{1}{2}}\mathbf{X}\mathbf{D}_c^{-\frac{1}{2}})(\mathbf{D}_r^{-\frac{1}{2}}\mathbf{X}\mathbf{D}_c^{-\frac{1}{2}})^T\mathbf{D}_r^{\frac{1}{2}}\mathbf{u}.$$

Hence ρ^2 is an eigenvalue of

$$(\mathbf{D}_r^{-\frac{1}{2}}\mathbf{X}\mathbf{D}_c^{-\frac{1}{2}})(\mathbf{D}_r^{-\frac{1}{2}}\mathbf{X}\mathbf{D}_c^{-\frac{1}{2}})^T = \mathbf{D}_r^{-\frac{1}{2}}\mathbf{X}\mathbf{D}_c^{-1}\mathbf{X}^T\mathbf{D}_r^{-\frac{1}{2}},$$

and has an associated eigenvector $(\mathbf{D}_r^{\frac{1}{2}}\mathbf{u})$. But these are just the square of the singular value and the associated singular vector in (9.6). Likewise, substituting equation (9.9) into equation (9.10) gives ρ^2 as an eigenvalue of $\mathbf{D}_c^{-\frac{1}{2}}\mathbf{X}^T\mathbf{D}_r^{-1}\mathbf{X}\mathbf{D}_c^{-\frac{1}{2}}$, and associated eigenvector $(\mathbf{D}_c^{\frac{1}{2}}\mathbf{v})$. Thus reciprocal averaging finds, in turn, all the singular values and singular vectors associated with correspondence analysis.

9.4.5 Two-way weighted dissimilarity coefficients

Cox and Cox (2000) use reciprocal averaging ideas to construct two sets of weighted dissimilarity coefficients from an $n \times p$ data matrix, $\mathbf{X}$. One set gives the dissimilarities between objects (rows) and one set the dissimilarities between variables (columns). The method extends Gower's general dissimilarity coefficient (Gower, 1971).

Let the dissimilarities for pairs of objects be $\{\delta_{rs}\}$ and the dissimilarities for pairs of variables be $\{\epsilon_{ij}\}$. As in Section 1.3.1 let the unweighted dissimilarity between the rth and sth objects, as measured by the i variable, be α_{rsi}. Let the unweighted dissimilarity between the ith and jth variables as measured by the rth object be β_{ijr}. Let the weight for the dissimilarity measure, δ_{rs}, for the ith variable be a_i and the weight for the dissimilarity measure, ϵ_{ij}

for the rth object be b_r. Let the weighted dissimilarities be given by

$$\delta_{rs} = \sum_i a_i \alpha_{rsi}$$

and

$$\epsilon_{ij} = \sum_r b_r \beta_{ijr}.$$

The weight a_i is chosen to be proportional to the sum of those dissimilarities which involve the ith variable, raised to a power γ_a,

$$a_i \propto \Big(\sum_j \epsilon_{ij} \Big)^{\gamma_a}.$$

Similarly, the weight b_r is chosen to be proportional to the sum of those dissimilarities which involve the rth object, raised to a power γ_b,

$$b_r \propto \Big(\sum_s \delta_{rs} \Big)^{\gamma_b}.$$

The choice of γ_a and γ_b dictate the intention of the weights. For instance, if $\gamma_a > 0$, then if variable i is in general similar to the other variables, then the dissimilarities it is involved with will be small and a_i will be a small weight. On the other hand, if variable i is, in general, different from the other variables, the larger dissimilarities it generates will give rise to a larger weight. For $\gamma_a < 0$ the opposite occurs for size of weights. For $\gamma_a = 0$ all weights are equal essentially leading to Gower's original dissimilarities. A similar situation regarding weights applies to the objects also. Cox and Cox discuss various situations where the choice of γ_a and γ_b is pertinent.

The two proportionalities above lead to the equations

$$\lambda_a a_i = \big(\sum_j \epsilon_{ij} \big)^{\gamma_a} = \big(\sum_j \sum_r b_r \beta_{ijr} \big)^{\gamma_a} = \big(\sum_r b_r \beta_{ir} \big)^{\gamma_a}, \quad (9.11)$$

$$\lambda_b b_r = \big(\sum_s \delta_{rs} \big)^{\gamma_b} = \big(\sum_s \sum_i a_r \alpha_{rsi} \big)^{\gamma_b} = \big(\sum_i a_r \alpha_{ri} \big)^{\gamma_b}, \quad (9.12)$$

where λ_a, λ_b are constants, $\alpha_{ri} = \sum_s \alpha_{rsi}$ and $\beta_{ir} = \sum_j \beta_{ijr}$.

The weights $\{a_i\}$ and $\{b_r\}$ can be arbitrarily scaled with the chosen scaling being $\sum a_i^2 = \sum b_r^2 = 1$. Equations (9.11) and (9.12)

are solved iteratively. Equations (9.11) and (9.12) illustrate the reciprocal averaging nature of the two sets of dissimilarities.

Special case, $\gamma_a = \gamma_b = 1$
For the case $\gamma_a = \gamma_b = 1$, equations (9.11) and (9.12) can be written as

$$\lambda_a \mathbf{a} = \mathbf{B}\mathbf{b} \tag{9.13}$$

$$\lambda_b \mathbf{b} = \mathbf{A}\mathbf{a} \tag{9.14}$$

where $\mathbf{a} = (a_1, \ldots, a_p)^T$, $\mathbf{b} = (b_1, \ldots, b_n)^T$, the $n \times p$ matrix $\mathbf{A}$ is given by $[\mathbf{A}]_{ri} = \alpha_{ri}$ and the $p \times n$ matrix $\mathbf{B}$ by $[\mathbf{B}]_{ir} = \beta_{ir}$.

Let $\lambda = \lambda_a \lambda_b$ and pre-multiplying by $\mathbf{A}$ in equation (9.13) and post-multiplying by $\mathbf{B}$ in equation (9.14) gives

$$\lambda \mathbf{b} = \mathbf{A}\mathbf{B}\mathbf{b},$$

$$\lambda \mathbf{a} = \mathbf{B}\mathbf{A}\mathbf{a}.$$

Thus λ is an eigenvalue of both $\mathbf{AB}$ and $\mathbf{BA}$. The eigenvectors of $\mathbf{BA}$ and $\mathbf{AB}$ are $\mathbf{a}$ and $\mathbf{b}$ respectively. The matrices $\mathbf{BA}$ and $\mathbf{AB}$ are non-negative matrices, and so by the Peron-Frobenius theorem, there is always a positive eigenvalue λ with non-negative eigenvectors $\mathbf{a}$ and $\mathbf{b}$. The weights $\mathbf{a}$ and $\mathbf{b}$ are found by solving these matrix equations. Cox and Cox (2000) discuss the choice of dissimilarity measures in various settings and illustrate the use of these reciprocal sets of disimilarities on three data sets using nonmetric multidimensional scaling.

9.5 Multiple correspondence analysis

Correspondence analysis is eminently suited to analysing two-way contingency tables – correspondence analysis needs all the elements of the data matrix $\mathbf{X}$ to be non-negative. Correspondence analysis can also be used on three-way or higher-way contingency tables. This is achieved by using indicator variables to convert the multi-way table into a two-way table. Suppose for a k-way table the number of categories for the ith way is c_i. An indicator variable is assigned to each category of each way of the table, giving $J = \sum_1^k c_i$ indicator variables in total. Each individual count out of the total count of n, then forms a row of an $n \times J$ table with the J indicator variables forming the columns. Each row of the new table will have k values of unity and $J - k$ of zero. An indicator variable has value

unity if the individual count is in the corresponding category of the original table. For example, the cancer data, although already a two-way table, can be put in this new form, giving a 400×7 table. Let the indicator variables be assigned: $I_1 = H$, $I_2 = S$, $I_3 = N$, $I_4 = I$, $I_5 = h$, $I_6 = t$, and $I_7 = e$. The first 22 rows of the table would be identical and equal to $(1, 0, 0, 0, 1, 0, 0)$. Then follows 2 rows of $(1, 0, 0, 0, 0, 1, 0)$, etc., the table ending with 28 rows of $(0, 0, 0, 1, 0, 0, 1)$.

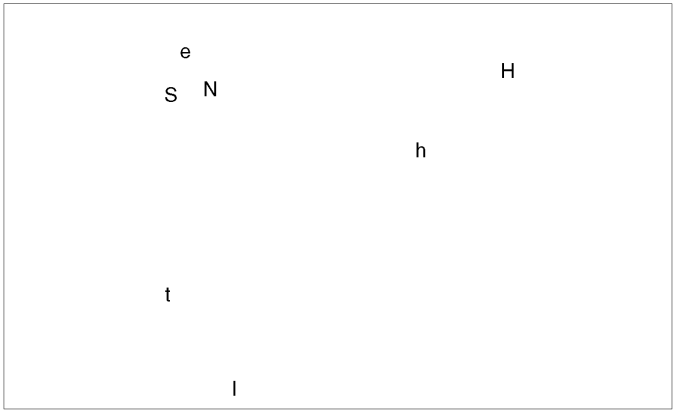

Figure 9.7 *Correspondence analysis of the cancer data represented by an indicator matrix.*

Figure 9.7 shows the correspondence analysis output for the cancer data using the indicator matrix. It can be seen that the positions of the four tumour types and three sites occupy similar positions to those from their previous analysis, noting however that this time the two axes have not been scaled by their respective singular values.

The eigenvalues of the two methods, i.e. the first using the usual correspondence analysis technique, and the second making use of an indicator matrix, are related by

$$\rho = (2\rho_I - 1)^2,$$

where ρ is an eigenvalue based on the original data matrix, and ρ_I an eigenvalue based on the indicator matrix. See Greenacre (1984) for further details.

Table 9.2 *Infant losses in relation to birth order and problem children. P – problem, C – controls.*

Numbers of mothers with	Birth order 2		3–4		5+	
	P	C	P	C	P	C
Losses	20	10	26	16	27	14
None	82	54	41	30	22	23

For a k-way contingency table, the indicator matrix can be written $\mathbf{Z} = [\mathbf{Z}_1, \ldots, \mathbf{Z}_k]$ where $\mathbf{Z}_i$ is an $n \times c_i$ matrix containing the c_i indicator variables for the ith way of the table. The matrix $B = \mathbf{Z}^T\mathbf{Z}$ is called the Burt matrix and contains the submatrices $\mathbf{Z}_i^T\mathbf{Z}_j$, the two-way contingency tables based on the ith and jth variables. Thus

$$\mathbf{B} = \begin{bmatrix} \mathbf{Z}_1^T\mathbf{Z}_1 & \mathbf{Z}_1^T\mathbf{Z}_2 & \ldots & \mathbf{Z}_1^T\mathbf{Z}_k \\ \mathbf{Z}_2^T\mathbf{Z}_1 & \mathbf{Z}_2^T\mathbf{Z}_2 & \ldots & \mathbf{Z}_2^T\mathbf{Z}_k \\ \vdots & \vdots & \ddots & \vdots \\ \mathbf{Z}_k^T\mathbf{Z}_1 & \mathbf{Z}_k^T\mathbf{Z}_2 & \ldots & \mathbf{Z}_k^T\mathbf{Z}_k \end{bmatrix}.$$

The submatrices $\mathbf{Z}_i^T\mathbf{Z}_i$ on the diagonal are simply diagonal matrices of column sums.

9.5.1 A three-way example

The three-way data in Table 9.2 are taken from Plackett (1981) and relate infant losses (e.g. stillbirths) for mothers to birth order and to whether there is a problem child in the family. A Burt matrix was found from the data which was then subjected to multiple correspondence analysis. Results are shown in Figure 9.8. Plackett's analysis indicated that only birth order affects the infant losses. This is confirmed in Figure 9.8 since the "problem/control axis" is nearly perpendicular to the "losses/none axis" with no pair of points being close. The "birth order axis" 2/3–4/5+ is more aligned with the losses/none axis indicating a relationship between these two, although this relationship would have appeared stronger if the "5+" had been closer to "losses".

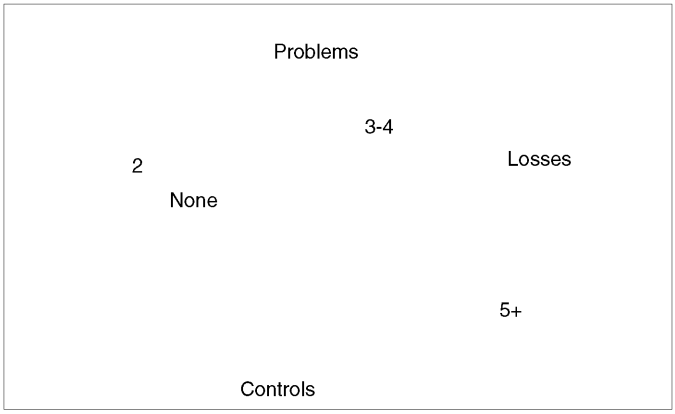

Figure 9.8 *Correspondence analysis of the three-way infant loss data*

For a comprehensive introduction to correspondence analysis, see Benzécri (1992). Some more recent articles on the subject are Tenenhaus and Young (1985), Greenacre and Hastie (1987), Choulakian (1988), Greenacre (1988), de Leeuw and van der Heijden (1988), Gower (1990). For correspondence analysis linked to log-linear models, see van der Heijden and de Leeuw (1985), van der Heijden and Worsley (1988), van der Heijden *et al.* (1989) and van der Heijden and Meijerink (1989). Bénasséni (1993) considers some perturbational aspects in correspondence analysis. Gilula and Ritov (1990), Pack and Jolliffe (1992) and Krzanowski (1993) consider some inferential aspects of correspondence analysis.

CHAPTER 10

Individual differences models

10.1 Introduction

Data analysed so far have generally been two-way, one- or two-mode data. This chapter investigates models for three-way, two-mode data, in particular for dissimilarities $\delta_{rs,i}$ where the suffices r and s refer to one set of objects and i to another. For example, N judges might each be asked their opinions on n objects or stimuli, from which N separate dissimilarity matrices are derived. The (r,s)th element of the ith dissimilarity matrix would be $\delta_{rs,i}$. Another example might be the production of a dissimilarity matrix each year for schools in a certain region, based on exam results. Then r and s refer to the rth and sth schools, and i is a time index. Individual differences modelling attempts to analyse such data taking into account the two different modes. For convenience, the suffix i will refer to "individuals" rather than any other objects, such as points in time. The whisky tasting experiment discussed in Chapter 1 is another example with a dissimilarity matrix produced for each of the N judges.

There were two basic approaches in the early work in this area. The first was to average over individuals, the second to compare results individual by individual. For example, metric or nonmetric MDS could be used on the dissimilarity matrix obtained by averaging dissimilarities over i, or alternatively by carrying out an analysis for each individual and then attempting a comparison.

10.2 The Tucker-Messick model

Tucker and Messick (1963) addressed the problems with the two early approaches to individual differences scaling, namely that averaging over individuals loses much information regarding the individual responses, and that comparing several different scalings can be a very difficult task. Tucker and Messick (see also Cliff, 1968) suggested placing the dissimilarities $\{\delta_{rs,i}\}$ into a matrix,

$\mathbf{X}$, with rows given by all the $\frac{1}{2}n(n-1)$ possible stimulus-pairs and columns given by the N individuals. Essentially, the singular valued decomposition (SVD) of $\mathbf{X}$ is then found,

$$\mathbf{X} = \mathbf{U}\boldsymbol{\Lambda}\mathbf{V}^T$$

and then the p dimensional least squares approximation to $\mathbf{X}$,

$$\hat{\mathbf{X}}_p = \mathbf{U}_p\boldsymbol{\Lambda}_p\mathbf{V}_p^T.$$

The matrix $\mathbf{U}_p$ gives the principal coordinates in a space for the pairs of stimuli, the matrix $\boldsymbol{\Lambda}_p\mathbf{V}^T$ gives the principal coordinates in a space for the individuals.

10.3 INDSCAL

Carroll and Chang (1970) proposed a metric model comprising two spaces: a group stimulus space and a subjects (or individuals) space, both of chosen dimension p. Points in the group stimulus space represent the objects or stimuli, and form an "underlying" configuration. The individuals are represented as points in the subjects space. The coordinates of each individual are the weights required to give the weighted Euclidean distances between the points in the stimulus space, the values that best represent the corresponding dissimilarities for that individual. Hence the acronym INDSCAL – INdividual Differences SCALing.

Let the points in the group stimulus space be given by x_{rt} ($r = 1, \ldots, n; t = 1, \ldots, p$). Let the points in the individuals space have coordinates w_{it} ($i = 1, \ldots, N; t = 1, \ldots, p$). Then the weighted Euclidean distance between stimuli r and s, for the ith individual is

$$d_{rs,i} = \left\{ \sum_{t=1}^{p} w_{it}(x_{rt} - x_{st})^2 \right\}^{\frac{1}{2}}.$$

The individual weights $\{w_{it}\}$ and stimuli coordinates $\{x_{rt}\}$ are then sought that best match $\{d_{rs,i}\}$ to $\{\delta_{rs,i}\}$.

10.3.1 The algorithm for solution

As with metric scaling of Chapter 2, dissimilarities $\{\delta_{rs,i}\}$ are converted to distance estimates $\{d_{rs,i}\}$ and then $\{w_{it}\}$, $\{x_{rt}\}$ are found

by least squares. The distances associated with each individual are doubly centred giving matrices $\mathbf{B}_i$, where

$$\begin{aligned}[\mathbf{B}_i]_{rs} = b_{rs,i} &= \sum_{t=1}^{p} w_{it} x_{rt} x_{st} \\ &= -\frac{1}{2}\left(d_{rs,i}^2 - \frac{1}{n}\sum_{r=1}^{N} d_{rs,i}^2 - \frac{1}{n}\sum_{s=1}^{N} d_{rs,i}^2 + \frac{1}{n^2}\sum_{r=1}^{N}\sum_{s=1}^{N} d_{rs,i}^2\right) \\ &= \mathbf{H}\mathbf{A}_i\mathbf{H},\end{aligned}$$

and $[\mathbf{A}_i]_{rs} = a_{rs,i} = -\frac{1}{2}d_{rs,i}^2$. Least squares estimates of $\{w_{it}\}$ and $\{x_{rt}\}$ are then found by minimising

$$S = \sum_{r,s,i}\left(b_{rs,i} - \sum_{t=1}^{p} w_{it} x_{rt} x_{st}\right)^2. \tag{10.1}$$

Carroll and Chang's algorithm uses a recursive least squares approach. Firstly, superscripts L and R (Left and Right) are placed on x_{rt} and x_{st} respectively in equation (10.1) to distinguish two estimates of the coordinates of the points in the group stimulus space, which converge to a common estimate. Thus equation (10.1) is

$$S = \sum_{r,s,i}\left(b_{rs,i} - \sum_{t=1}^{p} w_{it} x_{rt}^L x_{st}^R\right)^2.$$

The quantity S is firstly minimised with respect to $\{w_{it}\}$ for fixed $\{x_{rt}^L\}$, $\{x_{st}^R\}$. This is easily achieved if $\{x_{rt}^L x_{st}^R\}$ forms an $n^2 \times p$ matrix $\mathbf{G}$, where $[\mathbf{G}]_{\alpha t} = x_{rt}^L x_{st}^R$, with $\alpha = n(r-1)+s$, and $\{b_{rs,i}\}$ forms the $N \times n^2$ matrix $\mathbf{F}$ where $[\mathbf{F}]_{i\alpha} = b_{rs,i}$. Let the $N \times p$ matrix $\mathbf{W}$ be given by $[\mathbf{W}]_{it} = w_{it}$. Then the least squares estimate of $\mathbf{W}$ is given by

$$\hat{\mathbf{W}} = \mathbf{F}\mathbf{G}(\mathbf{G}^T\mathbf{G})^{-1}.$$

Next, a least squares estimate of $\{x_{rt}^L\}$ is found for fixed $\{w_{it}\}$, $\{x_{st}^R\}$. Let $\mathbf{G}$ now be the $Nn \times p$ matrix $[\mathbf{G}]_{\alpha t} = w_{it} x_{st}^R$, where now $\alpha = n(i-1)+s$. Let $\mathbf{F}$ be the $n \times Nn$ matrix $[\mathbf{F}]_{\alpha\beta} = b_{rs,i}$ where $\alpha = r$, $\beta = n(i-1)+s$. Let $\mathbf{X}^L$ be the $n \times p$ matrix $[\mathbf{X}^L]_{rt} = x_{rt}^L$. Then the least squares estimate of $\mathbf{X}^L$ for fixed $\{w_{it}\}$, $\{x_{st}^R\}$ is

$$\hat{\mathbf{X}}^L = \mathbf{F}\mathbf{G}(\mathbf{G}^T\mathbf{G})^{-1}.$$

This last step is now repeated interchanging $\{x_{rt}^L\}$ and $\{x_{st}^R\}$ to find the least squares estimate $\mathbf{X}^R$ of $\{x_{st}^R\}$ for fixed $\{w_{it}\}$, $\{x_{rt}^L\}$.

The process is repeated until convergence of $\hat{\mathbf{X}}^L$ and $\hat{\mathbf{X}}^R$. Carroll and Chang point out that $\hat{\mathbf{X}}^L$, $\hat{\mathbf{X}}^R$ converge only up to a diagonal transformation,

$$\mathbf{X}^L = \mathbf{X}^R\mathbf{C}$$

where $\mathbf{C}$ is a $p \times p$ diagonal matrix of non-zero entries. This is because $\sum_{t=1}^{p} w_{it}x_{rt}x_{st}$ can be replaced by $\sum_{t=1}^{p}(w_{it}/c_t)x^L_{rt}(x_{st}c_t)$ in equation (10.1), and hence the minimum sum of squares is not affected by $\{c_t\}$. To overcome this, the final step in the procedure is to set $\hat{\mathbf{X}}^L$ equal to $\hat{\mathbf{X}}^R$ and compute $\hat{\mathbf{W}}$ for a last time.

Notice one property of the INDSCAL model, that the dimensions of the resulting spaces are unique. Configurations cannot be translated or rotated. This implies that the dimensions may possibly be interpreted.

Normalization

Carroll and Chang address two normalization questions. The first is the weighting of the contributions to the analysis by the different individuals. Unless there are specific reasons to do so, they suggest that individuals are weighted equally, which is achieved by normalizing each individual's sum of squared scalar products, $\sum_{r,s} b^2_{rs,i}$. Secondly, the final solution for the stimulus space needs to be normalized since S in equation (10.1) is invariant to dilation of the configuration of points in the stimulus space with a corresponding shrinking in the subject space. Normalization can be carried out by setting the variance of the projections of the points on each axis equal to unity.

10.3.2 Identifying groundwater populations

One of the data sets (number 17) in Andrews and Herzberg (1985), concerns the estimation of the uranium reserves in the United States of America. These data will be subjected to analysis by INDSCAL. The data consist of twelve measurements made on groundwater samples taken at various sites. The variables are:

uranium (U); arsenic (AS); boron (B); barium (BA); molybdenum (MO); selenium (SE); vanadium (V); sulphate (SO4); total alkalinity (T_AK); bircarbonate (BC); conductivity (CT) and pH (PH).

Each groundwater sample was initially classified as coming from one of five rock formations:

Orgallala Formation (TPO); Quartermaster Group (POQ); Whitehorse and Cloud Chief Group (PGWC); El Reno Group and Blaire Formation (PGEB); and Dockum Formation (TRD).

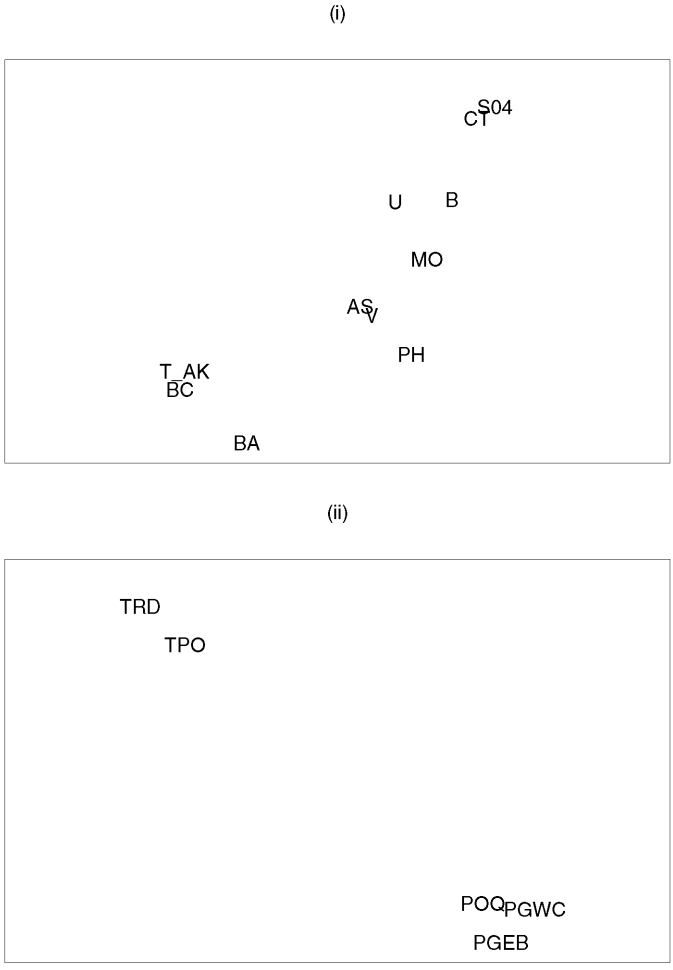

Figure 10.1 *INDSCAL analysis of groundwater samples, (i) group stimulus space, (ii) subject space*

For each of the five classes, the sample correlation matrix was used to give dissimilarities between the variables, using the transformation $\delta_{rs} = (1 - \rho_{rs})^{\frac{1}{2}}$. One variable (SE) was left out of the analysis since, for most samples, it was barely measurable. The five sets of dissimilarities $\{\delta_{rs,i}\}$ were then subjected to analysis by INDSCAL using a two dimensional group stimulus space and subject space.

Figure 10.1(i) shows the group stimulus space for the eleven remaining variables. Interesting groupings are {sulphate (SO4) and conductivity (CT)}, {total alkalinity (T_AK), bicarbonate (BC), and barium (BA) }, and {arsenic (AS), vanadium (V), uranium (U), boron (B), molybdenum (MO), and pH (PH)}.

Figure 10.1(ii) shows the subject space, where two groups can be clearly seen, {Ogallala Formation (TPO) and Dockum Formation (TRD)} and {Quartermaster Group (POQ), Whitehorse and Cloud Chief Group (PGWC) and El Reno Group and Blaire Formation (PGEB)}. The first group tends to shrink the group stimulus space along the first dimension and stretch it along the second. The second group does the opposite.

10.3.3 Extended INDSCAL models

MacCallum (1976a) carried out a Monte Carlo investigation of INDSCAL, where, for the ith individual, the angle between the axes in the group stimulus space was changed from 90° to θ_i, representing an error term. See also, MacCallum (1977a,b, 1979). He concluded that INDSCAL was susceptible to the assumption that individuals perceive the dimensions of the group stimulus space to be orthogonal. IDIOSCAL, a generalization of INDSCAL, can overcome this problem.

Winsberg and Carroll (1989a,b) extend the INDSCAL model to

$$d_{rs,i} = \left\{ \sum_{t=1}^{p} w_{it}(x_{rt} - x_{st})^2 + u_i(s_r + s_s) \right\}^{\frac{1}{2}},$$

where s_r is the "specificity" of the rth stimulus and u_i is the propensity of the ith individual towards specificities. The specificity for a stimulus can be thought of as a dimension solely for that stimulus. They use a maximum likelihood approach to fit the model.

Winsberg and De Soete (1993) adapt INDSCAL and assume

the N individuals each belong to a latent class or subpopulation. The probability that an individual belongs to latent class l is p_l $(1 \leq l \leq L)$. For those individuals in latent class l, their dissimilarities $\{\delta_{rs,i}\}$ are assumed to follow a common multivariate normal distribution. The coordinates of the points in the group stimulus space and the weights in the subject space are then found by maximum likelihood. They call their model CLASCAL.

10.4 IDIOSCAL

Carroll and Chang (1972) generalized their INDSCAL model to the IDIOSCAL model (Individual DIfferences in Orientation SCALing). They used the weighted Euclidean distance between stimuli r and s, for individual i

$$d_{rs,i} = \left\{ \sum_{t=1}^{p} \sum_{t'=1}^{p} (x_{rt} - x_{st}) w_{tt',i} (x_{rt'} - x_{st'}) \right\}^{\frac{1}{2}}.$$

Here $\mathbf{W}_i$ is a symmetric positive definite or semi-definite matrix of weights, $[\mathbf{W}_i]_{tt'} = w_{tt',i}$.

It is easily seen that

$$b_{rs,i} = \sum_{t} \sum_{t'} x_{rt} w_{tt',i} x_{st'},$$

and

$$\mathbf{B}_i = \mathbf{X}\mathbf{W}_i\mathbf{X}^T.$$

The IDIOSCAL model thus allows the group stimulus space to be manipulated to a further degree by individuals than the INDSCAL model, with various rotations and dilations of axes being allowed. Carroll and Wish (1974) give a good account of models which arise from IDIOSCAL using a suitable choice of $\mathbf{W}_i$. A summary of these models is given.

INDSCAL
When $\mathbf{W}_i$ is restricted to being a diagonal matrix, IDIOSCAL reduces to INDSCAL.

Carroll-Chang decomposition of $\mathbf{W}_i$
The spectral decomposition of $\mathbf{W}_i$ is used as an aid to interpretation. Thus

$$\mathbf{W}_i = \mathbf{U}_i \boldsymbol{\Lambda}_i \mathbf{U}_i^T,$$

where $\mathbf{U}_i\mathbf{U}_i^T = \mathbf{I}$, $\boldsymbol{\Lambda} = \text{diag}(\lambda_{ij})$, $(j = 1, \ldots, p)$, and

$$\begin{aligned}\mathbf{B}_i &= \mathbf{X}\mathbf{U}_i\boldsymbol{\Lambda}_i\mathbf{U}_i^T\mathbf{X}^T \\ &= (\mathbf{X}\mathbf{U}_i\boldsymbol{\Lambda}_i^{\frac{1}{2}})(\mathbf{X}\mathbf{U}_i\boldsymbol{\Lambda}_i^{\frac{1}{2}})^T,\end{aligned}$$

which gives the interpretation of the ith individual's configuration as an orthogonal rotation, $\mathbf{U}_i$, of the group stimulus space, followed by a rescaling of the axes by $\lambda_{ij}^{\frac{1}{2}}$. Unfortunately, the orthogonal transformation is not unique, since for any orthogonal matrix $\mathbf{V}$,

$$(\mathbf{U}_i\boldsymbol{\Lambda}_i^{\frac{1}{2}}\mathbf{V})(\mathbf{U}_i\boldsymbol{\Lambda}_i^{\frac{1}{2}}\mathbf{V})^T = (\mathbf{U}_i\boldsymbol{\Lambda}_i\mathbf{U}_i) = \mathbf{W}_i.$$

Tucker-Harshman decomposition of $\mathbf{W}_i$
Tucker (1972) and Harshman (1972) suggested the decomposition

$$\mathbf{W}_i = \mathbf{D}_i\mathbf{R}_i\mathbf{D}_i,$$

where $\mathbf{D}_i$ is a diagonal matrix, and $\mathbf{R}_i$ is a symmetric matrix with diagonal elements all equal to unity. The matrix $\mathbf{R}_i$ can be interpreted as a "correlation" matrix and $\mathbf{D}_i$ as a diagonal matrix of "standard deviations". If $\mathbf{R}_i = \mathbf{R}$ $(i = 1, \ldots, N)$ then the model reduces to Harshman's PARAFAC-2 model.

Tucker's 3-mode scaling
Tucker (1972) suggested a model for individual differences based on three-mode factor analysis (Tucker, 1966). See also MacCallum (1976a,b). The model is the IDIOSCAL model with the weight matrix, $\mathbf{W}_i$ decomposed by a set of $p \times p$ "core" matrices, $\{\mathbf{G}_m\}$.

Let the subjects space have p' dimensions possibly different from p. Let the coordinates for the individuals in this space be given by the matrix $\mathbf{Z} = [z_{rm}]$. Then the weight matrix is modelled by

$$W_i = \sum_{m=1}^{p'} \mathbf{G}_m z_{mr}$$

If all the $\mathbf{G}_m$ matrices were diagonal then an INDSCAL type solution would follow. MacCallum (1976b) develops a technique to transform $\{\mathbf{G}_m\}$ to be diagonal as "nearly as possible".

10.5 PINDIS

The PINDIS model (Procrustean INdividual DIfferences Scaling) was developed along the lines of the older methods of individual

differences scaling where scaling for each individual is carried out separately and then an overall comparison made. The model was developed after INDSCAL, but has not proved so popular. Relevant references are Borg (1977), Lingoes and Borg (1976, 1977, 1978).

PINDIS assumes that a scaling has been carried out for each individual by some method producing a configuration matrix $\mathbf{X}_i$ in each case. The actual scaling method is immaterial as far as PINDIS is concerned. The configurations $\mathbf{X}_i$ are then compared using Procrustes analysis. First, a centroid configuration, $\mathbf{Z}$, is established in a similar manner to that suggested by Gower (1975) (see Chapter 5) and then a hierarchy of translation, rotation and dilation models are applied to the configurations $\mathbf{X}_i$, to transform them individually, as best as possible, to the centroid configuration. The Procrustes statistic is used as an indication of the appropriate type of translation, rotation and dilation. The centroid configuration then represents the group stimulus space and the rotations etc. for the individuals represent the subjects space.

Firstly, all the N configurations $\mathbf{X}_i$ are centred at the origin and then dilated to have mean squared distance to the origin equal to unity, i.e. $\mathrm{tr}(\mathbf{X}_i^T\mathbf{X}_i) = 1$. The $\mathbf{X}_2$ configuration is rotated to the $\mathbf{X}_1$ configuration giving the first estimate of $\mathbf{Z}$ as $\frac{1}{2}(\mathbf{X}_1 + \mathbf{X}_2)$. Next $\mathbf{X}_3$ is rotated to $\mathbf{Z}$ and then a weighted average of $\mathbf{Z}$ and $\mathbf{X}_3$ gives the next estimate of $\mathbf{Z}$. This process is repeated until all the $\mathbf{X}_i$ configurations have been used.

Next the N configurations are each rotated to $\mathbf{Z}$ and a goodness of fit index calculated as

$$h = \frac{1}{N}\sum_i (1 - R_i^2(\mathbf{X}_i, \mathbf{Z}))^{\frac{1}{2}},$$

where $R(\mathbf{X}_i, \mathbf{Z})^2$ is the Procrustes statistic when $\mathbf{X}_i$ is rotated to $\mathbf{Z}$.

The average of the newly rotated $\mathbf{X}_i$ configurations gives the next updated estimate of the centroid $\mathbf{Z}$, and the goodness of fit index is recalculated. This procedure is repeated until h converges. The resulting $\mathbf{Z}$ is the centroid configuration.

The procedure so far has given the basic model. The centroid configuration $\mathbf{Z}$ is the group stimulus space, and the Procrustes rigid rotations $\mathbf{R}_i$ (rigid but with the possibility of a reflection) needed to rotate the individual configurations $\mathbf{X}_i$ to the centroid $\mathbf{Z}$ from the subject space. The rigidity of the rotations is now relaxed

and various models tried. The hierarchy of models is as follows, starting with the basic model.

1. Basic model: Rigid rotations only. The quantity

$$R_1(\mathbf{R}_i, \mathbf{Z}) = \sum_i \mathrm{tr}(\mathbf{X}_i\mathbf{R}_i - \mathbf{Z})^T(\mathbf{X}_i\mathbf{R}_i - \mathbf{Z})$$

is minimised over the set of matrices $\mathbf{X}_1, \ldots, \mathbf{X}_N$.

2. Dimension weighting: The dimensions of the group stimulus space are weighted. The quantity to be minimised is

$$R_2(\mathbf{R}_i, \mathbf{Z}) = \sum_i \mathrm{tr}(\mathbf{X}_i\mathbf{R}_i - \mathbf{ZSW})^T(\mathbf{X}_i\mathbf{R}_i - \mathbf{ZSW})$$

where $\mathbf{S}^T\mathbf{S} = \mathbf{I}$, and $\mathbf{W}$ is a diagonal matrix. Here, the centroid configuration $\mathbf{Z}$ is allowed to be rotated by $\mathbf{S}$ before weights are applied to the axes.

3. Idiosyncratic dimension weighting: The weighting of dimensions of the group stimulus space can be different for each individual. The quantity

$$R_3(\mathbf{R}_i, \mathbf{Z}) = \sum_i \mathrm{tr}(\mathbf{X}_i\mathbf{R}_i - \mathbf{ZSW}_i)^T(\mathbf{X}_i\mathbf{R}_i - \mathbf{ZSW}_i)$$

is minimised over $\mathbf{X}_1, \ldots, \mathbf{X}_N$.

4. Vector weighting: Each stimulus in the group stimulus space is allowed to be moved along the line through the origin to the stimulus before rotation occurs. The quantity to be minimised is

$$R_4(\mathbf{R}_i, \mathbf{Z}) = \sum_i \mathrm{tr}(\mathbf{X}_i\mathbf{R}_i - \mathbf{V}_i\mathbf{Z})^T(\mathbf{X}_i\mathbf{R}_i - \mathbf{V}_i\mathbf{Z}).$$

5. Vector weighting, individual origins: This is the same as model 4, except that the origin of $\mathbf{Z}$ for each individual can be moved to an advantageous position. The quantity to be minimised is

$$R_5(\mathbf{R}_i, \mathbf{Z}) = \sum_i \mathrm{tr}(\mathbf{X}_i\mathbf{R}_i - \mathbf{V}_i(\mathbf{Z} - \mathbf{1}\mathbf{t}_i^T))^T(\mathbf{X}_i\mathbf{R}_i - \mathbf{V}_i(\mathbf{Z} - \mathbf{1}\mathbf{t}_i^T))$$

where $\mathbf{t}_i$ is the translation vector for the centroid for the ith individual.

6. Double weighting: This allows both dimensional and vector weighting. The quantity

$$R_6(\mathbf{R}_i, \mathbf{Z}) = \sum_i \mathrm{tr}(\mathbf{X}_i\mathbf{R}_i - \mathbf{V}_i(\mathbf{Z} - \mathbf{1}\mathbf{t}_i^T)\mathbf{W}_i)^T \times (\mathbf{X}_i\mathbf{R}_i - \mathbf{V}_i(\mathbf{Z} - \mathbf{1}\mathbf{t}_i^T)\mathbf{W}_i)$$

is minimised over $\mathbf{X}_1, \ldots, \mathbf{X}_N$.

The models form a hierarchy with the first model always providing the poorest fit and the last model the best. Choice of model is made by assessing the improvement in fit made by going from one model to another in the hierarchy. Langeheine (1982) evaluated the measures of fit for the various models.

CHAPTER 11

ALSCAL, SMACOF and Gifi

In this chapter, three significant developments in multidimensional scaling are discussed. Firstly, ALSCAL and SMACOF, both of which are alternatives to the previously discussed gradient methods of the minimisation of stress. The third is the relationship to multidimensional scaling, of the Gifi system of nonlinear multivariate analysis together with a generalization.

11.1 ALSCAL

Takane, Young and de Leeuw (1977) developed ALSCAL (Alternating Least squares SCALing) along with other uses of the alternating least squares technique (see Young, de Leeuw and Takane (1976), and de Leeuw, Young and Takane (1976)). The attraction of ALSCAL is that it can analyse data that are: (i) nominal, ordinal, interval, or ratio; (ii) complete or have missing observations; (iii) symmetric or asymmetric; (iv) conditional or unconditional; (v) replicated or unreplicated; (vi) continuous or discrete – a Pandora's box!

An outline to the theory of ALSCAL is given, following Takane *et al.* (1977).

11.1.1 The theory

As for INDSCAL of Chapter 10, assume dissimilarity data $\{\delta_{rs,i}\}$ which can be any of the types (i)-(vi) above. The scaling problem can be stated as the search for a mapping ϕ, of the dissimilarities $\{\delta_{rs,i}\}$, giving rise to a set of disparities $\{\hat{d}_{rs,i}\}$,

$$\phi[\delta^2_{rs,i}] = \hat{d}^2_{rs,i},$$

where $\{\hat{d}^2_{rs,i}\}$ are least squares estimates of $\{d^2_{rs,i}\}$ obtained by

minimising the loss function called SSTRESS and denoted by SS, where

$$SS = \sum_r \sum_s \sum_i (d^2_{rs,i} - \hat{d}^2_{rs,i})^2. \tag{11.1}$$

Note that SSTRESS differs from STRESS in that it uses squared distances and disparities. This is done for algorithmic convenience.

The mapping ϕ has to take into account the restrictions that occur in the particular model and type of data. There are three types of restriction: process restrictions, level restrictions and conditionality restrictions.

Process restrictions

One process restriction is used for discrete data, another for continuous data. For discrete data, observations within a particular category should be represented by the same real number under the mapping ϕ. Following Takane *et al.*, let $\sim$ represent membership of the same category. So for discrete data

$$\phi: \quad \delta_{rs,i} \sim \delta_{r's',i'} \quad \Rightarrow \quad \hat{d}_{rs,i} = \hat{d}_{r's',i'}.$$

Continuous data have to be discretized, so as to make the data categorical: for example, an observation of 3.7 could be considered to be in the category of all those values in the interval [3.65, 3.75). The continuous restriction is then represented by

$$\phi: \quad \delta_{rs,i} \sim \delta_{r's',i'} \quad \Rightarrow \quad l \leq \hat{d}_{rs,i}, \hat{d}_{r's',i'} \leq u,$$

where $[l, u)$ is a real interval.

Level constraints

Different constraints on ϕ are needed for the type of data being analysed. For nominal data, no constraint is necessary once the process restraint has been taken into consideration. For ordinal data, the obvious constraint on ϕ is

$$\phi: \delta_{rs,i} \prec \delta_{r's',i} \quad \Rightarrow \hat{d}_{rs,i} \leq \hat{d}_{r's',i'}.$$

For quantitative data, $\hat{d}_{rs,i}$ is linearly related to $\delta_{rs,i}$, so that

$$\phi: \quad \hat{d}_{rs,i} = a_0 + a_1 \delta_{rs,i},$$

with $a_0 = 0$ for ratio data. Linearity can possibly be replaced by a polynomial relationship.

Conditionality constraints
Different experimental situations give rise to different conditions on the dissimilarities. If measurements made by different individuals are all comparable giving the unconditional case, then no constraints on ϕ are needed. If observations by different individuals are not comparable, then matrix conditionality is imposed where all dissimilarities within the matrix of dissimilarities for an individual are comparable, but not between matrices. This implies that ϕ is composed of N mappings $\{\phi_i\}$, one for each individual. Similarly, row conditionality gives rise to mappings $\{\phi_{ri}\}$. Here dissimilarities along a row of a matrix are comparable, but not between rows. For example, N judges may score the taste of p different whiskies.

11.1.2 Minimising SSTRESS

SSTRESS in (11.1) is minimised using an alternating least squares algorithm. Each iteration of the algorithm has two phases: an optimal scaling phase and a model estimation phase. Writing SSTRESS as $SS(\mathbf{X}, \mathbf{W}, \hat{D})$, where $\mathbf{X}$ is the matrix of coordinates, $\mathbf{W}$ is the matrix of weights, and $\hat{D}$ represents the disparities $\{\hat{d}_{rs,i}\}$, then the optimal scaling phase finds the least squares disparities $\hat{D}$ for fixed $\mathbf{X}$ and $\mathbf{W}$, which is followed by the model estimation phase which calculates new coordinates $\mathbf{X}$ and weights $\mathbf{W}$ for fixed $\hat{D}$.

The optimal scaling phase
Firstly, the distances $\{d_{rs,i}\}$ are calculated from current coordinate and weight matrices $\mathbf{X}, \mathbf{W}$. Then disparities $\{\hat{d}_{rs,i}\}$ are calculated. Conveniently, if all the disparities are placed in a vector $\hat{\mathbf{d}}$, and similarly the distances placed in vector $\mathbf{d}$, then

$$\hat{\mathbf{d}} = \mathbf{E}\mathbf{d},$$

where $\mathbf{E} = \mathbf{Z}(\mathbf{Z}^T\mathbf{Z})^{-1}\mathbf{Z}^T$, with $\mathbf{Z}$ depending on the type of transformation ϕ.

For ratio and interval data $\mathbf{Z}$ is a vector of squared dissimilarities $\{d^2_{rs,i}\}$ (placed conveniently into the vector). This can easily be seen by replacing $\hat{d}^2_{rs,i}$ in the SSTRESS equation (11.1) by $a+b\delta^2_{rs,i}$ and finding the least squares estimates of a and b.

For ordinal and nominal level data, $\mathbf{Z}$ is a matrix of dummy variables indicating which distances must be tied to satisfy the

measurement conditions. For example, with dissimilarities and distances given by

$$\delta_1^2 = 1.2 \quad \delta_2^2 = 1.7 \quad \delta_3^2 = 2.4 \quad \delta_4^2 = 3.2 \quad \delta_5^2 = 3.6$$

$$d_1^2 = 3.8 \quad d_2^2 = 4.6 \quad d_3^2 = 4.2 \quad d_4^2 = 5.4 \quad d_5^2 = 5.0,$$

for the ordinal transformation, least squares monotone regression will have $\hat{d}_2^2 = \hat{d}_3^2$, $\hat{d}_4^2 = \hat{d}_5^2$, giving

$$\mathbf{Z} = \begin{bmatrix} 1 & 0 & 0 \\ 0 & 1 & 0 \\ 0 & 1 & 0 \\ 0 & 0 & 1 \\ 0 & 0 & 1 \end{bmatrix}$$

and

$$\mathbf{Z}(\mathbf{Z}^T\mathbf{Z})^{-1}\mathbf{Z}^T = \begin{bmatrix} 1 & 0 & 0 & 0 & 0 \\ 0 & \frac{1}{2} & \frac{1}{2} & 0 & 0 \\ 0 & \frac{1}{2} & \frac{1}{2} & 0 & 0 \\ 0 & 0 & 0 & \frac{1}{2} & \frac{1}{2} \\ 0 & 0 & 0 & \frac{1}{2} & \frac{1}{2} \end{bmatrix}.$$

SSTRESS can now be written as

$$SS = \mathbf{d}^T(\mathbf{I} - \mathbf{E})\mathbf{d}$$

and normalized SSTRESS as

$$SS = \mathbf{d}^T(\mathbf{I} - \mathbf{E})\mathbf{d}/\mathbf{d}^T\mathbf{d}.$$

The last step in the optimal scaling phase is to normalize the solution, firstly with respect to the configuration and weights and other parameters, and secondly with regard to SSTRESS.

Model estimation phase

The model estimation phase finds the least squares estimates of the weight matrix, $\mathbf{W}$, for the current disparity values $\{\hat{d}_{rs,i}\}$ and coordinates $\mathbf{X}$ of the points in the group stimulus space. Then the least squares estimates of $\mathbf{X}$ are found for the current disparity values and weights $\mathbf{W}$.

For the first minimisation let the $\frac{1}{2}n(n-1)$ quantities $(x_{rt} - x_{st})^2$ make up the tth column $(t = 1, \ldots, p)$ of a matrix $\mathbf{Y}$. A similar

$\frac{1}{2}n(n-1) \times p$ matrix $\mathbf{D}^\star$ is composed of the disparities $\{\delta^2_{rs,i}\}$. Then SSTRESS can be written

$$SS = \text{tr}(\mathbf{D}^\star - \mathbf{W}\mathbf{Y}^T)^T(\mathbf{D}^\star - \mathbf{W}\mathbf{Y}^T)$$

and hence

$$\mathbf{W} = \mathbf{D}^\star\mathbf{Y}(\mathbf{Y}^T\mathbf{Y})^{-1}.$$

There can be a problem with negative estimated weights. Takane *et al.* show how these can be appropriately adjusted.

For the second minimisation the SSTRESS in (11.1) now has to be minimised with respect to the coordinates $\mathbf{X}$. Setting partial derivatives equal to zero gives rise to a series of cubic equations which can be solved using Newton-Raphson, possibly modified. The reader is referred to Takane et al. for further details.

In summary, the ALSCAL algorithm is as follows:

1. Find an initial configuration $\mathbf{X}$ and weights $\mathbf{W}$.
2. Optimal scaling phase: calculate D, $D^\star$ and normalize.
3. Terminate if SSTRESS has converged.
4. Model estimation phase: minimise $SS(\mathbf{W}|\mathbf{X}, D^\star)$ over $\mathbf{W}$; then minimise $SS(\mathbf{X}|\mathbf{W}, D^\star)$ over $\mathbf{X}$.
5. Go to step 2.

Details of further points relating to ALSCAL and reports on some Monte Carlo testing of the technique can be found in MacCallum (1977a, 1977b, 1978), MacCallum and Cornelius III (1977), Young and Null (1978), Young *et al.* (1978), Verhelst (1981) and ten Berge (1983).

To reiterate, the attraction of ALSCAL is that it is very versatile and can perform metric scaling, nonmetric scaling, multidimensional unfolding, individual differences scaling and other techniques. ALSCAL is available in the statistical computer packages SAS and SPSS.

11.2 SMACOF

As an alternative to the alternating least squares method for minimising SSTRESS, a method based on the majorization algorithm was initially proposed by de Leeuw (1977b). The method was then further refined and explored by de Leeuw and Heiser (1977, 1980), de Leeuw (1988), Heiser (1991), de Leeuw (1992) and Groenen (1993), and now has the acronym SMACOF, which stands for

Scaling by MAjorizing a COmplicated Function. Before describing SMACOF, the majorizing algorithm is briefly described. The following relies heavily on Groenen (1993).

11.2.1 The majorization algorithm

The majorization algorithm attempts to minimise a complicated function, $f(x)$, by use of a more manageable auxiliary function $g(x, y)$. The auxiliary function has to be chosen such that for each x in the domain of f

$$f(x) \leq g(x, y),$$

for a particular y in the domain of g, and also so that

$$f(y) = g(y, y).$$

So for graphs of f and g, the function g is always above the function f, and g touches f at the point $x = y$. The function g is then a majorizing function of f. This leads to an iterative scheme to minimise f. First, an initial value x_0 is used to start the minimisation. This then defines the appropriate majorizing function $g(x, x_0)$. This is minimised with its minimum at x_1 say. This value of x then defines the majorizing function $g(x, x_1)$. This, in turn, is minimised with minimum at x_2. The process is repeated until convergence.

An example
As an example of the majorizing algorithm, consider minimising the function, f, where

$$\begin{aligned} f &: [-1.5, 2.0] \longrightarrow R \\ f &: x \longmapsto 6 + 3x + 10x^2 - 2x^4. \end{aligned}$$

A graph of this function can be seen in Figure 11.1 as the solid line.

A majorizing function, g, is chosen as

$$g : \longmapsto 6 + 3x + 10x^2 - 8xy^2 + 6y^4.$$

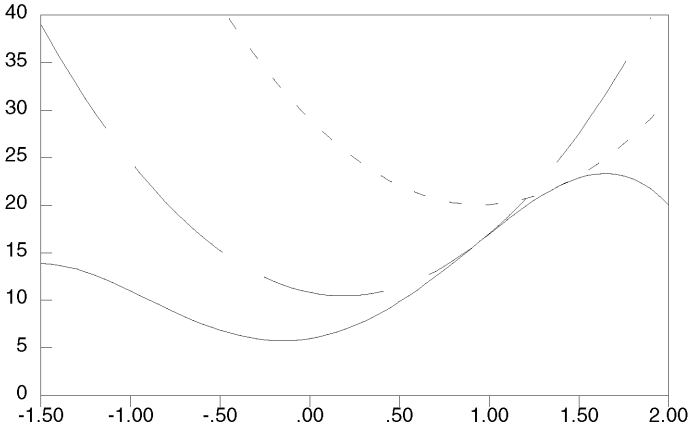

Figure 11.1 *Minimising the function* $f(x) = 6 + 3x + 10x^2 - 2x^4$ *using the majorizing function* $g(x, y) = 6 + 3x + 10x^2 - 8xy^3 + 6y^4$. *Solid line,* f*; short dashed line,* $g(x, 1.4)$*; long dashed line,* $g(x, 0.948)$.

The starting value for the algorithm is set at $x_0 = 1.4$, giving

$$g(x, 1.4) = 29.0496 - 18.952x + 10x^2,$$

a graph of which is shown in Figure 11.1 as the short dashed line. The mimimum of this quadratic function is easily found as $x = 0.948$. Hence $x_1 = 0.948$. The next iteration gives

$$g(x, 0.948) = 10.8460 - 3.7942x + 10x^2.$$

The graph of this function is shown as the long dashed line in Figure 11.1. The minimum of this function gives x_2, and the process continues until convergence at the minimum of f.

For metric MDS, consider the loss function which will be called stress as

$$S = \sum_{r<s} w_{rs}(\delta_{rs} - d_{rs})^2, \tag{11.2}$$

where, as usual, $\{w_{rs}\}$ are weights, $\{\delta_{rs}\}$ are dissimilarities and

$\{d_{rs}\}$ are Euclidean distances calculated from coordinates $\mathbf{X}$. Following Groenen (1993)

$$\begin{aligned} S &= \sum_{r<s} w_{rs}\delta_{rs}^2 + \sum_{r<s} w_{rs} d_{rs}^2(\mathbf{X}) - 2\sum_{r<s} w_{rs}\delta_{rs} d_{rs}(\mathbf{X}) \\ &= \eta_\delta^2 + \eta^2(\mathbf{X}) - 2\rho(\mathbf{X}). \end{aligned}$$

The stress S is now written in matrix form. Firstly,

$$\eta^2(\mathbf{X}) = \sum_{r<s} w_{rs}(\mathbf{x}_r - \mathbf{x}_s)^T(\mathbf{x}_r - \mathbf{x}_s) = \mathrm{tr}(\mathbf{X}^T\mathbf{V}\mathbf{X}),$$

where

$$[\mathbf{V}]_{rr} = \sum_{r\neq s} w_{rs} \qquad [\mathbf{V}]_{rs} = -w_{rs} \quad (r \neq s).$$

Next

$$\begin{aligned} \rho(\mathbf{X}) &= \sum_{r<s} \frac{w_{rs}\delta_{rs}}{d_{rs}} d_{rs}^2 \\ &= \sum_{r<s} \frac{w_{rs}\delta_{rs}}{d_{rs}} (\mathbf{x}_r - \mathbf{x}_s)^T(\mathbf{x}_r - \mathbf{x}_s) \\ &= \mathrm{tr}(\mathbf{X}^T\mathbf{B}(\mathbf{X})\mathbf{X}), \end{aligned}$$

where

$$\begin{aligned} [\mathbf{B}(\mathbf{X})]_{rs} &= w_{rs}\delta_{rs}/d_{rs}(\mathbf{X}) \quad \text{if } d_{rs}(\mathbf{X}) \neq 0, \\ &= 0 \quad \text{if } d_{rs}(\mathbf{X}) = 0. \end{aligned}$$

Then write stress as

$$S(\mathbf{X}) = \eta_\delta^2 + \mathrm{tr}(\mathbf{X}^T\mathbf{V}\mathbf{X}) - 2\mathrm{tr}(\mathbf{X}^T\mathbf{B}(\mathbf{X})\mathbf{X}).$$

A majorizing function, T, for stress S is given by

$$T(\mathbf{X}, \mathbf{Y}) = \eta_\delta^2 + \mathrm{tr}(\mathbf{X}^T\mathbf{V}\mathbf{X}) - 2\mathrm{tr}(\mathbf{X}^T\mathbf{B}(\mathbf{Y})\mathbf{Y}).$$

To show that T does majorize S,

$$\tfrac{1}{2}(T - S) = \rho(\mathbf{X}) - \tilde{\rho}(\mathbf{X}, \mathbf{Y}),$$

where

$$\tilde{\rho}(\mathbf{X}, \mathbf{Y}) = \mathrm{tr}(\mathbf{X}^T\mathbf{B}(\mathbf{Y})\mathbf{Y}).$$

Now

$$\begin{aligned}\rho(\mathbf{X}) &= \sum_{r<s} w_{rs}\delta_{rs}\{(\mathbf{x}_r - \mathbf{x}_s)^T(\mathbf{x}_r - \mathbf{x}_s)\}^{\frac{1}{2}} \\ &= \sum_{r<s} \frac{w_{rs}\delta_{rs}}{d_{rs}(\mathbf{Y})}\{(\mathbf{x}_r - \mathbf{x}_s)^T(\mathbf{x}_r - \mathbf{x}_s)(\mathbf{y}_r - \mathbf{y}_s)^T(\mathbf{y}_r - \mathbf{y}_s)\}^{\frac{1}{2}} \\ &\geq \sum_{r<s} \frac{w_{rs}\delta_{rs}}{d_{rs}(\mathbf{Y})}(\mathbf{x}_r - \mathbf{x}_s)^T(\mathbf{y}_r - \mathbf{y}_s) = \tilde{\rho}(\mathbf{X}, \mathbf{Y})\end{aligned}$$

by the Cauchy-Schwarz inequality, and hence $\rho(\mathbf{X}) \geq \tilde{\rho}(\mathbf{X}, \mathbf{Y})$. Also as $T(\mathbf{X}, \mathbf{X}) = S(\mathbf{X})$, T majorizes S.

To minimise T,

$$\frac{\partial T}{\partial \mathbf{Y}} = 2\mathbf{V}\mathbf{X} - 2\mathbf{B}(\mathbf{Y})\mathbf{Y} = \mathbf{0}. \tag{11.3}$$

Now $\mathbf{V}$ has rank $n-1$ since its row sums are all zero, and so the Moore-Penrose inverse is used to solve equation (11.3), giving

$$\mathbf{X} = \mathbf{V}^{+}\mathbf{B}(\mathbf{Y})\mathbf{Y},$$

which is known as the Guttman transform as it appears in Guttman (1968).

Thus, using the majorizing method for finding minimum stress simply has the Guttman transform as its updating equation. The algorithm gives rise to a non-decreasing sequence of stress values, which converge linearly (de Leeuw, 1988). One advantage of the majorizing method over gradient methods is that the sequence of stress values is always non-increasing. However, it shares the same problem of not necessarily finding the global minimum, but can get stuck at a local minimum.

11.2.2 The majorizing method for nonmetric MDS

For nonmetric MDS, the dissimilarities $\{\delta_{rs}\}$ are replaced by disparities $\{\hat{d}_{rs}\}$ in the loss function (11.2), and as with ALSCAL, there are two minimisations to be carried out. In one, the loss function or stress is minimised with respect to the distances $\{d_{rs}\}$, and in the other, it is minimised with respect to the disparities $\{\hat{d}_{rs}\}$. The first minimisation can be by the majorizing algorithm, the second by isotonic regression as discussed in Chapter 3.

11.2.3 Tunnelling for a global minimum

Groenen (1993) reviews methods for searching for global minima, and describes in detail the tunnelling method. Picturesquely, suppose you are at the lowest point of a valley in a mountainous region with only ascent possible in all directions. There is no direction in which you can descend, however you wish to be at a lower height above sea level. To overcome your predicament, you dig horizontal tunnels in various directions through the surrounding mountains until from one tunnel you reach the other side of the mountain and descent is again possible. See also Groenen and Heiser (1996).

The tunnelling method for stress first involves finding a configuration $\mathbf{X}^*$ which has local minimum stress. Then the tunnel is "dug" by finding other configurations with the same stress. The tunnelling function is defined as

$$\tau(\mathbf{X}) = \{S(\mathbf{X}) - S(\mathbf{X}^*)\}^{2\lambda}\left\{1 + \frac{1}{\sum_{rs}(d_{rs}(\mathbf{X}) - d_{rs}(\mathbf{X}^*))^2}\right\},$$

where λ is the pole strength parameter to be fixed, with $0 < \lambda < 1$.

The zero points of $\tau(\mathbf{X})$ then give configurations which have the same stress as that for $\mathbf{X}^*$. The reader is referred to Groenen for details of how these zero points can be found. Once a new configuration is found the stress can then possibly be reduced further and hopefully a global minimum eventually reached.

De Leeuw (1977b) shows how the majorization method can be extended to general Minkowski spaces. Heiser (1991) shows how the method can be adapted to allow for some of the pseudo-distances being negative. The pseudo-distances are the quantities obtained from transformation of the dissimilarities. For example, linear regression used on dissimilarities making them more distance-like could produce some negative pseudo-distances. Taking the method further, de Leeuw and Heiser (1980) show how the majorization method can be generalized to individual differences scaling.

Groenen *et al.* (1995) extend the majorization algorithm for least squares scaling so it can be used with Minkowski distances, $d_{rs} = [\sum_i |x_{ri} - x_{si}|^p]^{1/p}$, for $1 \leq p \leq 2$. For p outside this range algorithms based on the majorization approach are developed.

11.3 Gifi

Albert Gifi is the *nom de plume* of members, past and present, of the Department of Data Theory at the University of Leiden

who devised a system of nonlinear multivariate analysis that extends various techniques, such as principal components analysis and canonical correlation analysis. Their work is recorded in the book, Gifi (1990). It is not the purpose of this monograph to attempt coverage of all multivariate analysis techniques, but it is instructive to attempt a short summary of the Gifi system and its links with multidimensional scaling. The related distance approach to nonlinear multivariate analysis developed by Meulman (1986) which extends the Gifi system will also be briefly described. A summary of these two approaches is also given by Krzanowski and Marriott (1994).

11.3.1 Homogeneity

Underlying the Gifi system is the idea of homogeneity of variables and its maximisation. Let data be collected for n objects on m variables, $Z_1, \ldots, Z_m$. Let vector $\mathbf{z}_i$ $(i = 1, \ldots, m)$ contain the n observations made on the variable Z_i. Then two variables, Z_i and Z_j are homogenous if $\mathbf{z}_i$ and $\mathbf{z}_j$ are equal after any allowable transformations. Allowable transformations might be normalizing to unit length, or scaling by a constant. Let the transformed observations be denoted by $\mathbf{t}_i(\mathbf{z}_i)$.

Suppose the transformed $\mathbf{z}_i$ is compared with an arbitrary observation vector $\mathbf{x}$. Then if $\mathbf{x} \equiv \mathbf{t}_i(\mathbf{z}_i)$, then $\mathbf{z}_i$ is said to be *homogeneous* to $\mathbf{x}$. Otherwise the loss in homogeneity is defined as $(\mathbf{x} - \mathbf{t}_i(\mathbf{z}_i))^T(\mathbf{x} - \mathbf{t}_i(\mathbf{z}_i))$. The overall loss in homogeneity is

$$\sigma^2(\mathbf{x}, \mathbf{t}) = m^{-1} \sum_i (\mathbf{x} - \mathbf{t}_i(\mathbf{z}_i))^T(\mathbf{x} - \mathbf{t}_i(\mathbf{z}_i)).$$

The aim is to maximise homogeneity by minimising $\sigma^2(\mathbf{x}, \mathbf{t})$ with respect to $\mathbf{x}$ and the allowable transformations. To avoid trivial solutions, a normalizing condition usually has to be introduced.

Examples
A simple example is the case where tranformations of $\mathbf{z}_i$ are not allowed. Then

$$\sigma^2(\mathbf{x}) = m^{-1} \sum_i (\mathbf{x} - \mathbf{z}_i)^T(\mathbf{x} - \mathbf{z}_i).$$

Differentiating with respect to $\mathbf{x}$ and equating to $\mathbf{0}$ shows the minimum loss of homogeneity occurs when $\mathbf{x} = m^{-1}\sum_i \mathbf{z}_i = \bar{\mathbf{z}}$, and with minimum value $m^{-1}\sum_i(\bar{\mathbf{z}} - \mathbf{z}_i)^2$.

Now suppose the allowable transformation is that $\mathbf{z}_i$ can be scaled by a factor a_i. Assume also that $\mathbf{z}_i$ has been mean corrected. The loss of homogeneity is now

$$\sigma^2(\mathbf{x}, \mathbf{a}) = m^{-1}\sum_i (\mathbf{x} - a_i\mathbf{z}_i)^T(\mathbf{x} - a_i\mathbf{z}_i),$$

where $\mathbf{a} = (a_1, \ldots, a_m)^T$ and $\mathbf{x}^T\mathbf{x} = c$, a chosen constant to prevent the trivial solution $\mathbf{x} = \mathbf{a} = \mathbf{0}$.

The loss function is now minimised with respect to $\mathbf{x}$ and $\mathbf{a}$. This can be achieved using an alternating least squares algorithm where one step minimises $\sigma^2(\mathbf{x}, \mathbf{a})$ with respect to $\mathbf{x}$ for fixed $\mathbf{a}$ and the other minimises $\sigma^2(\mathbf{x}, \mathbf{a})$ with respect to $\mathbf{a}$ for fixed $\mathbf{x}$. In effect, the procedure is equivalent to finding the first principal component in a principal components analysis (PCA).

To increase dimensionality, let the allowable transformations be multidimensional, so that $\mathbf{z}_i$ is transformed to a matrix of scores $\mathbf{T}_i(\mathbf{z}_i)$. Let $\mathbf{X}$ be an arbitrary observation matrix. The loss of homogeneity is now

$$\sigma^2(\mathbf{X}, \mathbf{T}) = m^{-1}\sum_i \mathrm{tr}(\mathbf{X} - \mathbf{T}_i(\mathbf{z}_i))^T(\mathbf{X} - \mathbf{T}_i(\mathbf{z}_i))$$

which is minimised with respect to $\mathbf{X}$ and the allowable transformations $\mathbf{T}_i$. Gifi (1990) gives a table of variations of the loss functions together with their descriptions. The table is repeated here as Table 11.1.

From the table, it can be seen how the choice of σ^2 leads to nonlinear principal components analysis through the choice of the nonlinear function ϕ_i. The last two entries in the table require further explanation.

HOMALS

The acronym HOMALS stands for HOMogeneity analysis by Alternating Least Squares and is essentially multiple correspondence analysis. The matrix $\mathbf{Z}_i$ is the indicator matrix of variable Z_i (see Chapter 9) and $\mathbf{Y}_i$ is an $n \times q$ matrix of coefficients.

Table 11.1 *The table of loss functions in Gifi (1990)*

Loss function	Description
$\sigma^2(\mathbf{x}) = m^{-1}\sum_i(\mathbf{x}-\mathbf{z}_i)^T(\mathbf{x}-\mathbf{z}_i)$	Just averaging
$\sigma^2(\mathbf{x},\mathbf{a}) = m^{-1}\sum_i(\mathbf{x}-a_i\mathbf{z}_i)^T(\mathbf{x}-a_i\mathbf{z}_i)$	Linear PCA
$\sigma^2(\mathbf{X},\mathbf{A}) = m^{-1}\sum_i \mathrm{tr}(\mathbf{X}-\mathbf{z}_i\mathbf{a}_i^T)^T(\mathbf{X}-\mathbf{z}_i\mathbf{a}_i^T)$	Linear PCA: multiple solutions
$\sigma^2(\mathbf{x},\mathbf{a},\phi) = m^{-1}\sum_i(\mathbf{x}-a_i\phi_i(\mathbf{z}_i))^T(\mathbf{x}-a_i\phi_i(\mathbf{z}_i))$	Nonlinear PCA
$\sigma^2(\mathbf{x},\phi) = m^{-1}\sum_i(\mathbf{x}-\phi_i(\mathbf{z}_i))^T(\mathbf{x}-\phi_i(\mathbf{z}_i))$	Nonlinear PCA: wts. incorporated
$\sigma^2(\mathbf{x},\mathbf{y}) = m^{-1}\sum_i(\mathbf{x}-\mathbf{Z}_i\mathbf{y}_i)^T(\mathbf{x}-\mathbf{Z}_i\mathbf{y}_i)$	HOMALS: single solution
$\sigma^2(\mathbf{X},\mathbf{Y}) = m^{-1}\sum_i \mathrm{tr}(\mathbf{X}-\mathbf{Z}_i\mathbf{Y}_i)^T(\mathbf{X}-\mathbf{Z}_i\mathbf{Y}_i)$	HOMALS: multiple solutions

The loss function

$$\sigma^2(\mathbf{X},\mathbf{Y}) = m^{-1}\sum_i \mathrm{tr}(\mathbf{X}-\mathbf{Z}_i\mathbf{Y}_i)^T(\mathbf{X}-\mathbf{Z}_i\mathbf{Y}_i) \tag{11.3}$$

is minimised with respect to $\mathbf{X}$ and $\mathbf{Y}$ using an alternating least squares algorithm. In order to avoid the trivial solution, the condition $\mathbf{X}^T\mathbf{X} = n\mathbf{I}$ is imposed, and also $\mathbf{1X} = \mathbf{0}$. Details can be found in Gifi (1990) and also Michailidis and de Leeuw (1998).

For fixed $\mathbf{X}$, $\sigma^2(\mathbf{X},\mathbf{Y})$ is minimised by

$$\mathbf{Y}_i = (\mathbf{Z}_i^T\mathbf{Z}_i)^T\mathbf{Z}_i^T\mathbf{X} \ (i = 1,\ldots,m).$$

For fixed $\mathbf{Y}$, $\sigma^2(\mathbf{X},\mathbf{Y})$ is minimised by

$$\mathbf{X} = m^{-1}\sum_i \mathbf{Z}_i\mathbf{Y}_i.$$

However, $\mathbf{X}$ now has to be column centred and orthonormalized so that the two contraints are met.

Gifi (1990) and Michailidis and de Leeuw (1998) show how homogeneity analysis based on the loss function in (11.1) can be viewed as an eigenvalue and singular value decomposition problem. They also show it is also equivalent to correspondence analysis and hence can be viewed as a multidimensional scaling technique using "dissimilarities" as chi-square distances measured between row profiles.

The loss function in 11.1 is used extensively by Gifi (1990) to form a non-linear system of multivariate analysis.

Meulman (1986) extends the ideas of the Gifi system and relates several multivariate analysis techniques to multidimensional scaling. Essentially, data collected for m variables for a set of n objects can be viewed as n points in an m-dimensional "observational" space. A space of low dimension, p, is sought in which to represent these objects – the "representation" space. (This, of course, is not introducing a new idea in this book, as much of multidimensional scaling has this notion.) If a particular multivariate analysis technique, for instance canonical correlation analysis, can be formulated in such a manner that "distances" based on the data are defined between the objects, which are then used to find a configuration of points to represent the objects in representation space, then the technique is equivalent to a multidimensional scaling technique. The overall approach is more general than simply using the data to form Euclidean distances between objects directly, for example, and then using them as dissimilarities in classical scaling or nonmetric scaling. The essential difference is that the approach allows optimal transformations of the data.

Meulman (1986) uses the three types of loss function, STRIFE, STRAIN and STRESS. As before, $\mathbf{X}$ is the $n \times p$ matrix of coordinates representing the objects in representation space. Let $\mathbf{A}$ be the "rotation" matrix of PCA. Let $\mathbf{Q}$ be the matrix of data after it has been transformed, for instance by scaling the columns of $\mathbf{X}$ by varying amounts or a transformation based on splines. As a starting point, consider the formulation of PCA. This can be formulated as the minimisation of the loss function STRIFE,

$$\text{STRIFE}(\mathbf{X}, \mathbf{A}) = \text{tr}(\mathbf{Z} - \mathbf{X}\mathbf{A}^T)^T(\mathbf{Z} - \mathbf{X}\mathbf{A}^T),$$

with respect to $\mathbf{X}$ and $\mathbf{A}$ with the constraints $\mathbf{X}^T\mathbf{X} = \mathbf{I}$ and $\mathbf{A}^T\mathbf{A}$ is diagonal.

Now PCA can be generalized to allow transformation of the data $\mathbf{Z}$ to $\mathbf{Q}$ and so now the loss function is

$$\text{STRIFE}(\mathbf{Q}, \mathbf{X}, \mathbf{A}) = \text{tr}(\mathbf{Q} - \mathbf{X}\mathbf{A}^T)^T(\mathbf{Q} - \mathbf{X}\mathbf{A}^T),$$

and minimisation is with respect to $\mathbf{X}$, $\mathbf{A}$ and the allowable transformations of $\mathbf{Z}$.

Now let $\triangle$ be a distance operator that places Euclidean distances, $\delta(z_r, z_s) = \{(z_r - z_s)^T(z_r - z_s)\}^{1/2}$ (possibly viewed as dissimilarities), between objects r and s in a matrix denoted by

$\triangle(\mathbf{Z})$. Let $\triangle^2(\mathbf{Z})$ denote a corresponding matrix of squared Euclidean distances between the objects. Similarly, let D denote a distance operator for the points in the representation space, with $\mathbf{D}(\mathbf{X})$ a matrix of distances between points and $\mathbf{D}^2(\mathbf{X})$ a matrix of squared distances. PCA using squared distances in place of unsquared distances can be formulated as the minimisation of the STRAIN loss function,

$$\text{STRAIN}(\mathbf{X}) = \text{tr}\{\mathbf{H}(\triangle^2(\mathbf{Z}) - \mathbf{D}^2(\mathbf{X}))^T\mathbf{H}(\triangle^2(\mathbf{Z}) - \mathbf{D}^2(\mathbf{X}))^T\mathbf{H}\},$$

where $\mathbf{H}$ is the centring matrix. (See also ALSCAL) STRAIN is minimised over $\mathbf{X}$. Again, let the data be transformed to $\mathbf{Q}$ with a class of allowable transformations and then the STRAIN loss function becomes

$$\text{STRAIN}(\mathbf{Q}, \mathbf{X}) = \text{tr}\{\mathbf{H}(\triangle^2(\mathbf{Q}) - \mathbf{D}^2(\mathbf{X}))^T\mathbf{H}(\triangle^2(\mathbf{Q}) - \mathbf{D}^2(\mathbf{X}))^T\mathbf{H}\},$$

which is minimised with respect to $\mathbf{X}$ and $\mathbf{Q}$.

Now suppose dissimilarities are formed generally from the original data $\mathbf{Z}$, for example, using the Jaccard coefficient. Let $\triangle^*(\mathbf{Z})$ be the matrix of these dissimilarities. The third loss function is STRESS

$$\text{STRESS}(\mathbf{X}) = \text{tr}(\triangle^*(\mathbf{Z}) - \mathbf{D}(\mathbf{X}))^T(\triangle^*(\mathbf{Z}) - \mathbf{D}(\mathbf{X})).$$

The three loss functions, STRIFE, STRAIN and STRESS, can be modified to allow for groups of variables simply by summing over the groups. These are used for canonical coordinates analysis (the extension of canonical correlation analysis to more than two groups) and other multivariate techniques.

Meulman (1992) extends the use of the STRESS loss function for multivariate analysis techniques viewed from the distance approach. Suppose there are M groups of variables giving rise to data matrices $\mathbf{Z}_J$ $(1 \leq J \leq M)$. These can be transformed to $\mathbf{Q}_J$ with an allowable class of transformations. Additionally, these can be transformed again by the matrices $\mathbf{A}_J$ to $\mathbf{Q}_J\mathbf{A}_J$. The STRESS loss function is now

$$\text{STRESS}(\mathbf{Q}, \mathbf{A}, \mathbf{X}) = M^{-1}\sum_{J=1}^{M} \text{tr}(\triangle(\mathbf{Q}_J\mathbf{A}_J) - \mathbf{D}(\mathbf{X}))^T(\triangle(\mathbf{Q}_J\mathbf{A}_J) - \mathbf{D}(\mathbf{X})).$$

Meulman uses this loss function for several multivariate analysis techniques where choices of $\mathbf{Q}_J$ and $\mathbf{A}_J$ allow modifications and generalizations of these techniques. See also Meulman (1996) and Commandeur *et al.* (1999) for further details.

CHAPTER 12

Further m-mode, n-way models

This chapter gives brief descriptions of some more MDS models appropriate for data of various numbers of modes and ways.

12.1 CANDECOMP, PARAFAC and CANDELINC

CANDECOMP (CANonical DECOMposition) is a generalization of Carroll and Chang's (1970) INDSCAL model. The INDSCAL model, which is two-mode, three-way, is written as

$$b_{rs,i} = \sum_{t=1}^{p} w_{it} x_{rt} x_{st}.$$

This can be generalized to the three-way CANDECOMP model for three-mode, three-way data,

$$z_{rsi} = \sum_{t=1}^{p} w_{it} x_{rt} y_{st}. \tag{12.1}$$

An example of three-mode, three-way data is where N judges of whisky, each rank m liquor qualities for each of n bottles of whisky. The model is fitted to data using a similar algorithm to the INDSCAL model. The least squares loss function for the three-way model can be written as

$$S = \sum_{i=1}^{N} ||\mathbf{Z}_i - \mathbf{X}\mathbf{D}_i\mathbf{Y}^T||^2, \tag{12.2}$$

where $\mathbf{Z}_i$ is the $n \times m$ matrix $[\mathbf{Z}_i]_{rs} = z_{rsi}$, $\mathbf{X}$ is the $n \times p$ matrix giving coordinates for the second mode of the data (bottles of whisky), $\mathbf{Y}$ is the $m \times p$ matrix giving coordinates for the third mode of the data (qualities), and $\mathbf{D}_i$ is a diagonal matrix for the first mode (judges).

The model (12.2) now corresponds to Harshman's (1970) PARAFAC-1 (PARAllel profiles FACtor analysis) model. In Chapter 10

the PARAFAC-2 model was seen as a special case of IDIOSCAL. An alternating least squares algorithm for PARAFAC-2 is given by Kiers (1993). See also ten Berge and Kiers (1996) and Harshman and Lundy (1996).

CANDECOMP can be used for data of more than three modes with equation (12.1) being generalized further to

$$z_{r_1 r_2 \ldots r_m} = \sum_{t=1}^{p} x_{r_1 t}^{(1)} x_{r_2 t}^{(2)} \ldots x_{r_m t}^{(m)}.$$

The CANDECOMP model can be fitted with an iterative algorithm similar to that discussed for INDSCAL in Chapter 10; viz at each step S is minimised with respect to $\mathbf{D}_i$ $(i = 1, \ldots, N)$ for fixed $\mathbf{X}$ and $\mathbf{Y}$, then minimised with respect to $\mathbf{X}$ for fixed $\{\mathbf{D}_i\}$ and $\mathbf{Y}$ and then minimised with respect to $\mathbf{Y}$ for fixed $\{\mathbf{D}_i\}$ and $\mathbf{X}$. For further details, see Carroll and Chang (1970), and Harshman and Lundy (1984a,b). For an efficient algorithm for fitting the three-mode model, see Kiers and Krijnen (1991). Kruskal *et al.* (1989) and Lundy *et al.* (1989) report on degeneracies that can occur with the CANDECOMP model.

Several authors have discussed problems with using the CANDECOMP algorithm for INDSCAL since, for INDSCAL, $\mathbf{X}$ and $\mathbf{Y}$ have to be equivalent in the sense that they have to have equal columns up to scalar multiplication (see ten Berge and Kiers, 1991). Although in practice, the algorithm tends to work satisfactorily, ten Berge *et al.* (1988) used a particular data set to show that $\mathbf{X}$ and $\mathbf{Y}$ might not be equivalent. Also, ten Berge *et al.* (1993) show that negative weights can occur during the execution of the CANDECOMP algorithm, but explain how to overcome this.

Kruskal *et al.* (1989), Harshman and Lundy (1984b) and others consider the preprocessing of data before using CANDECOMP, for instance the removal of means or scaling rows/columns to specified values. ten Berge (1989) gives a summary of some of the problems of preprocessing and considers the use of the Deming-Stephan (1940) iterative method of rescaling the rows/columns to particular values. See also ten Berge and Kiers (1989).

For further references, see Rocci and ten Berge (1994) who consider the rank of symmetric 3-way arrays, Harshman and Lundy (1996) who give a generalization of the CANDECOMP model, and ten Berge and Kiers (1996) who give some uniqueness results for PARAFAC-2.

Carroll *et al.* (1980) introduced CANDELINC (CANonical DEcomposition with LINear Constraints) which is the CANDECOMP model, but incorporating constraints. The model is

$$z_{r_1 r_2 \ldots r_m} = \sum_{t=1}^{p} x_{r_1}^{(1)} x_{r_2}^{(2)} \ldots x_{r_m}^{(m)},$$

as before, but with the constraints

$$\mathbf{X}_i = \mathbf{D}_i \mathbf{T}_i,$$

where $\mathbf{D}_i$ are known design matrices and $\mathbf{T}_i$ are matrices of unknown parameters. The design matrices, for example, can be used when dissimilarities are collected in an experiment according to some experimental design.

12.2 DEDICOM and GIPSCAL

DEDICOM (DEcomposition into DIrectional COMponents) is a model devised by Harshman (1978) for analysing asymmetric data matrices. A one-mode two-way asymmetric $n \times n$ data matrix is decomposed as

$$\mathbf{X} = \mathbf{ARA}^T + \mathbf{N},$$

where $\mathbf{A}$ is an $n \times p$ matrix of weights ($p < n$), $\mathbf{R}$ is a $p \times p$ matrix representing asymmetric relationships among the p dimensions, and $\mathbf{N}$ is an error matrix. The model can be fitted by using an alternating least squares algorithm; see Kiers (1989) and Kiers *et al.* (1990). See Kiers (1993) for three-way DEDICOM and Takane and Kiers (1997) for latent class DEDICOM.

A problem with DEDICOM is that a convenient graphical representation of the results is not possible. Chino (1978, 1990) proposed the GIPSCAL model (Generalized Inner Product SCALing) which modelled the symmetric and skew-symmetric parts of $\mathbf{X}$ simultaneously and lent itself to graphical representation. Kiers and Takane (1994) generalized GIPSCAL to the model

$$\mathbf{X} = \mathbf{AA}^T + \mathbf{ARA}^T + c\mathbf{1}\mathbf{1}^T + \mathbf{E},$$

where $\mathbf{A}$ is an $n \times p$ matrix of coordinates of points representing the objects, c is a constant, $\mathbf{E}$ the error matrix and $\mathbf{R}$ is a block diagonal matrix with 2×2 blocks $\begin{bmatrix} 0 & \delta_l \\ -\delta_l & 0 \end{bmatrix}$, $l = 1, \ldots, [p/2]$. (If p is odd then a zero element is placed in the last position of the

diagonal.) The model can be fitted by an alternating least squares algorithm: see Kiers and Takane (1994) for further details.

12.3 The Tucker models

Kroonenberg (1983) relates models in the previous section to the Tucker (1966) models, under the name of three-mode principal components analysis. See also Kroonenberg (1992, 1994). A brief summary is given.

In Section 2.2.7, the connection between standard principal components analysis and classical scaling was discussed. The link between principal components analysis and the singular value decomposition of the data matrix forms the basis of the extension of principal components to three-way data. The sample covariance $n \times p$ matrix obtained from the mean-corrected data matrix, $\mathbf{X}$, is $(n-1)\mathbf{S} = \mathbf{X}^T\mathbf{X}$. Let the eigenvectors of $\mathbf{X}^T\mathbf{X}$ be $\mathbf{v}_i$ $(i = 1, \ldots, p)$, and placed in matrix $\mathbf{V}$. The component scores and component loadings are then given respectively by $\mathbf{XV}$ and $\mathbf{V}$.

However from Section 1.4.2 $\mathbf{V}$ is one of the orthonormal matrices in the singular value decomposition of $\mathbf{X}$,

$$\mathbf{X} = \mathbf{U}\boldsymbol{\Lambda}\mathbf{V}^T.$$

Thus the component scores are given by

$$\mathbf{XV} = \mathbf{U}\boldsymbol{\Lambda}\mathbf{V}^T\mathbf{V} = \mathbf{U}\boldsymbol{\Lambda}.$$

Hence principal components analysis is equivalent to the singular value decomposition of the data matrix,

$$\begin{aligned} \mathbf{X} &= \mathbf{U}\boldsymbol{\Lambda}\mathbf{V}^T \\ &= (\mathbf{U}\boldsymbol{\Lambda})\mathbf{V}^T \\ &= \text{component scores} \times \text{component loadings}, \end{aligned} \qquad (12.3)$$

and hence is an MDS technique since the component scores from the first few principal components are used to represent the objects or stimuli.

Write the singular value decomposition of $\mathbf{X}$ in (12.3) as

$$x_{ri} = \sum_{a=1}^{q}\sum_{b=1}^{q} u_{ra}v_{ib}\lambda_{ab} \qquad (r = 1, \ldots, n; i = 1, \ldots, p)$$

where $\mathbf{X}$ is of rank q. This gives the form of the generalization to

three- or higher-mode data. The generalization to give three-mode principal components analysis is

$$z_{rst} = \sum_{i=1}^{I}\sum_{j=1}^{J}\sum_{k=1}^{K} u_{ri}v_{sj}w_{tk}\lambda_{ijk} \qquad (12.4)$$
$$(r = 1, \ldots, R; s = 1, \ldots, S; t = 1, \ldots, T),$$

where there has been a change in some of the notation.

The number of elements in the three modes are R, S and T respectively. The $R \times K$ matrix $\mathbf{U}$, where $[\mathbf{U}]_{ri} = u_{ri}$, contains the I "components" for the first mode, and similarly for matrices $\mathbf{V}$ and $\mathbf{W}$ for the second and third modes. These matrices are orthonormal, $\mathbf{U}^T\mathbf{U} = \mathbf{I}$, $\mathbf{V}^T\mathbf{V} = I$, $\mathbf{W}^T\mathbf{W} = \mathbf{I}$. The three-way $I \times J \times K$ matrix $[\boldsymbol{\Lambda}]_{ijk} = \lambda_{ijk}$ is the "core matrix" containing the relationships between various components.

The Tucker-1 model is standard principal components analysis on the three modes, using one pair of modes at a time. Equation (12.4) gives the Tucker-3 model where all three modes are equivalent in status, each having an orthonormal matrix of principal components, i.e. $\mathbf{U}$, $\mathbf{V}$, $\mathbf{W}$ respectively. The Tucker-2 model has $\mathbf{W}$ equal to the identity matrix, and so

$$z_{rst} = \sum_{i=1}^{I}\sum_{j=1}^{J} u_{ri}v_{sj}\lambda_{ijt},$$

giving the third mode special status, e.g. for judges ranking attributes on several objects.

A small number of components is desirable for each mode. The models are fitted using a least squares loss function. For the Tucker-3 model

$$\sum_{r=1}^{R}\sum_{s=1}^{S}\sum_{t=1}^{T}(z_{rst} - \hat{z}_{rst})^2$$

is minimised where

$$\hat{z}_{rst} = \sum_{i=1}^{I}\sum_{j=1}^{J}\sum_{k=1}^{K} u_{ri}v_{sj}w_{tk}\lambda_{ijk},$$

to give the estimated component matrices $\mathbf{U}$, $\mathbf{V}$, $\mathbf{W}$ and the core matrix $\boldsymbol{\Lambda}$. Kroonenberg (1983) discusses algorithms for fitting the Tucker models; see also Kroonenberg and de Leeuw (1980), and ten Berge et al. (1987) for an alternating least squares approach.

12.3.1 Relationship to other models

If the core matrix $\boldsymbol{\Lambda}$ is chosen as the three-way identity matrix then the Tucker-3 model becomes

$$z_{rst} = \sum_{i=1}^{I} u_{ri} v_{si} w_{ti},$$

which is equivalent to the PARAFAC-1 model, or the three-mode CANDECOMP model.

Let $\boldsymbol{\Lambda}$ be a three-way identity matrix and also let $\mathbf{U} \equiv \mathbf{V}$. Then the Tucker-3 model becomes

$$z_{rst} = \sum_{i=1}^{I} u_{ri} u_{si} w_{ti},$$

which is the INDSCAL model.

In the Tucker-2 model let $\mathbf{U} \equiv \mathbf{V}$, then

$$z_{rst} = \sum_{i=1}^{I} \sum_{j=1}^{J} u_{ri} v_{sj} \lambda_{ijt},$$

which is the IDIOSCAL model. The PARAFAC-2 model can then be obtained by making the off-diagonal elements of $\boldsymbol{\Lambda}$ equal.

12.4 One-mode, n-way models

Cox *et al.* (1992) consider a one-mode, n-way model. The model is best illustrated for the three-way case, where data are in the form of "three-way dissimilarities". Three-way dissimilarities $\{\delta_{rst}\}$ are generalized from two-way dissimilarities, so that δ_{rst} measures "how far apart" or "how dissimilar" the objects r, s and t are when considered as a triple. The requirement for δ_{rst} is that it is a real function such that

$$\delta_{rst} \geq 0 \qquad (r \neq s \neq t)$$

$\delta_{rst} = \delta_{\pi(s,t,r)}$ (for all permutations $\pi(r, s, t)$ of r, s, t , $r \neq s \neq t$).

Dissimilarities δ_{rst} are only defined when r, s, t are distinct.

A configuration, $\mathbf{X}$, of points in a Euclidean space is sought that represents the objects, and a real-valued function, $d_{rst}(\mathbf{x}_r, \mathbf{x}_s, \mathbf{x}_t)$

constructed so that it satisfies the same conditions as the three-way dissimilarities. Possible functions are:

1. $d_{rst} = \max(d_{rs}, d_{rt}, d_{st})$, where d_{rs} is the Euclidean distance between the points r and s.
2. $d_{rst} = \min(d_{rs}, d_{rt}, d_{st})$.
3. $d_{rst} = (d_{rs}^2 + d_{rt}^2 + d_{st}^2)^{\frac{1}{2}}$.

For Euclidean distance between two points with coordinates $\mathbf{x}_r$ and $\mathbf{x}_s$,

$$d_{rs}^2 = \mathbf{x}_r^T\mathbf{x}_r + \mathbf{x}_s^T\mathbf{x}_s - 2\mathbf{x}_r^T\mathbf{x}_s.$$

If this is generalized to three points,

$$d_{rst}^2 = a(\mathbf{x}_r^T\mathbf{x}_r + \mathbf{x}_s^T\mathbf{x}_s + \mathbf{x}_t^T\mathbf{x}_t) + b(\mathbf{x}_r^T\mathbf{x}_s + \mathbf{x}_r^T\mathbf{x}_t + \mathbf{x}_s^T\mathbf{x}_t).$$

This function is symmetric in r, s, t. For invariance under rotation, translation and reflection, it is easily shown that $a + b$ must equal zero. Choose $a = 2$ and $b = -2$, then

$$d_{rst}^2 = d_{rs}^2 + d_{rt}^2 + d_{st}^2.$$

This function is the one chosen to represent the three-way dissimilarities.

Stress is defined as

$$S = \left\{ \frac{\sum(d_{rst} - \hat{d}_{rst})^2}{\sum d_{rst}^2} \right\}^{\frac{1}{2}},$$

and can be fitted using a Kruskal type algorithm. Gradient terms can be found in Cox *et al.* (1992). The fitting of this three-way model is denoted as MDS3. The extension to more than three ways, MDSn, is straightforward.

Cox *et al.* argue the case for three-way scaling by calculating dissimilarities based on the Jaccard coefficient, s_{rs}, for the following data matrix consisting of seven binary variables recorded for four individuals.

$$\mathbf{X} = \begin{bmatrix} 1 & 0 & 0 & 1 & 1 & 0 & 0 \\ 0 & 0 & 0 & 0 & 1 & 1 & 1 \\ 0 & 1 & 1 & 0 & 1 & 0 & 0 \\ 1 & 0 & 1 & 0 & 0 & 0 & 0 \end{bmatrix}.$$

Define $\delta_{rs} = 1 - s_{rs}$, and then $\delta_{12} = \delta_{13} = \delta_{14} = \delta_{23} = \delta_{24} = \delta_{34} = \frac{4}{5}$, giving no discriminatory information about the four individuals.

Define the three-way Jaccard coefficient, s_{rst}, as the number of

variables in which individuals r, s and t each score "1" divided by the number of variables in which at least one of them scores "1". Let $\delta_{rst} = 1 - s_{rst}$. For the above data, $\delta_{123} = \frac{6}{7}$, $\delta_{124} = \delta_{134} = \delta_{234} = 1.0$, showing that the individuals 1, 2 and 3 are in a group separated from individual 4. Cox *et al.* investigate one-mode, n-way scaling further on artificially constructed data, before applying it to some voting data from the 18th century in Great Britain.

Figure 12.1 *MDS2 – MDS7 for the 1768 election data from Maidstone, Kent.*

Prior to the Ballot Act of 1872, electors had their votes recorded. They often had to vote for two, three or even more canditates. The data used were the votes cast on the 20th of June 1768 in the town of Maidstone in the county of Kent. There were fifteen candidates competing for seven available seats. The electors could vote for up to seven candidates. The seven-way dissimilarity for a particular group of seven candidates was defined as the proportion of electors voting for the group subtracted from unity. MDS7 was then applied using a two dimensional space for the configuration. Results are shown in Figure 12.1(vi). The data can also be used to find 2, 3,...,6-way dissimilarities where, for instance, the dissimilarity among three particular candidates is the proportion of electors who voted for all three candidates among their seven votes subtracted from unity. Figures 12.1 (i) to 12.1 (v) show the configurations for MDS2 to MDS6 respectively. The stresses for the six configurations were 6%, 4%, 4%, 3%, 2%, and 1% respectively. The six configurations in Figure 12.1 are similar to each other. MDS2 (standard nonmetric MDS) splits the candidates into two groups $\{1, 2, 3, 4, 5, 6, 7\}$ and $\{9, 10, 11, 12, 13, 14, 15\}$ together with a singleton $\{8\}$. However MDS2 does not reveal all the information about the voting behaviour of the electors. MDS3 gives a very similar comfiguration to MDS2. MDS4-MDS7 show candidates 6 and 10 moving progressively closer to candidate 8.

A close look at the raw data shows that electors tended to vote for one of the two groups of candidates $\{1, 2, 3, 4, 5, 6, 7\}$, $\{9, 10, 11, 12, 13, 14, 15\}$, with candidate 8 noticeably not belonging to either of these groups. Several voters who voted mainly for the first group of candidates, often included candidate 10 for one of their votes. Similarly candidate 6 was often chosen by voters of the second group who wished for a wider choice.

Joly and Le Calve (1995) and Heiser and Bennani (1997) take the idea of three-way dissimilarities and distances further. Following the latter, they use the terms triadic dissimilarities and distances for these, and dyadic dissimilarities and distances for the usual two-way dissimilarities and distances between pairs of objects. Heiser and Bennani give the following properties that triadic

dissimilarities should satisfy:

$$\delta_{rst} \geq 0$$
$$\delta_{rst} = \delta_{\pi(r,s,t)}$$
$$\text{(for all permutations of } \pi(r,s,t) \text{ of } r,s,t)$$
$$\delta_{rrr} = 0$$
$$\delta_{rsr} = \delta_{rss}$$

and by symmetry $\delta_{rrs} = \delta_{ssr}$, etc. The dyadic dissimilarities between objects r and s are measured by the quantities $\delta_{rrs} = \delta_{rs}$. They also define triadic similarities s_{rst}.

Triadic distances are defined by d_{rst}, and a metric structure is considered where $\{d_{rst}\}$ satisfy the four properties for $\{\delta_{rst}\}$ above, but in addition $d_{rst} = 0$ only if $r = s = t$, and the triangle inequality for dyadic distances is replaced by the tetrahedral inequality

$$2d_{rst} \leq d_{rtu} + d_{stu} + d_{rsu}.$$

Let $d_{rs} = \frac{1}{2}d_{rrs}$. Heiser and Bennani prove the following results:

$$d_{rst} \leq d_{rtu} + d_{stu}$$
$$\tfrac{1}{3}(d_{rs} + d_{rt} + d_{st}) \leq d_{rst} \leq \tfrac{4}{3}(d_{rs} + d_{rt} + d_{st})$$
$$d_{rs} \leq \tfrac{5}{4}(d_{rt} + d_{st}).$$

Also if $d_{rrs} \leq d_{rst}$ then

$$\tfrac{2}{3}(d_{rs} + d_{rt} + d_{st}) \leq d_{rst} \leq \tfrac{4}{3}(d_{rs} + d_{rt} + d_{st})$$
$$d_{rs} \leq d_{rt} + d_{st}.$$

If d_{rst} is a triadic distance function, then so is $d_{rst}/(c + d_{rst})$, for c a positive constant.

Heiser and Bennani go on to consider triadic distances defined on dyadic distances, for example the Minkowski-p model where $d_{rst} = (d_{rs}^p + d_{rt}^p + d_{st}^p)^{1/p}$, and also on binary presence-absence variables. They use various MDS representations of triadic dissimilarities and illustrate the methods on data relating to: the unproductivity of teams of three individuals, the free sorting of kinship terms, a sensory experiment where undergraduates had to associate a colour with a taste and a sound.

Pan and Harris (1991) consider a one-mode, n-way model. Let s_{rst} be a three-way similarity. Again a Euclidean space is sought

in which points represent the objects. Let the coordinates be $\mathbf{x}_r$. Then the configuration is found such that

$$\lambda = \sum_{i=1}^{p} \lambda_i$$

is maximised, where

$$\lambda_i = -\frac{1}{2} \sum_{r \neq s \neq t} s_{rst} \frac{d_i^2(r,s,t)}{\sum_u x_{ui}^2},$$

$$d_i^2(r,s,t) = (x_{ri} - x_{si})^2 + (x_{ri} - x_{ti})^2 + (x_{si} - x_{ti})^2,$$

and $\mathbf{X}$ is constrained so that the centroid of the configuration is at the origin.

The problem can be written as the search for $\mathbf{X}$ that maximises

$$\lambda = \sum_{i=1}^{p} \frac{\mathbf{x}_i^T \mathbf{H} \mathbf{x}_i}{\mathbf{x}_i^T \mathbf{x}_i},$$

subject to $\mathbf{X}^T \mathbf{1} = \mathbf{0}$, where

$$[\mathbf{H}]_{rs} = h_{rs} = \sum_{t, r \neq s \neq t} (s_{rst} + s_{str} + s_{trs}) \qquad (r \neq s)$$

$$= - \sum_{t, r \neq s \neq t} h_{rt} \qquad (r = s).$$

Pan and Harris use their model on some geological data from the Walker Lake quadrangle which includes parts of California and Nevada. Samples of stream sediments were analysed and elements measured (Fe, Mg, etc.). Similarity between triples of elements was measured by a generalization of the sample correlation coefficient. Interesting results occurred. One justification for using triples of elements rather than standard MDS for pairs, was that it was important to identify those elements which are closely associated with gold and silver together.

One-mode, three-way data are uncommon, possibly because of a previous lack of an instrument for analysis. Further work is needed in this area to assess the impact of these newer triadic methods.

12.5 Two-mode, three-way asymmetric scaling

Okada and Imaizumi (1997) propose a model for multidimensional

scaling of asymmetric two-mode, three-way dissimilarities. For illustration, they use Japanese mobility data among eight occupational categories for the years 1955, 1965, 1975 and 1985. For each of these years there is an eight by eight table where the (r, s)th element is the number of sons whose occupations are in occupational category s and whose fathers' occupations are in occupational category r. Thus the data are two-mode, three-way, *occupational category* $\times$ *occupational category* $\times$ *year*. (To keep to the notions of INDSCAL the "years" will be thought of as subjects or individuals and the "occupational categories" will be thought of as stimuli.)

Let the three-way asymmetric dissimilarities be denoted by $\delta_{rs,i}$. Then a group stimulus space is found where each stimulus is represented by a point and a hypersphere centred at the point. Each individual has a symmetry weight representing individual differences in symmetric dissimilarity relationships. These are applied to the distances between points in the group stimulus space as with INDSCAL. Each individual also has a set of asymmetry weights that are applied to the radii of the hyperspheres in the directions of the various axes, distorting the hypersphere into a hyperellipse.

Let the coordinates of the point representing the rth stimulus be x_{rt} $(r = 1, \ldots, n; t = 1, \ldots, p)$, and let the hypersphere associated with this point have radius r_r. Let the symmetry weight for the ith individual be w_i and the set of asymmetry weights be u_{it}.Then the distance between the rth and sth stimuli for the ith individual is $d_{rs,i} = w_i d_{rs}$. The asymmetry weight u_{it} stretches or shrinks the radius of the hypersphere for stimulus r to $u_{it} r_r$ in the direction of the tth axis.

Let $m_{rs,i}$ be the distance along the line from the point on the circumference of the rth ellipsoid closest to the sth ellipsoid to the point on the circumference of the sth ellipsoid furthest from the rth ellipsoid,

$$m_{rs,i} = d_{rs,i} - \nu_{rs,i} r_r + \nu_{sr,i} r_s$$

where $\nu_{rs,i} = d_{rs,i} / (\sum_t (x_{rt} - x_{st})^2 / u_{it}^2)^{1/2}$.

Okada and Imaizumi now use a nonmetric approach involving STRESS to fit $\{\delta_{rs,i}\}$ to $\{m_{rs,i}\}$. The asymmetric dissimilarities $\delta_{rs,i}$ and $\delta_{sr,i}$ are represented by the differing distances $m_{rs,i}$ and $m_{sr,i}$. The amount by which $m_{rs,i}$ and $m_{sr,i}$ differ will depend on the asymmetric weights $\{u_{it}\}$ reflecting the difference between $\delta_{rs,i}$ and $\delta_{sr,i}$.

12.6 Three-way unfolding

DeSarbo and Carroll (1985) have devised a three-way metric unfolding model. It is a generalization of the unfolding model of Section 8.4. Let there be N judges and suppose the ith judge produces dissimilarities $\{\delta_{irt}\}$ for the rth stimulus on the tth occasion $(r = 1, \ldots, n; t = 1, \ldots, T)$. A common Euclidean space is found in which to place judges and stimuli as in the unfolding models of Chapter 8, together with a weight space for occasions. The weights in this space are applied to the common space to adjust for the particular occasions, in accordance with the ideas of INDSCAL. The three-way dissimilarities are modelled by the three-way squared Euclidean distances, d^2_{irt} as

$$\delta_{irt} = d^2_{irt} + \alpha_t = \sum_{m=1}^{p} w_{tm}(y_{im} - x_{rm})^2 + \alpha_t + \epsilon_{irt},$$

where $\{y_{im}\}$ are the coordinates for the judges, $\{x_{rm}\}$ are the coordinates for the stimuli, $\{w_{tm}\}$ are the weights representing the occasions, α_t is a constant for occasion t, and $\{\epsilon_{irt}\}$ are "errors".

The loss function to be minimised is

$$S = \sum_i \sum_r \sum_t \gamma_{irt}\epsilon^2_{irt},$$

where $\{\gamma_{irt}\}$ are weights defined by the analyst to weight δ_{irt} differentially. DeSarbo and Carroll give a weighted least squares algorithm for fitting the model and demonstrate its use on several data sets. The reader is referred to their paper for further details.

References

Abe, M. (1998) Error structure and identification condition in maximum likelihood nonmetric multidimensional scaling. *Eur. J. of Oper. Res.*, **111**, 216-227.

Ambrosi, K. and Hansohm, J. (1987) Ein dynamischer Ansatz zur Repräsentation von Objekten. In *Operations Research Proceedings 1986*, Berlin: Springer-Verlag.

Anderberg, M.R. (1973) *Cluster Analysis for Applications*, New York: Academic Press.

Andrews, D.F. and Herzberg, A.M. (1985) *Data*, New York: Springer-Verlag.

Apostol, I. and Szpankowski, W. (1999) Indexing and mapping of proteins using a modified nonlinear Sammon projection. *J. Computational Chem.*, **20**, 1049-1059.

Backhaus, W., Menzel, R. and Kreissl, S. (1987) Multidimensional scaling of colour similarity in bees. *Biol. Cybern.*, **56**, 293-304.

Barlow, R.E., Bartholomew, D.J., Bremner, J.M. and Brunk, H.D. (1972) *Statistical Inference under Order Restrictions*, London: Wiley.

Barnett, S. (1990) *Matrices: Methods and Applications*, Oxford: Oxford University Press.

Baulieu, F.B. (1989) A classification of presence/absence dissimilarity coefficients. *J. Classification*, **6**, 233-246.

Bell, P.W. and Cox, T.F. (1998) Bootstrap confidence regions in MDS. In Marx, B. and Friedl, H. (eds.), *Thirteenth International Workshop in Statistical Modelling*, New Orleans, 404-407.

Bell, P.W. and Cox, T.F. (2000) Measuring the variability in MDS configurations using shape analysis. (*In preparation.*)

Bénasséni, J. (1993) Perturbational aspects in correspondence analysis. *Computational Statistics & Data Anal.*, **15**, 393-410.

Bénasséni, J. (1994) Partial additive constant. *J. Stat. Computation Simulation*, **49**, 179-193.

Bennett, J.F. and Hays, W.L. (1960) Multidimensional unfolding: determining the dimensionality of ranked preference data. *Psychometrika*, **25**, 27-43.

Bennett, J.M. (1987) Influential observations in multidimensional scaling. In Heiberger, R.M. (ed.), *Proc. 19th Symp. Interface (Computer Science Statistics)*, Am. Stat. Assoc., 147-154.

Bentler, P.M. and Weeks, D.G. (1978) Restricted multidimensional scaling models. *J. Mathematical Psychol.*, **17**, 138-151.

Benzécri, J.P. (1992) *Correspondence Analysis Handbook*, New York: Marcel Dekker.

Bloxom, B. (1978) Constrained multidimensional scaling in N spaces. *Psychometrika*, **43**, 283-319.

Borg, I. (1977) Geometric representation of individual differences. In Lingoes, J.C. (ed.), *Geometric Representations of Relational Data*, Ann Arbor, MI: Mathesis Press.

Borg, I. and Groenen, P.G. (1997) *Modern Multidimensional Scaling.* New York: Springer-Verlag.

Borg, I. and Lingoes, J.C. (1980) A model and algorithm for multidimensional scaling with external constraints on the distances. *Psychometrika*, **45**, 25-38.

Bradu, D, and Gabriel, K.R. (1978) The biplot as a diagnostic tool for models of two-way tables. *Technometrics*, **20**, 47-68.

Brady, H.E. (1985) Statistical consistency and hypothesis testing for nonmetric multidimensional scaling. *Psychometrika*, **50**, 509-537.

Bricker, C., Tooley, R.V. and Crone, G.R. (1976) *Landmarks of Mapmaking: An Illustrated Survey of Maps and Mapmakers*, New York: Crowell.

Brokken, F.B. (1983) Orthogonal Procrustes rotation maximising congruence. *Psychometrika*, **48**, 343-349.

Browne, M.W. (1967) On oblique Procrustes rotation. *Psychometrika*, **32**, 125-132.

Büyükkurt, B.K. and Büyükkurt, M.D. (1990) Robustness and small-sample properties of the estimators of probabilistic multidimensional scaling (PROSCAL). *J. Mark. Res.*, **27**, 139-149.

Cailliez, F. (1983) The analytical solution of the additive constant problem. *Psychometrika*, **48**, 305–308.

Cailliez, F. and Kuntz, P. (1996) A contribution to the study of the metric and Euclidean structures of dissimilarities. *Psychometrika*, **61**, 241-253.

Calvert, T.W. (1970) Nonorthogonal projections for feature extraction in pattern recognition. *IEEE Trans. Comput.*, **19**, 447-452.

Carroll, J.D., and Arabie, P. (1980) Multidimensional scaling. *Annu. Rev. Psychol.*, **31**, 607-649.

Carroll, J.D. and Chang, J.J (1970) Analysis of individual differences in multidimensional scaling via an n-way generalization of "Eckart-Young" decomposition. *Psychometrika*, **35**, 283-319.

Carroll, J.D. and Chang, J.J. (1972) IDIOSCAL (Individual Differences

in Orientation Scaling): a generalization of INDSCAL allowing idiosyncratic references systems. Paper presented at Psychometric Meeting, Princeton, NJ.

Carroll, J.D. and Wish, M. (1974) Models and methods for three-way multidimensional scaling. In Krantz, D.H, Atkinson, R.L., Luce, R.D. and Suppes, P. (eds.), *Contemporary Developments in Mathematical Psychology, Vol. 2*, San Francisco: W.H. Freeman.

Carroll, J.D., Pruzansky, S. and Kruskal, J.B. (1980) CANDELINC: A general approach to multidimensional analysis of many-way arrays with linear constraints on parameters. *Psychometrika*, **45**, 3-24.

Chang, C.L. and Lee, R.C.T. (1973) A heuristic relaxation method for nonlinear mapping in cluster analysis. *IEEE Trans. Syst., Man. Cybern.*, **3**, 197-200.

Chatfield, C. and Collins, A.J. (1980) *Introduction to Multivariate Analysis*, London: Chapman and Hall.

Chen, C.H. (1996) The properties and applications of the convergence of correlation matrices. *Proc. Stat. Computing Section ASA Joint Stat. Meet. Chicago.*

Chen, C.H. and Chen, J.A (2000) Interactive diagnostic plots for multidimensional scaling with applications in psychosis disorder data analysis. *Unpublished manuscript.*

Chen, S.M. (1995) Measures of similarity between vague sets. *Fuzzy Sets Syst.*, **74**, 217-223.

Chen, S.M. (1997) Similarity measures between vague sets and between elements. *IEEE Trans. Syst., Man. Cybern. part B Cybern.*, **27**, 153-158.

Chino, N. (1978) A graphical technique for representing asymmetric relationships between n objects. *Behaviormetrika*, **5**, 23-40.

Chino, N. (1990) A generalized inner product model for the analysis of asymmetry. *Behaviormetrika*, **27**, 25-46.

Choulakian, V. (1988) Exploratory analysis of contingency tables by loglinear formulation and generalizations of correspondence analysis. *Psychometrika*, **53**, 235-250.

Chu, M.T. and Trendafilov, N.T. (1998) On a differential equation approach to the weighted or orthogonal Procrustes problem. *Statistics Computing*, **8**, 125-133.

Cliff, N. (1968) The "idealized individual" interpretation of individual differences in multidimensional scaling. *Psychometrika*, **33**, 225-232.

Cliff, N., Girard, R., Green, R.S., Kehoe, J.F. and Doherty, L.M. (1977) INTERSCAL: A TSO FORTRAN IV program for subject computer interactive multidimensional scaling. *Educational Psychological Meas.*, **37**, 185-188.

Commandeur, J.J.F (1991) *Matching Configurations*, Leiden, NL: DSWO Press.

Commandeur, J.J.F, Groenen, P.J.F. and Meulman, J.J (1999) A distance-based variety of nonlinear multivariate data analysis, including weights for objects and variables. *Psychometrika*, **64**, 169-186.

Constantine, A.G. and Gower, J.C. (1978) Graphical representation of asymmetry. *Appl. Statistics*, **27**, 297-304.

Coombs, C.H. (1950) Psychological scaling without a unit of measurement. *Psychol. Rev.*, **57**, 148-158.

Coombs, C.H. (1964) *A Theory of Data*, New York: Wiley.

Coombs, C.H. and Kao, R.C. (1960) On a connection between factor analysis and multidimensional unfolding. *Psychometrika*, **25**, 219-231.

Cooper, L.G. (1972) A new solution to the additive constant problem in metric multidimensional scaling. *Psychometrika*, **37**, 311-321.

Cormack, R.M. (1971) A review of classification (with Discussion). *J. R. Stat. Soc., A.*, **134**, 321-367.

Corradino, C. (1990) Proximity structure in a captive colony of Japanese monkeys (*Macaca fuscata fuscata*): an application of miltidimensional scaling. *Primates*, **31**, 351-362.

Coury, B.G. (1987) Multidimensional scaling as a method of assessing internal conceptual models of inspection tasks. *Ergonomics*, **30**, 959-973.

Cox, D.R. and Brandwood, L. (1959) On a discriminatory problem connected with the works of Plato. *J. R. Stat. Soc., B.*, **21**, 195-200.

Cox, M.A.A. and Cox, T.F. (1992) Interpretation of stress in nonmetric multidimensional scaling. *Statistica Applicata*, **4**, 611-618.

Cox, T.F. and Bell, P.W. (2000) The influence function for multidimensional scaling. (*In preparation.*)

Cox, T.F. and Cox, M.A.A. (1990) Interpreting stress in multidimensional scaling. *J. Stat. Comput. Simul.*, **37**, 211-223.

Cox, T.F. and Cox, M.A.A. (1991) Multidimensional scaling on a sphere. *Commun. Stat.*, **20**, 2943-2953.

Cox, T.F. and Cox, M.A.A. (2000) A general weighted two-way dissimilarity coefficient. *J. Classification*, **17**, 101-121.

Cox, T.F., Cox, M.A.A. and Branco, J.A. (1992) Multidimensional scaling for n-tuples. *Br. J. Mathematical Stat. Psychol.*, **44**, 195-206.

Cox, T.F. and Ferry, G. (1993) Discriminant analysis using multidimensional scaling. *Pattern Recognition*, **26**, 145-153.

Cramer, E.M. (1974) On Browne's solution for oblique Procrustes rotation. *Psychometrika*, **39**, 159-163.

Cressie, N.A.C. (1991) *Statistics for Spatial Data.* New York: Wiley.

Critchley, F. (1978) Multidimensional scaling: a short critique and a new method. In Corsten, L.C.A. and Hermans, J. (eds.), *COMPSTAT 1978*, Vienna: Physica-Verlag.

Davenport, M. and Studdert-Kennedy, G. (1972) The statistical analysis

of aesthetic judgements: an exploration. *J. R. Stat. Soc., C.*, **21**, 324-333.
Davidson, J.A. (1972) A geometrical analysis of the unfolding model: non-degenerate solutions. *Psychometrika*, **37**, 193-216.
Davidson, J.A. (1973) A geometrical analysis of the unfolding model: general solutions. *Psychometrika*, **38**, 305-336.
Davidson, M.L. (1983) *Multidimensional scaling*, New York: Wiley.
Davies, P.M. and Coxon, A.P.M. (1983) *The MDS(X) User Manual*, University of Edinburgh, Program Library Unit.
Defays, D. (1978) A short note on a method of seriation. *Br. J. Math. Stat. Psychol.*, **31**, 49-53.
De Jong, S., Heidema, J. and van der Knapp, H.C.M. (1998) Generalized Procrustes analysis of coffee brands tested by five European sensory panels. *Food Qual. Preference*, **9**, 111-114.
De Leeuw, J. (1977a) Correctness of Kruskal's algorithms for monotone regression with ties. *Psychometrika*, **42**, 141-144.
De Leeuw, J. (1977b) Applications of convex analysis to multidimensional scaling. In Barra, J.R., Brodeau, F., Romier, G. and van Cutsen, B. (eds.), *Recent Developments in Statistics*, Amsterdam: North Holland, 133-145.
De Leeuw, J. (1984) Differentiability of Kruskal's stress at a local minimum. *Psychometrika*, **49**, 111-113.
De Leeuw, J. (1988) Convergence of the majorization method for multidimensional scaling. *J. Classification*, **5**, 163-180.
De Leeuw, J. (1992) Fitting distances by least squares. *Unpublished report.*
De Leeuw, J. and Groenen, P.J.F. (1997) Inverse multidimensional scaling. *J. Classification*, **14**, 3-21.
De Leeuw, J. and Heiser, W. (1977) Convergence of correction matrix algorithms for multidimensional scaling. In Lingoes, J.C. (ed.), *Geometric Representations of Relational Data*, Ann Arbor, MI: Mathesis Press.
De Leeuw, J. and Heiser, W. (1980) Multidimensional scaling with restrictions on the configuration. In Krishnaiah, P.R. (ed.), *Multivariate Analysis V*, Amsterdam: North Holland.
De Leeuw, J. and Heiser, W. (1982) Theory of multidimensional scaling. In Krishnaiah, P.R. and Kanal, L.N. (eds.), *Handbook of Statistics, Vol. 2*, Amsterdam: North Holland, 285-316.
De Leeuw, J. and Stoop, I. (1984) Upper bounds for Kruskal's stress. *Psychometrika*, **49**, 391-402.
De Leeuw, J. and van der Heijden, P.G.M. (1988) Correspondence analysis of incomplete contingency tables. *Psychometrika*, **53**, 223-233.
De Leeuw, J., Young, F.W. and Takane, Y. (1976) Additive structure in qualitative data: an alternating least squares method with optimal scaling features. *Psychometrika*, **41**, 471-503.
Deming, W.E. and Stephan, F.F. (1940) On a least squares adjustment

of a sampled frequency table when the expected marginal totals are known. *Ann. Math. Stats.*, **11**, 427-444.

DeSarbo, W.S. and Carroll, J.D. (1985) 3-way unfolding via alternating weighted least-squares. *Psychometrika*, **50**, 275-300.

DeSarbo, W.S., Lehmann, D.R., Carpenter, G. and Sinha, I. (1996) A stochastic multidimensional unfolding approach for representing phased decision outcomes. *Psychometrika*, **61**, 485-508.

DeSarbo, W.S., Lehmann, D.R., Holbrook, M.B., Havlena, W.J. and Gupta, S. (1987) A stochastic three-way unfolding model for asymmetric binary data. *Appl. Psychol. Meas.*, **11**, 397-418.

Diday, E. and Simon, J.C. (1976) Clustering analysis. In Fu, K.S. (ed.), *Communication and Cybernetics 10 Digital Pattern Recognition*, Berlin: Springer-Verlag.

Digby, P.G.N. and Kempton, R.A. (1987) *Multivariate Analysis of Ecological Communities.* London: Chapman and Hall.

Diggle, P.J. (1983) *Statistical Analysis of Spatial Point Patterns.* London: Academic Press.

Dobson, A.J. (1983) *Introduction to Statistical Modelling.* London: Chapman and Hall.

Dryden, I.L. and Mardia, K.V. (1998) *The Statistical Analysis of Shape*, New York: Wiley.

Dryden, I.L., Faghihi, M.R., and Taylor, C.C. (1997) Procrustes shape analysis of planar point subsets. *J. R. Stat. Soc., B.*, **59**, 353-374.

Eckart, C. and Young, G. (1936) Approximation of one matrix by another of lower rank. *Psychometrika*, **1**, 211-218.

Ekman, G. (1954) Dimensions of colour vision. *J. Psychol.*, **38**, 467-474.

Fagot, R.F. and Mazo, R.M. (1989) Association coefficients of identity and proportionality for metric scales. *Psychometrika*, **54**, 93-104.

Faller, J.Y., Klein, B.P. and Faller, J.F. (1998) Characterization of cornsoy breakfast cereals by generalized Procrustes analyses. *Cereal Chem.*, **75**, 904-908.

Fan, J.L. and Xie, W.X. (1999) Some notes on similarity measure and proximity measure. *Fuzzy Sets Syst.*, **101**, 403-412.

Farewell, V.T. (1978) Jackknife estimation with structured data. *Biometrika*, **65**, 444-447.

Fawcett, C.D. (1901) A second study of the variation and correlation of the human skull, with special reference to the Naqada crania. *Biometrika*, **1**, 408-467.

Fenton, M. and Pearce, P. (1988) Multidimensional scaling and tourism research. *Ann. Tourism Res.*, **15**, 236-254.

Fichet, B. (1988) L_{-p} spaces in data analysis. In Bock, H.H. (ed.), *Classification and Related Methods of Data Analysis*, Amsterdam: North Holland, 439-444.

Fisher, R.A. (1940) The precision of discriminant functions. *Ann. Eugen.*, **10**, 422-429.

Fitzgerald, L.F. and Hubert, L.J. (1987) Multidimensional scaling: some possibilities for counseling psychology. *J. Counseling Psychol.*, **34**, 469-480.

Gabriel, K.R. (1971) The biplot graphical display of matrices with application to principal component analysis. *Biometrika*, **58**, 453-457.

Gabriel, K.R. (1981) Biplot display of multivariate matrices for inspection of data and diagnosis. In Barnett, V. (ed.) *Interpreting Multivariate Data*, Chichester, UK: Wiley, 147-174.

Gabriel, K.R. and Zamir, S. (1979) Lower rank approximation of matrices by least squares with any choice of weights. *Technometrics*, **21**, 489-498.

Gifi, A. (1990) *Nonlinear Multivariate Analysis*, New York: Wiley.

Gilula, Z. and Ritov, Y. (1990) Inferential ordinal correspondence analysis: motivation, derivation and limitations. *Int. Stat. Rev.*, **58**, 99-108.

Girard, R.A. and Cliff, N. (1976) A Monte Carlo evaluation of interactive multidimensional scaling. *Psychometrika*, **41**, 43-64.

Gold, E.M. (1973) Metric unfolding: data requirement for unique solution and clarification of Schönemann's algorithm. *Psychometrika*, **38**, 555-569.

Goodall, C. (1991) Procrustes methods in the statistical analysis of shape. *JRSS, Series B*, **53**, 285-339.

Goodall, D.W. (1967) The distribution of the matching coefficient. *Biometrics*, **23**, 647-656.

Goodhill, G.J., Simmen, M.W. and Willshaw, D.J. (1995) An evaluation of the use of multidimensional scaling for understanding brain connectivity. *Phil. Trans. R. Soc. Lon., Series B - Biological Sciences*, **348**, 265-280.

Gordon, A.D. (1990) Constructing dissimilarity measures. *J. Classification*, **7**, 257-269.

Gordon, A.D. (1995) Local transformation of facial features. *J. Applied Stats.*, **22**, 179-184.

Gordon, A.D. (1999) *Classification, 2nd ed.* London: Chapman and Hall/CRC Press.

Gower, J.C. (1966) Some distance properties of latent root and vector methods in multivariate analysis. *Biometrika*, **53**, 325-338.

Gower, J.C. (1968) Adding a point to vector diagrams in multivariate analysis. *Biometrika*, **55**, 582-585.

Gower, J.C. (1971) A general coefficient of similarity and some of its properties. *Biometrics*, **27**, 857-874.

Gower, J.C. (1975) Generalized Procrustes analysis. *Psychometrika*, **40**, 33-51.

Gower, J.C. (1977) The analysis of asymmetry and orthogonality. In Barra,

J.R. et al. (eds.), *Recent Developments in Statistics*, Amsterdam: North Holland.

Gower, J.C. (1984) Multivariate analysis: ordination, multidimensional scaling and allied topics. In Lloyd, E.H. (ed.), *Handbook of Applicable Mathematics, Vol. VI*, New York: Wiley.

Gower, J.C. (1985) Measures of similarity, dissimilarity and distance. In Kotz, S., Johnson, N.L. and Read, C.B. (eds.), *Encyclopedia of Statistical Sciences, Vol. 5*, 397-405.

Gower, J.C. (1990) Fisher's optimal scores and multiple correspondence analysis. *Biometrics*, **46**, 947-961.

Gower, J.C. (1990) 3-Dimensional biplots. *Biometrika*, **77**, 773-785.

Gower, J.C. (1992) Generalized biplots. *Biometrika*, **79**, 475-493.

Gower, J.C. (1994) Orthogonal and projection Procrustes analysis. In Krzanowski, W.J. (ed.) *Recent Advances in Descriptive Multivariate Analysis*, Oxford: Clarendon Press.

Gower, J.C. (1996) Unfolding a symmetric matrix. *J. Classification*, **13**, 81-105.

Gower, J.C. and Dijksterhuis, G.B. (1994) Multivariate analysis of coffee images - a study in the simultaneous display of multivariate quantitative and qualitative variables for several assessors. *Qual. Quantity*, **28**, 165-1845.

Gower, J.C. and Hand, D.J. (1996) *Biplots*, London: Chapman and Hall.

Gower, J.C. and Harding, S.A. (1988) Nonlinear biplots. *Biometrika*, **75**, 445-455.

Gower, J.C. and Legendre, P. (1986) Metric and Euclidean properties of dissimilarity coefficients. *J. Classification*, **3**, 5-48.

Gower, J.C. and Zeilman, B. (1998) Orthogonality and its approximation in the analysis of asymmetry. *Linear Algebra and its Applications*, **278**, 183-193.

Green, B.F. (1952) The orthogonal approximation of an oblique structure in factor analysis. *Psychometrika*, **17**, 429-440.

Green, B.F. and Gower, J.C. (1979) A problem with congruence. Paper presented at the annual meeting of the Psychometric Society, Monterey, California.

Green, P.J. and Sibson, R. (1978) Computing Dirichlet tesselations in the plane. *Computer J.*, **21**, 168-173.

Green, R.S. and Bentler, P.M. (1979) Improving the efficiency and effectiveness of interactively selected MDS data designs. *Psychometrika*, **44**, 115-119.

Greenacre, M.J. (1984) *Theory and Applications of Correspondence Analysis*, London: Academic Press Inc.

Greenacre, M.J. (1988) Correspondence analysis of multivariate categorical data by weighted least-squares. *Biometrika*, **75**, 457-467.

Greenacre, M.J. and Browne, M.W. (1986) An efficient alternating least-squares algorithm to perform multidimensional unfolding. *Psychometrika*, **51**, 241-250.

Greenacre, M.J. and Hastie, T. (1987) The geometrical interpretation of correspondence analysis. *JASA*, **82**, 437-447.

Greenacre, M.J., and Underhill, L.G. (1982) Scaling a data matrix in a low dimensional Euclidean space. In Hawkins, D.M. (ed.), *Topics in Applied Multivariate Analysis*, Cambridge: Cambridge University Press, 183-268.

Groenen, P.J.F. (1993) *The Majorization Approach to Multidimensional Scaling: Some Problems and Extensions.* Leiden, NL: DSWO Press.

Groenen, P.J.F. and Heiser, W.J. (1996) The tunneling method for global optimization in multidimensional scaling. *Psychometrika*, **61**, 529-550.

Groenen, P.J.F, Mather, R. and Heiser, W.J. (1995) The majorization approach to multidimensional scaling for Minkowski distances. *J. Classification*, **12**, 3-19.

Guttman, L. (1941) The quantification of a class of attributes: a theory and method of scale construction. In Horst, P. et al. (eds.), *The Prediction of Personal Adjustment*, New York: Social Science Research Council, 319-348.

Guttman, L. (1968) A general nonmetric technique for finding the smallest coordinate space for a configuration of points. *Psychometrika*, **33**, 469-506.

Hansohm, J. (1987) DMDS dynamic multidimensional scaling. Report, University of Augsburg.

Harshman, R.A. (1970) Foundations of the PARAFAC procedure: models and conditions for an "explanatory" multi-mode factor analysis. *UCLA Working Papers in Phonetics*, **16**.

Harshman, R.A. (1972) Determination and proof of minimum uniqueness conditions for PARAFAC-1. *UCLA Working Papers in Phonetics* , **22**.

Harshman, R.A. (1978) Models for analysis of asymmetrical relationships among N objects or stimuli. Paper presented at the First Joint Meeting of the Psychometric Society and the Society of Mathematical Psychology, Hamilton, Ontario.

Harshman, R.A. and Lundy, M.E. (1984a) The PARAFAC model for three-way factor analysis and multidimensional scaling. In Law, H.G., Snyder, C.W., Hattie, J.A. and McDonald, R.P. (eds.), *Research Methods for Multimode Data Analysis.* New York: Praeger, 122-215.

Harshman, R.A. and Lundy, M.E. (1984b) Data preprocessing and extended PARAFAC model. In Law, H.G., Snyder, C.W., Hattie, J.A. and McDonald, R.P. (eds.), *Research Methods for Multimode Data Analysis.* New York: Praeger, 216-284.

Harshman, R.A. and Lundy, M.E. (1996) Uniqueness proof for a family

of models sharing features of Tucker's three-mode factor analysis and PARAFAC/CANDECOMP. *Psychometrika*, **61**, 133-154.

Hartigan, J.A. (1967) Representation of similarity matrices by trees. *J. Am. Stat. Assoc.*, **62**, 1140-1158.

Hays, W.L. and Bennett, J.F. (1961) Multidimensional unfolding: determining configuration from complete rank order preference data. *Psychometrika*, **26**, 221-238.

Healy, M.J.R. (1986) *Matrices for Statistics*, Oxford: Clarendon Press.

Hefner, R.A. (1958) Extensions of the law of comparative judgement to discriminable and multidimensional stimuli. Doctoral dissertation, Univ. of Michigan.

Heiser, W.J. (1987) Correspondence analysis with least absolute residuals. *Computational Stats. Data Anal.*, **5**, 337-356.

Heiser, W.J. (1988) Multidimensional scaling with least absolute residuals. In Bock, H.H. *Classification and Related Methods of Data Analysis*, Amsterdam: North Holland, 455-462.

Heiser, W.J. (1991) A generalized majorization method for least squares multidimensional scaling of pseudodistances that may be negative. *Psychometrika*, **56**, 7-27.

Heiser, W.J. and Bennani, M. (1997) Triadic distance models: Axiomatization and least squares representation. *J. Mathematical Psychol.*, **41**, 189-206.

Heltshe, J.F. (1988) Jackknife estimator of the matching coefficient of similarity. *Biometrics*, **44**, 447-460.

Heltshe, J.F. and Forrester, N.E. (1983) Estimating species richness using the jackknife procedure. *Biometrics*, **39**, 1-11.

Hettmansperger, T.P. and Thomas, H. (1973) Estimation of J scales for unidimensional unfolding. *Psychometrika*, **38**, 269-284.

Hill, M.O. (1973) Reciprocal averaging: an eigenvector method of ordination. *J. Ecol.*, **61**, 237-251.

Hill, M.O. (1974) Correspondence analysis: a neglected multivariate method. *Appl. Stats.*, **23**, 340-354.

Hirschfeld, H.O. (1935) A connection between correlation and contingency. *Cambridge Phil. Soc. Proc.*, **31**, 520-524.

Horst, P. (1935) Measuring complex attitudes. *J. Soc. Psychol.*, **6**, 369-374.

Hubálek, Z. (1982) Coefficients of association and similarity based on binary (presence-absence) data; an evaluation. *Biol. Rev.*, **57**, 669-689.

Hubert, L. and Arabie, P. (1986) Unidimensional scaling and combinatorial optimization. In de Leeuw, J., Heiser, W.J., Meulman, J. and Critchley, F. (eds.),*Multidimensional Data Analysis*,Leiden, NL: DSWO Press.

Hubert, L. and Arabie, P. (1988) Relying on necessary conditions for optimization: unidimensional scaling and some extensions. In Bock, H.H.

(ed.), *Classification and Related Methods of Data Analysis*, Amsterdam: North Holland.

Hubert, L. and Arabie, P. (1992) Correspondence analysis and optimal structural representations. *Psychometrika*, **57**, 119-140.

Hubert, L., Arabie, P. and Meulman, J.J. (1997) Linear and circular unidimensional scaling for symmetric proximity matrices. *Br. J. Math. Stat. Psychol.*, **50**, 253-284.

Hurley, J.R. and Cattell, R.B. (1962) The Procrustes program: producing direct rotation to test a hypothesized factor structure. *Behavioral Science*, **7**, 258-262.

Ichino, M, and Yaguchi, H. (1994) Generalized Minkowski metrics for mixed feature-type data analysis. *IEEE Trans. Syst., Man. Cybern.*, **24**, 698-708.

Jackson, D.A., Somers, K.M. and Harvey, H.H. (1989) Similarity coefficients: measures of co-occurrence and association or simply measures of occurrence? *Am. Nat.*,**133**, 436-453.

Jackson, M. (1989) *Michael Jackson's Malt Whisky Companion: A Connoisseur's Guide to the Malt Whiskies of Scotland*, London: Dorling Kindersley.

Jardine, N. and Sibson, R. (1971)*Mathematical Taxonomy.* London: Wiley.

Jolliffe, I.T. (1986) *Principal Component Analysis*, New York: Springer-Verlag.

Joly, S. and Le Calve, G. (1995) 3-way distances. *J. Classification*, **12**, 191-205.

Kearsley, A.J., Tapia, R.A. and Trosset, M.W. (1998) The solution of the metric STRESS and SSTRESS problems in multidimensional scaling using Newton's method. *Computational Statistics*, **13**, 369-396.

Kelly, M.J., Wooldridge, L., Hennessy, R.T., Vreuls, D., Barneby, S.F., Cotton, J.C. and Reed, J.C. (1979) Air combat maneuvering performance measurement. Williams Air Force Base, AZ: Flying Training Division, Air Force Human Resources Laboratory (NAVTRAEQUIPCEN IH 315/AFHRL-TR-79-3).

Kendall, D.G. (1971) Seriation from abundance matrices. In Hodson, F.R., Kendall, D.G. and Tătu, P. (eds.), *Mathematics in the Archaeological and Historical Sciences*, Edinburgh: Edinburgh University Press.

Kendall, D.G. (1977) On the tertiary treatment of ties. Appendix to Rivett, B.H.P., Policy selection by structural mapping. *Proc. R. Soc. Lon.*, **354**, 422-423.

Kendall, D.G. (1984) Shape-manifolds, Procrustean metrics and complex projective spaces. *Bull. Lon. Math. Soc.*, **16**, 81-121.

Kendall, D.G., Barden, D., Carne, T.K. and Le, H. (1999) *Shape and Shape Theory*, Chichester, UK: Wiley.

Kiers, H.A.L. (1989) An alternating least squares algorithm for fitting

the two- and three-way DEDICOM model and the IDIOSCAL model. *Psychometrika*, **54**, 515-521.

Kiers, H.A.L. (1993) An alternating least squares algorithm for PARAFAC-2 and three-way DEDICOM. *Computational Stats. Data Anal.*, **16**, 103-118.

Kiers, H.A.L. and Groenen, P. (1996) A monotonically convergent algorithm for orthogonal congruence rotation. *Psychometrika*, **61**, 375-389.

Kiers, H.A.L. and Krijnen, W.P. (1991) An efficient algorithm for PARAFAC of three-way data with large numbers of observation units. *Psychometrika*, **56**, 147-152.

Kiers, H.A.L. and Takane, Y. (1994) A generalization of GIPSCAL for the analysis of nonsymmetric data. *J. Classification*, **11**, 79-99.

Kiers, H.A.L., ten Berge, J.M.F., Takane, Y. and de Leeuw, J. (1990) A generalization of Takane's algorithm for DEDICOM. *Psychometrika*, **55**, 151-158.

Klahr, D. (1969) A Monte Carlo investigation of the statistical significance of Kruskal's nonmetric scaling procedure. *Psychometrika*, **34**, 319-330.

Klein, R.W. and Dubes, R.C. (1989) Experiments in projection and clustering by simulated annealing. *Pattern Recognition*, **22**, 213-220.

Klir, G.J. and Folger, T.A. (1988) *Fuzzy Sets, Uncertainty, Inf.*, London: Prentice Hall.

Klock, H. and Buhmann, J.M. (1997) Multidimensional scaling by deterministic annealing. In *Proc. EMMCVPR97*, Venice.

Korth, B. and Tucker, L.R. (1976) Procrustes matching by congruence coefficients. *Psychometrika*, **41**, 531-535.

Koschat, M.A. and Swayne, D.F. (1991) A weighted Procrustes criterion. *Psychometrika*, **56**, 229-239.

Kristof, W. and Wingersky, B. (1971) Generalization of the orthogonal Procrustes rotation procedure to more than two matrices. In *Proc., 79th Annu. Convention Am. Psychol. Assoc.*, 81-90.

Kroonenberg, P.M. (1983) *Three-Mode Principal Components Analysis*, Leiden, NL: DSWO Press.

Kroonenberg, P.M. (1992) Three-mode component models: a review of the literature. *Statistica Applicata*, **4**, 73-96.

Kroonenberg, P.M. (1994) The Tuckals line - a suite of programs for 3-way data analysis. *Computational Stats. Data Anal.*, **18**, 73-96.

Kroonenberg, P.M. and de Leeuw, J. (1980) Principal components analysis of three-mode data by means of alternating least squares algorithms. *Psychometrika*, **45**, 69-97.

Kruskal, J.B. (1964a) Multidimensional scaling by optimizing goodness-of-fit to a nonmetric hypothesis. *Psychometrika*, **29**, 1-27.

Kruskal, J.B. (1964b) Nonmetric multidimensional scaling: a numerical method. *Psychometrika*, **29**, 115-129.

Kruskal, J.B. (1971) Monotone regression: continuity and differentiability properties. *Psychometrika*, **36**, 57-62.

Kruskal, J.B. (1984) Multilinear methods. In Law, H.G., Snyder Jr., J.A., Hattie, J.A. and McDonald, R.P. (eds.), *Research Methods for Multimode Data Analysis*, New York; Praeger, 36-62.

Kruskal, J.B., Harshman, R.A. and Lundy, M.E. (1989) How 3-MFA data can cause degenerate PARAFAC solutions, among other relationships. In Coppi, R. and Bolasco, S. (eds.), *Multiway Data Analysis*, Amsterdam: North Holland, 115-122.

Kruskal, J.B. and Wish, M. (1978) *Multidimensional Scaling.* Beverly Hills, CA: Sage Publications.

Krzanowski, W.J. (1988) *Principles of Multivariate Analysis: A User's Perspective*, Oxford: Clarendon Press.

Krzanowski, W.J. (1993) Attribute selection in correspondence analysis of incidence matrices. *Appl. Stats.*, **42**, 529-541.

Krzanowski, W.J. and Marriott, F.H.C. (1994) *Multivariate Analysis Part 1*, London: Edward Arnold.

Krzanowski, W.J. and Marriott, F.H.C. (1995) *Multivariate Analysis Part 2*, London: Edward Arnold.

Langeheine, R. (1982) Statistical evaluation of measures of fit in the Lingoes-Borg Procrustean individual differences scaling. *Psychometrika*, **47**, 427-442.

Langron, S.P. and Collins, A.J. (1985) Perturbation theory for generalized Procrustes analysis. *J.R. Stat. Soc. B.*, **47**, 277-284.

Lapointe, F.J. and Legendre, P. (1994) A classification of pure malt Scotch whiskies. *Appl. Stats.*, **43**, 237-257.

Lau, K.N., Leung, P.L. and Tse, K.K. (1998) A nonlinear programming approach to metric unidimensional scaling. *J. Classification*, **15**, 3-14.

Lawson, W.J. and Ogg, P.J. (1989) Analysis of phenetic relationships among populations of the avian genus Batis (Platysteirinae) by means of cluster analysis and multidimensional scaling. *Biom. J.*, **31**, 243-254.

Lee, S.Y. (1984) Multidimensional scaling models with inequality and equality constraints. *Commun. Stat.-Simula. Computa.*, **13**, 127-140.

Lee, S.Y. and Bentler, P.M. (1980) Functional relations in multidimensional scaling. *Br. J. Mathematical Stat. Psychol.*, **33**, 142-150.

Lerner, B., Guterman, H., Aladjem, M., Dinstein, I. and Romem, Y. (1998) On pattern classification with Sammon's nonlinear mapping - an experimental study. *Pattern Recognition*, **31**, 371-381.

Levin, J. and Brown, M. (1979) Scaling a conditional proximity matrix to symmetry. *Psychometrika*, **44**, 239-243.

Levine, D.M. (1978) A Monte Carlo study of Kruskal's variance based measure on stress. *Psychometrika*, **43**, 307-315.

Lim, T.M. and Khoo, H.W. (1985) Sampling properties of Gower's general coefficient of similarity. *Ecology*, **66**, 1682-1685.

Lingoes, J.C. (1971) Some boundary conditions for a monotone analysis of symmetric matrices. *Psychometrika*, **36**, 195-203.

Lingoes, J.C. and Borg, I. (1976) Procrustean individual differences scaling: PINDIS. *J. Mark. Res.*, **13**, 406-407.

Lingoes, J.C. and Borg, I. (1977) Procrustean individual differences scaling: PINDIS. *Sozial Psychologie*, **8**, 210-217.

Lingoes, J.C. and Borg, I. (1978) A direct approach to individual differences scaling using increasingly complex transformations. *Psychometrika*, **43**, 491-519.

Lingoes, J.C. and Roskam, E.E. (1973) A mathematical and empirical study of two multidimensional scaling algorithms. *Psychometrika Monograph Supplement*, **38**.

Lissitz, R.W., Schönemann, P.H. and Lingoes, J.C. (1976) A solution to the weighted Procrustes problem in which the transformation is in agreement with the loss function. *Psychometrika*, **41**, 547-550.

Lundy, M.E., Harshman, R.A. and Kruskal, J.B. (1989) A two stage procedure incorporating good features of both trilinear and quadrilinear models. In Coppi, R. and Bolasco, S. (eds.), *Multiway Data Analysis*, Amsterdam: North Holland, 123-130.

MacCallum, R.C. (1976a) Effects on INDSCAL of non-orthogonal perceptions of object space dimensions. *Psychometrika*, **41**, 177-188.

MacCallum, R.C. (1976b) Transformation of a three-mode multidimensional scaling solution to INDSCAL form. *Psychometrika*, **41**, 385-400.

MacCallum, R.C. (1977a) Effects of conditionality on INDSCAL and ALSCAL weights. *Psychometrika*, **42**, 297-305.

MacCallum, R.C. (1977b) A Monte Carlo investigation of recovery of structure by ALSCAL. *Psychometrika*, **42**, 401-428.

MacCallum, R.C. (1979) Recovery of structure in incomplete data by ALSCAL. *Psychometrika*, **44**, 69-74.

MacCallum, R.C. and Cornelius III, E.T. (1977) A Monte Carlo investigation of recovery of structure by ALSCAL. *Psychometrika*, **42**, 401-428.

MacKay, D.B. and Zinnes, J.L. (1995) Probabilistic multidimensional unfolding – an anisotropic model for preference ratio judgements. *J. Mathematical Psychol.*, **39**, 99-111.

Manton, K.G., Woodbury, M.A. and Tolley, H.D. (1994) *Statistical Applications Using Fuzzy Sets*, New York: Wiley.

Mardia, K.V. (1978) Some properties Classical multidimensional scaling. *Commun. Stat. Theor. Meth.*, **A7**, 1233-1241.

Mardia, K.V., Kent, J.T. and Bibby, J.M. (1979) *Multivariate Analysis*, London: Academic Press.

Mather, R. (1988) Dimensionality in constrained scaling. In Bock, H.H. (ed.), *Classification and Related Methods of Data Analysis*, Amsterdam: North Holland, 479-488.

Mather, R. (1990) Multidimensional scaling with constraints on the configuration. *J. Multivariate Anal.*, **33**, 151-156.

McElwain, D.W. and Keats, J.A. (1961) Multidimensional unfolding: some geometrical solutions. *Psychometrika*, **26**, 325-332.

Mead, A. (1992) Review of the development of multidimensional scaling methods. *The Statistician*, **41**, 27-39.

Messick, S.M. and Abelson, R.P. (1956) The additive constant problem in multidimensional scaling. *Psychometrika*, **21**, 1-15.

Meulman, J.J. (1986) *A Distance Approach to Nonlinear Multivariate Analysis*, Leiden, NL: DSWO Press.

Meulman, J.J. (1992) The integration of multidimensional scaling and multivariate analysis with optimal transformations. *Psychometrika*, **57**, 539-565.

Meulman, J.J (1993) Principal coordinates analysis with optimal transformation of the variables – minimizing the sum of squares of the smallest eigenvalues. *Br. J. Math. Stat. Psychol.*, **46**, 287-300.

Meulman, J.J. (1996) Fitting a distance model to homogeneous subsets of variables: Points of view analysis of categorical data. *J. Classification*, **13**, 249-266.

Michailidis, G. and de Leeuw, J. (1998) The Gifi system of descriptive multivariate analysis. *Stat. Science*, **13**, 307-336.

Milroy, W. (1998) *The Original Malt Whisky Almanac: A Taster's Guide*, Glasgow: Neil Wilson Publishing.

Mooijaart, A. and Commandeur, J.J.F. (1990) A general solution of the weighted orthonormal Procrustes problem. *Psychometrika*, **55**, 657-663.

New Geographical Digest (1986), London: George Philip.

Niemann, H. and Weiss, J. (1979) A fast-converging algorithm for nonlinear mapping of high-dimensional data to a plane. *IEEE Trans. Comput.*, **28**, 142-147.

Nishisato, S. (1980) *Analysis of Categorical Data: Dual Scaling and its Applications*, Totonto: University of Toronto Press.

Okada, A. and Imaizumi, T. (1997) Asymmetric multidimensional scaling of two-mode three way proximities. *J. Classification*, **14**, 195-224.

Olson, A.A. (1984) One-dimensional metric scaling. *Automation and Remote Control*, **45**, 783-788.

Pack, P. and Jolliffe, I.T. (1992) Influence in correspondence analysis. *Appl. Stats.*, **41**, 365-380.

Pan, G. and Harris, D.P. (1991) A new multidimensional scaling technique based upon associations of triple objects – Pijk and its application to the analysis of geochemical data. *Mathematical Geol.*, **6**, 861-886.

Pastor, M.V., Costell, E., Izquierdo, L. and Duran, L. (1996) Sensory profile of peach nectars - evaluation of assessors and attributes by generalized Procrustes analysis. *Food Science Technol. Int.*, **2**, 219-230.

Peay, E.R. (1988) Multidimensional rotation and scaling of configurations to optimal agreement. *Psychometrika*, **53**, 199-208.

Plackett, R.L. (1981) *The Analysis of Categorical Data*, London: Griffin.

Pliner, V. (1984) A class of metric scaling models. *Automation and Remote Control*, **45**, 789-794.

Pliner, V. (1986) The problem of multidimensional metric scaling. *Automation and Remote Control*, **47**, 560-567.

Pliner, V. (1996) Metric unidimensional scaling and global optimization. *J. Classification*, **13**, 3-18.

Polzella, D.J. and Reid, G.R. (1989) Multidimensional scaling analysis of simulated air combat maneuvering performance data. *Aviat. Space, Environ. Med.*, **60**, 141-144.

Poste, L.M. and Patterson, C.F. (1988) Multidimensional scaling – sensory analysis of yoghurt. *Can. Inst. Food Sci. Technol. J.*, **21**, 271-278.

Ramsay, J.O. (1977) Maximum likelihood estimation in multidimensional scaling. *Psychometrika*, **42**, 241-266.

Ramsay, J.O. (1978a) Confidence regions for multidimensional scaling analysis. *Psychometrika*, **43**, 145-160.

Ramsay, J.O. (1978b) *MULTISCALE: Four Programs of Multidimensional Scaling by the Method of Maximum Likelihood.* Chicago: International Educational Services.

Ramsay, J.O. (1980) Some small sample results for maximum likelihood estimation in multidimensional scaling. *Psychometrika*, **45**, 141-146

Ramsay, J.O. (1982) Some statistical approaches to multidimensional scaling data. *J. R. Stat. Soc., A.*, **145**, 285-312.

Ramsay, J.O. (1991) *Multiscale Manual*, McGill University.

Rao, C.R. (1982) Diversity and dissimilarity coefficients: a unified approach. *Theor. Pop. Biol.*, **21**, 24-43.

Richardson, M. and Kuder, G.F. (1933) Making a rating scale that measures. *Personnel J.*, **12**, 36-40.

Richman, M.B. and Vermette, S.J. (1993) The use of Procrustes target analysis to discriminate dominant source regions of fine sulphur in the Western USA. *Atmospheric Environ. Part A*, **27**, 475-481.

Ripley, B.D. (1981) *Spatial Statistics.* New York: Wiley.

Rivett, B.H.P. (1977) Policy selection by structural mapping. *Proc. R. Soc. Lon.*, **354**, 407-423.

Roberts, G., Martyn, A.L., Dobson, A.J. and McCarthy, W.H. (1981) Tumour thickness and histological type in malignant melanoma in New South Wales, Australia. 1970-76. *Pathology*, **13**, 763-770.

Rocci, R. and ten Berge, J.M.F. (1994) A simplification of a result by Zellini on the maximal rank of symmetrical 3-way arrays. *Psychometrika*, **59**, 377-380.

Rodgers, J.L. and Thompson, T.D. (1992) Seriation and multidimensional

scaling - a data-analysis approach to scaling asymmetric proximity matrices. *Appl. Psychological Meas.*, **16**, 105-117.

Ross, J. and Cliff, N. (1964) A generalization of the interpoint distance model. *Psychometrika*, **29**, 167-176.

Saito, T. (1978) The problem of the additive constant and eigenvalues in metric multidimensional scaling. *Psychometrika*, **43**, 193-201.

Sammon, J.W. (1969) A nonlinear mapping for data structure analysis. *IEEE Trans. Comput.*, **18**, 401-409.

Schiffman, S.S, Reynolds, M.L. and Young, F.W. (1981) *Introduction to Multidimensional Scaling: Theory, Methods and Applications*, New York: Academic Press.

Schneider, R.B. (1992) A uniform approach to multidimensional scaling. *J. Classification*, **9**, 257-273.

Schobert, R. (1979) *Die Dynamisierung komplexer Marktmodelle mit Hilfe von Verfahren der mehrdimensionalen Skalierung*, Berlin: Duncker and Humblot.

Schoenberg, I.J. (1935) Remarks to Maurice Fréchet's article "Sur la définition axiomatique d'une classe d'espaces vectoriels distanciés applicables vectoriellement sur l'espace de Hilbert". *Ann. Math.*, **36**, 724–732.

Schönemann, P.H. (1966) A generalized solution of the orthogonal Procrustes problem. *Psychometrika*, **31**, 1-10.

Schönemann, P.H. (1970) On metric multidimensional unfolding. *Psychometrika*, 35, 349-366.

Schönemann, P.H. and Carroll, R.M. (1970) Fitting one matrix to another under choice of a central dilation and a rigid motion. *Psychometrika*, **35**, 245-256.

Shepard, R.N. (1962a) The analysis of proximities: multidimensional scaling with an unknown distance function I. *Psychometrika*, **27**, 125-140.

Shepard, R.N. (1962b) The analysis of proximities: multidimensional scaling with an unknown distance function II. *Psychometrika*, **27**, 219-246.

Shepard, R.N. and Carroll, J.D. (1966) Parametric representation of nonlinear data structures. In *Proceedings of the International Symposium on Multivariate Analysis*, New York: Academic Press, 561-592.

Sherman, C.R. (1972) Nonmetric multidimensional scaling: a Monte Carlo study of the basic parameters. *Psychometrika*, **37**, 323-355.

Sibson, R. (1978) Studies in the robustness of multidimensional scaling: Procrustes statistics. *J. R. Stats. Soc., B.*, **40**, 234-238.

Sibson, R. (1979) Studies in the robustness of multidimensional scaling; perturbational analysis Classical sacaling. *J. R. Stats. Soc., B.*, **41**, 217-229.

Sibson, R., Bowyer, A. and Osmond, C. (1981) Studies in the robustness of multidimensional scaling: Euclidean models and simulation studies. *J. Stats. Comput. Simul.*, **13**, 273-296.

Siedlecki, W., Siedlecki, K. and Sklansky, J. (1988) An overview of mapping techniques for exploratory pattern analysis. *Patt. Recog.*, **21**, 411-429.

Simantiraki, E. (1996) Unidimensional scaling: a linear programming approach minimising absolute deviations. *J. Classification*, **13**, 19-25.

Simmen, M.W. (1996) Multidimensional scaling of binary dissimilarities: Direct and derived approaches. *Multivariate Behavioral Research*, **31**, 47-67.

Sinesio, F and Moneta, E. (1996) Sensory evaluation of walnut fruit. *Food Qual. Preference*, **8**, 35-43.

Smith, N.J. and Iles, K. (1988) A graphical depiction of multivariate similarity among sample plots. *Can. J. For. Res.*, **18**, 467-472.

Smith, W., Kravitz, D. and Grassle, J.F. (1979) Confidence intervals for similarity measures using the two-sample jackknife. In Orloci, L., Rao, C.R. and Stiteler, W.M. (eds.), *Multivariate Methods in Ecological Work*, Fairland, MD: International Cooperative Publishing House, 253-262.

Sneath, P.H.A. and Sokal, R.R. (1973) *Numerical Taxonomy.* San Francisco: W.H. Freeman and Co.

Snijders, T.A.B., Dormaar, M., van Schuur, W.H., Dijkman-Caes, C. and Driessen, G. (1990) Distribution of some similarity coefficients for dyadic binary data in the case of associated attributes. *J. Classification*, **7**, 5-31.

Söderkvist, I. (1993) Perturbation analysis of the orthogonal Procrustes problem. *BIT*, **33**, 687-694.

Spaeth, H.J. and Guthery, S.B. (1969) The use and utility of the monotone criterion in multidimensional scaling. *Multivariate Behavioral Research*, **4**, 501-515.

Spence, I. (1970) Local minimum solutions in nonmetric multidimensional scaling. *Proc. Soc. Stats. Section Am. Stat. Assoc.*, **13**, 365-367.

Spence, I. (1972) A Monte Carlo evaluation of three nonmetric multidimensional scaling algorithms. *Psychometrika*, **37**, 461-486.

Spence, I. and Domoney, D.W. (1974) Single subject incomplete designs for nonmetric multidimensional scaling. *Psychometrika*, **39**, 469-490.

Spence, I. and Lewandowsky, S. (1989) Robust multidimensional scaling. *Psychometrika*, **54**, 501-513.

Spence, I. and Ogilvie, J.C. (1973) A table of expected stress values for random rankings in nonmetric multidimensional scaling. *Multivariate Behavioral Research*, **8**, 511-517.

Stenson, H.H. and Knoll, R.L. (1969) Goodness of fit for random rankings in Kruskal's nonmetric scaling procedure. *Psychological Bull.*, **71**, 122-126.

Storms, G. (1995) On the robustness of maximum-likelihood scaling for violations of the error model. *Psychometrika*, **60**, 247-258.

Takane, Y. (1978a) A maximum likelihood method for nonmetric multidimensional scaling: I. The case in which all empirical pairwise orderings are independent – theory. *Japanese Psychological Res.*, **20**, 7-17.

Takane, Y. (1978b) A maximum likelihood method for nonmetric multidimensional scaling: I. The case in which all empirical pairwise orderings are independent – evaluation. *Japanese Psychological Res.*, **20**, 105-114.

Takane, Y. (1981) Multidimensional successive categories scaling: a maximum likelihood method. *Psychometrika*, **46**, 9-28.

Takane, Y. and Kiers, H.A.L. (1997) Latent class DEDICOM. *J. Classification*, **14**, 225-247.

Takane, Y., Kiers, H.A.L. and de Leeuw, J. (1995) Component analysis with different sets of constraints on different dimensions. *Psychometrika*, **60**, 259-280.

Takane, Y., Young, F.W. and de Leeuw, J.(1977) Nonmetric individual differences multidimensional scaling: an alternating least squares method with optimal scaling features. *Psychometrika*, **42**, 7-67.

Ten Berge, J.M.F. (1977) Orthogonal Procrustes rotation for two or more matrices. *Psychometrika*, **42**, 267-276.

Ten Berge, J.M.F. (1983) A generalization of Verhelst's solution for a constrained regression problem in ALSCAL and related MDS-algorithms. *Psychometrika*, **48**, 631-638.

Ten Berge, J.M.F. (1989) Convergence of PARAFAC preprocessing procedures and the Deming-Stephan method of iterative proportional fitting. In Coppi, R. and Bolasco, S. (eds.), *Multiway Data Analysis*, Amsterdam: North Holland, 53-63.

Ten Berge, J.M.F. (1997) Reduction of asymmetry by rank-one matrices. *Computational Stat. Data Anal.*, **24**, 357-366.

Ten Berge, J.M.F. and Bekker, P.A. (1993) The isotropic scaling problem in generalized Procrustes analysis. *Computational Stat. Data Anal.*, **16**, 201-204.

Ten Berge, J.M.F., de Leeuw, J. and Kroonenberg, P.M. (1987) Some additional results on principal components analysis of three-mode data by means of alternating least squares algorithms. *Psychometrika*, **52**, 183-191.

Ten Berge, J.M.F. and Kiers, H.A.L. (1989) Convergence properties of an iterative procedure of ipsatizing and standardizing a data matrix, with applications to PARAFAC/CANDECOMP preprocessing. *Psychometrika*, **54**, 231-235.

Ten Berge, J.M.F. and Kiers, H.A.L. (1991) Some clarifications of the CANDECOMP algorithm applied to INDSCAL. *Psychometrika*, **56**, 317-326.

Ten Berge, J.M.F. and Kiers, H.A.L. (1996) Some uniqueness results for PARAFAC2. *Psychometrika*, **61**, 123-132.

Ten Berge, J.M.F., Kiers, H.A.L. and Commandeur, J.J.F. (1993) Orthogonal Procrustes rotation for matrices with missing values. *Br. J. Math. Stat. Psychol.*, **46**, 119-134.

Ten Berge, J.M.F. and Kiers, H.A.L. and de Leeuw, J. (1988) Explicit CANDECOMP/PARAFAC solutions for a contrived $2\times2\times2$ array of rank three. *Psychometrika*, **53**, 579-584.

Ten Berge, J.M.F., Kiers, H.A.L. and Krijnen, W.P. (1993) Computational solutions for the problem of negative saliences and nonsymmetry in INDSCAL. *J. Classification*, **10**, 115-124.

Ten Berge, J.M.F. and Knol, D.L. (1984) Orthogonal rotations to maximal agreement for two or more matrices of different column orders. *Psychometrika*, **49**, 49-55.

Ten Berge, J.M.F. and Nevels, K. (1977) A general solution to Mosier's oblique Procrustes problem. *Psychometrika*, **42**, 593-600.

Tenenhaus, M. and Young, F.W. (1985) An analysis and synthesis of multiple correspondence analysis, optimal scaling, dual scaling, homogeneity analysis and other methods for quantifying categorical multivariate data. *Psychometrika*, **50**, 91-119.

Ter Braak, C.J.F. (1992) Multidimensional scaling and regression. *Statistica Applicata*, **4**, 577-586.

Tijssen, R.J.W. and Van Raan, A.F.J. (1989) Mapping co-word structures: a comparison of multidimensional scaling and leximappe. *Scientometrics*, **15**, 283-295.

Tong, S.T.Y. (1989) On nonmetric multidimensional scaling ordination and interpretation of the matorral vegetation in lowland Murcía. *Vegetatio*, **79**, 65-74.

Torgerson, W.S. (1952) Multidimensional scaling: 1. Theory and method. *Psychometrika*, **17**, 401-419.

Torgerson, W.S. (1958) *Theory and Method of Scaling*, New York: Wiley.

Trosset, M.W. (1998) A new formulation of the nonmetric strain problem in multidimensional scaling. *J. Classification*, **15**, 15-35.

Tucker, L.R. (1951) A method for synthesis of factor analytic studies. Personnel Research Section Report No. 984, Department of the Army, Washington, DC.

Tucker, L.R. (1966) Some mathematical notes on three-mode factor analysis. *Psychometrika*, **31**, 279-311.

Tucker, L.R. (1972) Relations between multidimensional scaling and three-mode factor analysis. *Psychometrika*, **37**, 3-27.

Tucker, L.R. and Messick, S. (1963) An individual differences model for multidimensional scaling. *Psychometrika*, **28**, 333-367.

Van der Heijden, P.G.M. and de Leeuw, J. (1985) Correspondence analysis used complementary to log-linear analysis. *Psychometrika*, **50**, 429-447.

Van der Heijden, P.G.M. and Meijerink, F. (1989) Generalized correspondence analysis of multi-way contingency tables and multi-way (super-)

indicator matrices. In Coppi, R. and Bolasco, S. (eds.), *Multiway Data Analysis.* Amsterdam: North Holland, 185-202.

Van der Heijden, P.G.M and Worsley, K.J. (1988) Comment on "Correspondence analysis used complementary to log-linear analysis". *Psychometrika*, **53**, 287-291.

Van der Heijden, P.G.M., de Falguerolles, A. and de Leeuw, J. (1989) A combined approach to contingency table analysis using correspondence analysis and log-linear analysis. *Appl. Stats.*, **38**, 249-292.

Verboon, P. and Gabriel, K.R. (1995) Generalized Procrustes analysis with iterative weighting to achieve resistance. *Br. J. Math. Stat. Psychol.*, **48**, 57-73.

Verboon, P. and Heiser, W.J. (1992) Resistant Orthogonal Procrustes Analysis. *J. Classification*, **9**, 237-256.

Verboon, P. and Heiser, W.J. (1994) Resistant lower rank approximation of matrices by iterative majorization. *Computational Stats. Data Anal.*, **18**, 457-467.

Verhelst, N.D. (1981) A note on ALSCAL: the estimation of the additive constant. *Psychometrika*, **46**, 465-468.

Wagenaar, W.A. and Padmos, P. (1971) Quantitative interpretation of stress in Kruskal's multidimensional scaling technique. *Br. J. Math. Stat. Psychol.*, **24**, 101-110.

Wang, W.J. (1997) New similarity measures on fuzzy sets and on elements. *Fuzzy Sets Syst.*, **85**, 305-309.

Weeks, D.G. and Bentler, P.M. (1982) Restricted multidimensional scaling models for asymmetric proximities. *Psychometrika*, **47**, 201-208.

Winsberg, S. and Carroll, J.D. (1989a) A quasi-nonmetric method for multidimensional scaling of multiway data via a restricted case of an extended INDSCAL model. In Coppi, R. and Bolasco, S. (eds.), *Multiway Data Analysis*, Amsterdam: North Holland.

Winsberg, S. and Carroll, J.D. (1989b) A quasi-nonmetric method for multidimensional scaling of multiway data via a restricted case of an extended Euclidean model. *Psychometrika*, **54**, 217-229.

Winsberg, S. and De Soete, G. (1993) A latent class approach to fitting the weighted Euclidean model, CLASCAL. *Psychometrika*, **58**, 315-330.

Winsberg, S. and De Soete, G. (1997) Multidimensional scaling with constrained dimensions: CONSCAL. *Br. J. Math. Stat. Psychol.*, **50**, 55-72.

Wish, M. and Carroll, J.D. (1982) Theory of multidimensional scaling. In Krishnaiah, P.R. and Kanal, L.N. (eds.), *Handbook of Statistics, Vol. 2*, Amsterdam: North Holland, 317-345.

Wish, M., Deutsch, M. and Biener, L. (1972) Differences in perceived similarity of nations. In Romney, A.K., Shepard, R.N. and Nerlove, S.B. (eds.), *Theory and Applications in the Behavioural Sciences, Vol. 2*, New York: Seminar Press, 289-313.

Young, F.W. (1987) *Multidimensional Scaling: History, Theory and Applications*, Hamer, R.M. (ed.), Hillsdale, NJ: Lawrence Erlbaum.

Young, F.W. and Cliff, N.F (1972) Interactive scaling with individual subjects. *Psychometrika*, **37**, 385-415.

Young, F.W. and Null, C.H. (1978) Multidimensional scaling of nominal data: the recovery of metric information with ALSCAL. *Psychometrika*, **43**, 367-379.

Young, F.W., de Leeuw, J. and Takane, Y. (1976) Regression with qualitative and quantitative variables: an alternating least squares method with optimal scaling features. *Psychometrika*, **41**, 505-529.

Young, F.W., Takane, Y. and Lewyckyj, R. (1978) Three notes on ALSCAL. *Psychometrika*, **43**, 433-435.

Young, G. and Householder, A.S. (1938) Discussion of a set of points in terms of their mutual distances. *Psychometrika*, **3**, 19–22.

Young, M.P., Scannell, J.W., O'Neill, M.A., Hilgetag, C.C., Burns, G. and Blakemore, C. (1995). Nonmetric multidimensional scaling in the analysis of neuroanatomical connection data and the organization of the primate cortical visual-system. *Phil. Trans. R. Soc. Lon., Series B - Biological Sci.*, **348**, 281-308.

Zegers, F.E. (1986) A family of chance-corrected association coefficients for metric scales. *Psychometrika*, **51**, 559-562.

Zegers, F.E. and ten Berge, J.M.F. (1985) A family of association coefficients for metric scales. *Psychometrika*, **50**, 17-24.

Zielman, B. and Heiser, W.J. (1993) Analysis of asymmetry by a slide-vector. *Psychometrika*, **58**, 101-114.

Zielman, B. and Heiser, W.J. (1996) Models for asymmetric proximities. *Br. J. Math. Stat. Psychol.*, **49**, 127-146.

Zinnes, J.L. and Griggs, R.A. (1974) Probabilistic, multidimensional unfolding analysis. *Psychometrika*, **39**, 327-350.

Zinnes, J.L. and MacKay, D.B. (1983) Probabilistic multidimensional scaling: complete and incomplete data. *Psychometrika*, **48**, 27-48.

APPENDIX

Computer programs for multidimensional scaling

A.1 Computer programs

Early computer programs for nonmetric MDS were Kruskal's MDSCAL, Guttman and Lingoes' smallest space analysis program SSA, and Young and Torgerson's TORSCA. The program MDSCAL was later developed into KYST by Kruskal, Young and Seery. SSA was developed into MINISSA by Guttman, Lingoes and Roskam. Young also developed another program, POLYCON.

Carroll and Chang introduced INDSCAL for individuals scaling, and later with Pruzansky, SINDSCAL. Later came Takane, Young and de Leeuw's ALSCAL, their alternating least squares program. Ramsay introduced MULTISCALE, a program for his maximum likelihood approach. SMACOF was developed by Heiser and de Leeuw. In 1981, the MDS(X) series of programs was commercially launched, and included the following:

1. CANDECOMP – CANonical DECOMPosition;
2. HICLUS – HIerarchical CLUStering;
3. INDSCAL-S – INdividual Differences SCALing;
4. MDPREF – MultiDimensional PREFerence scaling;
5. MINICPA – Michigan-Israel-Nijmegen Integrated series, Conditional Proximity Analysis;
6. MINIRSA – MINImum Rectangular Smallest space Analysis;
7. MINISSA – Michigan-Israel-Nijmegen Integrated Smallest Space Analysis;
8. MRSCAL – MetRic SCALing;
9. MVNDS – Maximum Variance Non-Dimensional Scaling;
10. PARAMAP – PARAmetric MAPping;
11. PINDIS – Procrustean INdividual DIfferences Scaling;
12. PREFMAP – PREFerence MAPping;
13. PROFIT – PROperty FITting;

14. TRIOSCAL – TRIadic similarities Ordinal SCALing;
15. UNICON – UNIdimensional CONjoint measurement.

The package is available from: Program Library Unit, University of Edinburgh, 18 Buccleuch Place, Edinburgh, EH8 9LN, UK. It is now somewhat dated in its presentation.

More commonplace statistical packages which offer MDS are SPSS and SAS, both of which have an alternating least squares option, ALSCAL. NAG also produces subroutines which carry out MDS. More limited are SYSTAT, STATISTICA and SOLO which will carry out nonmetric MDS on a PC. Schiffman *et al.* (1981) discuss fully programs for MDS and the results obtained when they are used on various data sets. They also give addresses from where the programs can be obtained. More recently, Borg and Groenen (1997) have given a good summary of computer programs for MDS, together with examples of their use. They cover ALSCAL, KYST, SYSTAT, SAS, STATISTICA, MULTISCALE, MINISSA, FSSA and PROXSCAL.

A.2 The accompanying CD-ROM

The accompanying CD-ROM contains programs which run under DOS to carry out some of the multidimensional scaling techniques which have been described in the text. The programs can be run individually, or more conveniently, from a menu program provided. The aim is to give the reader some "hands on" experience of using the various techniques. However, the condition of its use is that the authors and publisher do not assume any liability for consequences from the use of the CD-ROM. A Windows version will be available at the end of 2000.

Minimum system requirements
Windows 95, 98 or NT 4.0
Minimum – 640×480 256 colour display
Recommended – 800×600 16-bit or higher colour display
12 megabytes of free disk space
Minimum 16 megabytes of RAM
Recommended – 32 megabytes of RAM

*Please see CRC Press Downloads and Updates
http://www.crcpress.com/e_products/downloads/default.asp

A.2.1 Installation instructions

Windows Users

1. Place the CD in the CD-ROM drive.

2. Select Run from the Start Menu.

3. Type "**command**" for Windows 95/98 or "**cmd**" for Windows NT. Click O.K.

4. Type **d:** and hit enter (where d:\ is the CD-ROM drive letter).

5. At the d:\ prompt (again, where d:\ is the drive letter of your CD-ROM) type **install c mds** (where c is the destination drive, and mds the directory where the application will be installed). Hit enter.

6. Follow the prompt: type **mds** then hit enter.

To install an icon for the menu on your desktop, follow these instructions:

7. Open Windows Explorer (start → programs).

8. Open the MDS folder.

9. Right-click on the menu.exe.

10. Select Create Shortcut from the menu.

11. Drag the "Shortcut to menu" to the desktop.

If desired:

12. Rename the icon on the desktop by right-clicking on it and choosing Rename.

Once the installation is complete, you may run the program by double-clicking on the newly created icon on the desktop.

DOS Users

1. Place the CD in the CD-ROM drive.

2. Create a DOS window (by typing "**command**" from the start → run in Windows 95/98, or "**cmd**" in Windows NT). Click O.K.

3. At the prompt type **d:** (where d:\ is the drive letter of your CD-ROM).

4. Install the application by typing **install c mds** (where **c** is the destination drive, and mds the directory where the application will be installed.

5. Run the application by typing **mds**.

A.2.2 Data and output

By default, all data to be analysed and output generated will be located in the directory c:\mds\data. However, this default location for the data can be changed using the menu program. For instance, the user may wish to place data and ouput for each "project" undertaken in a separate directory, e.g. c:\mds\project1, c:\mds\project2, etc. To change the directory, use the menu program (see below), type 1001, and then type the name of the new directory where data and output are to be located. (Note the directory must already exist, having been created from Windows or otherwise.) To return to using the default directory, use the menu again and type in the default directory.

Data provided

The data files provided are of five types:
(i) those that end .VEC (e.g. KELLOG.VEC) – these contain an $n \times p$ data matrix, i.e. data for n objects measured on p variables. The data are to be viewed as p vectors of length n.
(ii) those that end .DIS (e.g. UK_TRAVE.DIS) – these contain dissimilarity data $\{\delta_{rs}\}$.
(iii) those that end .MAT (e.g. CANCER.MAT) – these contain two-way data in the form of a matrix. The data could be a contingency table, for instance.
(iv) those that end .IND (e.g. BIRTH.IND) – these are for indicator matrices.
(v) those that end .DEG – these contain coordinates of points on a sphere.
For the user to input his/her own data, see below.

A.2.3 To run the menu

There are three ways to run the menu program:
(i) create a DOS window, change directory to c:\mds\data, and type mds. (Note: mds can be typed from any directory.)
(ii) run mds from Windows (e.g. for Windows 95 and 98 click start, click run, type mds, click OK)
(iii) double click on the mds icon (if created)
In all three cases, a menu will appear in a DOS window. It has three columns of numbers and descriptions. Each number refers

to a program. The first column of programs (nos. 10-23) manipulate data ready for MDS analysis. The second column of programs (nos. 100-110) carry out the MDS analyses. The third column of programs (nos. 1000-1008) are for plotting and menus and to stop.
To run a program, simply type the program number.
To obtain a description of a program, type the program number followed by ,D (e.g. 22,D).

A.2.4 Program descriptions

Data manipulation programs
10 DAT2TRAN – transposes a matrix or vector, switching rows and columns
11 DAT2UNF – converts a matrix of dissimilarities ready for the unfolding program
12 HISTORY – this program is used on the historical voting data of Chapter 12 to produce dissimilarities ready for input into MDSCAL_2/3
13 IND2CON – transforms an indicator matrix into a contingency table
14 MAT2DISS – converts a binary data matrix into dissimilarity data
15 MDS_INPU – allows the user to input dissimilarities data (one at a time)
16 RAN_DATS – selects a subset of the data at random for analysis
17 RAN_VECG – generates random data for existing objects in a file
18 RAND_CAT – generates random categorical data for existing objects in a file (see Cox and Cox, 1998)
19 RECAVDIS – generates general two-way dissimilarity data according to Cox and Cox (2000) (see page 193)
20 VEC_JOIN – combines two sets of vectors into a single set: useful for plotting two configurations simultaneously
21 VEC2CSV – converts vector output files into comma separated values suitable for importing into a spread sheet.
22 VEC2DISS – generates dissimilarity data from data vectors
23 VEC2GOWE – generates Gower's general dissimilarities from a data matrix

MDS techniques
100 BIPLOT – Biplots (does not plot the biplot)
101 CLSCAL – Classical scaling
102 INDSCAL – Individual Differences Scaling, INDSCAL
103 LEAST_SQ – Least squares scaling
104 MDSCAL_T – Spherical MDS
105 MDSCAL_2 – Nonmetric scaling
106 MDSCAL_3 – Nonmetric scaling (one-mode, three-way)
107 PROCRUST – Procrustes analysis
108 RECIPEIG – Reciprocal averaging
109 UNFOLDIN – Unfolding
110 UNI_SCAL – Unidimensional scaling

Plotting and menus
1000 LINEAR – Linear biplots (plots the biplot)
1001 MENU – The menu program
1002 MENU_DAT – A menu of the data sets
1003 MOVIE_MD – Nonmetric MDS plotting the configuration at each step
1004 NONLIN – Non-linear biplots
1005 SHEP_PLO – Shepard plot for nonmetric MDS
1006 THETA_PL – Three dimensional plotting program for spherical MDS
1007 VEC_PLOT – Two dimensional plot of the first two columns in a file
1008 EXIT – (or use return key)

A.3 The data provided

Various data sets are in the directory c:\mds\data. Typing 1002 in the MDS menu will give a menu for the data sets. Each data set is given a number and typing this number produces a short decription of the data. Note that the data menu cannot be used to select files for anlysis.

The data sets
UK_TRAVE.DIS (Chapter 1)

SKULLS.VEC, PLATO.VEC (Chapter 2)

KELLOG.VEC (Chapter 3, Chapter 5)

WORLD_TR.MAT (Chapter 3, Chapter 4)

WORLD_TR.DEG (Chapter 4)

HANS_70.DAT HANS_71.DAT HANS_72.DAT HANS_73.DAT (Chapter 4)

ORD_SURV.VEC SPEED.VEC (Chapter 5)

MONK_84.DIS MONK_85.DIS (Chapter 6)

WHISKY.MAT (Chapter 6, Chapter 9)

AIR_EXPE.VEC AIR_NOVI.VEC (Chapter 6)

YOGHURT.VEC (Chapter 6)

SCORES.VEC (Chapter 7)

NATIONS.VEC (Chapter 8)

CANCER.MAT (Chapter 9)

MUNSINGE.MAT (Chapter 9)

BIRTH.IND (Chapter 9)

PGEB.VEC PGWC.VEC POQ.VEC TPO.VEC TRD.VEC (Chapter 10)

MAIDSTONE.68 (Chapter 12)

Figures in the text
Some of the configurations in the text can be reproduced using the following programs and data sets.

Figure 1.1	CLSCAL VEC_PLOT	UK_TRAVE.DIS
Figure 2.1	VEC2DISS CLSCAL VEC_PLOT	SKULLS.VEC
Figure 2.2	VEC2DISS LEAST_SQ VEC_PLOT	SKULLS.VEC
Figure 3.2 and Figure 3.4	VEC2GOWE MDSCAL_2 VEC_PLOT SHEP_PLO	KELLOG.VEC

Figure 3.12	MAT2DISS MDSCAL_2 VEC_PLOT	WORLD_TR.MAT
Figure 4.2	VEC2DISS MDSCAL_2 PROCRUST	HANS_70.VEC HANS_71.VEC HANS_72.VEC HANS_73.VEC
Figure 4.3	MAT2DISS MDSCAL_T THETA_PL	WORLD_TR.MAT WORLD_TR.DEG
Figure 5.2(ii)	PROCRUST VEC_PLOT	ORD_SURV.VEC SPEED.VEC
Figure 6.1	MDSCAL_2 PROCRUST VEC_PLOT	MONK_84.DIS MONK_85.DIS
Figure 6.2	MAT2DISS MDSCAL_2 VEC_PLOT	WHISKY.MAT
Figure 6.3	PROCRUST VEC_PLOT	AIR_EXPE.VEC AIR_NOVI.VEC
Figure 6.4	VEC_DISS MDSCAL_2 VEC_PLOT	YOGHURT.VEC
Figure 7.1 7.2, 7.3	LINEAR	SCORES.VEC
Figure 7.4	NONLIN	SCORES.VEC
Figure 8.3	DAT2UNF UNFOLDIN VEC_JOIN VEC_PLOT	NATIONS.VEC
Figure 9.2	RECIPEIG VEC_PLOT	CANCER.MAT
Figure 9.4	RECIPEIG VEC_PLOT	MUNSINGE.MAT
Figure 9.5	RECIPEIG VEC_PLOT	WHISKY.MAT

Figure 9.7	IND2CON RECIPEIG VEC_PLOT	CANCER.DAT
Figure 9.8	IND2CON RECIPEIG VEC_PLOT	BIRTH.IND
Figure 10.1	VEC2DISS INDSCAL VEC_PLOT	PGEB.DAT POQ.DAT PGWC.DAT TPO.DAT TRD.DAT
Figure 12.1 (i)	HISTORY MDSCAL_2 VEC_PLOT	MAIDSTONE.68
Figure 12.1 (ii)	HIST MDSCAL_3 VEC_PLOT	MAIDSTONE.68

A.4 To manipulate and analyse data

This section gives some examples of how the various programs are invoked. It is suggested that users follow these examples for practice before attempting analysis of their own data. The return key is symbolized as ↩.

Example 1: Classical scaling of the skull data
From the menu type 22 ↩ (to construct dissimilarities from the raw data)
Now type:

a1 ↩	(file name for a record of the session)
1 ↩	(choose Euclidean distance as a measure of dissimilarity)
n ↩	(choose not to transpose rows and columns)
y ↩	(standardize columns)
skulls.vec ↩	(input raw data from the file)
↩	(no more data required)
a2 ↩	(file for output of dissimilarities)
↩	(continue, back to the menu)
101 ↩	(choose classical scaling from the menu)
a2 ↩	(input the dissimilarities)

a3 ↩	(file to record the output)
(Eigenvalues are displayed)	
y ↩	(to save coordinates for plotting)
a4 ↩	(file for saving the coordinates; the program suggests the user enters a file name ending in .VEC, to show the type of file, but this is not necessary.)
↩	(to continue, return to the menu)
1007 ↩	(choose the plotting program)
a4 ↩	(input the coordinates)
n ↩	(do not wish to reset the axes)
↩	(to plot the configuration on the screen)
↩	(to return from the plot)
s ↩	(stop the plotting program)
↩	(to return to the menu)

Hint: to delete the files that have been created in this analysis either do this in Windows (e.g. from Windows Explorer), or if using DOS directly, exit the menu program (or use another DOS window) change directory to c:\mds\data (cd command) if not already in this directory and delete the files (delete a?).

Example 2: Nonmetric MDS of the Kellog data

From the menu type 23 ↩ (to construct dissimilarities based on Gower's general dissimilarity coefficient)

Now type:

kellog.vec ↩	(input the raw data)
b1 ↩	(file name for a record of the session)
b2 ↩	(file to store the dissimilarities)
ord ↩	(several times; the program checks whether the data are categorical or ordinal)
y ↩	(to standardize variables)
↩	(return back to the menu)
105 ↩	(choose nonmetric mds from the menu)
b2 ↩	(input the dissimilarities)
b3 ↩	(file to record the output)
↩	(choose a random starting configuration)
2 ↩	(choose a 2-dimensional solution)
200 ↩	(choose 200 iterations of the algorithm)
b4 ↩	(file for saving the coordinates)
b5 ↩	(file to save Shepard plot)

↩	(to continue, return to the menu)
1007 ↩	(choose the plotting program)
b4 ↩	(input the coordinates)
n ↩	(do not wish to reset the axes)
↩	(to plot the configuration on the screen)
↩	(to return from the plot)
s ↩	(stop the plotting program)
1005 ↩	(to draw the Shepard plot)
b5 ↩	(to input plot file)
↩	(to return to the menu)

Example 3: Least squares scaling and Procrustes analysis of the Kellog data

It is assumed that the dissimilarities have been constructed as in Example 2.

From the menu type 103 ↩ (to choose Least-Squares Scaling from the menu)

Now type:

b2 ↩	(input the dissimilarities)
c2 ↩	(file name to record the session)
↩	(choose a random starting configuration)
2 ↩	(choose a 2-dimensional solution)
200 ↩	(choose 200 iterations of the algorithm)
c4 ↩	(file for saving the coordinates)
↩	(to continue, return to the menu)
	(plot the configuration as in Example 2)
107 ↩	(choose Procrustes analysis from the menu)
c3 ↩	(file to record the session)
b4 ↩	(target configuration from Example 2)
c4 ↩	(mobile configuration)
c5 ↩	(modified configuration)
↩	(to return to the menu)

(plot configurations as required)

Example 4: Individual differences scaling of groundwater samples

22 ↩	(to generate dissimilarities)
d1 ↩	(file to record the session)
10 ↩	(choose correlations)
y ↩	(transpose rows and columns)

(note there is a maximum of 15 stimuli allowed)

y ↩	(standardize columns)

pgeb.vec ↩ (enter raw data, 5 files in total)
pgwc.vec ↩
poq.vec ↩
tpo.vec ↩
trd.vec ↩
↩ (to terminate input)
d2 ↩ (file to save dissimilarities)
↩ (return to menu)
102 ↩ (choose INDSCAL from the menu)
d2 ↩ (input the dissimilarities)
d3 ↩ (file to record the session)
-1 ↩ (use default tolerance)
-1 ↩ (use default number of cycles)
2 ↩ (number of dimensions)
↩ (no starting vector)
↩ (no starting vector)
↩ (no starting vector)
y ↩ (save results)
d4 ↩ (individuals space)
d5 ↩ (group stimulus space)
↩ (return to menu)
(now plot configurations)

Example 5: Biplot of the Renaissance painters
From the menu type 1000 ↩ (to choose Linear Biplot)
Then type
scores.vec ↩ (input the data)
e1 ↩ (file to record the session)
y ↩ (to standardize the columns)
1.0 ↩ (choose principal components biplot)
n ↩ (do not reset axes for plotting)
↩ (to plot)
↩ (to end plot)
↩ (return to the menu)

Example 6: Reciprocal Averaging of the Munsingen data
From the menu type 108 ↩ (to choose Reciprocal Averaging)
Then type
munsinge.mat ↩ (input the data)
f1 ↩ (file to record the session)
y ↩ (to save the vector for objects)

f2 ↩ (file for results)
y ↩ (to save the vector for attributes)
f3 ↩ (file for results)
↩ (return to the menu)
(now use plot_vec as in previous examples for f2 and f3)

A.5 Inputting user data

The user may analyse his/her own data contained in a pre-prepared file. The menu does allow input of dissimilarity data directly, but not general data. Data has to be placed in files according to the following formats.

A.5.1 Data format

Vectors need to be in the following (FORTRAN) format:

	FORMAT
Heading	**A80**
I,J,K,ALPHA	**3I3,G12.5**
ACR,COL,X (for i=1,...,I)	**2A4,25G12.5** or comma separated values

where: I is number of individuals; J is number of dimensions for the solution; K is number of cycles performed in the analysis; ALPHA is final gradient calculated; ACR is an identifier (acronym) for individual i; COL is a descriptor (colour) for individual i; X is the vector position of individual i in J dimensions.
Note that, apart from ACR and COL, the data may be entered as comma separated values.

Note: this structure is designed for use with multidimensional scaling. However, it is adopted for all the programs. In general, the parameters K and ALPHA may be omitted.

Dissimilarities need to be in the following FORMAT:

	FORMAT
Heading	**A80**
I	**I3**
dij (for i=2,...,I; j=1,...,i-1)	**G16.9**

ACR,COL	**2A4**
(for i=1,...,I)	

where: I is the number of individuals; dij is the dissimilarity between individuals i and j (assign missing values a negative dissimilarity); ACR is an identifier (acronym) for individual i; COL is a descriptor (colour) for individual i.

Note that the dissimilarities are input by rows. Since the matrix is symmetric, only the lower triangle is required. In general, the parameters ACR and COL may be omitted. If required, successive integers will be adopted to label the points.

In general, if a dissimilarity is missing, simply assign it a negative value.

Dissimilarities for Individual Differences Scaling

The format closely follows that of the dissimilarity data files.

	FORMAT
Heading	**A80**
I,J	**2I3**
dijk	**G16.9**
(for i=1,...,I;	
j=2,...,J;	
k=1,..., j-1)	
ACR,COL	**2A4**
(for i=1,...,I)	
ACR1,COL1	**2A4**
(for j=1,...,J)	

where: I is the number of individuals; J is the number of dissimilarity matrices; dijk is the dissimilarity for individual i between objects j and k; ACR is an identifier (acronym) for individual i; COL is a descriptor (colour) for individual i; ACR1 is an identifier (acronym) for object j; COL1 is a descriptor (colour) for object j.

Note that the dissimilarities are input by rows. Since the matrix is symmetric, only the lower triangle is required. Missing dissimilarities are unacceptable for this technique. In general, the parameters ACR, COL and ARC1, COL1 may be omitted. If required, successive integers will be adopted to label the points.

Contingency tables

The following is for contingency tables or data matrices with integer values.

	FORMAT
Heading	**A80**
I,J	**2I3**
A	**80I3** or comma separated values
(for i=1,...,I)	
ACR,COL	**2A4**
(for i=1,...,I)	
ACR1,COL1	**2A4**
(for j=1,...,J)	

where: I is the number of individuals (rows); J is the number of attributes (columns); A is the J dimensional row vector of attributes for individual i; ACR is an identifier (acronym) for individual i; COL is a descriptor (colour) for individual i; ACR1 is an identifier (acronym) for attribute j; COL1 is a descriptor (colour) for attribute j.

In general, the parameters ACR, COL and ARC1, COL1 may be omitted. If required, successive integers will be adopted to label the points.

Indicator Matrix

This "indicator matrix" stores the values in a contingency table in compact form for use in multiple correspondence analysis. For example, from page 138, the 28 rows of (0, 0, 0, 1, 0, 0, 1) would have a single line entry in the matrix as 28 4 3.

Heading	**A80**
Frequency, Levels	**11I3** or comma separated values
(for i=1,...,I)	
ACR,COL	**2A4**
(for i=1,...,I)	

where: I is the number of levels; ACR is an identifier (acronym) for individual i; COL is a descriptor (colour) for individual i.

In general, the parameters ACR and COL may be omitted. If required, successive integers will be adopted to label the points.

A.6 Error messages

All file allocations and parameters specific to the programs are set interactively at run time. In particular, a file containing a record of the run is compiled. Appropriate data files, as described above, are prepared in advance.
Any errors associated with the run, which typically arise if too large a data set is considered, will be reported on the screen. In addition, stopping codes are produced; a value of 0 (STOP 0) is associated with a successful run. The other stopping codes are summarised below.

BIPLOT

1 - no file containing a data matrix provided
2 - no file to record the output provided
3 - no file to record the final X configuration provided
4 - no file to record the final Y configuration provided
5 - increased array bounds required for the matrix provided
6 - increased array bounds required for working space
7 - increased array bounds required for the sort subroutine
8 - an eigenvalue is less than zero

CLSCAL

1 - no file of dissimilarities provided
2 - no file to record the output provided
3 - no file to record the final configuration provided
4 - too many individuals required
5 - a missing value was encountered in the dissimilarity list
6 - increased array bounds required for the sort subroutine

DAT2TRAN

1 - no file containing an information matrix is provided
2 - too many individuals required
3 - too many attributes required
4 - no file to record the transposed matrix provided

DAT2UNF

1 - no file to record the output provided
2 - no file containing a contingency table provided

3 - increased array bounds required for the data provided
4 - a missing value is unsuitable for unfolding
5 - no file to record the final configuration provided

HISTORY

1 - no data file provided
2 - too many candidates - array overload
3 - too many pairings of candidates - array overload
4 - too many triples of candidates - array overload

IND2CON

1 - no file to record the output provided
2 - no file containing a data matrix provided
3 - too much data (too many rows) input
4 - too much data (too many columns) input
5 - no file to record the final configuration provided

INDSCAL

1 - no file of dissimilarities provided
2 - no file to record the output provided
3 - no file to record the final configuration provided
4 - no file to record the attribute weights provided
5 - too few individuals provided
6 - too many individuals required
7 - too many attributes required
8 - a missing value was encountered in the dissimilarity list

LEAST_SQ

1 - no file of dissimilarities provided
2 - no file to record the output provided
3 - too many cycles required
4 - no file to record the final configuration provided
5 - too many individuals required
6 - the solution is required in too many dimensions

LINEAR

1 - no file containing a data matrix provided
2 - no file to record the output provided

3 - a graphics adaptor is needed to run this program
4 - increased array bounds required for the matrix provided
5 - increased array bounds required for working space
6 - increased array bounds required for the sort subroutine
7 - an eigenvalue is less than zero

MAT2DISS

1 - insufficient storage for local variables
2 - no file containing a data matrix provided
3 - no file to record the output provided
4 - no file to record the individual dissimilarities provided
5 - no file to record the attribute dissimilarities provided
6 - too many individuals required
7 - too many attributes required
8 - a non-binary variable was encountered

MDSCAL_2

1 - no file of dissimilarities provided
2 - no file to record the output provided
3 - too many cycles required
4 - no file to record the final configuration provided
5 - no file to record the results for a Shepard plot
6 - too many individuals required
7 - too high a dimensional solution required
8 - increased array bounds required for the sort subroutine

MDSCAL_3

1 - no file of dissimilarities provided
2 - no file to record the output provided
3 - too many cycles required
4 - no file to record the final configuration provided
5 - no file to record the results for a Shepard plot
6 - too many individuals required
7 - too high a dimensional solution required
8 - increased array bounds required for the sort subroutine

MDSCAL_T

1 - no file of dissimilarities provided
2 - no file to record the output provided

3 - too many cycles required
4 - no file to record the final configuration provided
5 - no file to record the results for a Shepard plot
6 - too many individuals required
7 - increased array bounds required for the sort subroutine

MDS_INPU

1 - no file to record the output provided
2 - no file to record the dissimilarities provided

MENU

1 - no appropriate data file provided

MENU_DAT

1 - too many file names provided
2 - selected item too high
3 - no appropriate data file provided

MOVIE_MD

1 - no file of dissimilarities provided
2 - no file to record the output provided
3 - too many cycles required
4 - no file to record the final configuration provided
5 - no file to record the results for a Shepard plot
6 - too many individuals required
7 - too high a dimensional solution required
8 - increased array bounds required for the sort subroutine
9 - a graphics adaptor is needed to run this program

NONLIN

1 - no file containing a data matrix provided
2 - no file to record the output provided
3 - a graphics adaptor is needed to run this program
4 - increased array bounds required for the matrix provided
5 - increased array bounds required for working space
6 - increased array bounds required for the sort subroutine

PROCRUST

1 - no file to record the output provided
2 - no file containing a target configuration provided
3 - no file containing a mobile configuration provided
4 - no file to record the final configuration provided
5 - too many individuals in the target configuration
6 - too high a dimension in the target configuration
7 - too many individuals in the mobile configuration
8 - too high a dimension in the mobile configuration
9 - the vectors have no points in common
10 - the input vectors are only one dimensional
11 - negative eigenvalues generated
12 - increased array bounds required for the sort subroutine
13 - Gram-Schmidt orthogonalisation has failed

RAND_CAT

1 - no file containing a data vector provided
2 - no file to record the output provided
3 - failed to generate partitioning planes
4 - no file to record the final configuration provided
5 - too many individuals required

RAN_DATS

1 - no file containing a data vector or matrix provided
2 - too many individuals required - vector input
3 - too many attributes required - vector input
4 - no file to record the final configuration provided
5 - too many individuals required - matrix input
6 - too many attributes required - matrix input
7 - no file to record the selected subset is provided

RAN_VECG

1 - no file containing vector or dissimilarity data provided
2 - no file to record the final configuration provided
3 - insufficient acronyms provided

RECAVDIS

1 - no file containing an information matrix is provided

2 - no file to record the output provided
3 - exponentiation error - numerical overflow
4 - data type not recognized
5 - no file of dissimilarities provided
6 - no appropriate eigenvalues located
7 - increased array bounds required for the matrix provided
8 - increased array bounds required for working space
9 negative dissimilarity generated
10 conflict when combining two categories
11 increased array bounds required for the sort subroutine

RECIPEIG

1 - no file containing an information matrix is provided
2 - no file to record the output provided
3 - no file to record the final individual configuration provided
4 - no file to record the final attributes configuration provided
5 - increased array bounds required for the matrix provided
6 - increased array bounds required for working space
7 - the data contains an excess of missing values
8 - increased array bounds required for the sort subroutine

SHEP_PLO

1 - no file containing a configuration provided
2 - a graphics adaptor is needed to run this program

THETA_PL

1 - no file containing a configuration provided
2 - no file to record the output provided
3 - all transformations are zero
4 - a graphics adaptor is needed to run this program
5 - too many data points required

UNFOLDIN

1 - no file of dissimilarities provided
2 - no file to record the output provided
3 - no file to record the final X configuration provided
4 - no file to record the final Y configuration provided
5 - insufficient space for the X dimension
6 - insufficient space for the Y dimension

7 - insufficient space for the dimensions required
8 - increased array bounds required for the sort subroutine
9 - a null vector has been generated

UNI_SCAL

1 - no file of dissimilarities provided
2 - no file to record the output provided
3 - no file to record the final configuration provided
4 - too many individuals required
5 - increased array bounds required for the sort subroutine

VEC2CSV

1 - no file containing a vector file provided
2 - no file provided to record the output vector

VEC2DISS

1 - no file to record the output provided
2 - too many files required
3 - too many rows required
4 - too many columns required
5 - no file to record the dissimilarities provided
6 - negative dissimilarity generated

VEC2GOWE

1 - no file containing a data vector provided
2 - no file to record the output provided
3 - no file to record the dissimilarities provided
4 - data type not recognized
5 - increased array bounds required for the matrix provided
6 - increased array bounds required for working space

VEC_JOIN

1 - no file containing a first vector provided
2 - no file containing a second vector provided
3 - no file to record the combined vector is provided
4 - increased array bounds required for the vector provided

VEC_PLOT

1 - no file containing a configuration provided
2 - a graphics adaptor is needed to run this program
3 - too much data input